"Time Dependent Deformation of Long Span Prestressed

Concrete Beams Having Low Relaxation Strands"

by

Timothy E. Bradberry, B.S.C.E.

A Report Submitted in Partial Fulfillment

of Requirements for the Degree of

Master of Science in Civil Engineering

The University of Texas at Austin

Austin, Texas

May 1986

To my parents,
my sister and my brother and all those persons who have played
the role of my family while I have been away from home

A C K N O W L E D G M E N T S

Carrasquillo for his assistance during the instrumentation development and installation and for his advice concerning the laboratory tests on companion concrete cylinders.

TABLE OF CONTENTS

TABLE OF CONTENTS (continued)

TABLE OF CONTENTS (continued)

LIST OF FIGURES

LIST OF FIGURES (continued)

viii

LIST OF FIGURES (continued)

LIST OF TABLES

C H A P T E R   1

INTRODUCTION

1.1 General

The serviceability limit state is extremely important in the design of long span composite prestressed concrete slab-girder bridges. Deflection control and dependability vitally affect riding quality. As the span length is increased, the effects of excessive and deficient beam camber are magnified. The differential camber between adjacent beams causes difficulties in forming composite decks and has resulted in very thick decks being used to "level out" slabs [39]. Minimization of these effects could result in substantial savings [28]. Some long span girders have exhibited substantial sag [39]. Such bridges would be more aesthetically appealing if excessive camber or deflection were minimized. Recent advances in the production of high strength concrete [37] has led to studies of increased optimization of prestressed concrete standard sections, such as the AASHTO-PCI Type IV girder investigated herein. As these sections are optimized and stretched in length the serviceability limit state will become even more important.

Serviceability limit states can only be considered if practical and dependable prediction of time-dependent deformations can be made. At present, a number of analytical

models have been developed [46, 44, 25] which predict the time-dependent behavior of pretensioned prestressed concrete girders constructed with materials of known properties. Results from these models sometimes are in conflict and some have not been verified for local conditions. Thus, verification of these analytical models is necessary before practical application can be made. Such verification can best be made when field data of the time-dependent deformations of slab-girder bridges is collected along with knowledge of the construction materials' instantaneous and time-dependent properties. After the accuracy of the model is verified for the known conditions, the sensitivity of the prediction to variable variations can be studied analytically.

The Center for Transportation Research at the University of Texas at Austin, in cooperation with the Texas State Department of Highways and Public Transportation and the Federal Highway Administration, has been conducting a research project to collect long term deformation data on a pair of prototype long span slab-girder bridges being constructed in Austin, Texas. This report is the first of two reports to be written concerning the study.

1.2 Background

If practical prediction and allowance for variations of time-dependent deformations is to be recognized by practitioners an understanding of the basic prestressed concrete deflection problem is necessary. In Fig. 1.1 the deflection of a prestressed concrete beam under full dead load is broken down into two parts. On the one hand there is the downward deflection, Δ_d, due to the dead weight of the beam and supported structure which is also affected by the creep and shrinkage of concrete. On the other hand there is the upward camber, Δ_u, due to the eccentricity and inclination of the prestressing force. This camber tends to increase with time due to concrete creep and to decrease with time due to loss of prestress force. Loss of prestress force is caused by the time-dependent concrete creep, concrete shrinkage and steel relaxation. Superimposed on these are deflection deviations due to temperature gradients. The two opposing deformations shown in Fig. 1.1 are each of much greater magnitude than their algebraic sum. The actual visual deformation is the difference in these large numbers, $\Delta_d - \Delta_u$. Thus errors in predicted net deflections ($\Delta_n = \Delta_d - \Delta_u$) may seem large when predictions are compared with field measurements on actual structures. However, this error is often not significant when compared to the sum of the absolute magnitudes of the two separate components of beam deformation--$|\Delta_d| + |\Delta_u|$.

$$\Delta_n = \Delta_d - \Delta_u$$

$$\frac{W\ell}{2} \qquad\qquad \frac{W\ell}{2}$$

II

$$\Delta_d$$

$$\frac{W\ell}{2} \qquad\qquad \frac{W\ell}{2}$$

+

$$\Delta_u$$

F_{pe}

F_{pe}

0.12 ℓ

Effect of draped tendon
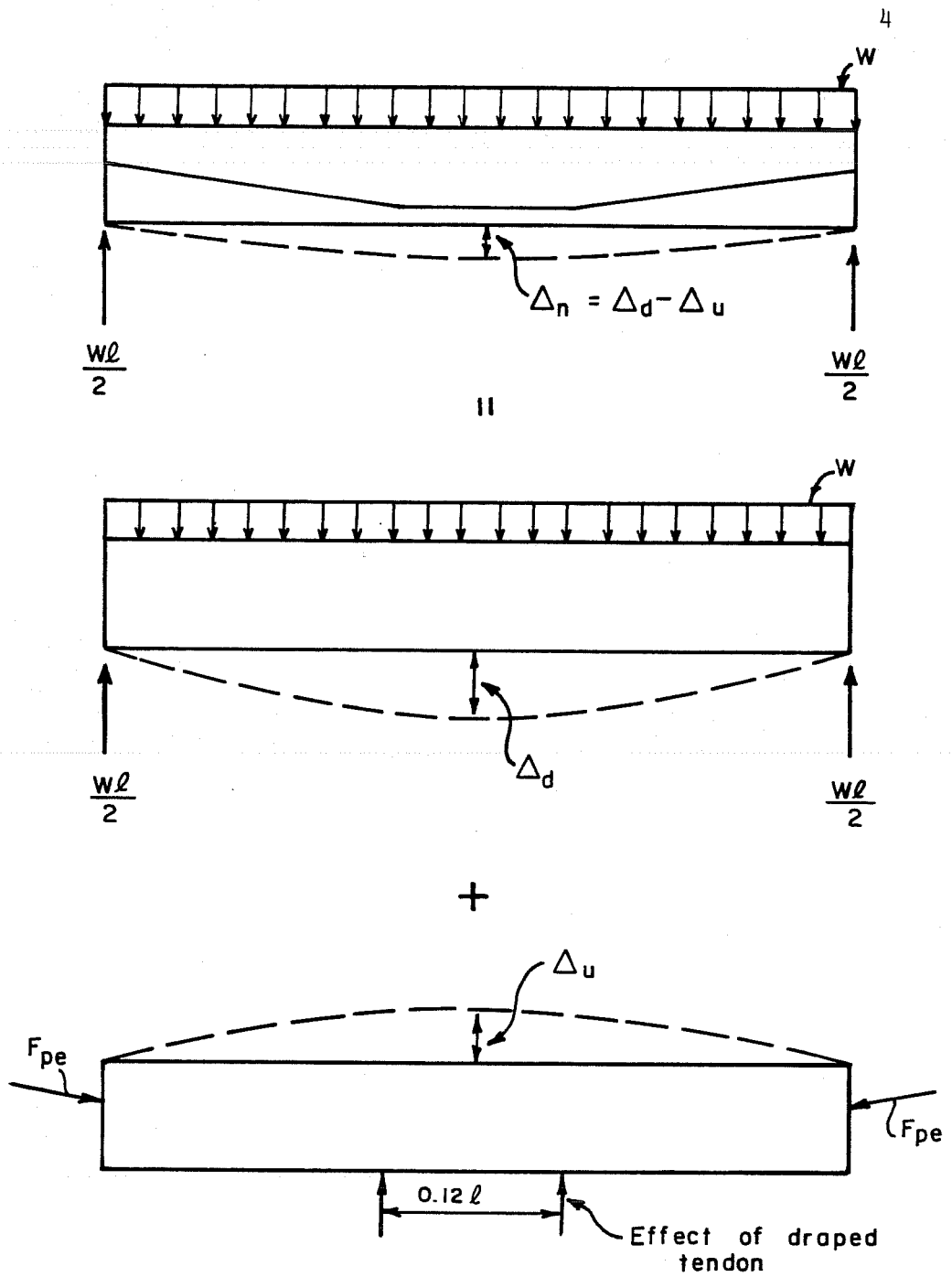
Fig. 1.1 Basic Prestressed Concrete Deflection Problem

The effects of girder and supported structure dead loads are generally an instantaneous elastic problem while those of creep, shrinkage, and relaxation are time-dependent, interdependent, and greatly affected by environmental and material factors. Furthermore, loss of prestress, though often calculated assuming an instantaneous elastic response, is also time dependent. The environmental and material factors can be statistically calculated only if assessments of their effects in the given geographic region have been previously made. The designer must understand that the actual location and climate where the structure is built will have a major impact on its time-dependent deformation behavior. Unless given this data, the designer cannot hope to make a reasonable estimation of the time-dependent deformations that he wishes to consider.

1.2.1 <u>Creep</u> <u>and</u> <u>Shrinkage</u> <u>Effects.</u> A significant factor affecting time-dependent deformations of pretensioned prestressed concrete bridge girders is the creep of the concrete. Concrete creep, concrete shrinkage and steel stress relaxation each contribute to loss of prestress resulting in loss of camber (downward deflection). However, only the creep of concrete and the effective prestress force contribute to girder upward camber. The primary effect of creep is to accentuate the net movement (upward effect) while the secondary effect is loss of prestress (downward effect). The amount of upward camber is a major factor

in the final deformed shape of the girder. Thus the importance of creep of concrete must be properly understood.

Creep and shrinkage effects for pretensioned prestressed concrete are influenced by almost every variable related to concrete maturity, material make-up and environmental chemistry, and load conditions throughout the life of the member [18]. In order to assist practitioners, a number of studies have been devoted to the determination of a "global" creep law based on constant stress laboratory creep tests [43, 16, 45, 1, 13]. No such law has been found which accurately predicts creep of concrete for field structures of arbitrary concrete constituents and environmental conditions. Early studies [43, 32] did not consider the interaction of creep and shrinkage and little was understood concerning temperature induced creep. Consequently, early investigators were satisfied to fit mathematical curves to creep data for specific laboratory tests under specific conditions [43]. More recent investigations [23, 1, 45, 14, 30] include the complex interaction of creep, shrinkage and temperature in their formulations in at least a qualitative sense. However, before these interactions can be evaluated quantitatively, statistical studies of creep of concrete and of environmental and material factors in various geographic regions should be carried out. In the meanwhile, available knowledge concerning creep and shrinkage of concrete can be assessed,

combined with knowledge of steel relaxation, and applied to the prediction of time-dependent deformations of pretensioned prestressed concrete field structures.

1.2.2 Loss of Prestress. The loss of prestress force plays a major role producing downward deflection components in prestressed concrete members with time. Some downward action may be attributed to primary creep effects but this is small due to the fact that most members are old enough at the time of casting of the deck that the creep of the aged girder concrete is relatively small compared to that of young concrete.

The loss of prestress directly lowers the effective prestress force and opposes the effect of the downward action of the dead weight of the girder and supported structure which tend to raise the effective prestress force because the center of gravity of the prestressing steel is below the neutral axis.

Loss of prestress was of major concern at the dawn of the prestressed concrete era. Loss of prestress was thought to be the "Achilles Heel" of prestressed concrete because the loss of prestress was large compared to the total prestress force. The development of high strength prestressing steel alleviated this problem. Subsequently, loss of prestress became of importance only in assessing the serviceability limit state of the prestressed concrete structure since the loss is usually less than 50 percent of the initial transferred force.

More recently, with the advent of low relaxation prestressing steel, loss of prestress due to steel relaxation has been further reduced. Due to this, the level of initial effective prestress force has generally been raised, thereby allowing a reduction in the number of required strands.

1.2.3 Analysis of Time-Dependent Deformations. The complex interaction of concrete creep, concrete shrinkage and steel relaxation combined with the incomplete knowledge of environmental and material factors make the "close" prediction of time-dependent deformations of prestressed concrete structures impossible if net deflections are used as the measuring stick. However, satisfactory results are possible if the present knowledge of these phenomena are applied and the judgement of the adequacy of predicted deformations reflect the overall or combined magnitudes of upward and downward actions.

Suttikan [46] has reviewed some available analytical procedures including the work of Corley, Sozen and Siess [18], Sinno and Furr [44], Gamble et al. [25, 33, 19] Branson [15], Dilger et al. [41, 47] Grouni [22], Huang [27], the P.C.I. Committee on Prestress Losses [36], Hays and Matlock [24], Lytton [41], Atkins [12], Pierce [38], Chang [17], and Lo [31].

Suttikan developed a rational analytical procedure, based on a discrete element technique capable of predicting both strength and long-term load responses of prestressed concrete

beams, providing that instantaneous and time-dependent material properties are available. One of the objectives of Suttikan's work was to develop a computer program capable of

> utilizing known material properties, when complete data are available.... A further objective [was] to show the validity of the proposed method by comparing the analytical results with the [then] existing observed values from actual beam tests....

Suttikan did not verify his method for the case where complete material property data is available.

The computer program developed by Suttikan will be used by Kelly [10] to predict the time-dependent deformations of the bridge girders being investigated herein.

1.2.4 Impetus for This Study. The impetus for this study came from the observation in the past several years of difficulty in predicting the actual deflections of several long-span prestressed concrete Type IV beams 120 to 135 feet long. It was observed that a recent serious deflection discrepancy incident in the State of Texas involved Type IV beams 130 feet feet long fabricated using low-relaxation strands.

Concern was expressed that use of such strands might aggravate the prediction problem in some unknown way. The construction of a new bridge in Austin, Texas afforded an opportunity to learn more about long term behavior of this type of structure. The planned length of certain spans and type of

standard girder were very much in the range of interest so this bridge was chosen to instrument and monitor. In the original project plan the intent was to instrument two spans. One span was to have beams fabricated with regular stress-relieved strands. The other was to have beams fabricated with special low-relaxation strands. A determination of the effects of using low-relaxation strands could be made by comparison of the behavior of the two spans. Unfortunately, since low-relaxation strand also meets all the requirements for normal stress-relieved strand, the actual contract wording implicitly permitted the fabricator to substitute low-relaxation strands for regular stress-relieved strands. The fabricator exercised this option and hense both spans were made with the same type strand although at different initial strand tension levels.

1.2.5 Previous Work. There have been relatively few studies where field data of the time-dependent deformations of the type of bridge system being investigated have been collected from a prototype field structure. Three studies conducted at the University of Illinois have concerned long term testing of this type [42, 26, 20].

Reynolds and Gamble [42] conducted a study in 1967 to develop instrumentation systems for long-term field testing of prestressed reinforced concrete highway bridges. The authors

evaluated the alternative systems for measuring five different parameters:

1. stress and strain in the prestressing steel,

2. strain in the concrete,

3. temperature gradients across beam sections,

4. deflections of the structure, and

5. relative humidity in the concrete.

They tested applicable instrumentation systems on laboratory specimens so that the alternative could be evaluated for each parameter of interest.

Gamble [20] measured camber, strain, creep and shrinkage on a four-span (46 ft, 73 ft, 73 ft, and 46 ft) precast, pretensioned, prestressed concrete highway bridge and concrete specimens over a period of two years. Most important changes in camber and concrete strains occurred within the first few weeks after release although some minor movements were measured after the deck was cast up to about 3.3 years. Shortening of the girders as much as 1 in. was measured. Strains measured showed cyclic expansion and contraction on an annual basis. "A re-evaluation of the methods currently used to estimate camber change, loss of prestress, and changes in length of members should be made in light of the results of the creep tests and the measurements on the girders" [20].

Houdeshell, Anderson and Gamble [26] measured camber, strain, creep, and shrinkage on a three-span (73 ft each) prestressed concrete highway bridge and concrete specimens over a period of two years. Although most important changes in beam camber occurred within 200 days after release, measurable movements were still occurring after more than two years. Similar changes in fiber strain occurred. Creep and shrinkage measurements indicate that shrinkage in the field was much less than in the laboratory, but that "creep values were comparable in the two environments. Further work is required to define the magnitude of creep of concrete subjected to variable environmental conditions, as most accepted present concepts are not adequate" [26].

1.3 Bridge System Being Investigated

The slab-girder bridge being investigated consists of pretensioned prestressed concrete AASHTO-PCI Type IV girders made composite with a cast-in-place deck. The bridge is a multispan system with girders supported on bent caps poured compositely with vertical piers. The deck consists of stay-in-place prestressed concrete panels upon which the passive deck reinforcement is placed and the remaining deck concrete cast. Figure 1.2 is a schematic of the bridge system being investigated. Fig. 1.2a shows an elevation view of a typical

Span L

Parapet

Abutment

Deck

Type IV Girder

Retaining Wall

Bent
Cap

Pier

a) bridge elevation

Reinforced Deck

Pretensioned Girder, Type IV(Typ.)
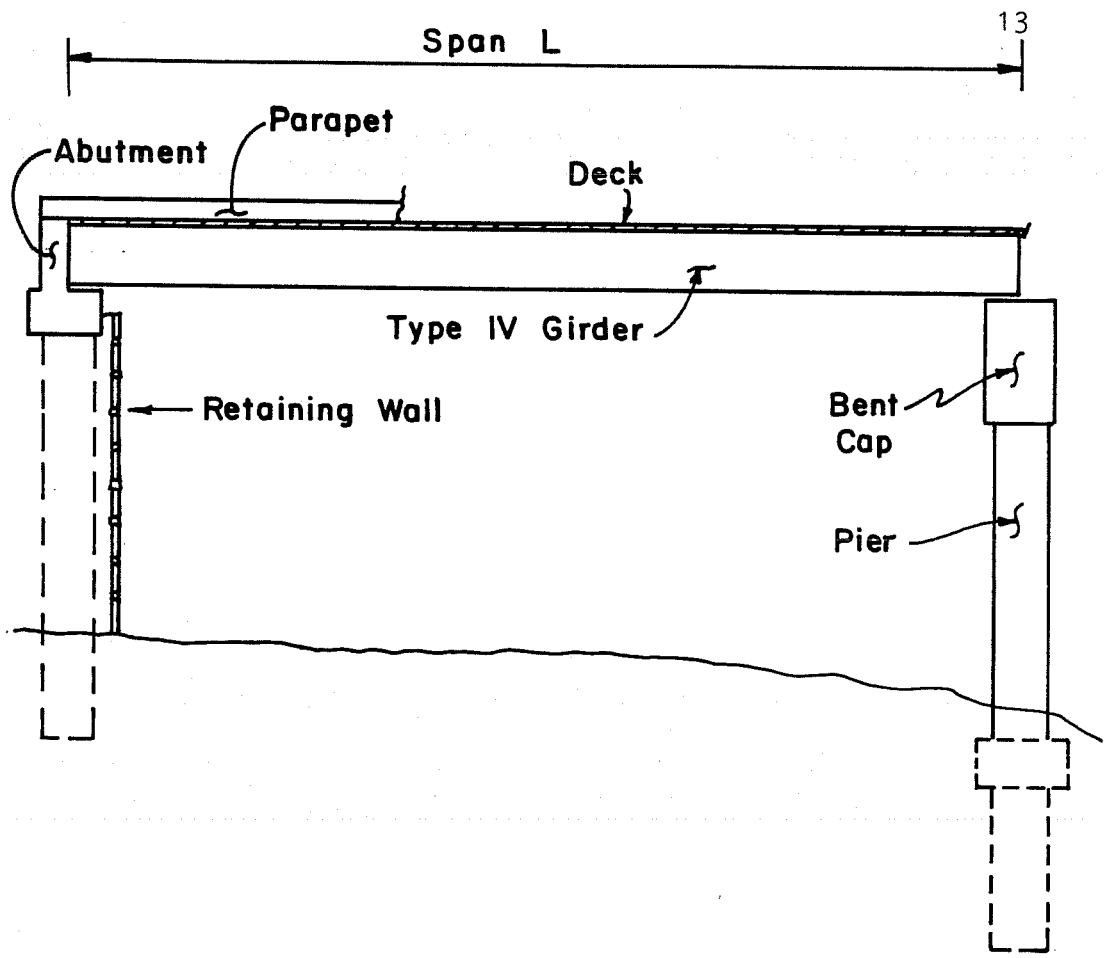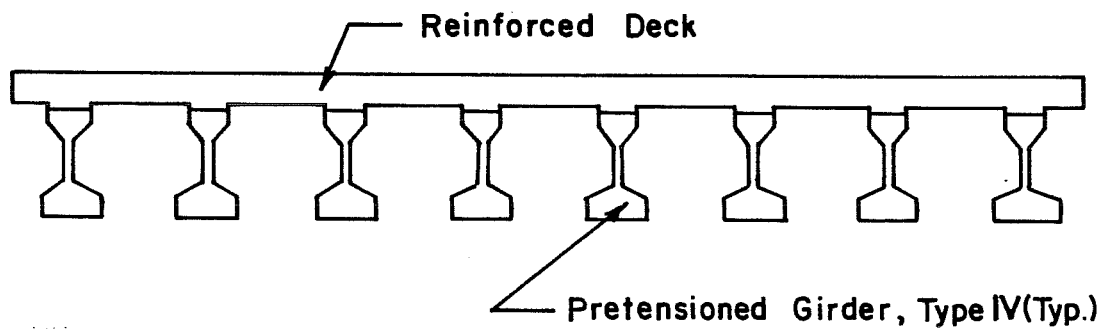
b) bridge cross section

Fig. 1.2 Schematic of the Bridge System Being Investigated

instrumented span and in Fig. 1.2b the cross section of the span is shown.

In this bridge system there are at least five stages of non-composite girder behavior. These stages are illustrated in Figures 1.3a to 1.3e. They are:

1. The pre-transfer stage, at which time the strands are anchored to the stressing abutments and are under tension equal to their initial stress minus any relaxation which has occured since they were stressed; the girder has no applied stress and thus no deformations (Fig. 1.3a);

2. The transfer stage, at which time the prestress force is transferred from the stressing abutments to the girder, the strands having lost a stress proportional to the elastic deformation of the concrete at the center of gravity of the prestressing steel; the girder has curvature and a deformed shape as shown qualitatively in Fig. 1.3b;

3. The storage stage, at which time the girder is placed on supports in the stock pile; the girder is supported at some distance in from either end thus increasing the camber and curvature which also is growing as time goes by due to concrete creep; the girder has a curvature

DEFORMED SHAPE   CURVATURE

a) Pre-Transfer Stage   (in prestressing bed) $\phi = 0$

CAMBER (Initial Instantaneous)

b) Transfer Stage   (in prestressing bed) ϕ_i

Camber (Increased & Growing)

c) Storage Stage (in stock pile with decreased span length) $\phi_i + \frac{d\phi}{dt}(t) + \phi_{\text{due to change in support conditions}}$

Camber (Decreased)

d) In- Place Unloaded Stage $\phi_{\text{end of storage stage}} - \phi_{\text{due to change in support conditions}}$

Camber (Decreased Again)

e) In-Place Deck-Load Stage $\phi_{\text{before deck is cast}} - \phi_{\text{due to deck load}} + \frac{d\phi}{dt}(t)$

Fig. 1.3 Non-Composite Girder Behavior

and a deformed shape as shown qualitatively in Fig. 1.3c;

4. The in-place-but-unloaded stage where the girder has been erected but no panels have yet been placed; there is some decrease in camber and curvature and a deformed shape due to changes in support conditions; the girder has curvature as shown qualitatively in Fig. 1.3d; and

5. The in-place-deck-load stage at which time the full load of the panels and deck are supported by the girders themselves; here the mid-span camber is further decreased (Fig. 1.3e) as is the mid-span curvature.

The intermediate partial and full panel load stage where some and then all of the deck panels have been placed is now shown. The addition of parapets and any deck overlay will be carried by the composite section of girders and deck slab rather than the girders alone.

Note that at each stage the girders are simply supported and thus statically determinate. This means that except for span length changes as the girder deforms over time there is a continuous redistribution of stress such that the resultant stress components and girder reactions do not change. These stress resultants and girder reactions do not change unless the applied load or span length changes. This makes possible the

simple determination of temperature induced camber even when the temperature distribution is non-linear [21]. Deflection corrections due to variations in support conditions should also be easily calculated for this determinate structure.

1.4 Stress-Relieved and Low-Relaxation Strands

1.4.1 Background. Early producers and researchers of prestressed concrete products noted that within a short period of time after the prestressing strands had been pulled to the required tension there was a noticeable drop in the measured load. They spoke of the strand creeping over time. Later they determined that the concept of relaxation of the strand was more realistic. Creep is the change in strain under constant applied stress while pure stress relaxation is the change in stress under a constant strain. Although the exact nature of this relaxation phenomena was not (and is still not) fully understood it has been agreed that a strand which minimizes this effect tends to minimize losses and so is desirable from the standpoint of optimum design of prestressed members. Thus, a method to produce low relaxation or "stabilized" strand has been devised and implemented; the specifications for this product are contained in Supplement I of ASTM A416 [4].

1.4.2 Specifications. The specifications for both normal stress-relieved and special low-relaxation strands are

covered by ASTM A416 [4]. The testing methods for these strands are contained in ASTM A370 [3] and E328 [9], respectively.

According to ASTM A416, the physical requirements for normal and low-relaxation strands are the same except as noted in Sections S4 and S5 of Supplement I. The physical requirements are abbreviated below, along with other requirements that are of interest:

1. Strength – The breaking strength of the finished strand shall be such that the minimum nominal ultimate stress is equal to the grade of the strand in ksi (i.e., grade 250 or 270) based on the specified nominal areas [Sec. 6.1].

2. Yield – Minimum yield at 1% extension under load shall not be less than 85% of specified breaking strength (except 90% for low-relaxation strand) [Sec. 6.2].

3. Strain – The total elongation under load of the strand shall be not less than 3.5% and shall be measured in a gage length of not less than 24 in. (or 610 mm). If the minimum elongation is met prior to rupture it is not necessary to determine the final elongation value [Secs. 6.3.1 and 6.3.3].

4. Sampling – One specimen for testing shall be taken from each 20-ton (18-Mg) production lot of finished strand [Sec. 9.1].

5. Marking - Low-relaxation strand produced meeting the requirements of Supplement I must be specially identified [Sec. 11.2].

6. Certification - The manufacturer shall, when requested in the order, furnish a representative load-elongation curve for each size and grade of strand shipped [Sec. 13.2].

A review of the supplement to ASTM A416 reveals the differences between the specifications of each type of strand. The physical requirements for special low-relaxation strand include all those of normal stress-relieved strand. In addition to these specifications, low-relaxation strand has the added requirement that the relaxation loss after 1000 hours shall be not more than 2.5% when initially loaded to 70% of specified minimum breaking strength, or not more than 3.5% when when loaded to 80% of said breaking strength.

Also, low-relaxation strand shall have a 5% higher yield than does normal stress-relieved strand. No limit on the relaxation loss of normal stress-relieved strand is specified.

1.4.3 <u>Manufacturing Processes</u>. The manufacturing process for low-relaxation strand is identical to that of normal stress-relieved strand up to the point of heat treating the strand. Both strands begin as seven individual wires which are drawn through dies to diameters within the specified tolerances.

Six of the seven wires are helically placed around the slightly larger diameter center wire and have a uniform pitch of not less than 12 and not more than 16 times the nominal diameter of the strand.

In order to "relieve" the strand wires of stresses induced by the stranding process, the strand is uniformly heat treated. At this point the manufacturing processes for normal and low-relaxation strands diverge.

According to a spokesman for Florida Wire and Cable Company (FWC) there are three commonly used methods of stress relieving prestressing strand:

1. Pull the strand through a bath of molten lead controlling the temperature and the rate of movement of the strand.

2. Run the strand through a gas fired furnace with the same controls on temperature and rate of movement.

3. Heat the strand through induction using induction coils and tracking the temperature by infrared cameras.

Simply treating the strand by one of the three methods listed above will produce normal stress-relieved strand. If, however, while heat-treating the strand, it is tensioned to produce a 1% extension after treatment, the resulting product is low-relaxation or "stabilized" strand. When asked if FWC had ever manufactured normal stress-relieved strand and these had met

the specifications of low-relaxation strand, the spokesman said,
in essence, that it is impossible to produce stabilized strand
without substantially tensioning the strand during heat
treatment; this could not be done accidentally. He added, "I can
tell you whether a strand is stabilized simply by looking at it;
stabilized strand is much straighter and stiffer than stress-
relieved strand." It was also discovered that strand which is
manufactured as low-relaxation strand but does not meet the
additional specifications may be used as stress relieved strand
by the buyer but still retains the low-relaxation marking.

A spokesman for Shinko Wire America, Inc. (SWAI) said
that the 0.5 in. diameter Shinko low-relaxation strand is
tensioned to between 7 and 8 tons during heat treatment. He also
indicated that the test they are required to submit to the
Highway Department for the low-relaxation strand does not always
indicate the 1000 hour relaxation properties of the strand. The
test, which is completed in 30 minutes, requires that the
relaxation of the strand during that period of time be less than
1.001% with the strand loaded to 80% of its minimum breaking
strength. Apparently when this relaxation is extrapolated to
1000 hours a small error in the measured relaxation in 30 minutes
will throw the 1000 hour relaxation off substantially. According
to Preston [40] the purpose of this short term test is not to

accurately determine the 1000 hour relaxation but to separate stress-relieved and low-relaxation strand.

1.4.4 Relaxation Behavior.

"Pure stress relaxation is the time dependent loss of prestress which occurs when the strand is maintained at a constant strain.... The former [low-relaxation strands] exhibit linear behavior in log time, $R = A + B*log(t)$, when $t > 10$ hours, whilst the latter [normal relaxation strand] exhibit a linear log-log relationship, $log(R) = C + D*log(t)$, with $t > 5$ hours.... It is apparent that the fundamental relaxation characteristics of the two types of strand are different" [29: 12-13].

This type of "intrinsic" relaxation is not what occurs in practice because the length of a stressed strand is practically never held constant. In a prestressed concrete beam the strain of the prestressing steel is constantly changing due to creep, shrinkage, temperature and load effects and changes in support conditions. Thus, the actual relaxation loss is normally less than the "intrinsic" relaxation loss due to the decrease in strand strain caused by other losses. This agrees with the findings of Gamble [20] and Houdeshell, Anderson and Gamble [26] in their field investigations.

For the tests reported in Ref. 29 (which take into account the relaxation that occurs in the first minute after loading) the average measured 1000 hour total relaxation for low-relaxation strand at 70% of the specified breaking strength is 2.28% while that for normal relaxation strand is 3.55%. If the

tests conducted are normalized to the standard tests found in the codes those 1000 hour values are 1.92% and 3.00% respectively. Therefore, for the tests reported in Ref. 29, the difference between the 1000-hour relaxation of low-relaxation and normal stress-relieved strands both loaded to 70% is either 1.27% or 1.08% depending on which test method is used.

   1.4.5 <u>Testing</u>. A recent state-of-the-art report by Preston [40] indicates that special equipment and test procedures prohibit accurate widespread testing of seven-wire prestressed concrete strand.

   For strength and yield tests special gripping devices and elongation measuring devices are necessary along with some experience in order to obtain the required degree of accuracy.

   For relaxation tests the strand must "have a stress loss that does not exceed the specified amount when loaded to the specified load for the specified time under the specified conditions" listed in the ASTM specifications. The strand must be maintained at 68 $\pm$°F throughout the duration of the test. Because the strand must be held at a constant strain and the load measuring device must be able to accurately detect very small changes in load, Preston says, "the special equipment required for this test is generally available only in the laboratories of fabricators of low-relaxation strand" [40].

Although a modulus of elasticity (MOE) test is not specified by ASTM A416, pretentioned prestressed concrete manufacturing procedures require that the MOE of the strand be known in order to determing the necessary elongation required. According to Preston the actual MOE of two strands produced on the same equipment and meeting the same specifications may differ by as much as 2.4%. This is due to variations in pitch and wire diameters. The tolerances allowed by ASTM result in variations in actual MOE values. If the MOE in the laboratory is computed based on actual strand cross-sectional area and that used in the field to determine the required elongation is based on nominal strand area the errors in actual strand force of as much as 1.2% will be made. Once again, special testing equipment and procedures requiring some experience are necessary to accurately assess strand MOE.

1.5 Objective and Scope

This study was undertaken for the following reasons:

1. To develop a field instrumentation program along with a material test program suitable for documenting the behavior of a long-span prestressed concrete slab-girder bridge,

2. To implement the field and laboratory programs by making measurements on an actual prestressed concrete bridge made using low-relaxation strands,

3. To collect long term data from the field and the laboratory, and

4. To evaluate the predictive capability of analytical models by comparing calculated results with the collected field measurements.

This study was designed specifically for application to a multi-span bridge in which each span consists of several simply supported pretensioned standard I-section girders.

This report includes the findings of Phase 1 of the investigation which documents the behavior of the instrumented girders from the time of casting to the time of their placement on the bents at the job site. The development of the instrumentation, monitoring, and laboratory test program is also discussed.

The development of the instrumentation system as well as the material testing program is discussed in Chapter 2. Field work which covers the implementation of the field instrumentation program as well as monitoring the instrumentation and collecting companion material specimens is presented in Chapter 3. Chapter 4 covers the procedures and results of laboratory tests conducted to obtain realistic engineering properties from the field

collected companion material specimens. Chapter 5 is a presentation of the data collected in the field. Chapter 6 summarizes the conclusions of Phase 1 of the research project and offers recommendations for implementation of the findings and for further research.

CHAPTER 2

DEVELOPMENT OF INSTRUMENTATION AND LABORATORY TESTS

2.1 General

Since this investigation involves monitoring a full scale field structure it differs from a typical laboratory study. The unique characteristics of this field study are as follows:

1. The instrumentation used must be simple, rugged, and able to be monitored under varied and uncontrollable environmental conditions for several years.

2. There is a third party involved, namely the contractor, requiring open communication and cooperation between this party and the research team.

3. If the fabricating plant and/or job site is not close by the research laboratory, much time and expense is spent on transportation that could otherwise be used for needed laboratory material tests.

4. Access to instrumentation for monitoring may be hindered by conditions existing during handling, storage, and final placement.

The characteristics above are general constraints which must be satisfied by this study to fulfill the objectives. This chapter discusses how the various subsystems of this

27

investigation were chosen, tested, and developed. Any subsequent field changes are discussed in Chapter 3.

2.1.1 Selection of Field Instrumentation. The four basic field measurements desired were:

1. surface concrete strains,

2. prestressing steel strains,

3. internal and ambient temperatures, and

4. beam camber/deflections.

Losses in prestressing force due to elastic shortening, shrinkage, and creep of concrete can be determined from knowledge of the concrete strain distribution history measured from the pre-release state of the member. Therefore, measurements of surface concrete strains were of interest to evaluate these losses directly. Measurements of the prestressing steel strains were of interest because the time-dependent loss of the prestressing force can be determined by knowledge of (1) steel relaxation and (2) elastic shortening of the strands. Steel relaxation can only be estimated by knowing the average relaxation properties of the prestressing steel. Direct measurement of the prestressing steel strains gives knowledge of the elastic shortening of the prestressing steel due to creep, shrinkage, temperature, and changes in load or support conditions.

The temperature measurements were needed for (1) knowledge of the temperature history of the members and their environment and (2) an evaluation of deformations induced by temperature changes and gradients so that creep, shrinkage, and load effects may be corrected for these independent strains. The ambient and internal temperature histories are of interest because they are among the factors affecting concrete strength, creep, and shrinkage properties.

Finally, the beam deflections were of primary interest because of questions concerning the predictive capability of computer programs used in design and analysis. The correlation of the predicted camber and deflection with that measured in the field will be a key component of this overall study and will be reported by Kelly [10]. This correlation was pointed out in Chapter 1 where the impetus for this study was discussed.

2.1.2 <u>Selection</u> <u>of</u> <u>Laboratory</u> <u>Tests</u>. If the computer programs used to predict the behavior of pretensioned prestressed concrete members in slab-and-girder bridges are to be rational and accurate in their analysis they must assume realistic material properties. Therefore, to provide the maximum possible information regarding the instantaneous and time-dependent properties of the materials used in the members investigated an extensive companion test program was needed. This information

could subsequently be put in a form that was acceptable as input into the analytical model.

Material properties of interest in this investigation include:

1. concrete compressive strength at various ages,

2. concrete time-dependent creep and shrinkage,

3. concrete stress-strain relationship at various,

4. prestressing steel relaxation properties, and

5. prestressing steel instantaneous elastic modulus.

Compressive tests on standard companion concrete cylinders were needed at various ages because of widespread use of this parameter in comparison of research results. Also the aging effects of hydrating cement on the compressive strength of the concrete was needed for input into the analytical model.

Creep and shrinkage properties of the concrete have a primary effect on the time-dependent deformations of pretensioned prestressed concrete members. Thus tests were needed to assess the creep and shrinkage behavior over time of companion cylinders so that these properties could also be included as input into the analytical model.

Concrete elastic modulus at the time of transfer of prestress determines the initial camber of a pretensioned member for a given prestressing force and eccentricity. Thus, it was desirable to measure the elastic modulus of companion cylinders

as close to the time of transfer as possible. Subsequent tests could yield the stiffening effect of aging concrete giving a modulus versus time curve which could provide even further useful information to the analytical model.

As mentioned previously, relaxation properties of the prestressing steel are needed to estimate the loss of prestress due to this stress level and time dependent phenomenon. Therefore, a determination of the relaxation behavior of companion strand samples was needed so that relaxation effects of the actual materials could be considered by the analytical model.

Lastly, the elastic modulus of both the gross prestressing strand and the individual wires which make up the strand were needed to (1) provide instantaneous elastic response information about the prestressing steel to the analytical model and (2) interpret the prestressing strain data recorded in the field to give losses due to elastic shortening of the strands.

Where applicable and possible, all laboratory tests were generally performed within the constraints of ASTM standard test methods. However, in almost all cases, environmental contraints outlined by ASTM for tests on companion concrete cylinders were not adhered to. In fact, most concrete cylinders were purposely stored in an environment, both before and during the early testing, that was similar to the environments of the prestressed members being investigated.

2.2 Concrete Strain Instrumentation

From the initial stages of this investigation it was decided that the most reliable scheme for monitoring the strain distribution over the depth of the Type IV girders would be a proven mechanical system. This decision was based on an understanding that pressure cells and electrical resistance strain gages for application to concrete have not yet proven to be reliable over long time periods, while mechanical systems employed in the past have generally worked well. Although such systems as vibrating-wire acoustic gages have been developed and used in Europe, no such system was available for this investigation.

A number of decisions concerning the concrete strain monitoring system were still to be made. Which hardware system provided the most reliable results was a primary concern. Other decisions which needed to be made included (1) at what depths of the girder section should the gage points be located and (2) how should the points be attached to the specimens.

Of the mechanical strain gage systems available--Whittimore, Demec, and Soil-Test--the Demec system, as shown in Fig. 2.1, provided the highest precision and ease of handling. One drawback of this system, however, was that the instrument and gage points could only be obtained directly from the manufacturer, who is located in England. Thus, procurement of
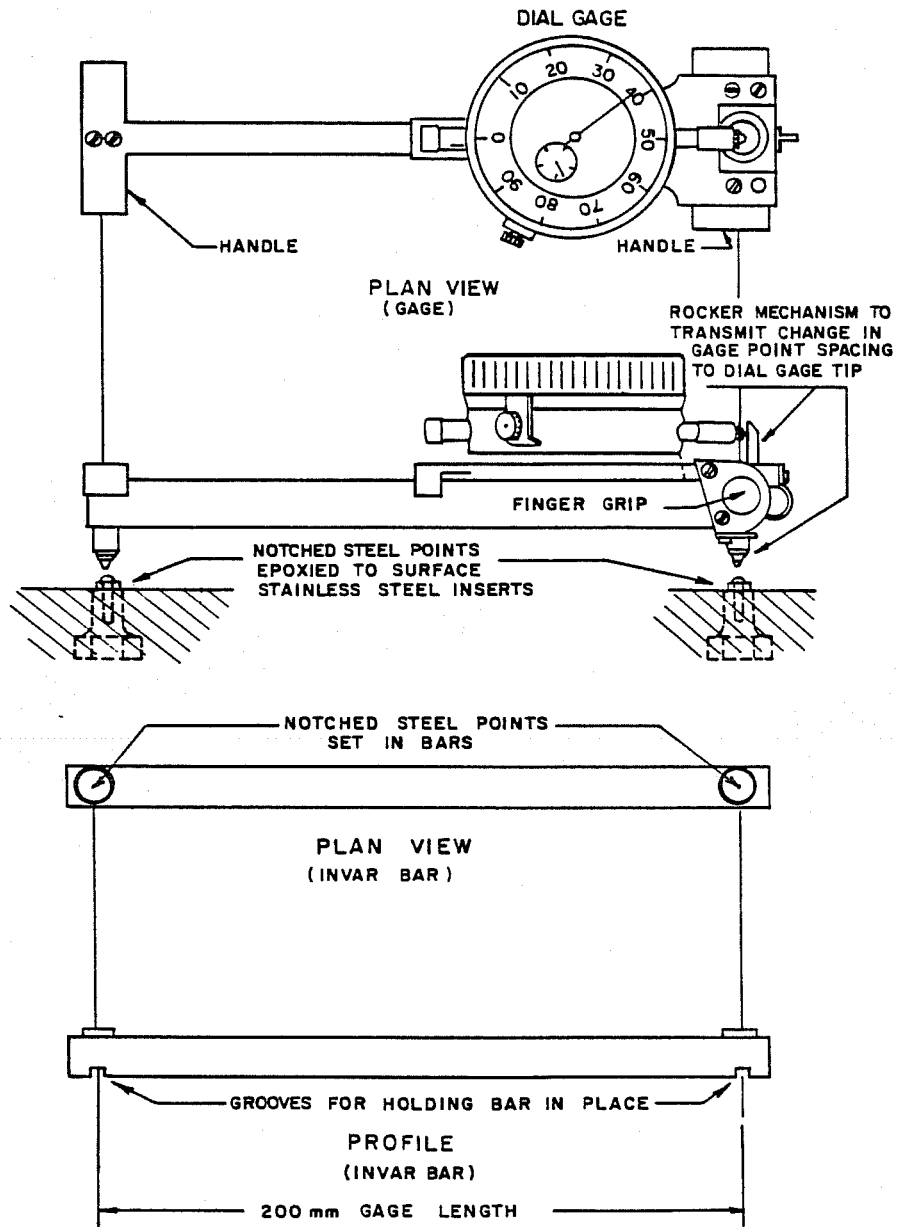
Fig. 2.1 Demec Mechanical Strain Monitoring System

additional instruments needed to perform laboratory and field
measurements was very difficult and actually required a full year
to complete. Such possible delays in getting equipment (or
materials) must be considered long before a field investigation
such as this is undertaken.

For preliminary testing of the concrete strain
monitoring system a full-scale laboratory prestressed concrete
bridge girder being constructed at the Ferguson Structural
Engineering Laboratory for a study reported by Overman [34] was
instrumented with gage points at the quarter points, and at mid-
span. The points were affixed to the specimens at gage lines
about 3, 23, and 37 in. from the bottom fiber. The exact
elevations of the points above the bottom fiber of the beam
varied from location to location along the span, as shown in Fig.
2.2a. This was because the points were hand-placed on the bare
concrete without the aid of preset locations or a template. This
method of placing the points on the girder was undesirable for
the field testing and thus inserts were manufactured to provide
preset locations for gage points in the field cast specimens.
Figure 2.2b shows the strain distribution across the depth of
section of the laboratory specimen as measured by the Demec
concrete strain monitoring system at the south quarter point,
mid-span, and the north quarter point respectively. The strain
distributions at transfer of prestress and about 2 days later are

a)   demec points placement
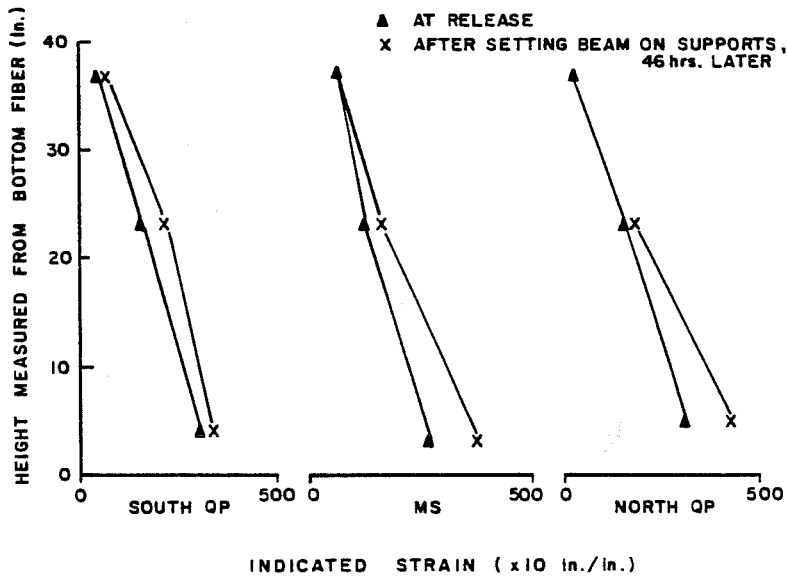
b)   strain distributions as measured by demec system

Fig. 2.2   Testing Demec System on a Laboratory Specimen

shown. With the exception of the 3 in. elevation gage line at the south quarter point, all gage lines gave strain readings qualitatively consistent with those expected. The apparent error in the 46-hr reading on the bottom gage line at the south quarter point may be due to a loose Demec point, a problem which became acute during the early field monitoring portion of this investigation when the epoxy lost adherence.

2.3 Strand Strain Monitoring System

Electrical resistance strain monitoring systems employing high quality strain gages applied to test specimens at points of interest and connected by lead wires to strain indicating equipment have been used widely in the laboratory as well as in the field for short duration structural testing. Application of such instrumentation to long term testing, especially of field constucted structures and structural members, has several practical pitfalls:

1. Strain indicators cannot be left out in the weather and expected to perform properly over long periods of time.

2. The resistance of lead wires and connections changes over time due to corrosion.

3. Workman who are unaware of, or insensitive to, the delicate nature of the strain gage instrumentation can

ruin the instrumentation during construction and handling of the test specimen.

4. The vibration of plastic concrete during placement may result in damage to strain gages or lead wires.

Some steps were therefore taken to minimize these undesirable effects.

Since the resistance of the connection will change between the time a lead wire is removed and later reconnected to the strain indicating equipment for subsequent readings, some way of accounting for this change was necessary. Hardware was available which had been used on a previous project to perform this function. The hardware consisted of galvanized junction-boxes each having a multiple channel switch, one channel of which was connected to a precision resistor of supposedly constant resistance. The precision resistor was used as a calibrator for any changes in resistance caused by the connection or switch thereby eliminating the need for a continuously field connected switch and balance unit. By balancing the strain indicator to the calibrating resistor, strain gage readings unaffected by the changes in connection resistance should be attainable. Alternatively, by reading and recording the indicated resistance of the calibrator each time strain gage readings are taken variation resistance corrections to the apparent strain gage readings can be made. Variations in switch resistance between

channels cannot be accounted for by this hardware system. For example, if the resistance of the channel that is connected to the calibrating resistance changes over time independent of the lead connected channels, indicated strain gage readings will be in error by the amount of this change at the time of recording readings.

In order to test the system and acclimate researchers to strain gage instrumentation procedures, the laboratory specimen used to test surface strain instrumentation was fitted with strain gage hardware. The test specimen referred to in Sec. 2.2 was instrumented with strain gages near its north end. Six gages were attached using standard strain gage procedures to three of the 0.5 in., seven-wire strands prior to placement of the strands in the casting bed and thus prior to the stressing operation.

Pairs of gages were affixed to a single strand on different wires about 3 in. apart on three different strands. Gages 1 and 4 were enclosed by a section of PVC pipe to protect them from damage caused by mechanical vibration of the concrete. The lead wires from all six gages were connected to a data acquistion unit which was in turn connected to a computer scanner. After stressing the strands, three of the six lead wires (those for Gages 4, 5, and 6) were disconnected from the data acquistion unit and connected to the calibrating switch box.

Figure 2.3 shows indicated strain versus time for all electronic strain gages attached to the laboratory specimen. Gage 2 malfunctioned after stressing giving erroneously large indicated strain readings. Of the remaining five gages, Gage 5 gave erroneous readings 2 out of the 5 times it was read. This could be the result of a bad channel on the switch box, a problem which arose later during the field work. Gage 6 appeared to not follow the same shape curve as the three remaining gages. Considering only the three gages whose readings did not hint of error (i.e., Gages 1, 3, and 4) it can be concluded that the strand strain gage system as tested in the laboratory was only 50% reliable. That is, for every two strain gages placed, only one gage yielded untainted results. However, if the instrumented strands are considered as a whole then the strand strain monitoring system was 67% reliable because the strains of two out of the three strands instrumented could be reliably determined over the short time period of 21 days. Both gages protected with PVC pipe seemed to perform well but it could not be determined whether this was due to the added protection. Unfortunately, the conclusions drawn from this investigation of the strain monitoring system are very limited since not enough readings were taken and no comparison with theoretical strains are offered.

Since it was very unlikely that reliable results would be obtained in the field from more than 50% of the applied strain
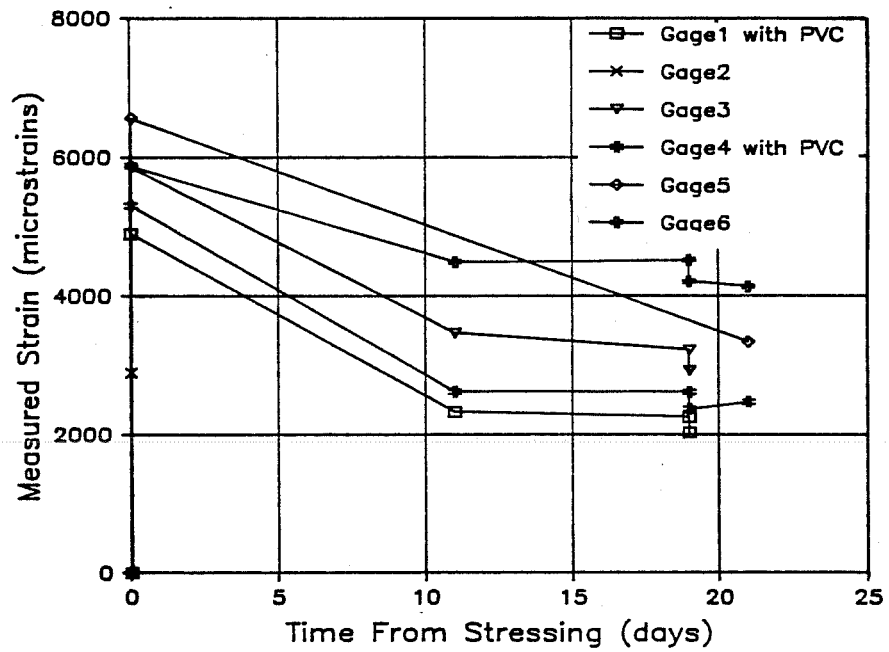
Fig. 2.3 Measured Strand Strain vs. Time for Laboratory
         Specimen as Measured by Electronic Strain Gages

gages or 67% of instrumented strands the subsequent field work employed two gages per instrumented strand per point of interest and were applied to a total of five strands per instrumented girder. The gages were applied after stressing the strands, thus yielding only information on the elastic loss of strand strain. No extra protection was given to the gages beyond the normal application of standard procedures and a thick gummy barrier material.

2.4 Temperature Instrumentation

Reliability of temperature monitoring instrumentation was not of concern in the initial planning phase of the investigation as thermocouples were known to have given consistent performance in the past. Thus, no testing was done as had been with other instrumentation systems.

The only decisions which were therefore required concerning the monitoring of the internal temperature of the field specimens were where and how many thermocouples should be placed. It was decided to place three thermocouples at each instrumentation location along the beams--one in each of the flanges, top and bottom, and one at the centroidal axis of the girder cross-section.

2.5 Long-Time Deflection Monitoring System

The development of the system for monitoring the instantaneous and time-dependent deflections of the girders was begun at the earliest stages of the project because the deflection data was considered the most important to be obtained. The system developed is unique and holds much promise for application to future research in the area of behavior of full scale field constructed prestressed concrete highway bridges and bridge components. The system has already been applied, in a modified form, to the load testing of a highway bridge at Happy, Texas [39], and has thereby proven to give results consistent with theory for such instantaneous deflection measurements.

2.5.1 Requirements of the Deflection Monitoring System.

The system used to monitor the time-dependent camber/deflection behavior of the girders had to meet the general requirements set out in Sec. 2.1. In addition, this system had to meet the specific needs of a long-span, pretensioned, prestressed concrete, slab-and-girder bridge system as follows:

1. Accurate transverse cambers/deflections (to within 0.01 in.) from the pre-transfer state of the girder until some extended time after the bridge is placed in service should be attainable.

2. The camber/deflection monitoring system should be easily transported and maintained.

3. The presence of wind should not interfere excessively while taking readings.

4. Damage to components of the camber/deflection monitoring system caused by negligent parties should minimize loss of reference to the initial undeformed state of the specimen.

5. The system should not cause problems with bridge clearance.

2.5.2 Deflection Monitoring System Alternatives. Two previous investigations were examined specifically for their approach to determining the deflected shape of the specimens tested [35, 11]. Also, White and Breen were consulted as to the performance of the system that White was using to collect deflection data for the study reported in Ref. 48.

Armstrong, Leyendecker, and Breen [11] developed an elaborate system to monitor the deflections of pan formed slab-girder bridges. The system, shown schematically in Fig. 2.4, could not meet the requirement of measuring the deformations at the time of prestress transfer although, theoretically, it could be employed once the girders were placed on the bents. However, the cost of this movable, under-bridge dial gage system would be prohibitive for the length of span being investigated. Also, this system would have violated clearance requirements of the bridge.

SLAB

ABUTMENT

ROLLERS (TYP.)

BAR JOIST

BENT CAP (TYP.)

TRACK ANGLE

BOLT-IN INSERT (TYP.)

ELEVATION

BRIDGE GIRDERS (TYP.)

JOIST

CROSS PIECE (Aluminum Box Channel)

DIAL GAGE (TYP.)

SECTION A-A
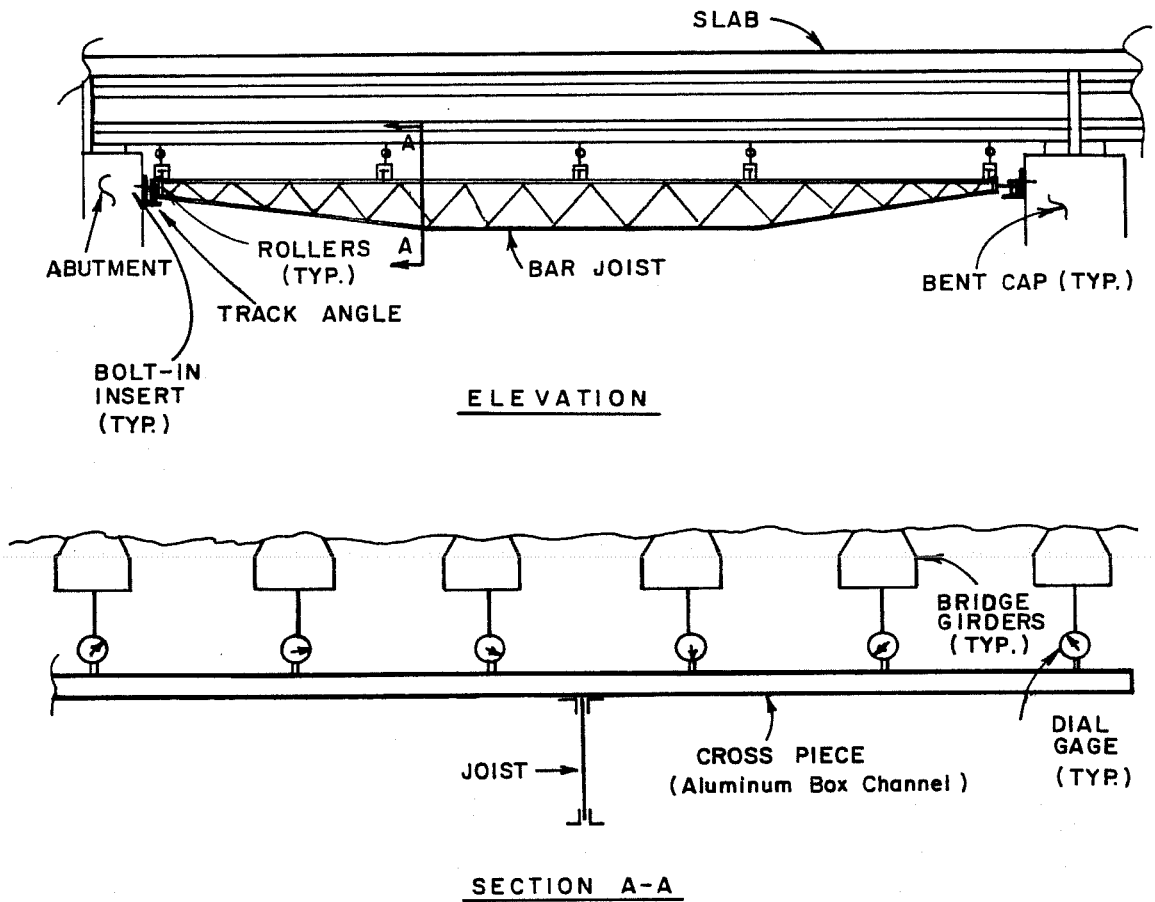
Fig. 2.4   Elaborate Under-Bridge Deflection Monitoring System

Pauw and Breen [35] developed a base line system which consisted of a tensioned wire stretched between two fixed reference points, as is shown schematically in Fig. 2.5. The tension in the wire was maintained by a suspended weight at one end. Deflections of the girders could be determined by measuring the distance between the base line and brass inserts, both initially, before prestressing, and at the desired time thereafter, and computing the difference. The measurements were made with a touch activated deflection meter which could be attached to the girder by bolt inserts and which permitted an accuracy in measurement of 1/1000 in. A temporary base line was used to get the initial deflection measurements prior to installing the girders on the bent caps.

The system used by White and Breen [48] employed a precision remote optical micrometer level sighting on leveling rods resting on bench marks, as shown schematically in Fig. 2.6. Considering both the performance of the remote optical system in the investigation sited and the prior experience of the writer and others, with pretensioned, prestressed concrete construction, the remote optical system would not be reliable, for the length of span being investigated.

Electronic systems employing linear potentiometers could not meet the requirements of durability and long term reliability. Also considered was an electronic laser system
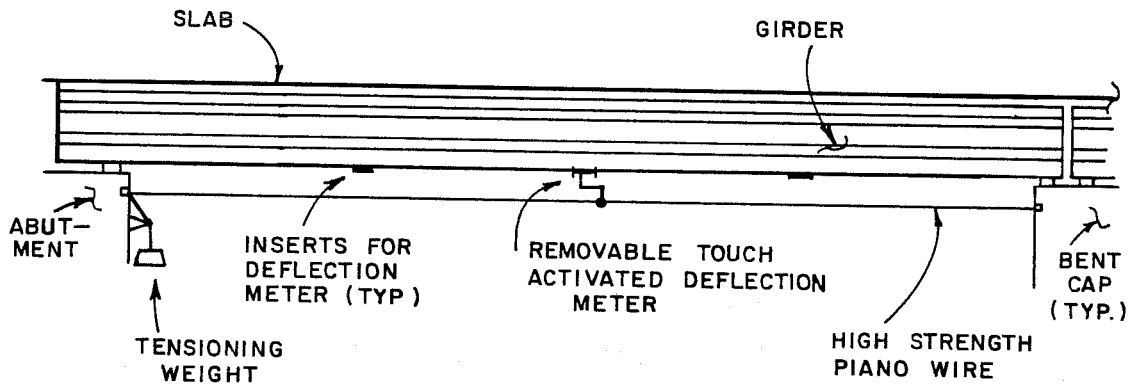
a) girder in place

b) girder in prestressing plant

Fig. 2.5 Base Line Deflection Monitoring System

MICROMETER
LEVEL

BENCH
MARKS
(TYP.)

LEVELING
ROD

SLAB

GIRDER
(IN PLACE)

ABUTMENT

BENT
CAP

a) girder in place

SCALED LEVEL
TARGETS

GIRDER

CASTING
BED

PICK-UP
TRUCK
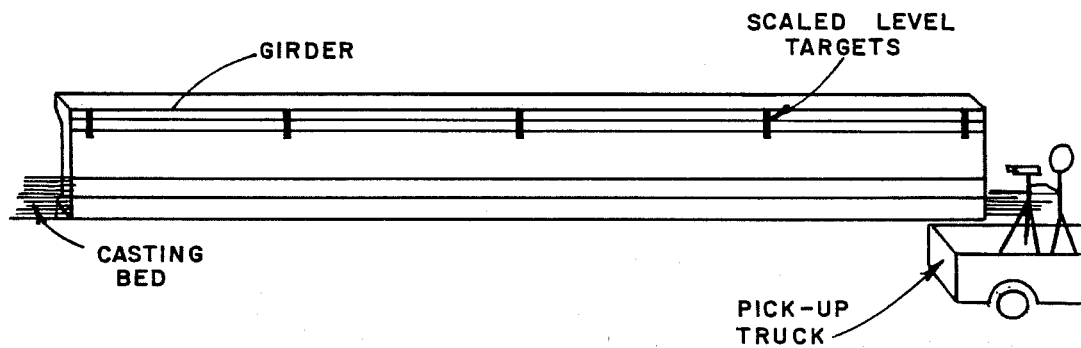
b) girder in casting bed

Fig. 2.6 Remote Optical Deflection Monitoring System

employing a high density, narrow beam laser. Such a laser could be mounted to one end of the girders, as shown in Fig. 2.7, sighted on a mirror at the opposite end, and used as a reference line from which deflection measurements could be made. The scales used to make deflection measurements could be attached to hinges mounted on the girders' bottom flanges and thus could rotate into and out of the beam reference line. Since the accuracy of such a system depends on the width of the beam of light produced by the laser, the diffusion effect for the required length of projected laser light would prohibit accurate readings from being taken with conventional lasers. The cost of such a system, if an appropriate laser were available, would certainly be too high.

2.5.3 <u>Selection of the Best Deflection Monitoring System Alternative</u>. Of the deflection monitoring schemes considered, the one which best met the requirements of both the general investigation and the deflection monitoring system was the high tensioned base line method. Therefore, a base line and scale method consisting of a base line reference system made up of high strength piano wire under controlled tension and visually readable scales affixed to the girder was developed. Figure 2.8 illustrates the general principles of this deflection monitoring system. The system is simple, durable, transportable (self-contained), able to accurately measure (to within 0.01 in.)

CALIBRATING MIRROR
AND SCALE (Fixed to
Laser Unit)

REFLECTED
LASER
BEAM

GIRDER
(In Casting Bed,
in Storage, or in
Place)

SCALES MOUNTED ON HINGES
FOR MAKING DEFLECTION
READINGS

R

R

LASER
(To be leveled and
rotated upon calibration)

REFERENCE LINE
LASER BEAM

ADJUSTABLE
MIRROR
(To be leveled and
rotated for
calibration)
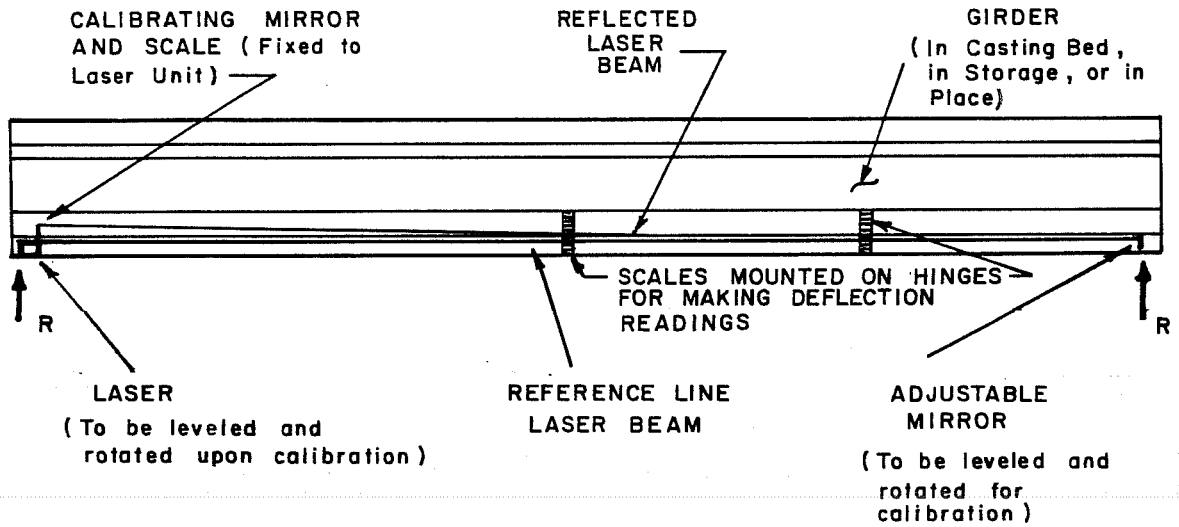
Fig. 2.7 Laser Deflection Monitoring System

PIANO WIRE ANCHOR
(Removable)

PIANO WIRE
ANCHOR
(Removable)

€ DEFLECTION SCALE

DETAIL. A

BASE LINE
CORRECTION
SCALE (FIXED)

$\frac{1}{4}$ PT. DEFLECTION
SCALE (Smallest Div. = $\frac{1}{64}$")
(Typ.)

HIGH STRENGTH
PIANO WIRE UNDER
CONTROLLED
TENSION (Removable)

BASE LINE
CORRECTION
SCALE (FIXED)
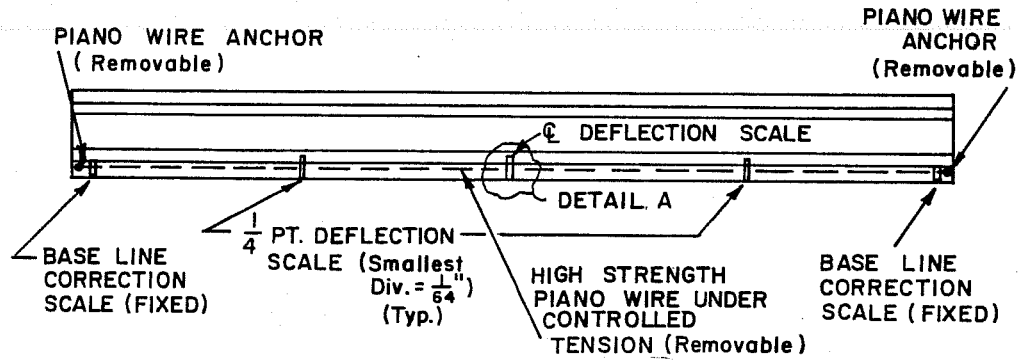
a) prerelease state of pretensioned girder showing all
attached deflection monitoring instrumentation
(Girder has zero vertical deflection throughout its
length)

DIRECTION OF INCREASE
READING IS ▲

OTHER SIDE OF
SCALE IS ▼

SAY 4 + $\frac{38}{64}$ INCHES

NOTE:

APPARENT IMMEDIATE
VERTICAL DEFLECTION

$= 4 + \frac{38}{64} - (2 + \frac{47}{64})$

$= 1 + \frac{53}{64}" = 1.828"$

DETAIL A

SAY 2 + $\frac{47}{64}$ INCHES
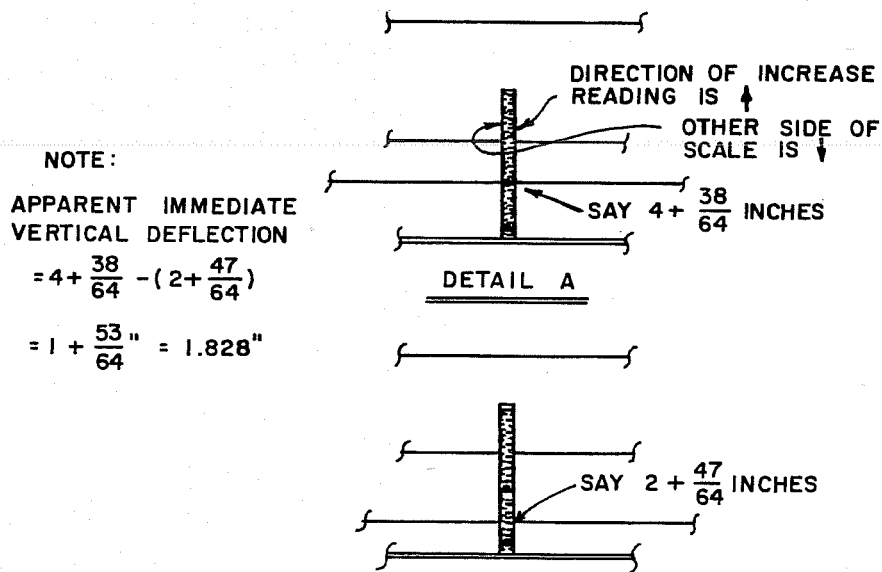
b) Detail A for the immediate response of the pretensioned
girder upon transfer of prestress

Fig. 2.8 General Principles of Chosen Deflection Monitoring
System

vertical camber/deflections from the pre-transfer state of the girders, and easily maintained and adjusted. The system, however, requires that the points of interest along the span of the girder be accessed directly in order to make readings. Also, the system's performance may be hindered by the presence of excessive wind.

2.5.4 <u>Development</u> <u>of</u> <u>the</u> <u>Chosen</u> <u>Deflection</u> <u>Monitoring</u> <u>System</u>. The development of the piano wire system can be divided into two phases. The first phase consisted of testing the system on a full scale laboratory constructed prestressed concrete bridge girder (see Fig. 2.9). This gave an opportunity to adapt the hardware of the system to the construction environment as well as to evaluate the system reliability. The second phase involved determining exactly how to control the tension in the piano wire from the pre-transfer state of the girder through the subsequent monitoring of girder deflections in the field.

2.5.4.1 Testing of Piano Wire System on the Laboratory Specimen. For the first phase of initial testing of the piano wire system coil-loop inserts were cast in the side face of the bottom flange of the laboratory specimen at the support points, 4 in. from the surface of the casting bed. After removal of the forms and prior to the transfer of the prestressing force to the girder a 0.031 in. diameter high strength (approx. 330 ksi) piano wire was hung between special anchors attached to the coil loops.
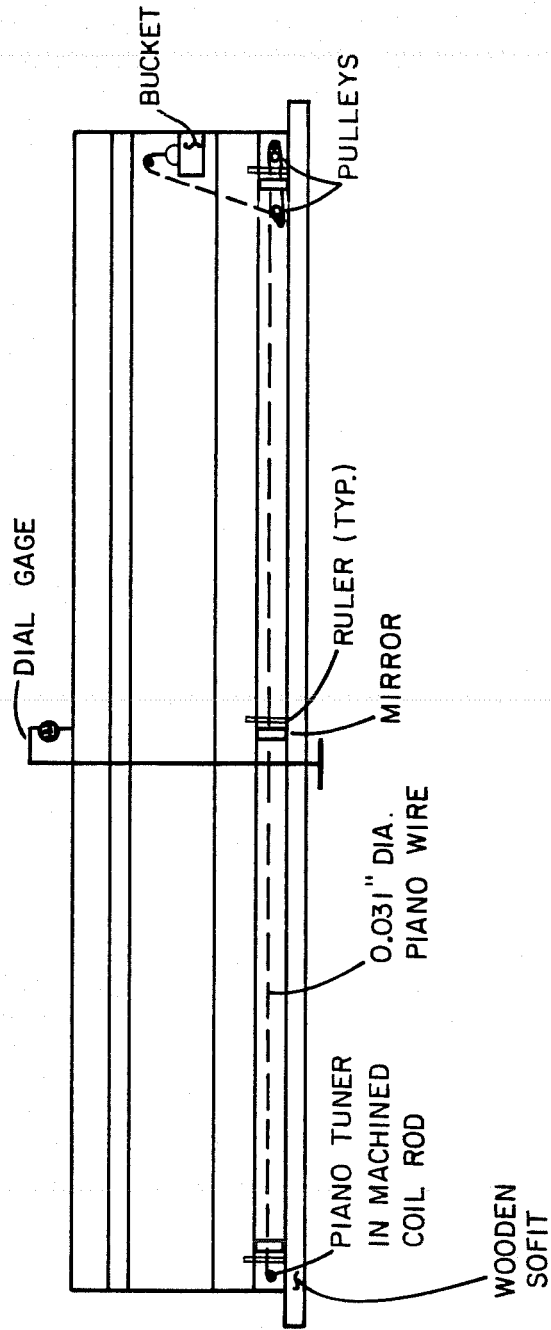
Fig. 2.9 Laboratory Specimen Instrumented with Experimental Deflection Monitoring
System

At the "live" end, the anchor consisted of a specially machined coil rod with an attached pulley through which the piano wire extended and then was tied to a bucket of known weight. At the "dead" end, the piano wire was passed through and twisted around a piano tuner. The tuner was screwed into a wooden bearing which had been drilled and pressed into a machined coil rod anchor. The tension in the piano wire was maintained at a constant value by the force exerted by the bucket. In order to measure the relative movement of the bottom flange of the beam with respect to the initial shape of the piano wire, sections of metric tape were affixed, using quick-setting epoxy, to the flange at points of interest along the beam (the quarter points and mid-span) as well as next to the piano wire anchors. It was necessary to place the scales near the anchors so variations in the elevation of the wire ends due to adjusting the piano tuner and replacing the wire could be accounted for and the necessary linear corrections made to the readings taken. Mirrors were affixed to the girder next to the scales to insure that the readings were always taken from an eye level exactly the same elevation as the piano wire. This was accomplished by lining up the image of the piano wire with the wire itself while making readings.

2.5.4.1.1 Initial Camber Measurements Using Piano Wire System and a Dial Gage. Upon transfer of prestress, the laboratory specimen showed an immediate upward camber of 0.295

in. as measured by the piano wire system and of 0.233 in. as
determined from dial gage readings. The difference between the
two values of initial camber can be explained by considering the
elastic deformations of the precasting bed at the ends of the
girder. The wooden soffit which supported the girder before
transfer of prestress undoubtedly experienced additional vertical
elastic deformation at the ends of the girder when the weight of
the girder was transfered from uniform soffit support to point
loads on the soffit at the ends of the girder. However, these
deformations were not measured by dial gages at the girder ends.
Thus, the midspan dial gage measured an upward vertical camber
which was less than the actual camber by the amount of elastic
deformation of the wooden soffit. Since no dial gages were used
at the ends, no correction to the camber was experimentally
determined.

    2.5.4.1.2 Reliability of Piano Wire System for Live
Load Deflection Measurements. In evaluating the reliability of
the piano wire system for determining time dependent vertical
camber/deflections of the test specimen it should be noted that
the piano wire used in the laboratory was slightly greater than
0.03 in. in diameter. Since the metric tape had least divisions
of 1 mm (0.0394 in.) the accuracy of the laboratory system is
0.04 in., which is 1/4 that desired. Unfortunately, piano wire
readings were not made immediately before and after forming for

and casting of the composite slab. Thus, the deflection versus time curve could not be determined with the piano wire system for comparison with the dial gage determined curve. Therefore, this test was not conclusive as to the reliability of the piano wire system for monitoring time-dependent camber/deflections. However, the results of this test indicated a smaller diameter piano wire should be used in order to enhance the system's accuracy.

Live load deflections of the laboratory specimen as measured by the piano wire system were compared with those obtained from dial gage readings. As can be seen from Fig. 2.10, the piano wire system used in the laboratory yields deflection measurements which are very close to those obtained from dial gage readings. In fact, for the initial loading of the specimen, the piano wire system gave more consistent deflections than did the dial gage system. The average difference between the results given by the two deflection monitoring system is well within the 0.04 in. accuracy of the piano wire system used.

2.5.4.2 Fine Tuning of Piano Wire System. These preliminary tests indicated that the piano wire system had great possibilities. In order to further refine the system to the point where it could readily be used in the field it was necessary to extend the testing to a more representative length of wire. Anchorage attachments were affixed between columns in
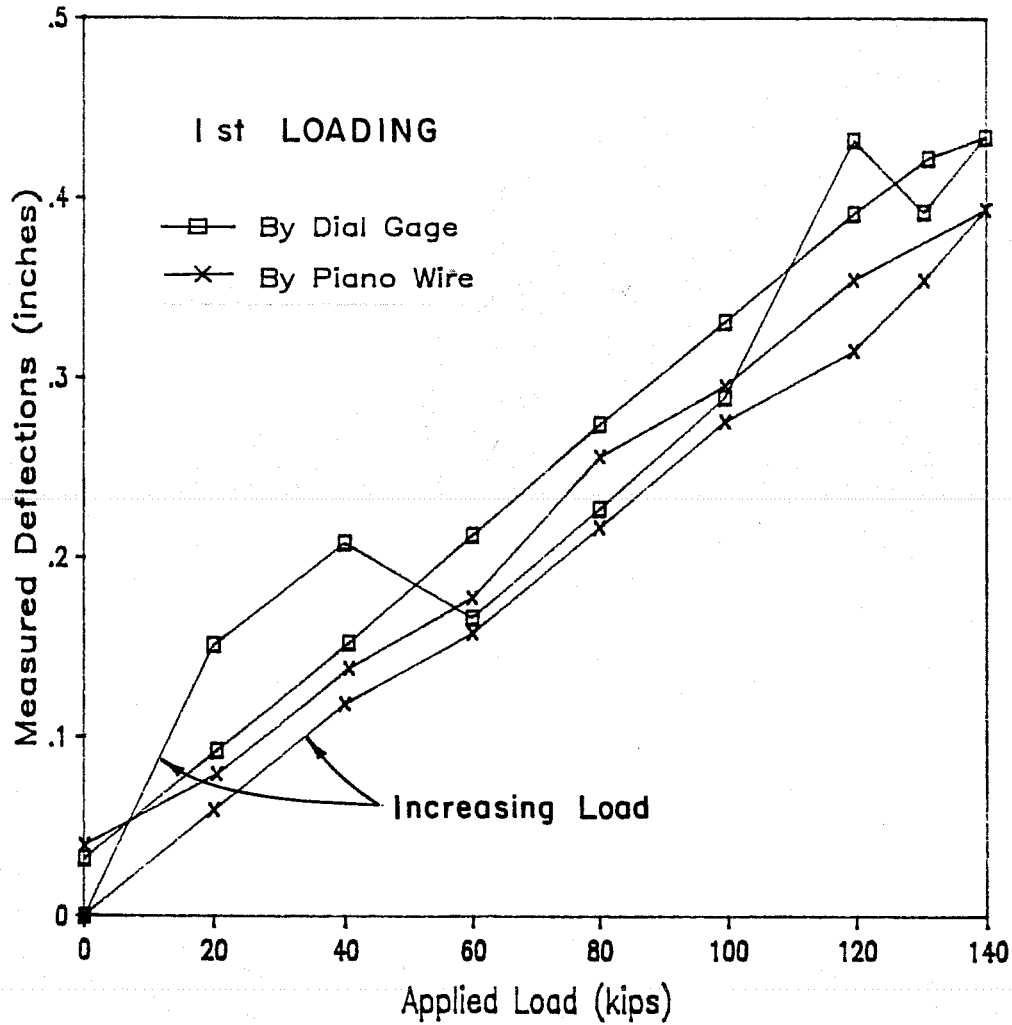
a) deflection vs. load for first loading of laboratory beam

Fig. 2.10 Verification of Reliability of Base Line System for Monitoring Live-Load Deflections
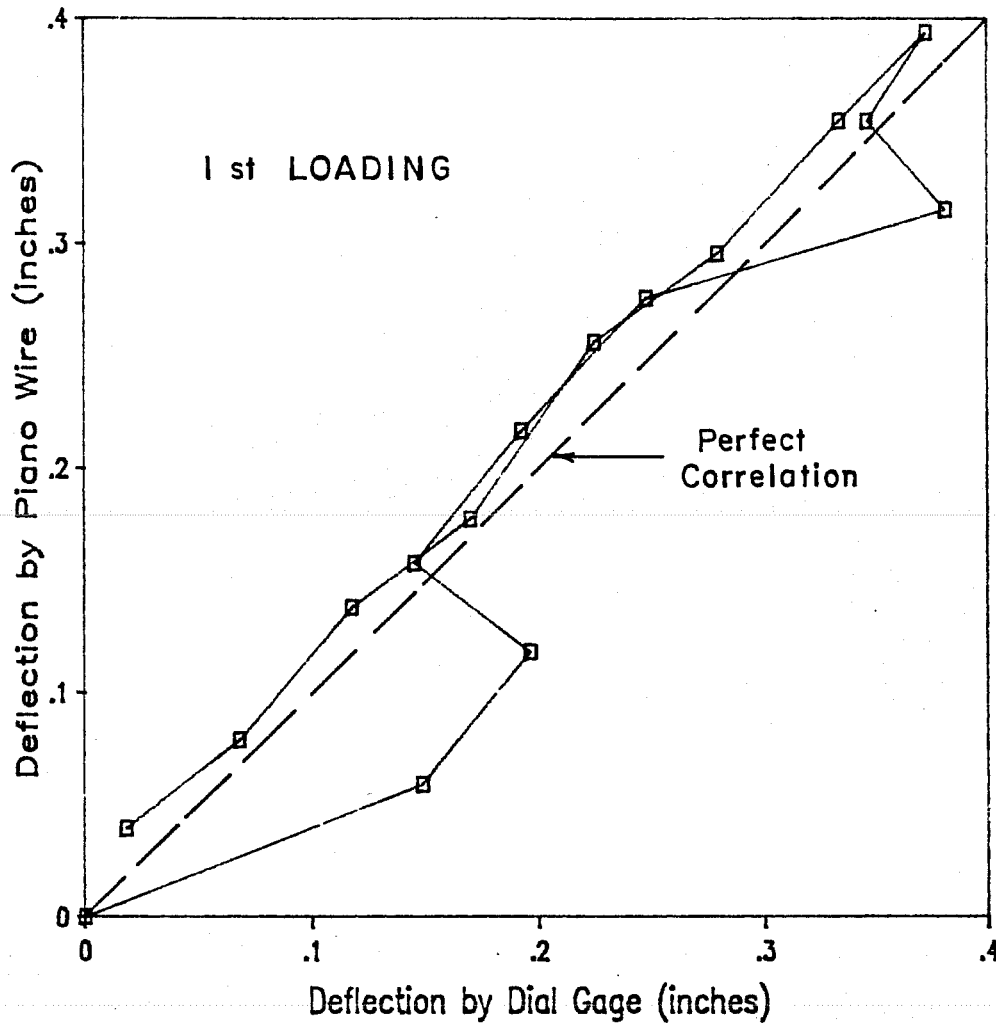
b) correlation of dial gage and piano wire determined deflections for first loading of laboratory beam

Fig. 2.10 Verification of Reliability of Base Line System for Monitoring Live-Load Deflections (cont'd)
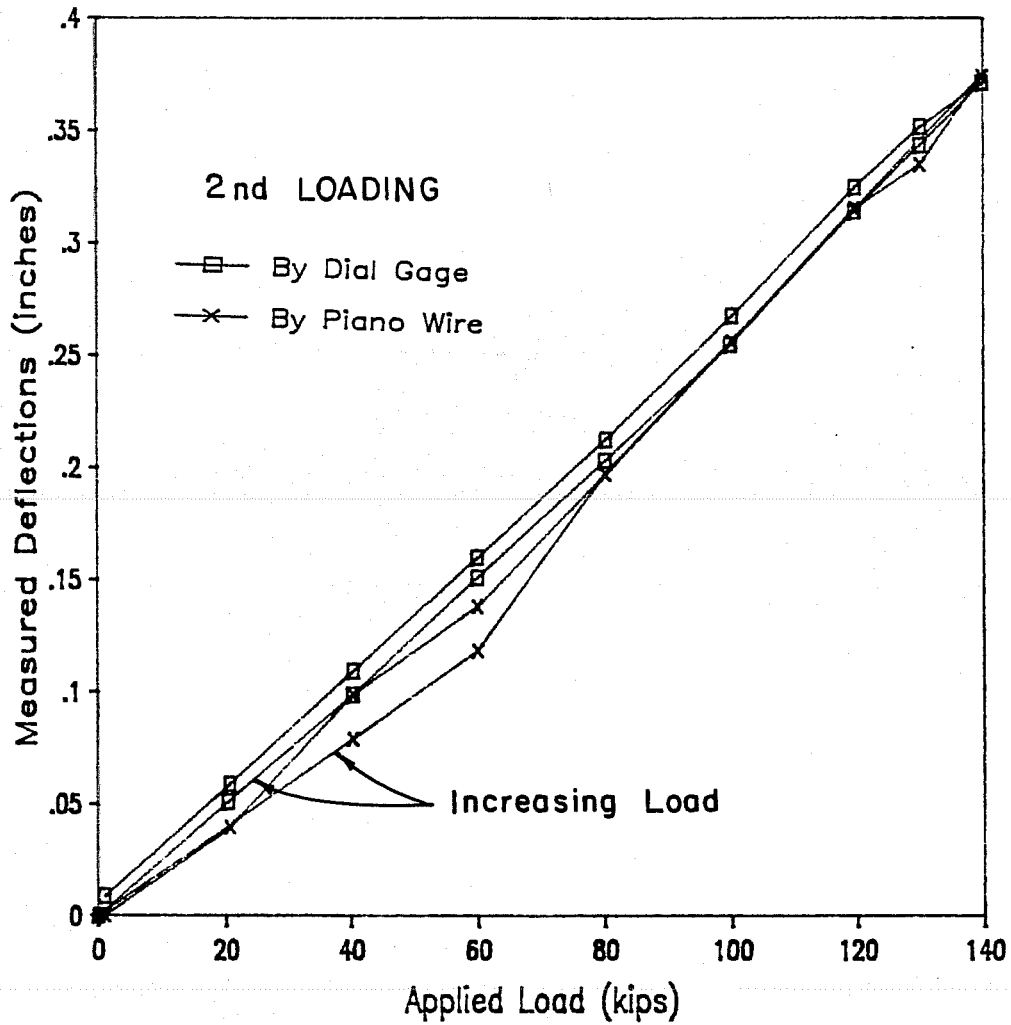
c) deflection vs. load for second loading of laboratory
beam

Fig. 2.10 Verification of Reliability of Base Line System for
Monitoring Live-Load Deflections (cont'd)

d) correlation of dial gage and piano wire determined
deflections for first loading of laboratory beam

Fig. 2.10 Verification of Reliability of Base Line System for
Monitoring Live-Load Deflections (cont'd)

ULTIMATE LOADING

—☐— By Dial Gage
—✕— By Piano Wire

Measured Deflections (inches)

Applied Load (kips)
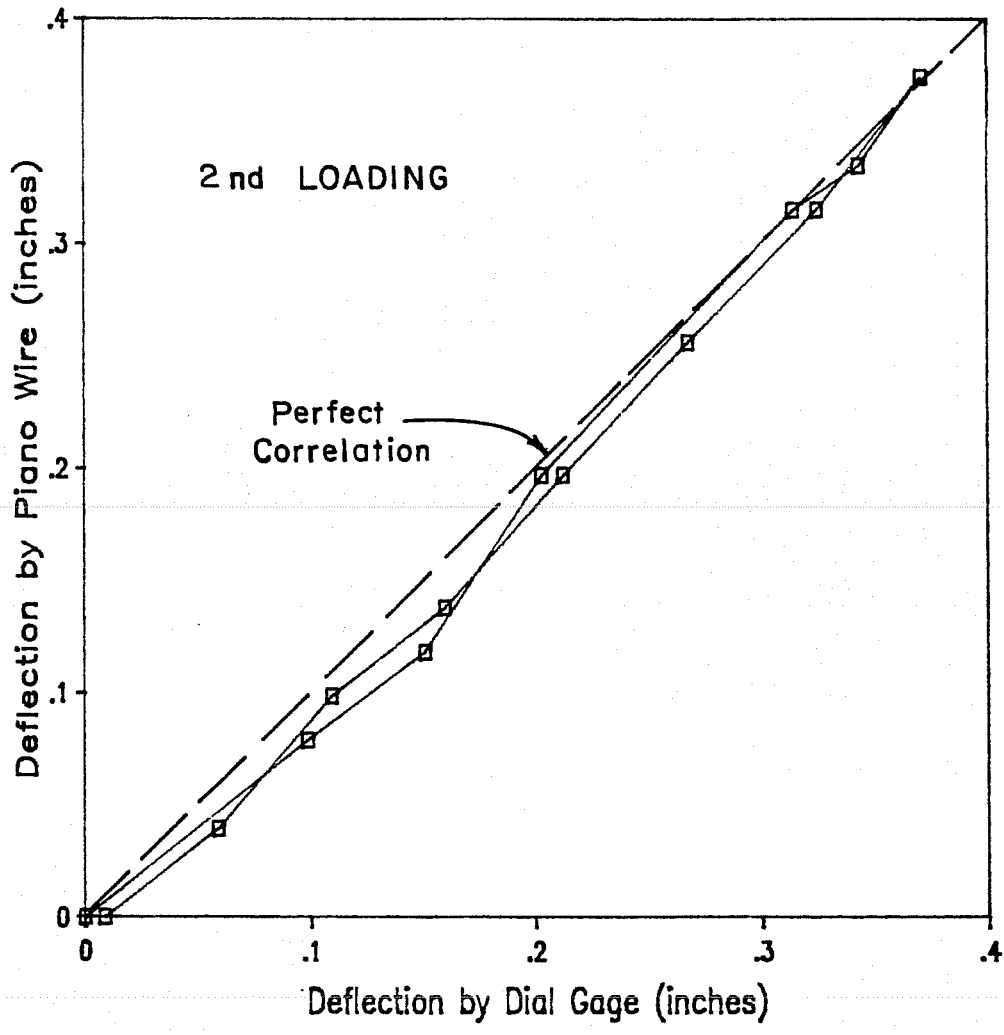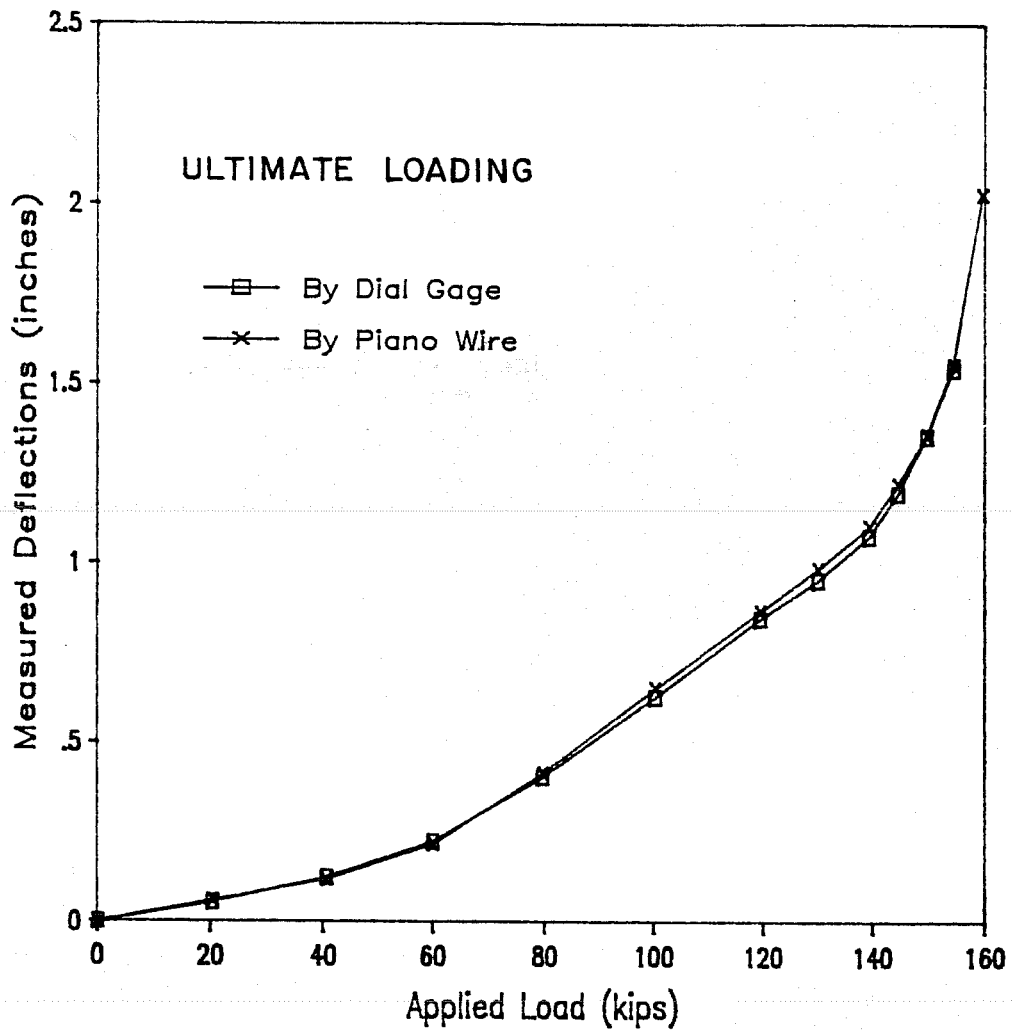
e) deflection vs. load for ultimate loading of laboratory
   beam

Fig. 2.10 Verification of Reliability of Base Line System for
           Monitoring Live-Load Deflections (cont'd)
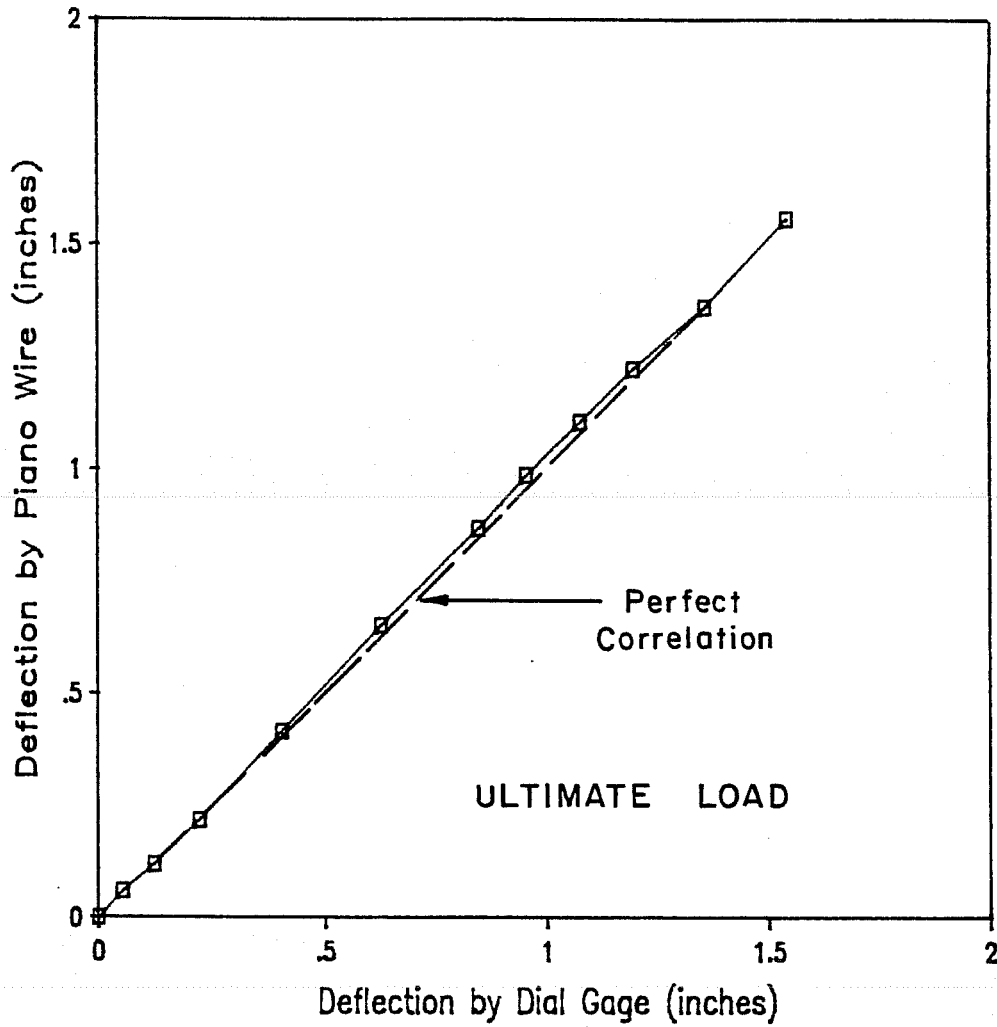
f) correlation of dial gage and piano wire determined
   deflections for ultimate loading of laboratory beam

Fig. 2.10   Verification of Reliability of Base Line System for
            Monitoring Live-Load Deflections (cont'd)

the laboratory 140 ft apart. A smaller diameter piano wire was then hung between the anchors.

Phase II involved the following:

1. determining the breaking strength of the piano wire,

2. developing a method of duplicating the shape of the hanging wire each time it was replaced or lost any initial tension, and

3. designing an anchorage device for the piano wire which would allow adjustment of the tension in the wire.

Step 1 was easily accomplished by performing a tension test on various gages of wire. The force which a wire resisted up to failure was of particular interest when "pretensioning" the wire during attachment to the specimen in the field. Since the load versus sag curve of a horizontal string, wire, or cable has a non-linear, catenary shape with decreasing sag for increasing tension it was desirable to stress the piano wire as high as possible to minimize error in duplicating the deflected shape. For this reason the piano wire was stressed to over 90% of its breaking strength. The 0.017 in. diameter wire used in the field work had a breaking strength of about 41 lbs. Thus, it was typically tensioned to more than 37 lbs in the field.

The base line system used by Pauw and Breen [35] had employed a hanging weight to maintain constant tension in the high strength wire. Since the piano wire system being developed

for this application was to be placed on the bottom flange of the instrumented girders it was undesirable to use a massive hanging weight as there would be very little clearance in the casting bed. If a hanging weight was used it would have required a temporary deflection monitoring system be employed during casting and storage of the girders as in the study made previously [35]. This was undesirable from the standpoint of instrumentation simplicity. Therefore, another method of maintaining the piano wire base line initial shape was developed.

Three methods of maintaining the piano wire shape were considered and tested:

1. the elongation method,

2. the torque method, and

3. the standard weight deflection method.

The elongation method proved unworkable because it was a very subjective method which would have required the determination of the amount of "prestress" with which the wire was initially pulled while attaching it to the anchors. Also, some way of determining how much wire was taken up at each end due to tightening would be necessary. Most detrimental of all was the fact that shrinkage, creep, and curvature induced girder shortening and lengthening would have invalidated the method.

The torque method was not a workable solution because of the possible variation in frictional resistance of the anchors

both during tensioning, due to increased shear force, and over time, due to corrosion. Also, since the range of torque which needed to be applied was so small (40 to 80 in.-lbs) fine tuning of the piano wire was not possible with this method.

After discarding the first two alternatives, a method was developed in which a small weight increment was attached to the wire at mid-span producing a deflection increment which could be duplicated from time to time by adjusting the wire's tension. This system is both rational and simple. The rationale behind the system is that the deflection of a horizontal wire at a specified location due to an applied load is directly related to the level of tension in the wire and thus to its sagging shape without the applied load. Figure 2.11 illustrates the procedure used to establish and maintain the level of wire tension by the standard weight deflection method.

Preparing an anchorage device for the piano wire was simple. A 1/2-in. diameter bolt, approximately 2-1/2 in. long was machined and drilled to have a 3/4-in. long by 1/8-in. deep recess in the shank along with a 1/8-in. diameter hole thru which the piano wire could be passed. The recess provided an area upon which to take up the piano wire during adjustment. The recessed bolt worked well as an anchorage device for the piano wire in the laboratory and in the field.

65
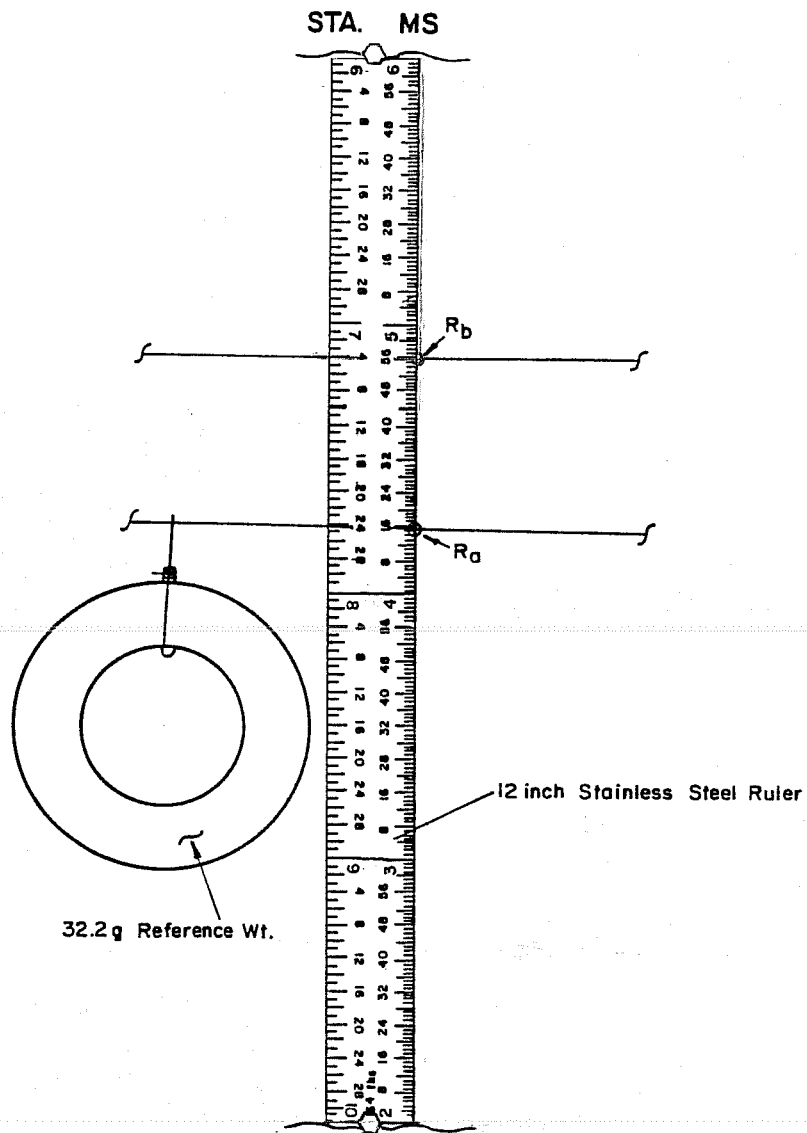
a)   calibration procedure

Fig. 2.11   Standard Weight Deflection Method of Establishing and
Maintaining a Fixed Reference Curve with High Strength
Wire
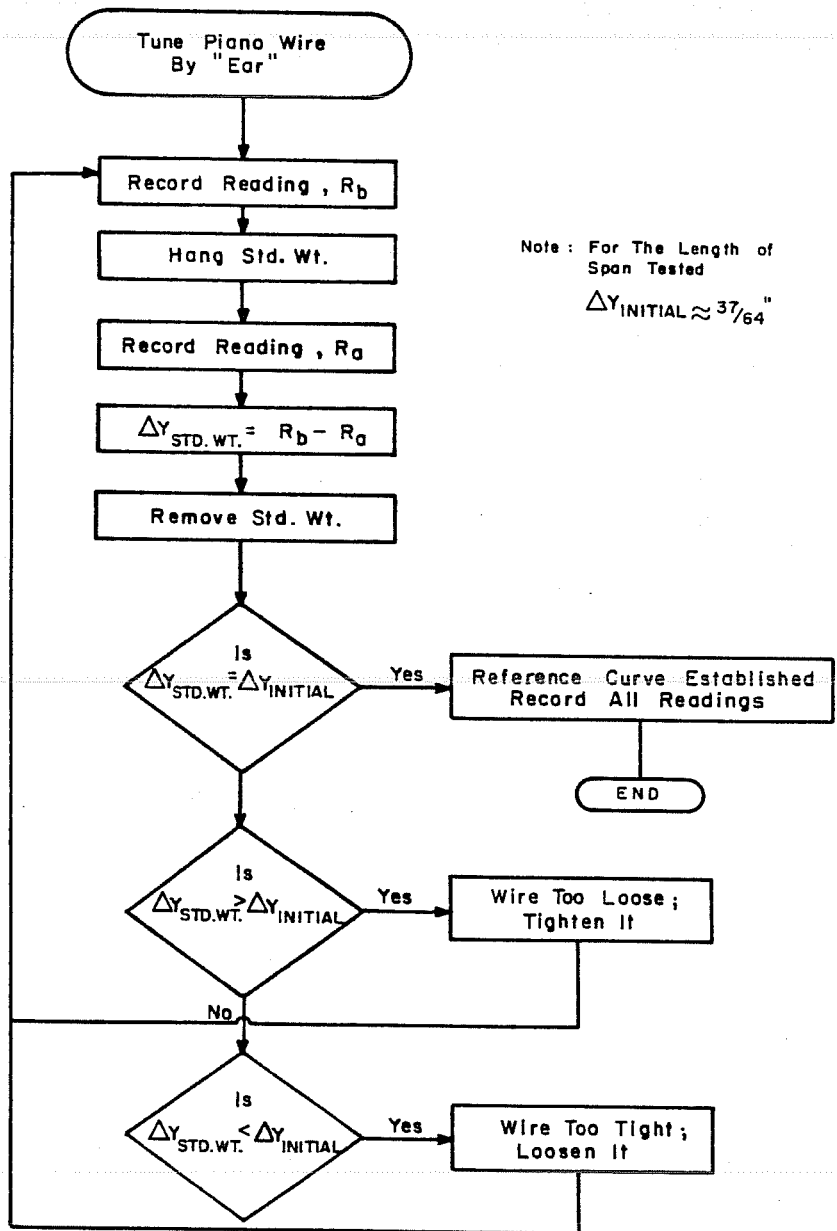
b) calibration operations

Fig. 2.11 Standard Weight Deflection Method of Establishing and
Maintaining a Fixed Reference Curve with High Strength
Wire (cont'd)

Fig. 2.12 Creep Test Loading Frame

2.6 Pilot Creep Test Series

Most of the material tests of companion specimens required in this investigation were well established, having either applicable standard methods, or standard testing apparatuses, or both. However, in the planning stages of the investigation there was some question as to the applicability of the standard method (as per ASTM) of determining the creep properties of the girder concrete for input into the analytical model. Also, test facilities had to be procured, erected, and placed before any tests could be performed. Consequently, a series of pilot creep tests was conducted to,

1. obtain familiarity with the testing procedures,

2. refine the test set-up procedures,

3. fabricate necessary test facilities, and

4. examine the suitability of ASTM Standard Method C512-76 for application to this field study.

Making use of available concrete from concurrent laboratory projects, enough cylinders were cast to perform five creep tests of two specimens each including unloaded control cylinders to compensate for shrinkage and temperature effects. The specimens, groups PA, PB, and PC were cast from three different concrete mixes within 32 days of each other in late winter and early spring of 1984. Two tests were performed on cylinders from group PA, one from group PB, and three from group

PC. Each test consisted of loading two stacked cylinders in a loading frame like that shown in Fig. 2.12. Cylinders PA1, PA2, PB1, PC1, PC2, and PC3 were loaded to 39%, 35%, 40%, 59%, 36%, and 52% of their measured compressive strength at age 18, 25, 28, 3, 7, and 7 days respectively.

The resulting creep coefficient versus time curves are shown in Fig. 2.13. Each curve represents the creep coefficients based on the average creep strains of two loaded cylinders using three equally spaced vertical gage lines with readings corrected for temperature and shrinkage effects. With the exception of the curve for PA1, all creep curves are consistent with those expected by creep theory which states that creep is proportional to the applied stress for a given age of loading as long as the applied stress is not greater than 50% of the strength of the concrete at the age of loading. It should be noted that the applied load was allowed to fluctuate as much as $\pm$ 4.9% and thus was not kept within 2% of the initial value for all tests as is recommended by ASTM C512-76 [8]. Whenever this requirement was exceeded the apparent creep coefficient is slightly lower or higher than the actual coefficient varying as the actual load is lower or higher than the initial load.

In these pilot tests, researchers were able to familiarize themselves with the testing procedures and fabricated enough creep frames to conduct the subsequent tests on concrete
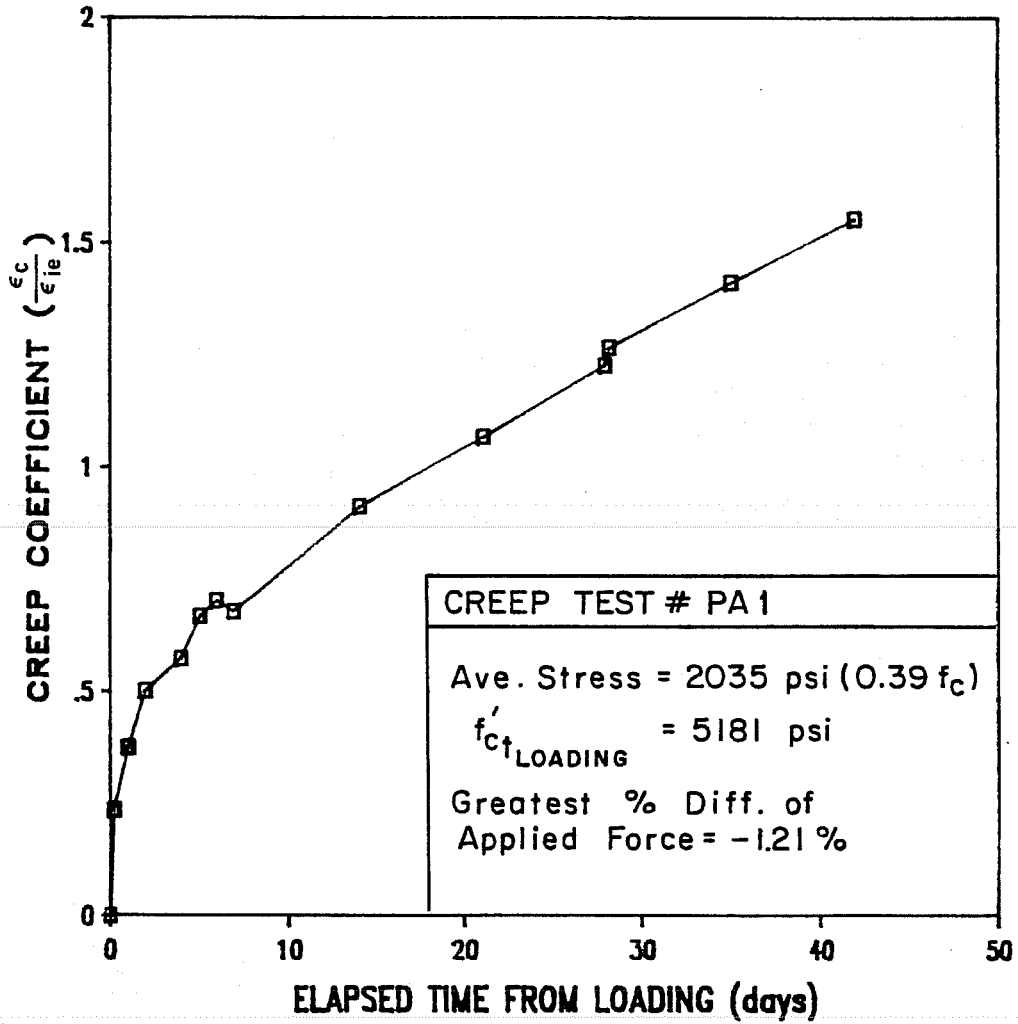
a) preliminary creep test no. PA1

Fig. 2.13 Creep Coefficient vs. Time Curves for Preliminary Creep
Tests

CREEP TEST # PA 2

Ave. Stress = 2295 psi (0.35 f_c)

$f'_{ct_{LOADING}}$ = 6472 psi

Greatest % Diff. of
Applied Force = 0.75 %
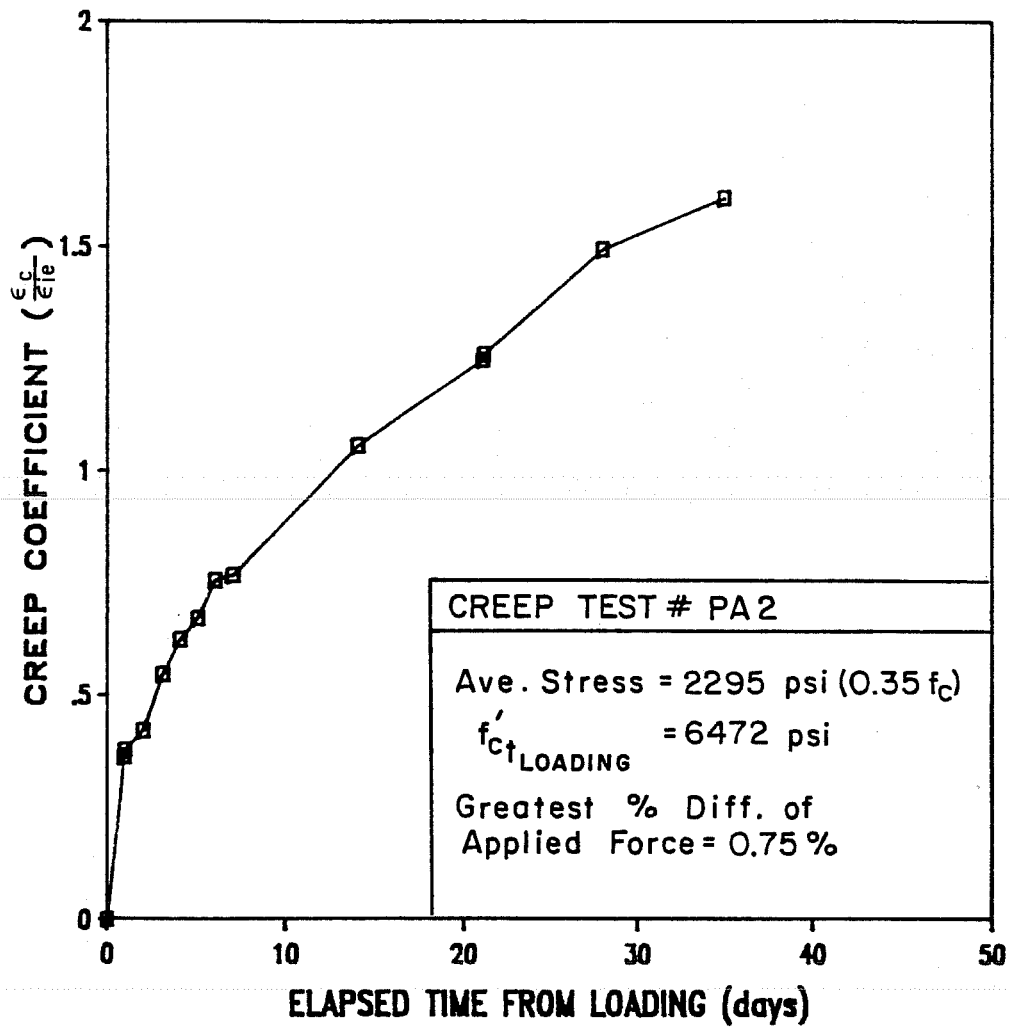
b) preliminary creep test no. PA2

Fig. 2.13   Creep Coefficient vs. Time Curves for Preliminary Creep
Tests (cont'd)

CREEP TEST # PB 1

Ave. Stress = 1837 psi (0.40 f_c)

$f'_{c_{t_{LOADING}}}$ = 4650 psi

Greatest % Diff. of
Applied Force = −3.63 %
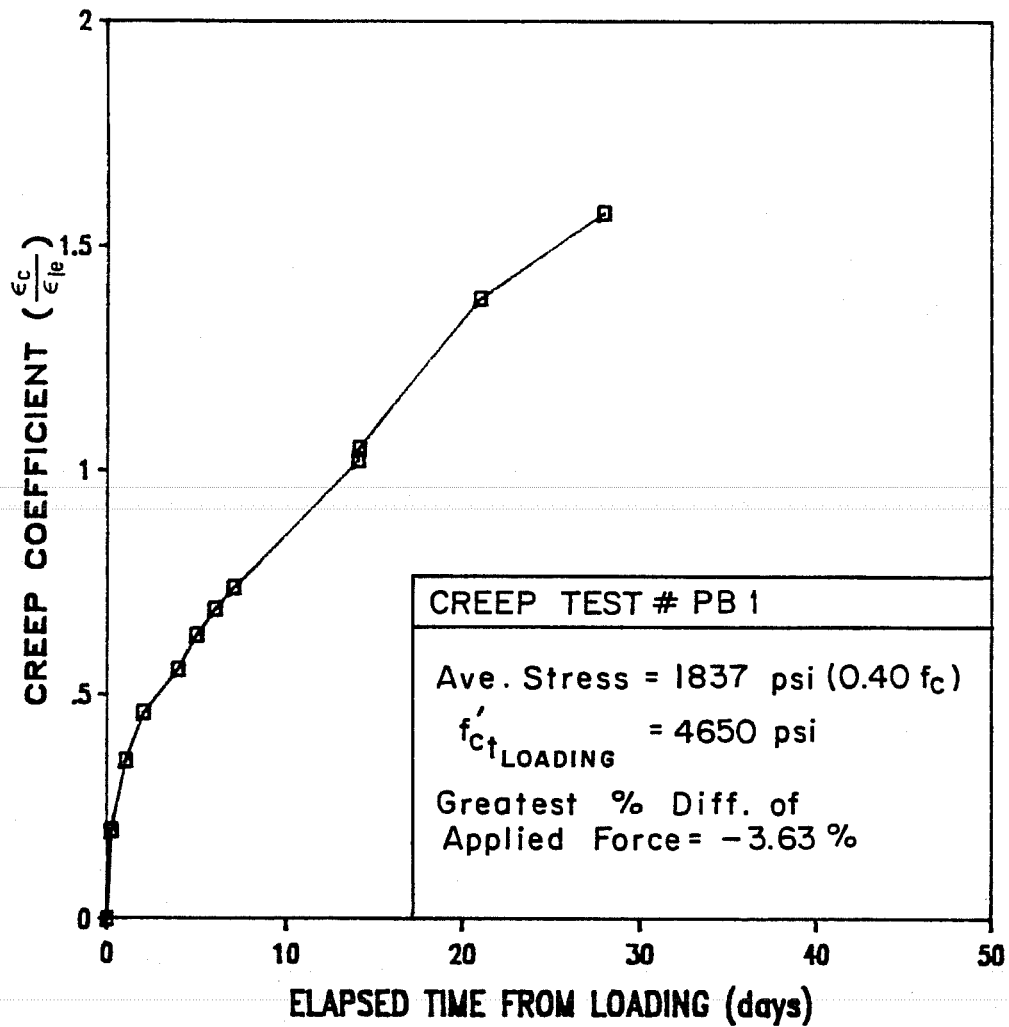
c) preliminary creep test no. PB1

Fig. 2.13 Creep Coefficient vs. Time Curves for Preliminary Creep
Tests (cont'd)
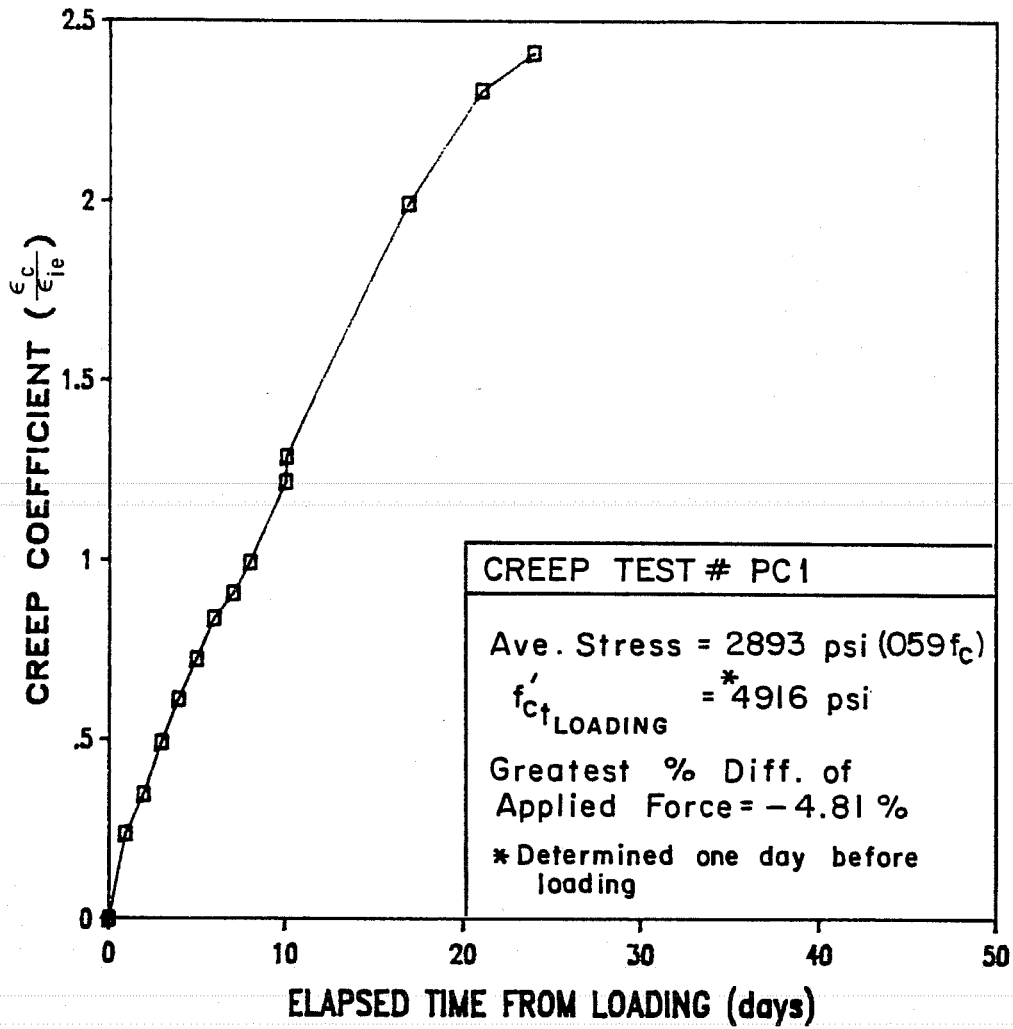
d) preliminary creep test no. PC1

Fig. 2.13 Creep Coefficient vs. Time Curves for Preliminary Creep Tests (cont'd)

CREEP COEFFICIENT $\left(\frac{\epsilon_c}{\epsilon_{le}}\right)$

ELAPSED TIME FROM LOADING (days)

CREEP TEST # PC2

Ave. Stress = 1837 psi (0.36 f_C)

$f'_{Ct}{}_{LOADING}$ = 5128 psi

Greatest % Diff. of
Applied Force = − 2.13 %
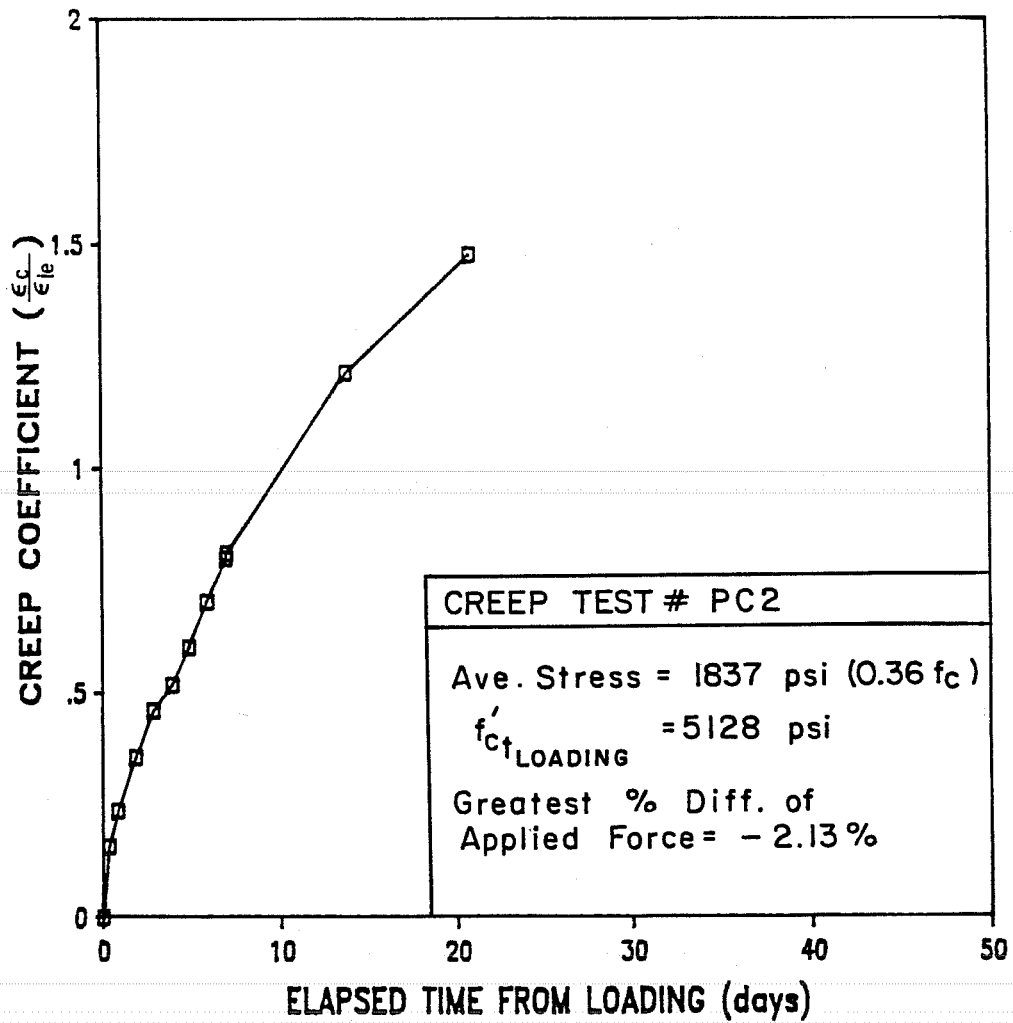
e)   preliminary creep test no. PC2

Fig. 2.13   Creep Coefficient vs. Time Curves for Preliminary Creep
Tests (cont'd)

CREEP TEST # PC3

Ave. Stress = 2667 psi $(0.52 f_c')$

$f_{c}'{}_{\text{LOADING}}$ = 5,128 psi

Greatest % Diff. of
Applied Force = −2.29%
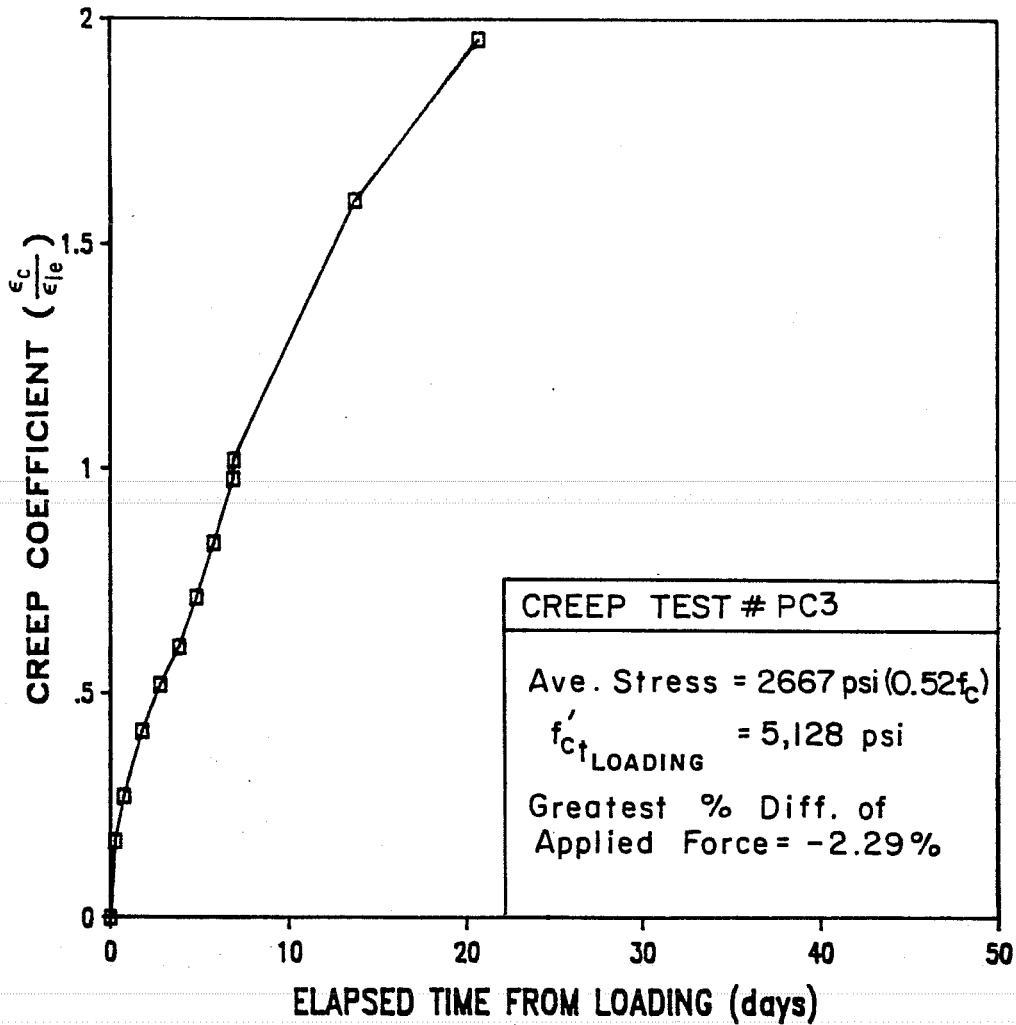
f) preliminary creep test no. PC3

Fig. 2.13 Creep Coefficient vs. Time Curves for Preliminary Creep
Tests (cont'd)

from the beams investigated in the field study. Also, a method
of setting up the test specimens in a way which minimized
eccentric loading and stress concentrations was developed from
the pilot tests. However, the suitability of ASTM Method C512-76
for application to the determination of time dependent
deformations of prestressed concrete structures was not veri-
fiable from these pilot creep tests.

The major drawbacks of ASTM Method C512-76 are:

1. Section 1.1 of Method C512-76 disclaims this standard
    from providing a means for calculating time-dependent
    deformations of reinforced or prestressed concrete
    structural members, and

2. ASTM Method C512-76 is limited to specimens of concrete
    under controlled conditions of temperature and relative
    humidity.

Therefore, the creep properties of the various
concretes used in this field investigation can only be
interpreted in light of the known conditions under which the
tests were conducted and comparison of these properties to the
creep properties of other concretes should be carefully
qualified.

C H A P T E R 3

FIELD WORK

3.1 General

As noted in Chapter 2, a distinctive characteristic of a field study is that other parties are involved, such as contractors or workmen who have little or no interest in the investigation. This presents both an opportunity and a burden. The opportunity is that of closing the necessary feedback loop from industry to research. The burden is the possible handicaps to the research due to conflicts because of the contractor's schedule and mode of operation. Often the contractor has no pecuniary incentive to modify his schedule and procedures to satisfy the needs of research. The research team and contractor should agree from the onset to give mutual cooperation and respect. Each should be willing to compromise when conflicts of interest arise so that both parties will "win" in the long run.

Fortunately, in this study the fabricator cooperated very well. This chapter discusses the field work and the fabricator's cooperation in that work.

3.1.1 Presentation Format.

Field work is presented in chronological order for a typical specimen casting. The particulars of specific castings are mentioned where they differed from the norm. Sufficient detail is given so that one

could repeat the investigation or benefit from the lessons
learned should similar future studies be made.

3.1.2 <u>Overview</u> <u>of</u> <u>Program</u> <u>of</u> <u>Field</u> <u>Investigation</u>. The
program of field investigation was divided into the following
parts:

1. Direct monitoring of beam vertical deflections;

2. Direct monitoring of surface concrete strains;

3. Monitoring of prestress losses (except relaxation
   losses) using electrical resistance strain gages; and

4. Monitoring of internal concrete temperatures as well
   as external ambient temperatures.

The instrumentation monitoring locations are 2.0 ft for
station END, 32.2 ft for station QP, and 63.4 ft for station MS
from the south end of each specimen as it was oriented in the
casting yard. The external instrumentation hardware was placed
on only one side of each specimen. Girders placed side by side
in the bridge had instrumentation facing one another, thus
allowing access to two specimens' monitoring stations at a time.
Four girders per bridge were instrumented with full or partial
instrumentation.

Figure 3.1 is the layout of a typical casting of
instrumented girders along with elevation views of the specimens
as cast in both positions 1 and 2. The elevation views show the
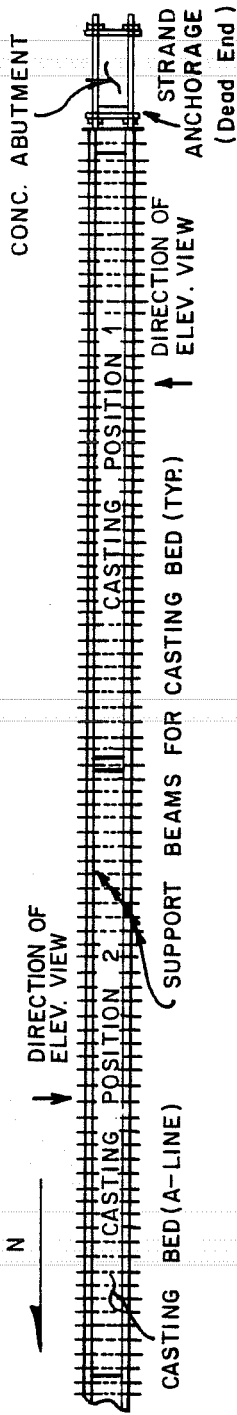
a) plan--casting positions 1 and 2
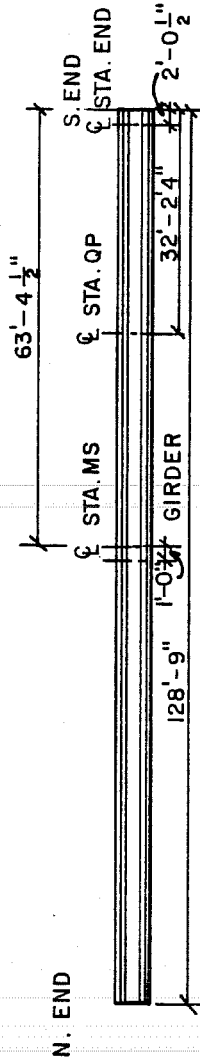
b) elevation--casting position 1 (looking east)
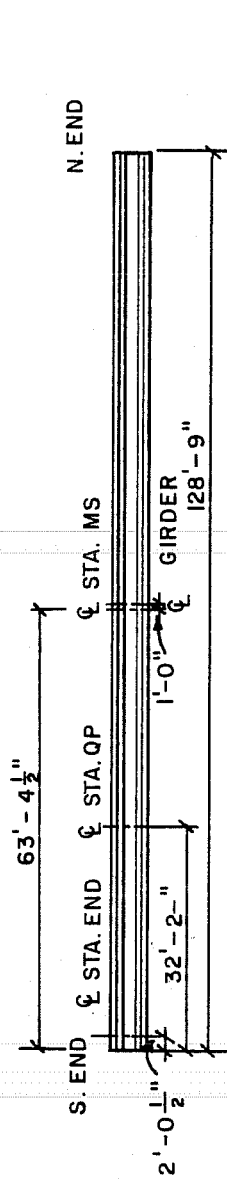
c) elevation--casting position 2 (looking west)

Fig. 3.1 General Layout of Typical Girder Instrumentation and Casting Orientation

locations of the various monitoring stations. Instrumentation location details are given in Fig. 3.2.

Assuming symmetry, only one quarter point (QP) of each girder was instrumented. This greatly reduced the amount of field work required. Holes necessary for attaching inserts to the forms were pre-drilled in the forms prior to the first casting. Note that the mid-span (MS) monitoring stations were placed on a 1 ft offset to avoid conflict with the mid-span diaphragms.

While eight girders were instrumented, only four girders included strain gages on the strands and thermocouples in the concrete. The instrumented girders designated by both the erection marks and appropriate research identification are listed in Table 3.1.

Figure 3.3 shows the internal instrumentation of fully instrumented girders at station MS for each strand pattern used. For the higher strand stress level design (i.e., the design with only 46 strands) strain gages were placed on draped strands causing the gages to actually be at different levels at station QP and at station MS.

Table 3.2 lists as-built information for each specimen cast. This information may be used as input data for the analytical model.
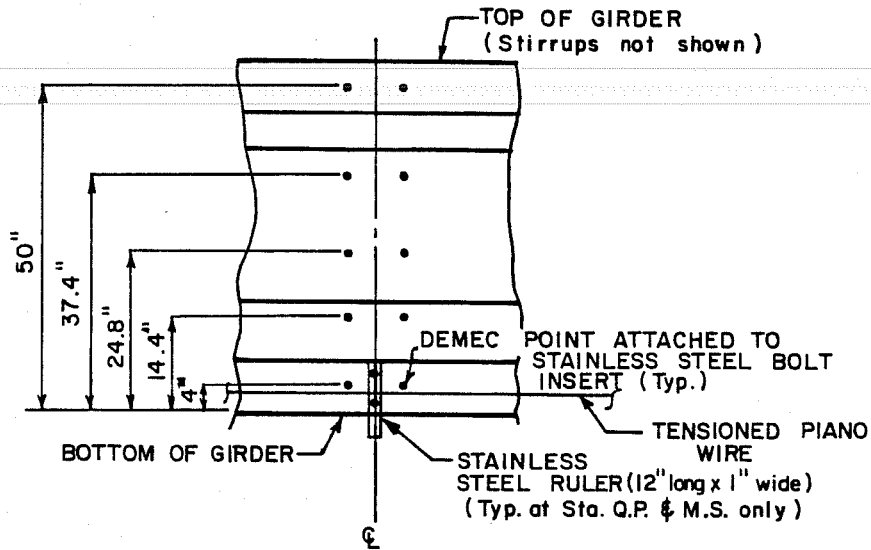
a) detail--typical monitoring station
(internal instrumentation not shown)
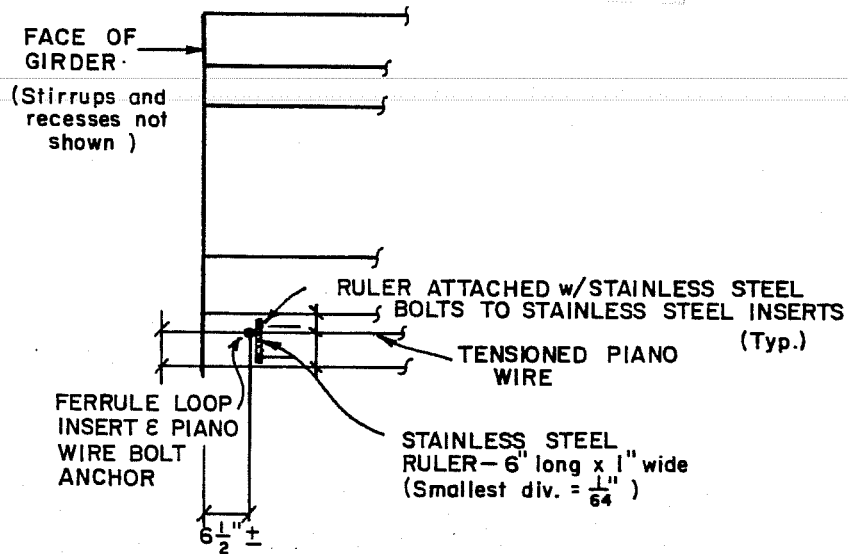
b) detail--north end -casting position 1 (as shown)
-casting position 2 (reversed)
--south end -casting position 2 (as shown)
-casting position 1 (reversed)

Fig. 3.2 Details of External (Mechanical) Girder
Instrumentation

TABLE 3.1   Instrumented Girders

Erection Mark	Research ID[1]	Date Cast	Bridge[2]	Instrumentation
B18A	L-I1	06/25/84	RML	Full
B18B	L-I2	06/25/84	RML	Partial
B18	L-01	07/09/84	RML	Full
B18	L-02	07/09/84	RML	Partial
B2	H-01	10/02/84	LML	Full
B2	H-02	10/02/84	LML	Partial
B2B	H-I1	11/12/84	LML	Full
B2A	H-I2	11/12/84	LML	Partial

[1] The following is an explanation of the elements of the research ID:

L = the strand stress level upon stressing of $0.70f_{pu}$

H = the strand stress level upon stressing of $0.75f_{pu}$

I = a girder placed near the middle (or interior) of the bridge

0 = a girder placed near the edge (or outside) of the bridge

1 = a girder which was cast in casting position 1

2 = a girder which was cast in casting position 2

[2] RML and LML stand for the right and left main lanes respectively
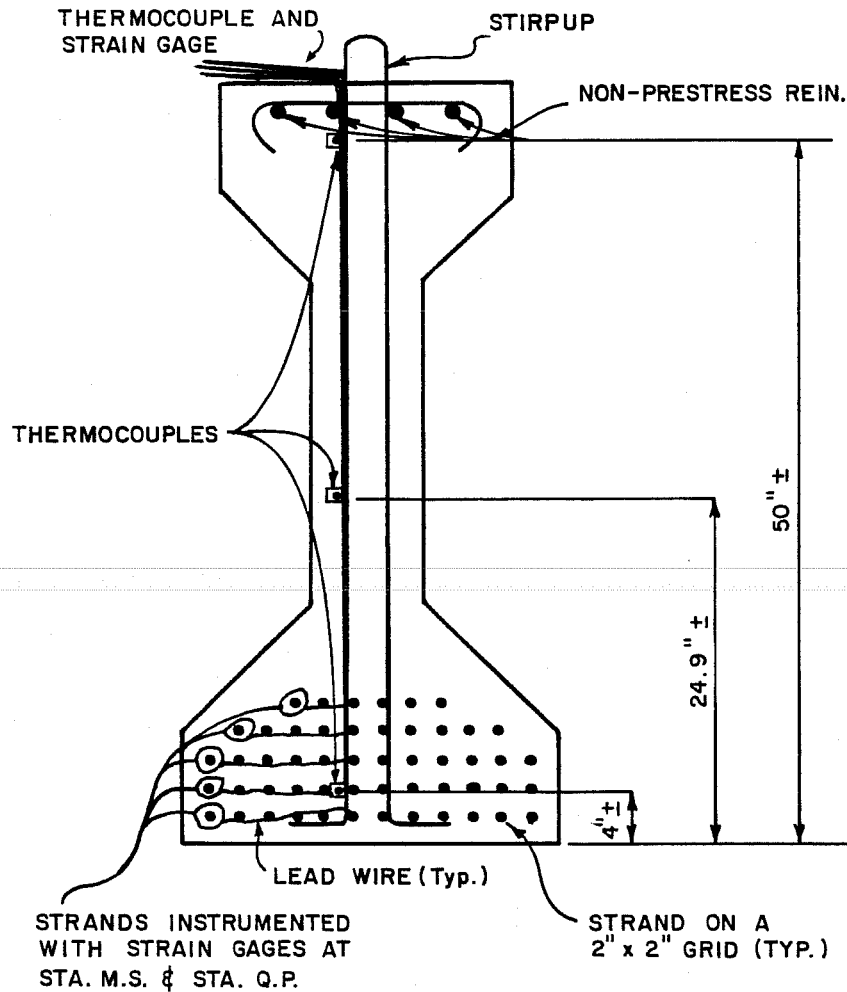
a) all electronic instrumentation for low strand stress level
   girders

Fig. 3.3   Section Details Showing Internal Electronic Instrumenta-
           tion Placement

STIRRUP

NON-PRESTRESSED
REINFORCEMENT (#11
BARS)

STRANDS INSTRUMENTED
WITH STRAIN GAGES AT
STA. M.S. ₵ STA. Q.P.

STRAND ON A
2" x 2" GRID (TYP.)
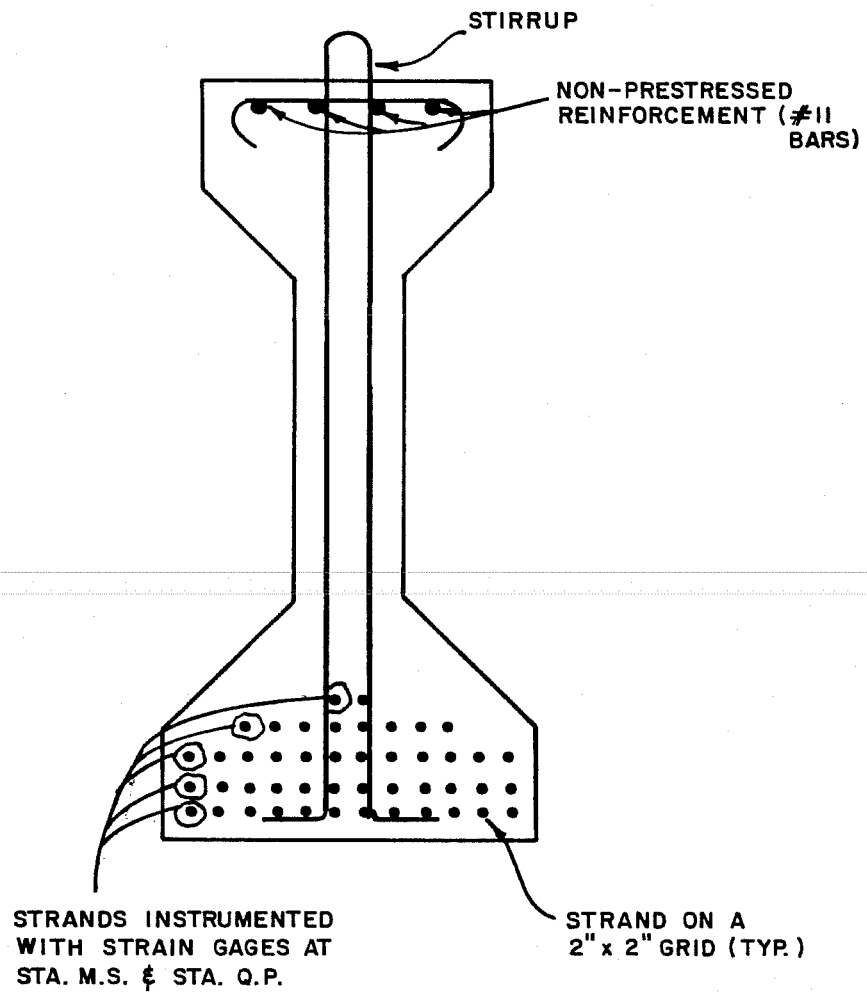
b)   instrumented strands for high strand stress level girders

Fig. 3.3   Section Details Showing Internal Electronic Instrumenta-
tion Placement

TABLE 3.2 As-Built Strand Data

Specimen	L-I1	L-I2	L-01	L-02	H-01	H-02	H-I1	H-I2
No. of Straight Strands	42	42	42	42	36	36	36	36
No. of Draped Strands	10	10	10	10	10	10	10	10
North End to Drape Pt. (ft)	57.16	57.42	57.54	57.38	57.10	------	57.58	57.33
South End to Drape Pt. (ft)	57.12	56.71	57.40	57.35	55.92	------	57.58	57.33
Overall Length (ft) (measured)	128.72	128.73	128.71	128.73	------	------	------	------

3.2 Form Preparation

To place the mechanical inserts into the specimens, it was necessary to drill 17/64-in. diameter holes in the forms. The fabricator gave full cooperation and all inserts were placed within 1 in. of their target locations.

3.3 Strand Installation and Stressing Operations

The actual girder prestress force developed is an important factor in the production of serviceable bridge girders. The procedure used to develop this force may vary from one fabricator to another. Pertinent details of the strand installation and stressing procedures are included here to document strand stresses.

3.3.1 Prestressing Strand Used. The original design of all girders for the right main lane bridge called for exclusive use of normal stress relieveed seven-wire strand while the left main lane girders were to be fabricated with low-relaxation seven-wire strands. This was specified so that a direct comparison could be made of the effects of low relaxation strands on girder behavior. As soon as the field work was begun it was discovered (Fig. 3.4) that the fabricator planned to use low relaxation strands for all girders since the low-relaxation strand met or exceeded the normal stress relieved strand specifications in all requirements. Thus, the normal stress

a) FWC 0.5 in. 270K low-relaxation strand
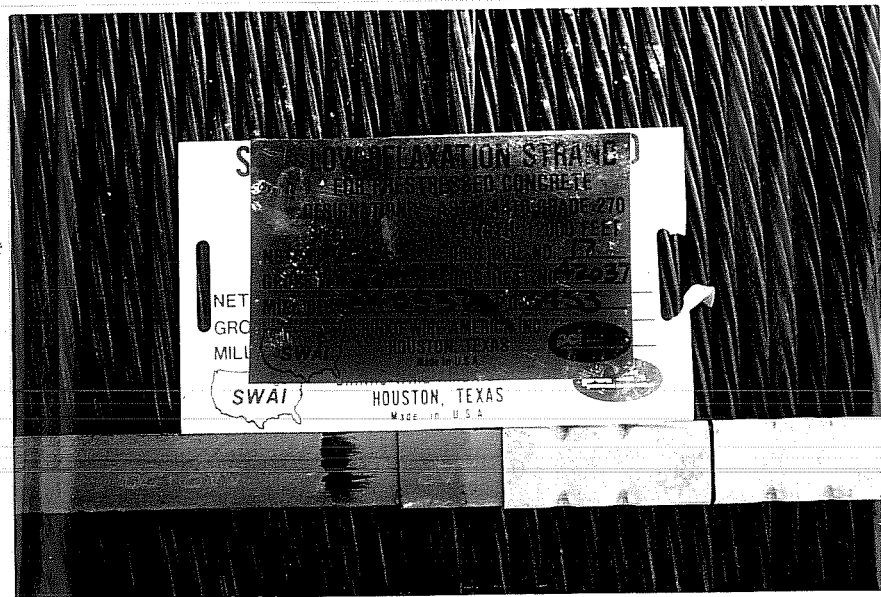
b) SWAI 0.5 in. 270K low-relaxation strand

Fig. 3.4   Type of Prestressing Strand Used in Specimens
Investigated

relieved strand requirement for the right main lane girders was legally bypassed by the contractor through substitution of low-relaxation strands. This was unfortunate as it made impossible one of the primary proposed objectives of this investigation. After detailed consultation with the sponsor, it was decided that the program should continue with the major variable being the comparison of the effects of using low-relaxation strand at two different stress levels, 0.70 F_{pu} and 0.75 F_{pu} respectively.

Strand used in the fabrication of the field specimens was purchased by the fabricator from two suppliers, Florida Wire and Cable Co. of Jacksonville, Florida (Fig. 3.4a) and Shinko Wire America Inc. of Houston, Texas (Fig. 3.4b). The strand was shipped in packs (coils) weighing approximately 6250 lbs and containing about 12,000 lineal ft of 1/2-in. strand each.

3.3.2 <u>Placement of the Prestressing Strand.</u> The coils were set in racks and the strands threaded through the appropriate holes in the header forms. The strands were then attached in groups of about 10 each to a pulling device and stretched some 508 ft to the "live" or stressing end abutment. At the "dead" or holding end of the casting bed the strands were cut, passed through holes in the "dead end" anchor plates and chucked. At the "live" end the slack in each strand was taken up and the strand initially tensioned using a pair of come-alongs attached to a load measuring device to about 2000 lbs. Drape

strands were placed and the header forms pulled to their final positions. Frames for holding up the draped strands were placed at the ends of the girder line and between girder header forms. The appropriate strands were looped over the hold-up hardware and the strands straightened and tensioned to 2000 lbs each. This operation completed the strand placement process.

3.3.3 Stressing of Prestressing Strands.

The stressing operation was performed by jacking between the stressing abutment bearing and pulling plates using two hydraulic rams (a large ram for stressing straight strands and a smaller ram for stressing draped strands). The plates between which the rams were placed rested on greased rails. The Norcath Multiple-Strand Stressing System rams had been calibrated and certified. The total load applied to each set of strands was based on the pressure indicated by the gages on the hydraulic pump. The parameter used to control stressing was not the ram pressure but rather the measured strand elongations. The desired elongation had been previously marked on the threaded rods used to transfer the force to the strand stressing plates. When the marked portions of the rods were pulled to the backside of the reference abutment bearing plates, the lock nuts were tightened down, the ram pressure noted and the hydraulic rams unloaded.

Table 3.3 summarizes the jacking loads reported by the State inspectors for the specimens fabricated. The loads are

Table 3.3 Strand Load Data

Specimens Fabricated	L-I1, 2	L-01, 2	H-01, 2	H-I1, 2
Design Strand Load	28,910 lb	28,910 lb	30,982 lb	30,982 lb
Average Strand Load Based on Actual Ram Pressure (Straight Strands Only)	29,119 lb	28,950 lb	32,004 lb	32,186 lb
Average Strand Load Based on Actual Strand Elongations (Deflected Strand Only)	28,939 lb	28,736 lb	31,137 lb	31,912 lb
Indicated Strand Load Upon Stressing (Based on Load Cells)	–	25,500 lb	29,807 lb	–
Indicated Strand Load Upon Release (Based on Load Cells)	–	24,250 lb	30,540 lb	25,830 lb
Indicated Strand Wire Load Upon Release (Based on Strain Indicated by Attached SR-7 Gage)	–	–	–	30,312 lb
Strand Modulus of Elasticity (Based on Mill Test Reports)	28,900 ksi	28,000 ksi	28,600 ksi	28,000 ksi
Wire Modulus of Elasticity (Assumed)	–	–	–	30,000 ksi

average load per strand for both the draped and straight strands.
The loads based on elongations assume infinitely stiff abutments
which is reasonable considering the size of the abutments. Also
listed for some of the specimens are the strand loads as per the
load monitoring system installed, as discussed later, in order to
independently check the jacking forces.

3.3.4 Depressing Draped Strands. Stressing of the
draped and straight strands were performed simultaneously but
independently using two separate hydraulic systems. This was
necessary because the indicated draped strand elongations were
not the same as those of the straight strand due to the
additional strand length required by the draped pattern. In some
prestressing plants the draped strands are held down while
stressing or pulled up after stressing. In this plant the draped
strands are depressed after stressing.

No matter how it is performed the draping of
prestressing strands is a dangerous operation. In fact, between
the fabrication of the last two sets of specimens a workman was
fatally injured when a hold-down chuck failed, releasing the
draped strands with their tremendous kinetic energy. This
unfortunate event stalled the fabrication of the last two
specimens. After a second hold-down unit failed the following
week without causing injury, steps were taken to ensure the
safety of all parties involved. The problem was traced to a

faulty half-size chuck used to passively lock the hold-down hardware in place. A regular full-size chuck was substituted for the "half" chuck. An extra heavy high strength chain was placed around the strand and casting bed in hopes that it would dissipate some of the energy should the hold-down systems fail again. In this type of accident, the victim could very easily have been one of the research team. The researchers spent a lot of time in intimate contact with the stressed strands while installing instrumentation. The failure occurred without warning.

The draped strands were slowly depressed using a special twin-shaft h hydraulic ram. Although this operation presents one of the greatest apparent dangers during the stressing procedures, the accident which claimed the life of the worker occurred long after the strand depressing operation had been completed and without any warning. The only event which seemed to have set off the explosive failure was the bending over of the hold-down strand by the worker in order to tie it off to one of the straight strands, which was standard procedure (see (Fig. 3.5).

3.3.5 Independent Monitoring of Strand Jacking Forces. After the first casting it was decided to place load cells on two of the prestressing strands in order to independently monitor the applied jacking force at the dead end of the bed during the
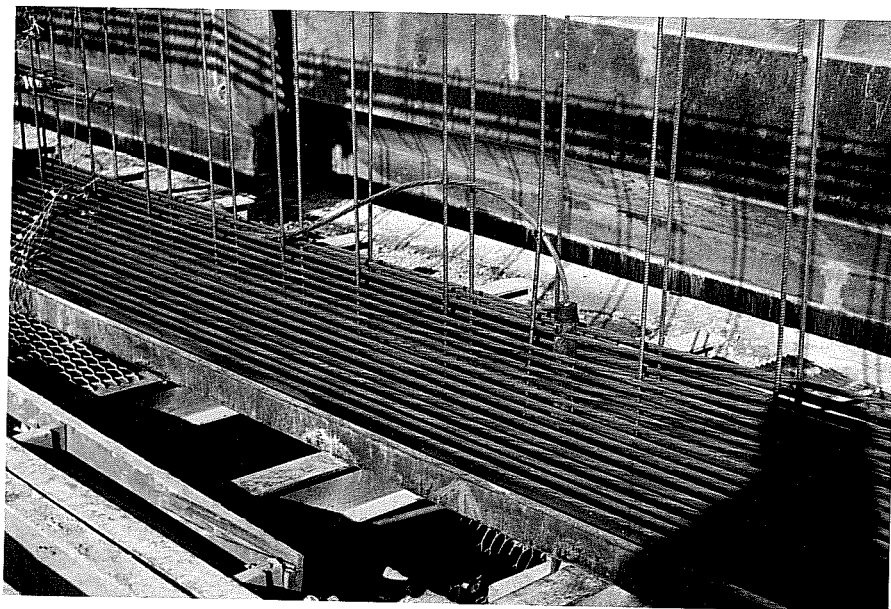
Fig. 3.5 Hold-Down Hardware for Draped Strands

stressing and release (transfer of prestress) operations of subsequently fabricated specimens. Two special "chairs" were fabricated by welding an approximately 10- to 12-in. long, 1.875-in. OD extra heavy structural pipe to a 4- x 4- x 1-in. steel bearing plate. These chairs provided seats for the load cells--which had a 4-in. diameter bearing area--away from the surrounding strand chuck. The decrease in stress caused by the 15-in. or so of additional strand length was negligible for the 6103 in. original strand length used. This loss turns out to be less than 1/5 the magnitude of the seating loss of a typical strand.

On the day of the stressing operation calibrated load cells were placed on two of the strands using the specially fabricated chairs. The load cells were attached through a switch and balance unit to a strain indicator before application of any force to the strands.

This system was used on specimens L-01, L-02, H-I1, and H-I2. No such system was available at the time of casting of the first specimens, L-I1 and L-I2, and only one load cell was used for specimens H-01 and H-02.

3.4 Attachment of Inserts

On the day following the initial strand stressing operation the installation of the four beam instrumentation

systems was begun. The inserts for the mechanical instrumentation were loosely attached to the forms. Later, the inserts were tightened so that they would no be vibrated loose during the mechanical vibration of the concrete. Two or three of the ferrule loop inserts which served as attachments for the piano wire anchors had to be removed during the form setting operation and were replaced once the appropriate form had been set in place. This was necessary because the forms were slid longitudinally along the bed next to the placed reinforcement and the loop portion of the insert was positioned between the second and third levels of strands.

3.5 Installation of Electronic Instrumentation

While the mechanical inserts were being loosely attached to the Type IV forms, installation of strain gage instrumentation was begun. Electrical resistance strain gages were applied to the selected strands in pairs at stations QP and MS of the girder to be fully instrumented. The gages were applied at the levels noted in Table 3.4. Standard procedures were employed in attaching the gages to the strands. However, because the gages were placed by hand without the aid of clear plastic tape, perfect alignment of all gages along the axis of the strand wires was not achieved.

TABLE 3.4 Strand Strain Gage Placement

Strain Gage Desig.	For L-I1 Level (in.)	For L-I1 Switch Channel	For L-01 Level (in.)	For L-01 Switch Channel	For H-01 Level (in.)	For H-01 Switch Channel	For H-I1 Level (in.)	For H-I1 Switch Channel
QP2N	2	#1	2	#1	2	#1	2	#1
QP2S	2	#2	2	#2	2	#2	2	#3
QP4N	4	#3	4	#3	4	#3	4	#4
QP4S	4	#4	4	#4	4	#4	4	#5
QP6N	6	#5	6	#5	6	#5	6	#6
QP6S	6	#6	6	#6	6	#7	6	#7
QP8N	98#7	8	#7	8	#8	8	#9	
QP8S	8	#8	8	#8	8	#9	8	#10
QP10N	10	#9	10	#9	25-7/8	#10	28-5/8	#11
QP10S	10	#10	10	#10	25-7/8	#11	28-5/8	#12
MS2N	2	#1	2	NA	2	#1	2	#1
MS2S	2	#2	2		2	#11	2	#2
MS4N	4	#3	4		4	#3	4	#3
MS4S	4	#4	4		4	#4	4	#4
MS6N	6	#5	6		6	#5	6	#5
MS6S	6	#6	6		6	#6	6	#6
MS8N	8	#7	8		8	#7	8	#7
MS8S	8	#8	8		8	#8	8	#8
MS10N	10	#9	10		10	#9	10	#9
MS10S	10	#10	10	NA	10	#10	10	#10

Once the gages were affixed to the strands, the gage
lead wires were lifted from the strand surface and a small ball
of Barrier E, a gumming insulating material, was placed
underneath. This provided insulation between the leads
themselves and between the leads and the strand. At this point
the gages were checked with an ohmeter to ensure that they were
functioning properly. Previously prepared two lead wires,
approximately 30 ft long, were soldered to each gage and threaded
through the strands and up the nearest stirrup. The free end of
each lead wire was labeled as to the gage it served. A liberal
number of plastic ties were used to tie the lead wires to each
strand they crossed as well as to the stirrup. This was done to
ensure that the wires and gages would not be damaged by being
pulled loose during the mechanical vibration of the concrete.

Next, the gages, lead connections, and surrounding
surface were painted with a white insulating material called M-
Coat, which was allowed to dry for at least two hours before
strips of Barrier E were wrapped around the gages to protect
them. While the M-Coat was drying the lead wires were bundled,
wrapped with duct tape and attached to the calibrating switch
boxes. Connection to the strain indicator was then made and the
readings of all gaged channels of the switch box were checked for
stability. In some cases the readings were not found to be very
stable due to problems with a particular channel on the switch in

the calibrating switch box. Table 3.4 lists the corresponding switch box channels for each applied strain gage for all fully instrumented specimens.

If time permitted, several readings of the strain gages were taken on the day of installation to further assess the relative stability of the strain gage system. Such recorded readings could be used to determine possible deviations of strains from their measured values. The strain gage system used was not temperature compensating.

The last step of the installation of the electronic instrumentation was the placement of the thermocouple wire. For all but the first casting the thermocouple wires, as well as the strain gage lead wires, were made up in the laboratory prior to the installation period. This preparation greatly accelerated the installation process. Labeled thermocouple sets were attached to the stirrups at all three instrumentation stations.

Figure 3.6 shows a typical monitoring station with all electronic instrumentation installed prior to the placement of the remaining stirrups. Note that both the calibrating switch box and the ends of the thermocouple wires with connectors were placed in a plastic bag to protect them from direct moisture. The switch boxes were waterproofed before installation but precautions were taken to further protect the lead wire connections from the weather.
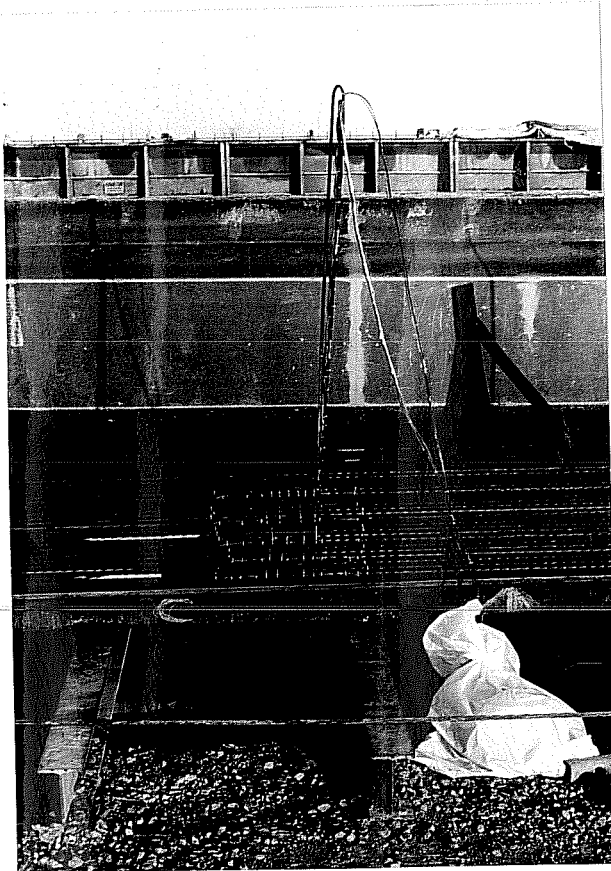
Fig. 3.6 Typical Monitoring Station Immediately after all
          Electronic Instrumentation Was Installed

3.6 Fabrication, Casting, and Remaining Instrumentation

Procedures

Two days after the gage and insert installation procedures, fabrication of the girders was continued as the stirrups and end steel were placed. Except for beams H-01 and H-02, concrete was placed on the third day after strand stressing. On the H-01 and H-02 specimens, the casting operation was delayed until the fourth day. Because these specimens were cast early in the morning of the fourth day and released the following morning, they were almost 1/2 day older at release than those specimens cast late on the third day and released early on the fourth day.

During the casting operation, standard 6-in. diameter concrete cylinder specimens were made for the subsequent material testing to be performed in Austin. Enough cylinders were made from random batches for each casting to allow creep, shrinkage, compressive strength and modulus of elasticity tests to be performed periodically. The total number of cylinders made varied from casting to casting but averaged about 32 each. Samples of prestressing steel were also cut directly from the coils used for each set of specimens fabricated so that laboratory tests could be performed. Table 3.5 is a summary of all material samples collected. No samples of passive reinforcement were obtained.

TABLE 3.5   Concrete Slump or Strand Designation for Material
            Samples Collected

	L-I1&2	L-O1&2	H-O1&2	H-I1&2
Total N	33 ea	~36 ea	~30 ea	28 ea
Batch Selected:				
1st	7 in. ~11 ea	2-1/4 in. ~9 ea	8-7/8 in. ~10 ea	7-1/4 in. 14 ea
2nd	4" ~11 ea	5-1/2" ~9 ea	8-1/2" ~10 ea	9-1/4" 14 ea
3rd	6" ~11 ea	8-3/4" ~9 ea	7-1/2" ~10 ea	not made
4th	not made	9" ~9 ea	not made	not made
Strand Supplier	FWC	SWAI	FWC	SWAI
Bin:				
#1	Coil # 371851	Heat 42048 Coil #17	Heat 16304 Coil #433202	Heat 42111 Coil #19
#2	Coil # 371973	Heat 42048 Coil #9	Heat 42080 Coil #42080	Heat 42111 Coil #17
#3	Coil # 371992	None	Heat 15278 Coil #418921	Heat 42111 Coil #16
#4	None	Heat 42048 Coil #10	Heat 16304 Coil #433342	Heat 42095 Coil #28
#5	None	Heat 42048 Coil #8	Heat 16304 Coil #433343	Heat 42111 Coil #20
#6	None	Heat 42048 Coil #14	Heat 16304 Coil #433331	Heat 42111 Coil #21
#7	None	Heat 42048 Coil #20	Heat 16304 Coil #433233	Heat 42111 Coil #22
#8	None	Heat 42048 Coil #24	Heat 16304 Coil #433203	Heat 42095 Coil #34 & 27

On the day following the casting operation release cylinders were broken to determine if the girder concrete had developed sufficient strength to allow the prestress force to be safely transferred. Specified release strengths for the lower stress level and higher stress level designs were 5270 psi and 5025 psi respectively. Table 3.6 contains the averages of the release cylinder breaks for each casting along with the age of the release cylinders when they were tested. The cylinder breaks indicate that release strengths were obtained within 24 hours.

Once it was determined that the concrete had achieved sufficient strength to allow the transfer of the prestressing force to the girders, the forms were prepared to be removed. All bolts used to secure the mechanical hardware to the forms were removed early on the day of release to allow the forms to be removed without damage to the inserts. Unfortunately, for beams H-01 and H-02 the form stripping crew began removing the form ties late on the day of casting, because the casting operation had been completed earlier that morning. This resulted in most of the bolts holding the inserts to the forms having their heads sheared or popped off.

As soon as the first form was removed installation of the necessary mechanical instrumentation was begun. This time period, which lasted from 40 to 60 minutes, was the most critical period of the investigation of each pair of specimens. It

TABLE 3.6   Concrete Strength at Release

	For L-I1&2	For L-01&2	For H-01&2	For H-I1&2
Casting Date	06/25/84	07/09/84	10/02/84	11/12/84
Time Casting Begun	2:30pm	4:45pm	7:30am	2:00pm
Time Required to Complete Casting	3 hrs.	2 hrs.	2 hrs.	2-1/4 hrs.
Release Date	06/26/84	07/10/84	10/03/84	11/13/84
Time of Release	~2:20pm	~10:45am	~10:45am	~10:45am
Avg. Release Cylinder Break (psi)	5437	5427	6694	5505
Age of Release Cyls. (hrs)	20-1/2	13	22	15-1/2

required close communication between the research team and the release crew in order to ensure that accurate initial readings were taken for all systems prior to release (i.e., transfer of prestress). This was achieved for all specimens except L-I1 and L-I2. For these two specimens, which were the first specimens cast, the release crew began to transfer the prestress force before all the instrumentation systems had been completely monitored. Fortunately, initial "zero level" readings were obtained for the deflection monitoring systems of these two specimens. As soon as it was recognized that the prestress force was being transferred prematurely, appropriate action was taken to stop the release crew and the supervisor was informed of the unacceptability of transferring the prestress before the research team had completed all initial readings. Upon subsequent castings the release crew gave the research team their full cooperation. The effect of this error upon the reported results is that the initial measured strains of the concrete surface are slightly smaller in absolute value than the actual strains were. Subsequent measured strains are also in error by the amount of unmeasured strains for these girders only.

Operations required to complete the instrumentation installation were:

1.   Attach all 1/4-in. stainless steel bolts to inserts for mechanical strain gage points.

2. Glue all mechanical strain gage points to these bolt heads with epoxy.

3. Bolt stainless steel rulers to bottom flange inserts at station QP, MS and at the ends of the girders next to the piano wire anchors.

4. Attach adjustable bolt anchors for the piano wire to their ferrule inserts.

5. Uncoil an appropriate amount of piano wire, threading it through the bolt anchor, cutting it about 1 ft longer than the distance between the anchors, and applying an initial tension of about 37 lbs.

6. Adjust tension in the piano wire to maintain a sag due to an attached 32.2g weight at mid-span of about 35/64 in.

As soon as the installation procedures for a system were completed, initial "zero level" readings were taken and recorded. The surface concrete strain readings were made with the mechanical, Demec strain measuring instrument. Deflection readings were obtained by placing a mirror next to each ruler, lining up the mirror image of the wire with the wire itself and recording the indicated ruler reading to the nearest 1/2 of the least scale division (1/64 in.). Electronic instrumentation was monitored, the readings recorded, and permission granted to the release crew to cut the hold-down ties and transfer the

prestressing force to the girders. For all specimens except L-I1 and L-I2 instrumentation was monitored immediately after the completion of prestress transfer while the girders were still in the casting bed. For specimens L-I1 and L-I2 the first monitoring of girder instrumentation after release was done once the girders had been transported to storage.

Figure 3.7a is a view of the south end of specimen L-I2 after the attachment of all mechanical instrumentation hardware. Note the tensioned piano wire attached to the mechanical bolt anchor. The machined nut tightened up against the concrete is the lock nut used to prevent the bolt from backing out of the ferrule insert. The ferrule inserts had been filled with grease before attaching them to the forms and thus there was little friction between the threads of the insert and those of the bolt anchor to resist the torque applied by the high tensioned wire. Whenever adjustments were to be made to the piano wire tension a wrench was first placed on the bolt anchor and held while the lock nut was loosened with another wrench. This prevented the tensioned piano wire from backing out the bolt anchor. The full size ruler shown here was used at the ends of only specimens L-I1 and L-I2. On subsequent specimens only a half ruler was used at the ends because a full size ruler was unnecessary and the sharp ends were a safety hazard.

a) view of bottom flange at the south end of L-I2

This figure is now
being used in
Dominic Kelly's thesis
Fig. 2.19

b) view of bottom flange at station MS of instrumented girder

Fig. 3.7 Piano Wire Instrumentation in Place

Figure 3.7b shows a typical view of the bottom flange of a specimen at stations MS after all mechanical instrumentation hardware was installed. Deflection readings were always taken using the scale which increased in magnitude from bottom to top. Also note in Fig. 3.7b that the points for the mechanical Demec strain gage were glued to the heads of the 1/4-in. diameter stainless steel bolts.

As mentioned previously, the form stripping crew began loosening the H-01 and H-02 specimens' forms before the 1/4-in. bolts used to hold the inserts in place had been removed. This resulted not only in the shearing and popping off of most of the 1/4-in. bolt heads but also in some damage to the concrete around the area of the inserts at station END of specimen H-01. The force applied to the inserts by the forms almost produced a pull-out failure of the concrete. Because it was feared the inserts might have to be removed the Demec points were offset about 10 in. north. A further complication was the loss of the ferrule loop insert used to attach the bolt anchor for the deflection monitoring system. The insert was not bolted tightly to the form and thus vibrated loose during consolidation of the concrete. Also, the force applied to the two inserts for attaching the ruler badly cracked the surrounding concrete which was later chipped away and subsequently patched by the girder maintenance crew.

Thus, even if the insert had not vibrated loose it would have been removed along with the damaged concrete. Alternatively, one of the Demec point inserts was used to anchor the piano wire and the rulers was glued to the concrete. A wooden chamfer strip was used to wedge the piano wire out away from the concrete surface. This alternative anchorage system required all adjustments to the piano wire tension to be made from the opposite end of this specimen. The small error in measured vertical deformation due to the fact the piano wire was anchored away from the support point is certainly negligible.

3.7 Acquisition and Reduction of Data

Because of the nature of this field investigation, acquisition of all field data had to be performed manually. Appropriate standard data sheets for each instrumentation system were designed to provide uniform format for the recording of data and field notes. In addition, field notebooks were kept to record other detailed information.

Supplementary information was obtained from external sources such as the State Highway inspectors at the plant, Texas SDHPT District 9, one of the prestressing strand suppliers, and the National Climatic Data Center in Asheville, North Carolina. This information included the concrete mix designs, strand stressing data, design and release cylinder tests, strand mill

tests (including relaxation tests) and local climatological conditions in Austin and San Antonio for the period of testing.

All of the field data gathered was reduced to tables and plots using a microcomputer "spread sheet" program. The program was used to produce overlay "spread sheets" stored on diskettes for each data set into which the field recorded data could be input line by line or dumped and the resulting interpreted results calculated by the "pre-constructed" overlay "spread sheet." This spread sheet software was also used in the reduction of data from the laboratory companion test program.

3.8 Coordination of Efforts

Project management of this investigation required the most concerted efforts. Unfortunately, prearrangement of certain functions of the investigation was very difficult. Lack of familiarity with the mode of operation of this particular plant is to blame for certain mistakes of the research team, such as the failure to communicate the importance of allowing all zero readings to be made prior to any release operations.

The critical path for each pair of specimens fabricated contained several parallel operations that required more research personnel than were available as well as many series operations that left some people standing around doing nothing. This was further complicated by the remoteness of the prestressing plant

from the research laboratory. For example, it was desirable to load the creep cylinders on the day of release. However, this would have required the transportation of the necessary cylinders 45 miles to the laboratory and the preparation and loading of the specimens by personnel who were not available because they had to be at the plant installing and monitoring instrumentation. A possible solution to this problem would have been to set up the creep frames at the prestressing plant. For the case of a series operation the example is the events of the casting day. Because the exact time when the forms were to be placed was unknown and because the instrumentation systems required that the research team be involved in the form setting operation, research personnel were required to stand around for hours doing practically nothing while the preparations were being made to set the girder forms.

Fortunately, on the day of release when many parallel operations had to be performed in a very short period, the research team was usually able to get the prestressing plant to adjust their mode of operation slightly. The plant personnel are to be commended for their cooperation in these areas as well as their cooperation throughout the investigation in providing cranes when necessary to move specimens.

3.9 Evaluation of Instrumentation Performance

Each of the field instrumentation systems employed in this investigation has given certain indications as to the appropriateness and/or reliability of the system for the application made. The performance of each system in providing reliable data can be estimated by the variations of the data from time to time and from specimen to specimen. This evaluation of instrumentation performance can be divided into five parts for each system as follows:

1. preparability;

2. installability;

3. durability;

4. accessability; and

5. reliability.

Each system is evaluated based on these five areas and the conclusions as to the performance of the system noted.

3.9.1 Performance of Concrete Strain Monitoring System.

The hardware required for the concrete strain monitoring system was very difficult to prepare. The bolt inserts, which were also used for portions of the deflection monitoring system, were made of high grade stainless steel. The required threaded hole in the end of the 3/4-in. stainless steel bolt had to be drilled and tapped in the laboratory. Because of the hardness of the stainless steel, drilling and tapping of the bolts required

about four man-weeks to complete as there were some 240 bolts for

this system to be done alone at about 20 minutes each.

Originally, brass bolts had been contemplated for this

application but their cost was considered prohibitive and so

stainless steel was chosen instead. It is the author's opinion

that the trade off of initial cost for a labor and tool intensive

operation was certainly not a very efficient use of resources.

Thus, working with the materials chosen, the preparability of the

surface strain instrumentation was very poor.

Fortunately, the installation of the concrete strain

instrumentation was much easier than was the preparation of the

required inserts. The most difficult part of the installation

procedure, the drilling of holes in the Type IV form, had to be

performed only once. After that was completed it was simply a

matter of maintaining the forms in their proper order and

spending an hour or so bolting the inserts to the forms on the

day of instrumentation installation. There was some difficulty

in setting the forms with the inserts bolted as there was little

or no clearance between the bolt heads and the top flange

reinforcement holding the passive longitudinal reinforcement in

place. This resulted in some of the inserts becoming loose when

setting the forms requiring that they be tightened after the

forms were in place and in some cases requiring that the bolt

holding an insert on be replaced as it was bent by the impact of

the transverse re-bar. Fortunately, no insert set for the placement of a Demec point was ever vibrated off during the consolidation of the concrete. The problem mentioned previously concerning the inserts of specimens H-01 and H-02 was not a result of poor installability of the insert but rather was the result of poor management on the part of the author. The clearance problem, if it had been recognized, could have been prevented by machining the heads of the 3/4-in. stainless steel bolts but that would have further handicapped the system's preparability.

As mentioned previously, the inserts for the mechanical strain gage system were sufficiently durable to survive the installation and fabrication procedures. Because the inserts were made of stainless steel no problems of corrosion of the inserts was anticipated or has been observed. However, the long-term durability of the surface strain gage system was affected by the type of epoxy used to set the Demec points on the 1/4-in. diameter bolt heads. Because of the need to set the points quickly for obtaining the initial and transfer response readings, a quick setting epoxy was used rather than drilling Demec gage holes in the bolts. This epoxy appeared to withstand the environmental conditions during the summer. However, when the rains came in the fall this epoxy lost its adhesion rather quickly. Not only did the moisture and/or lower temperature

affect the old epoxy but points affixed to specimens H-01, H-02, H-I1, and H-I2, which were cast in October and November, lasted only a short while before the epoxy yellowed and lost its adhesion. As quickly as possible after the problem was recognized, temporary points were epoxied to all specimens until the proper epoxy could be used to affix permanent points. Fortunately, the fabricator allowed the researchers to use some of the epoxy with which the beams were being patched by the girder maintenance crews. This latter epoxy is designed to be more durable than the concrete itself. All Demec points were affixed permanently to the bolt heads with this fabricator supplied epoxy in December 1984. This problem of lost Demec points has resulted in several discontinuities in the surface strain versus time curves for each specimen investigated. Of course, this problem had a minimum effect on the surface strain-time curve of the first set of specimens cast. The durability of the surface strain monitoring system was therefore found dependent on the quality of epoxy used. A better system procedure would have been to use brass bolts and drilled Demec reference holes directly in the brass bolts eliminating epoxy altogether.

No problems of unaccessibility to the surface strain monitoring systems of any of the specimens was encountered during the plant stage of the investigation reported herein.

The reliability of the surface strain monitoring system
as used in this investigation has been affected by several
things:

1.   the quality of the Demec gages used;

2.   the frequency of monitoring the surface strain systems;

3.   the stability of gage points; and

4.   the number of operators involved.

The first four specimens cast, L-I2, L-01, and L-02,
were monitored with an old Demec gage with a slightly worn pivot.
The gage would indicate differences of reacings when making three
consecutive readings of the standard bar prior to each field
monitoring session. If the gage was flipped around on the
standard bar the readings would differ. When the fifth specimen
was fabricated, a new Demec gage was available and then all
subsequent readings of this specimen, the four previous
specimens, and the three specimens still to be fabricated were
made using this gage. Appropriate continuity readings on
previously fabricated specimens were made with both gages at the
time the new instrument was employed. This new gage gave more
consistent standard bar readings as long as the bar was oriented
the same way each time it was read. However, when the bar was
flipped around the readings would differ.

The more frequently the surface strains were monitored,
the more reliable were the indicated strains. This was partially

due to the resulting increase in operator proficiency. The more frequently the operator made readings, the more likely it was that he would hold the gage in a consistent manner. Also, the operator was more familiar with what the readings had been previously and thus could look for problems when a reading seemed dramatically different than it had been on the previous monitoring session. Related to this is also the fact that lost Demec points could be replaced more quickly when the frequency of monitoring the specimen was high.

As noted earlier, the stability of the gage points, due previously to the effectiveness or lack thereof of the epoxy used, had a primary effect on the reliability of the system. Any point that was found missing or loose automatically introduced a discontinuity in the recorded data for that particular gage line. The longer the time between taking the previous reading and finding the point defective, the greater was the effect of the discontinuity on the final results. Points which were found defective early in the monitoring period introduced discontinuities in the data during the period of greatest change in strain and thus had a greater impact on the final results.

3.9.2 Performance of Strand Strain Monitoring System. The preparation for installation of the strand strain monitoring system consisted of obtaining the gages, lead wires, and calibrating switch boxes, precutting and soldering the lead wire,

cleaning up and/or putting together the calibrating switch boxes, and gathering the necessary materials and equipment needed to complete the installation procedure. With regard to the preparability of the surface strain monitoring system, the strand strain monitoring system required less man hours but more technical labor.

Although there was some savings in time during the preparation period for the strand strain monitoring system, the amount of time required to install the system far exceeded that of the other systems. Of course, no additional installation procedures were necessary on the day of release as were with two of the other three systems. The SR7 gages were placed on the strands after the stressing at the request of the fabricator. This simplified the installation procedures somewhat as the gages could be placed in their final position along the specimens span and the stressed strands were separated so that hands could be easily slipped between them. Overall, the installability of the strand strain monitoring system was time/labor intensive.

The durability of the strand strain monitoring system during the casting stage of specimen fabrication was better than anticipated. Only a few of the 80 gages appeared to have suffered damage during the casting of the girders. Subsequently, many more gages gave indications that they were manfunctioning. It is not known at this time whether the gages that have appeared

to malfunction are themselves defective or whether there is a problem with those particular calibrating switch box channels. The latter may very well be the case as some channels of the switches in the calibrating switch boxes were found defective during installation requiring other channels to be used instead.

Although the strand strain monitoring system installed survived the casting operation, one system (for L-01), as mentioned previously, suffered the loss of all gages at station MS due to the lead wires being inadvertently ground in two at the surface of the concrete. This unfortunate occurrence might have been prevented if proper instruction had been given to the fabricator as to the delicate nature of the instrumentation.

Access to the strand strain monitoring system was not a problem with the specimens stored in the fabricating plant. Long-term durability of the strand gages was poor. Little dependable data were obtained after a three-month life.

3.9.3 Performance of Internal Temperature Monitoring System. The preparation and installation of the copper-constantine thermocouplers to monitor internal concrete temperatures was by far the easiest procedure of all instrumentation systems prepared and installed. Preparation involved simply cutting the thermocouple wire to the proper lengths, stripping the ends of the wires, attaching a male connector to one end of each wire and making sure the free end of

the wire was twisted together to complete the circuit. The thermocouple wires for a particular monitoring station were taped together in such a manner that positioning of the free end of the bottom wire 4 in. from the casting bed would place the free ends of the other two wires in the proper locations. Thus, installation involved simply placing the set of three thermocouple wires along a stirrup with the free end of the bottom wire being 4 in. from the casting bed and tying the wires to the stirrup with plastic ties.

The temperature monitoring systems gave no indications that they were damaged in any way throughout the plant stage of this investigation. Readings were easily made utilizing a multichanneled temperature indicator. Readings were reasonable for a given monitoring session for all such sessions. Thus, it is believed that the temperature data colelcted from this instrumentation system is very reliable.

Accessibility of the temperature instrumentation in this investigation was not a problem during the plant stage reported herein.

3.9.4 Performance of Time Camber/Deflection Monitoring System. Preparation of the system used to monitor vertical beam deflections involved the machining of 16 1/2-in. diameter bolts (plus a few extras) as noted in Sec. 2.5.4.2. In order to keep the bolts from backing out of the inserts, 1/2-in. lock nuts were

also machined to be half as thick as normal. Machining of inserts for attaching the rulers was also required. Also required was the procurement of the necessary ferrule loop inserts, piano wire and stainless steel rulers. The rulers were pre-drilled with a special extra hard 1/4-in. bit in the laboratory and some were cut in half. Overall, the preparability of the camber/deflection monitoring system was good.

Installation of the deflection monitoring equipment began with the attachment of the inserts. The ferrule loop inserts were loosely attached on the Saturday before casting as were the inserts for attaching the rulers. The same inserts were used to attach the rulers as were used to provide places for the Demec points. Some of the ferrule loop inserts used to attach the 1/2-in. diameter machined bolts for anchoring the piano wire had to be removed and then replaced during the form setting operation as noted in Sec. 3.4. The pre-drilled rulers were easily attached to the bottom flange of each specimen with stainless steel 1/4-in. bolts after the forms were removed. The installation of the piano wire was a nerve-wracking operation. Care had to be taken in uncoiling the piano wire as it was easily tangled and not easily untangled. The pressure to install the instrumentation as quickly as possible so that the fabricator could carry on his operation especially effected this instrumentation procedure. Once the wire was attached to the

bolts (which were hopefully locked down) it had to be tightened or loosened as required so that the attachment of the standard weight at midspan would produce the desired sag. Installability of the camber/deflection monitoring system was much better than that of the strand strain monitoring system and about as good as the concrete surface strain monitoring system.

The "piano wire system" used to measure girder camber/deflection was designed so that the temporary loss of the piano wire or either anchor would not result in the loss of reference to initial readings. This meant that the system was virtually indestructable although from time to time the piano wire had to be replaced as it was found broken or it broke during adjustment.

There was no problem gaining access to the camber/deflection monitoring system monitoring station during Phase 1 of this overall investigation.

The reliability of the "piano wire" camber/deflection monitoring system is felt to be very high. A comparison of the camber curves of two beams cast at the same time and monitored concurrently reveals that the system yields consistent results between beams. That is, the plotting of the time-cambers for a particular pair of beams are similar in shape.

CHAPTER 4

MATERIAL TESTS OF COMPANION SPECIMENS

4.1 General

4.1.1 Guidelines for Testing. In general, guidelines by which material tests on companion specimens were performed have been taken from applicable ASTM standard methods. However, because "the differences between laboratory and field conditions may cause a notable difference in the behavior of the control specimens and the field structure" [18], the controlled conditions requirements of ASTM for tests on concrete cylinders were modified for most tests performed to reflect field conditions. Companion concrete cylinders were cured, stored and tested under conditions similar to those existing in the field. Details of the actual conditions underwhich the creep and shrinkage tests were performed are reported so that the test results can be properly assessed.

4.1.2 Format of Presentation. In this chapter the material tests performed are described in sufficient detail to allow deviations from ASTM standard methods to be noted. Such descriptions of procedure are given to aid in the proper interpretation of the results. Following the description of each test method used, the results of tests performed are presented.

4.2 Tests on Concrete

The concrete properties of interest, as noted in Sec. 2.1.2, were:

1. age-compressive strength relationships,

2. time-dependent creep and shrinkage properties, and

3. age-stress-strain relationships.

Most compressive strength tests were performed at the same time as stress-strain tests using the same specimens and so are described concurrently herein.

4.2.1 Test Specimens. Specimens used in all tests were standard 6 in. diameter by 12-in. long cylinders made from selected batches of field cast concrete according to ASTM Method C-31, "Making and Curing Concrete Test Specimens in the Field" [5]. Early curing and storage (less than 28 days) of most concrete cylinders was under the ambient conditions existing at the plant. Beginning with those tested within the first four weeks after each casting, concrete specimens were progressively transported to the laboratory and stored under the ambient conditions existing at the laboratory storage and testing areas which may be assumed to be similar to those existing in the outdoor area where creep and shrinkage tests were performed.

Concrete mix design information for each casting is given in Table 4.1. Calculations of the results of all tests on companion concrete cylinders assume perfect 6-in. diameter

TABLE 4.1a   Concrete Materials Data

	L Series Beams	H Series Beams
Aggregate Characteristics		
Fine Aggregate (FA):		
Specific Gravity	2.61	2.63
SSD Unit Wt (lbs/cu.ft.)	97.56	101.02
% Solids	59.80	61.50
Coarse Aggregate (CA):		
Specific Gravity	2.58	2.58
SSD Unit Wt (lbs/cu.ft.)	95.34	95.34
% Solids	59.10	59.10
Cement Origin	Alamo; TXI; Type III	Alamo; Type III
Design Factors		
Cement Factor (CF)	6.5 sacks/cy	7.0 sacks/cy
Coarse Aggregate Factor (CAF)	0.72	0.72
Water Factor (WF)	4.3 gals/sk	4.1 gals/sk
Air Factor	---	---
Yield (vol. conc/sack cement)	4.154	3.857
Fine Aggregate Factor (vol. FA/FA solids x vol. mortar)	0.93	0.87
Admixtures:		
Spec. 494 (oz/sack)	7	7
Mighty 150 (oz/sack)	16	16

TABLE 4.1b Concrete Mix Design Data

Specimens	L-I*	L-O*	H-O*	H-I*
Design Specifications				
Cement	Type III; 611 lbs/cy	Type III; 611 lbs/cy	Type III; 658 lbs/cy	Type III; 658 lbs/cy
Fine Aggregate	FM = 2.67; 1446 lbs/cy	FM = 2.67; 1408 lbs/cy	FM = 2.48; 1333 lbs/cy	FM = 2.48; 1362 lbs/cy
Coarse Aggregate	3/4 in.; 1830 lbs/cy	3/4 in.; 1853 lbs/cy	3/4 in.; 1852 lbs/cy	3/4 in.; 1852 lbs/cy
W/C Ratio	0.38	0.38	0.38	0.38
Unit Paste Volume	0.255	0.255	0.268	0.268
Mix Proportions **(cement:sand:** **gravel)**	1:2.37:3	1:2.3:3.03	1:2.03:2.82	1:2.07:2.82
Admixtures				
Spec. 494 (oz/cy)	45.5	45.5	49	49
Mighty 150 (oz/cy)	104	104	112	112

cylinders. Unit weights (reported later) were determined from measurements of one cylinder from each batch made several months after the casting of the youngest specimens.

4.2.2 Stress-Strain and Strength Tests Procedures. Compressive strength tests were performed on some concrete cylinders according to ASTM Method C-39, "Test for Compressive Strength of Cylindrical Concrete Specimens" [6] but most compressive strengths were determined by breaking the stress-strain test cylinders during the second loading. Some of the breaks were obtained from the State, and thus are of cylinders cured under laboratory conditions if they were performed on design strength specimens. Other breaks obtained from the State are of release cylinders, and thus are of cylinders cured under field conditions. In the presentation of the results, the origin of each reported cylinder break is noted.

The stress-strain-strength tests were performed according to ASTM Method C-469-81, "Static Modulus of Elasticity and Poisson's Ratio of Concrete in Compression" [7]. A suitable compressometer, as shown in Fig. 4.1, was used for all tests performed. The testing apparatus employed was a hydraulically driven, 600 kip capacity, Satec Systems, Inc. machine. It has a metric load scale so all load readings were converted from kN to kips by multiplying by the factor 0.2248.
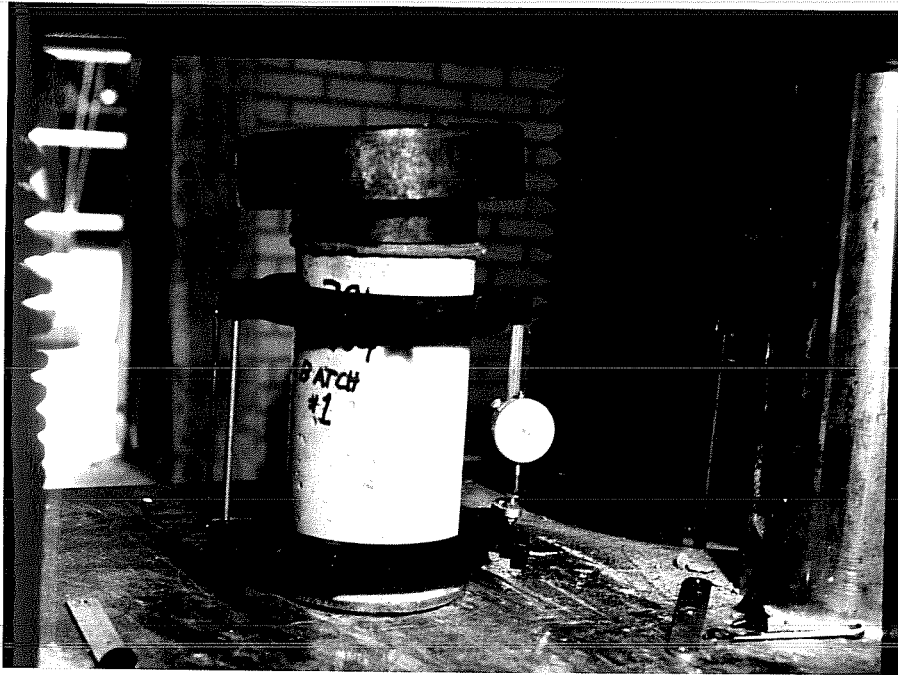
Fig. 4.1 Compressometer Used to Perform Modulus of Elasticity
(MOE) Tests on Concrete Cylinder Specimens

The intended load rate was 40 psi/s for each specimen tested which falls in the 30 to 40 psi/s range specified by Method C-469. The loading rate has an important effect on the shape of the resulting stress-strain curve and thus care was taken to minimize loading rate differentials between tests. It is believed that the actual loading rates for all tests performed were between 35 and 45 psi/s.

Two loadings per cylinder were performed and the resulting average stress-strain curve and modulus of elasticity determined from the recorded data. Preparation and testing procedure was as follows:

1. Mark two diametrically opposed vertical lines on each test specimen measuring down 2 in. from the top of the cylinder along each line and making a horizontal mark.

2. Cap specimens with high strength capping compound.

3. Place compressometer around specimen and screw in top clamps such that their points embed in the concrete at the intersection of the lines previously drawn.

4. After tightening top and bottom clamps measure and record the distance from both the center of the gage and the rod to the edge of the cylinder.

5. With a spherical head on top place the instrumented specimen in the testing machine and center it on the lower platen.

6. Check to obtain uniform seating of the upper platen on top of the spherical head when lowering the platen.

7. Load specimen to seat platens checking for proper functioning of the dial gage and correct any unusual behavior without recording any readings.

8. Load specimen two more times as follows:

   a. Apply load continuously without shock.

   b. Apply load at the specified constant rate.

   c. Record, without interruption of loading, the applied load and dial gage reading for each 100 kN (22.48 kip) increment of load up to 40% of the assumed ultimate strength of the cylinder for the first loading and thereafter for each 50 kN (11.24 kip) or smaller increment up to ultimate, if possible, for the second loading.

For the two loadings performed on each specimen the resulting average stress-strain curve and modulus of elasticity were determined according to the calculation procedures of Method C-469. The maximum compressive load applied to a cylinder upon the second loading was noted for each test.

4.2.3 **Stress-strain and Strength Tests Results.** Tables 4.2a through 4.2d summarize the results of all stress-strain and strength tests performed. In these tables the age of each cylinder is given in days from casting. "FSEL" stands for

Table 4.2 MOE and Compressive Strength of Companion Concrete Cylinders

a) for specimens L-I1&2

AGE	TEST FACILITY	CYLINDER IDENTIFICATION	UNIT WEIGHT	COMPRESSIVE STRENGTH	Ec	ACI RECOMMENDED Ec	ACI Ec COEFFICIENT
.0							
.6	STATE LAB	C-L-IR1	N/A	4,804	N/A	3.994	
.8	STATE LAB	C-L-IR2	N/A	5,071	N/A	4.103	
.9	STATE LAB	C-L-IR3	N/A	5,482	N/A	4.266	
.9	STATE LAB	C-L-IR4	N/A	5,391	N/A	4.231	
.9	FSEL	C-L-IB1-1	148.4	5,709	5.122	4.508	37.5
1.0	FSEL	C-L-IB2-1	147.3	5,772	5.112	4.482	37.6
.9	FSEL	C-L-IB3-1	145.8	5,414	5.163	4.275	39.9
2.0	FSEL	C-L-IB1-2	148.4	6,909	N/A	4.959	
2.0	FSEL	C-L-IB2-2	147.3	6,790	N/A	4.861	
2.0	FSEL	C-L-IB3-2	145.8	6,718	N/A	4.762	
7.0	STATE LAB	C-L-ID1	N/A	7,438	N/A	4.969	
7.0	STATE LAB	C-L-ID2	N/A	7,545	N/A	5.005	
7.0	STATE LAB	C-L-ID3	N/A	7,446	N/A	4.972	
8.0	FSEL	C-L-IB1-3	148.4	7,172	5.108	5.052	33.4
8.0	FSEL	C-L-IB2-3	147.3	7,847	5.482	5.226	34.6
8.0	FSEL	C-L-IB3-3	145.8	7,036	4.898	4.873	33.2
21.0	FSEL	C-L-IB1-4	148.4	8,316	5.077	5.440	30.8
21.0	FSEL	C-L-IB2-4	147.3	8,229	5.140	5.352	31.7
21.0	FSEL	C-L-IB3-4	145.8	8,886	5.593	5.477	33.7
28.0	FSEL	C-L-IB1-5	148.4	9,135	5.468	5.702	31.6
28.0	FSEL	C-L-IB2-5	147.3	8,563	5.296	5.459	32.0
28.0	FSEL	C-L-IB3-5	145.8	8,173	5.162	5.252	32.4
92.0	FSEL	C-L-IB1-6	148.4	9,282	5.952	5.748	34.2
92.0	FSEL	C-L-IB2-6	147.3	8,984	5.805	5.592	34.3
92.0	FSEL	C-L-IB3-6	145.8	8,865	5.673	5.470	34.2
325.7	FSEL	C-L-IB2-7	147.3	10,952	5.652	6.174	30.2
325.7	FSEL	C-L-IB3-7	145.8	10,475	5.687	5.946	31.6

Table 4.2 MOE and Compressive Strength of Companion Concrete
Cylinders (cont'd)

b) for specimens L-01&2

AGE	TEST FACILITY	CYLINDER IDENTIFICATION	UNIT WEIGHT	COMPRESSIVE STRENGTH	Ec	ACI RECOMMENDED Ec	ACI Ec COEFFICIENT
.0							
.5	STATE LAB	C-L-OR1	N/A	5,374		4.224	
.5	STATE LAB	C-L-OR2	N/A	5,480		4.265	
.9	FSEL	C-L-OB1-1	N/A	6,854	4.815	4.770	33.3
.9	FSEL	C-L-OB2-1	N/A	6,813	4.832	4.756	33.5
2.2	FSEL	C-L-OB1-2	N/A	8,205		5.219	.
2.2	FSEL	C-L-OB2-2	N/A	8,078		5.179	
6.9	FSEL	C-L-OB1-3	N/A	8,786	5.520	5.401	33.7
6.9	FSEL	C-L-OB2-3	N/A	9,406	5.337	5.588	31.5
13.9	FSEL	C-L-OB1-4	N/A				
13.9	FSEL	C-L-OB2-4	N/A	8,984	5.483	5.461	33.1
14.0	FSEL	C-L-OB3-1	146	9,326	5.778	5.622	34.3
13.9	FSEL	C-L-OB4-1	146	8,372	5.347	5.327	33.5
14.0	STATE LAB	C-L-OD1	N/A	9,645		5.659	
14.0	STATE LAB	C-L-OD2	N/A	9,500		5.616	
14.0	STATE LAB	C-L-OD3	N/A	9,429		5.595	
20.8	FSEL	C-L-OB1-5	N/A	9,350	6.041	5.571	35.8
20.8	FSEL	C-L-OB2-5	N/A	9,024	5.747	5.474	34.6
20.9	FSEL	C-L-OB3-2	146	9,262	5.632	5.603	33.5
20.9	FSEL	C-L-OB4-2	146	9,760	5.724	5.751	33.2
27.8	FSEL	C-L-OB1-6	N/A	10,137	5.982	5.801	34.0
27.8	FSEL	C-L-OB2-6	N/A	8,845	5.753	5.419	35.0
27.8	FSEL	C-L-OB3-3	146	10,137	5.559	5.861	31.3
27.8	FSEL	C-L-OB4-3	146	9,859	5.474	5.780	31.6
311.7	FSEL	C-L-OB3-4	146	9,899	5.198	5.792	29.9
311.8	FSEL	C-L-OB4-4	146	11,389	5.744	6.213	30.8

c)   for specimens H-01&2

AGE	TEST FACILITY	CYLINDER IDENTIFICATION	UNIT WEIGHT	COMPRESSIVE STRENGTH	Ec	ACI RECOMMENDED Ec	ACI Ec COEFFICIENT
.0							
.9	STATE LAB	C-H-OR1	N/A	6,667	N/A	4.705	
.9	STATE LAB	C-H-OR2	N/A	6,720	N/A	4.723	
2.3	FSEL	C-H-OB1-1	145.4	7,552	4.962	5.007	32.6
1.3	FSEL	C-H-OB2-1	145.9	6,973	4.631	4.811	31.5
2.3	FSEL	C-H-OB3-1	146.1	7,748	5.008	5.130	32.2
14.2	STATE LAB	C-H-OD1	N/A	9,504	N/A		
14.2	STATE LAB	C-H-OD2	N/A	9,716	N/A		
14.2	STATE LAB	C-H-OD3	N/A	9,610	N/A		
28.8	FSEL	C-H-OB1-2	145.4	9,346	N/A	5.593	
29.3	FSEL	C-H-OB2-2	145.9	10,170	N/A	5.865	
28.8	FSEL	C-H-OB3-2	146.1	9,010	N/A	5.469	
160.9	FSEL	C-H-OB1-3	145.4	9,899	5.068	5.733	29.1
160.9	FSEL	C-H-OB2-3	145.9	10,892	5.391	6.013	29.3
160.0	FSEL	C-H-OB3-3	146.1	10,674	5.588	6.021	30.6

d)   for specimens H-I1&2

AGE	TEST FACILITY	CYLINDER IDENTIFICATION	UNIT WEIGHT	COMPRESSIVE STRENGTH	Ec	ACI RECOMMENDED Ec	ACI Ec COEFFICIENT
.0							
.6	STATE LAB	C-H-IR1	N/A	5,443	N/A	4.251	
.6	STATE LAB	C-H-IR2	N/A	5,567	N/A	4.299	
1.0	FSEL	C-H-IB1-1	145.80	6,043	4.74	4.516	34.6
.9	FSEL	C-H-IB2-1	147.00	4,762	4.07	4.059	33.1
3.0	FSEL	C-H-IB1-2	145.80	8,134	N/A	5.240	
3.0	FSEL	C-H-IB2-2	147.00	7,162	N/A	4.977	
13.9	STATE LAB	C-H-ID1	N/A	9,965	N/A	5.752	
13.9	STATE LAB	C-H-ID2	N/A	9,770	N/A	5.695	
13.9	STATE LAB	C-H-ID2	N/A	9,894	N/A	5.731	
119.0	FSEL	C-H-IB1-3	145.80	10,594	5.76	5.980	31.8
119.0	FSEL	C-H-IB2-3	147.00	8,984	5.22	5.575	30.9

Ferguson Structural Engineering laboratory. Cylinder

designations ending in R# are release cylinders tested by the

State prior to transfer of prestress. Cylinder designations

ending in D# are design cylinders tested by the State. Cylinder

designations ending in B#-# are cylinders made from each batch

sampled by researchers (the first number indicates the batch

while the second indicates the order of testing). Elastic

modules are in million psi. The ACI recommended moduli [2] are

based on the formula:

$$q_{ct}w^{1.5} \sqrt{f'_c} \; psi$$

where q_{ct} = unitless coefficient assumed to be 33,

w = unit weight of concrete in lb/ft^3

f'_c = compressive strength of concrete in psi

For some batches, no measurement of unit weights were available

and thus the ACI recommended moduli for these batches have been

calculated based on an assumed unit weight of 145 lb/ft^3.

The ACI coefficient q_{ct} is taken as 33 for moderate to

low strength concrete as specified by ACI 209 [2]. For batches

of known tested concrete, this coefficient has been calculated as

an indication of how close or far off the measured moduli are

from the ACI 209 recommended calculations of E_c. The range of

values for q_{ct} represented by the test data is reasonable

considering the scatter apparent in the tests performed herein and elsewhere.

Figures 4.2a through 4.2d are plots of average measured compressive strength versus age of concrete for each field specimen casting. These measured strength gain curves are compared with the ACI 209 recommended strength gain function. In all cases, the early strength of concrete (age less than 28 days) predicted by the ACI 209 recommended function, $(t/(2.3 + 0.92t))(f'_c)_{28d}$, is substantially lower than the measured values. The function in Fig 4.2d does not use the ACI recommended coefficients but instead uses a function normalized to the measured three-day strength and fitted to the measured data. Also, the last average break reported in Fig. 4.2a is erroneously high. The compressive tests performed when compared with the ACI 209 recommended strength gain function for moist cured concrete indicates that the recommended function under-predicts strength at early ages. At ages 28 days and greater, the ACI recommended function more accurately predicts concrete strengths.

Figure 4.3 shows two typical stress-strain curves generated by the data from modulus of elasticity tests. The first curve is typical for most of such tests performed. The second curve is typical of a few tests performed where the full range of the ascending portion of the stress-strain curve was tracked. Figures 4.4a through 4.4d are plots of average measured
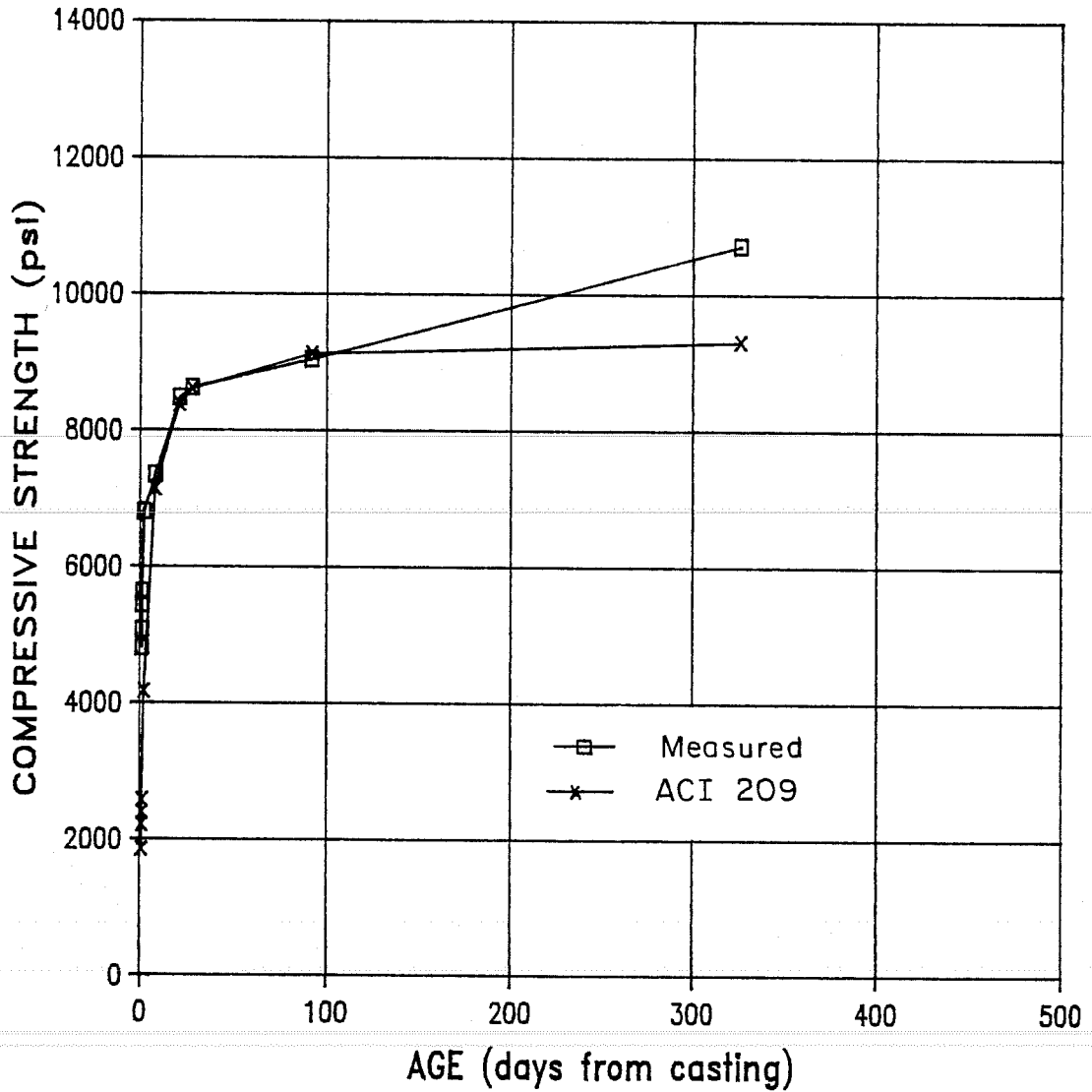
a) measured and predicted strength curves for specimens L-I1&2

Fig. 4.2 Strength vs. Time Curves for Concrete from Field
Specimens Investigated
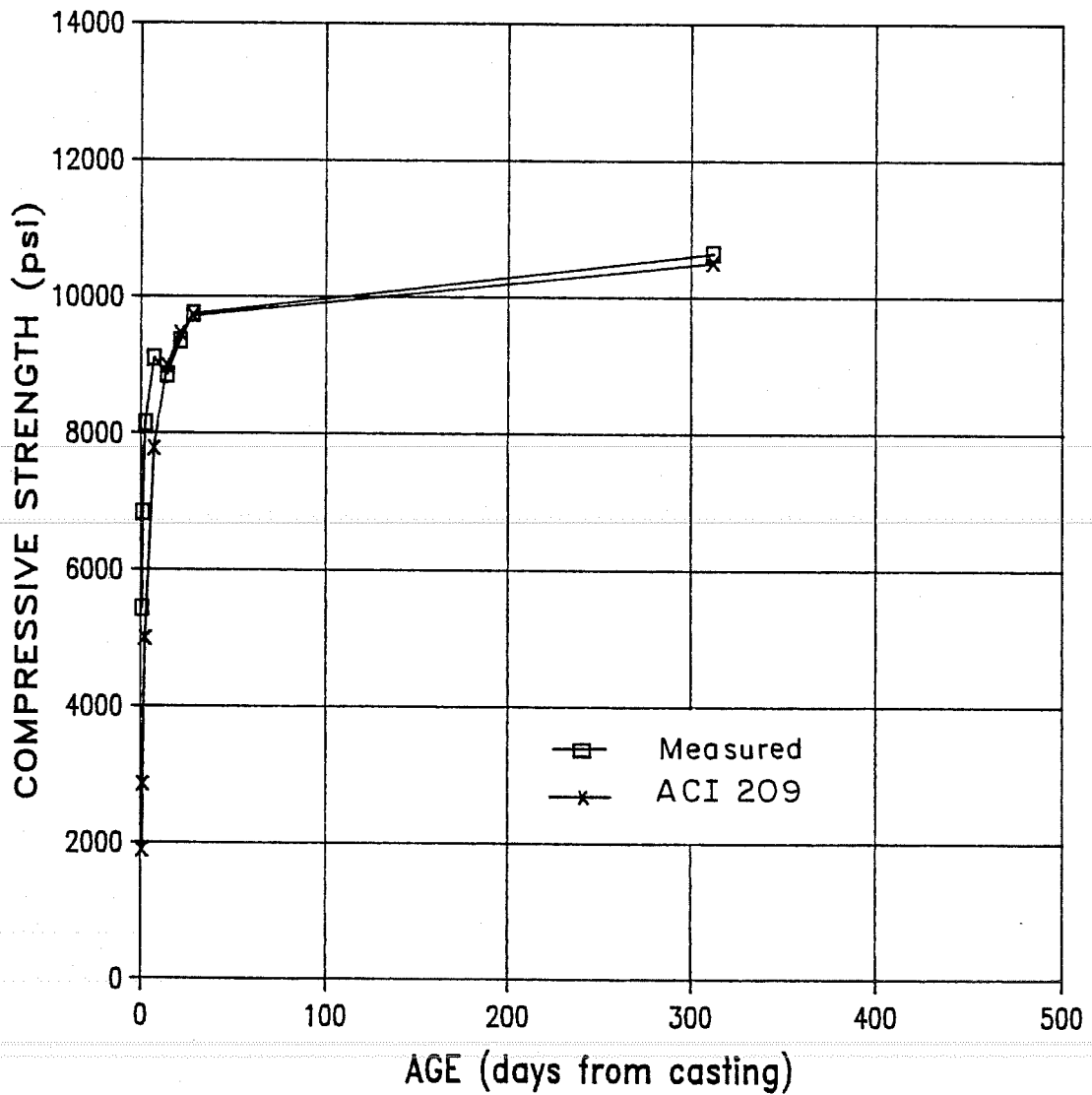
b) measured and predicted strength curves for specimens L-01&2

Fig. 4.2 Strength vs. Time Curves for Concrete from Field
Specimens Investigated (cont'd)
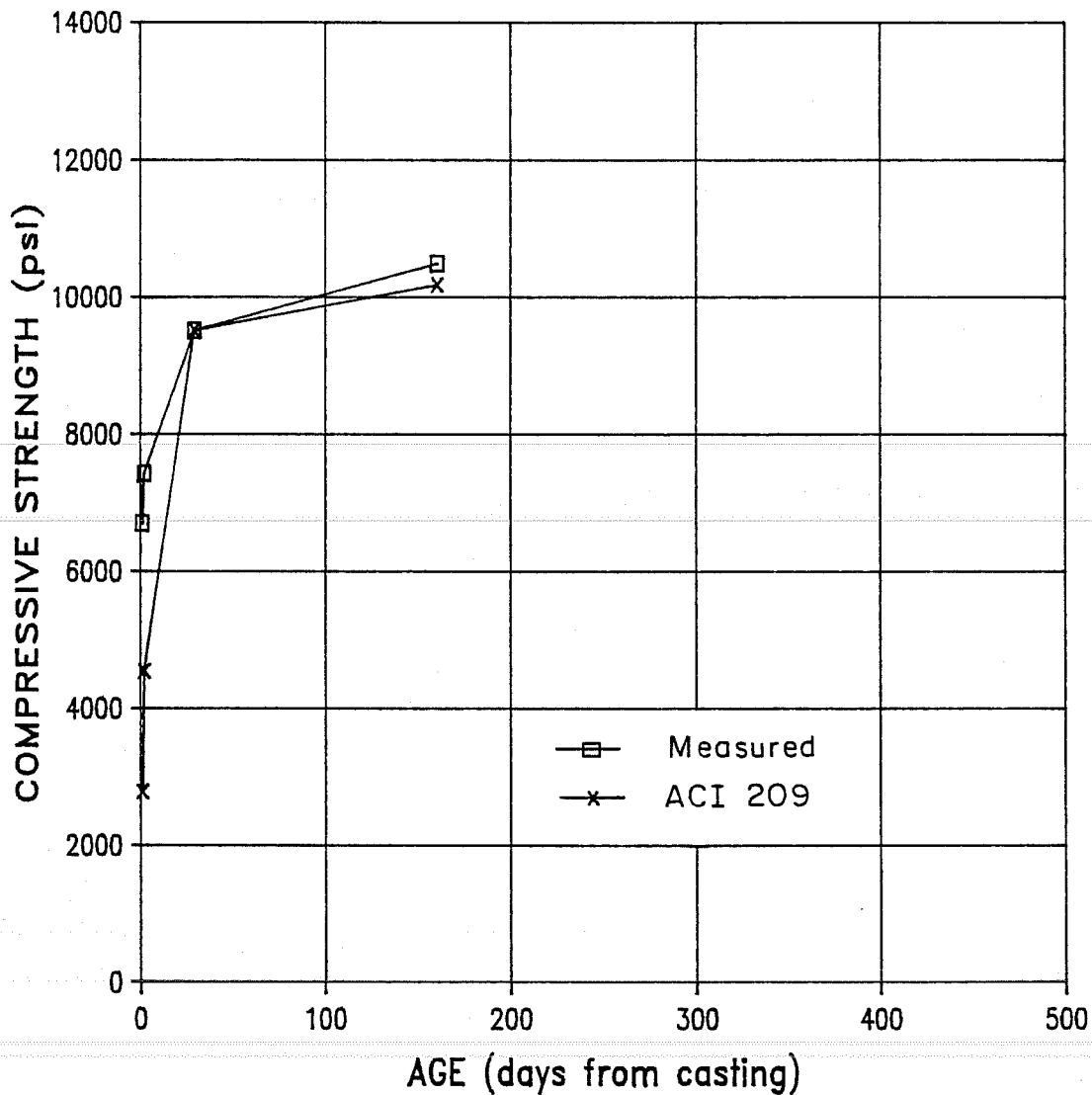
c) measured and predicted strength curves for specimens H-01&2

Fig. 4.2   Strength vs. Time Curves for Concrete from Field
          Specimens Investigated (cont'd)
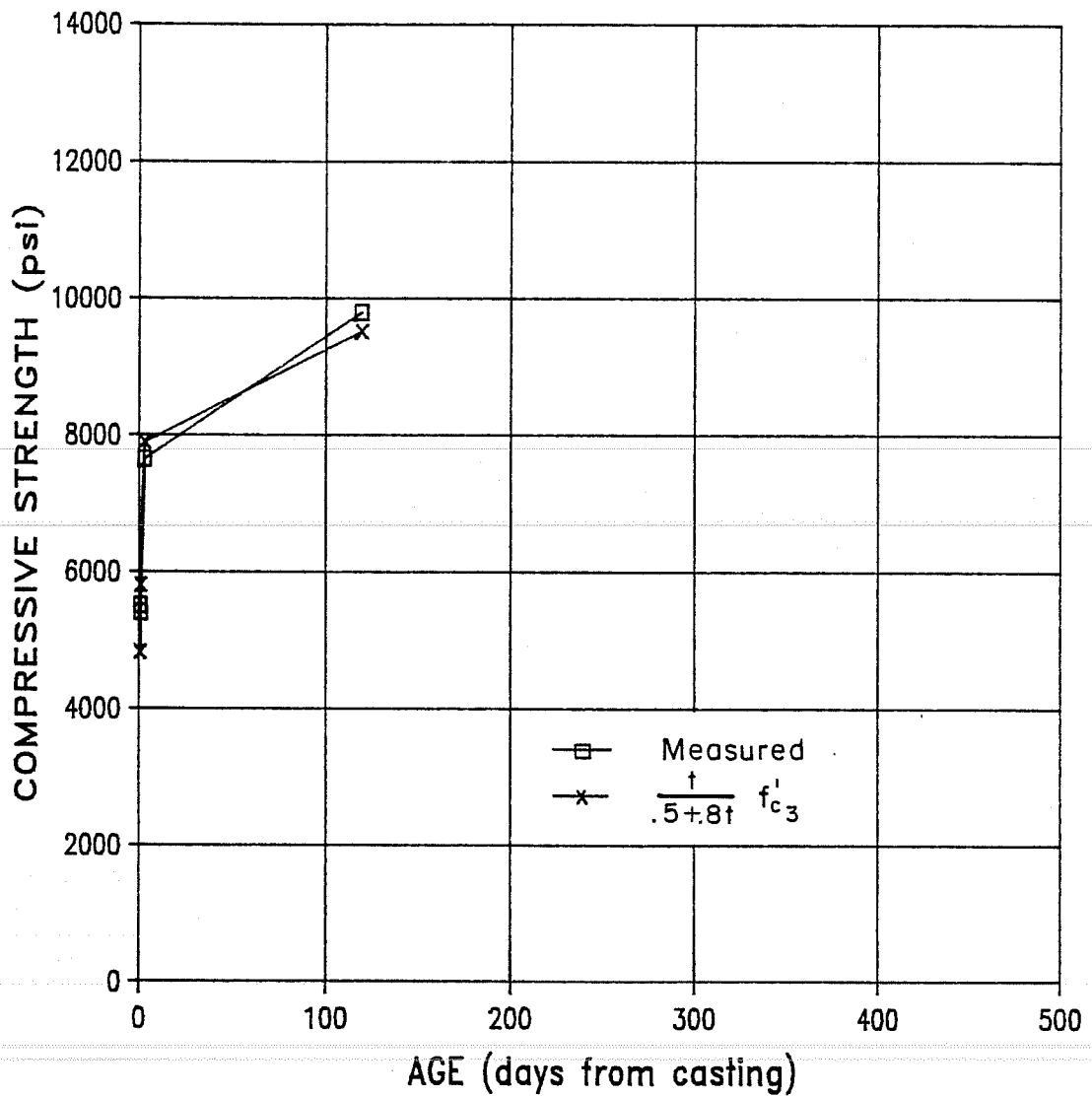
d) measured and predicted strength curves for specimens H-I1&2

Fig. 4.2 Strength vs. Time Curves for Concrete from Field
Specimens Investigated (cont'd)
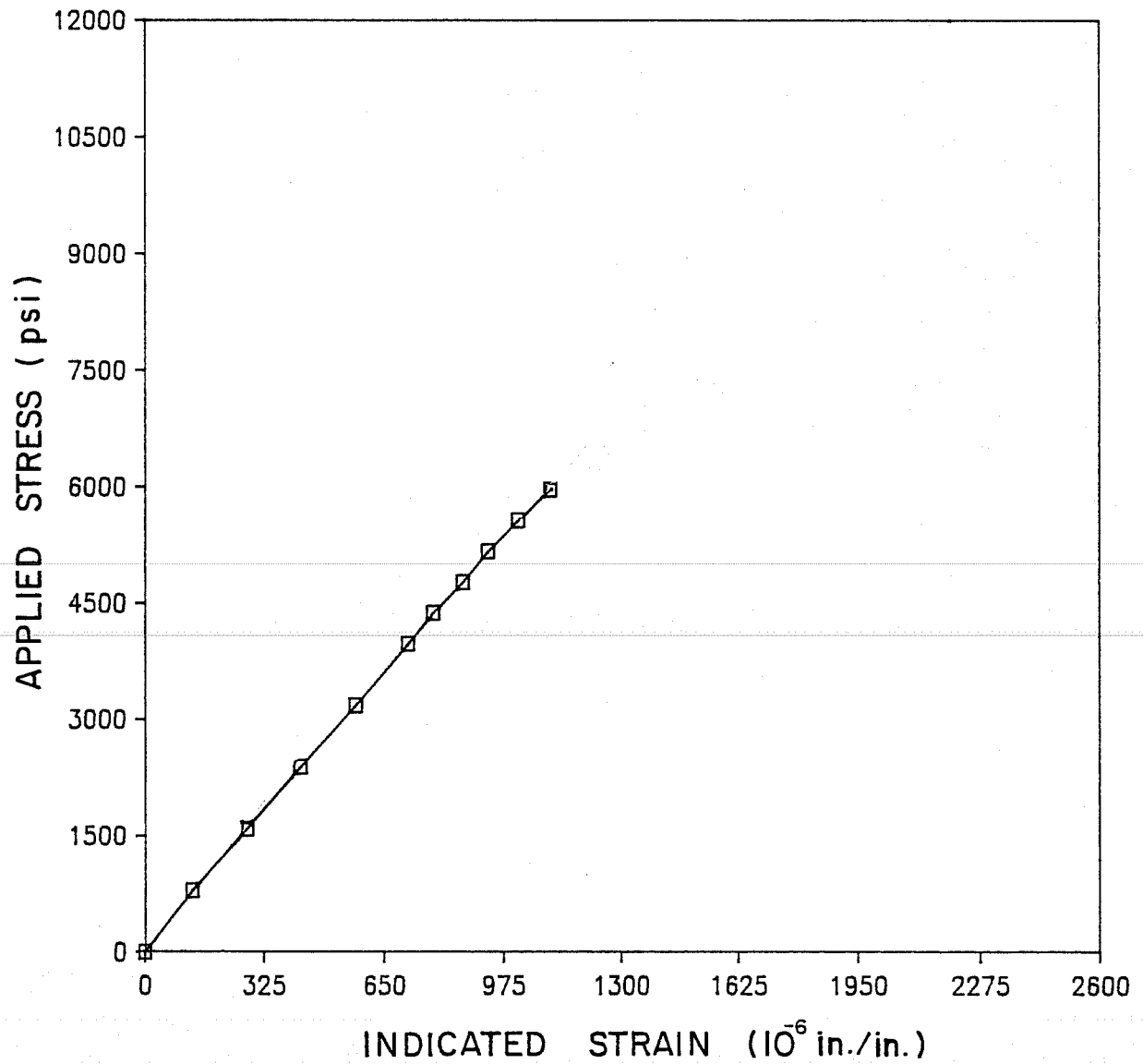
a) typical curve for most modulus tests performed

Fig. 4.3 Typical Stress-Strain Curves from Concrete MOE Tests
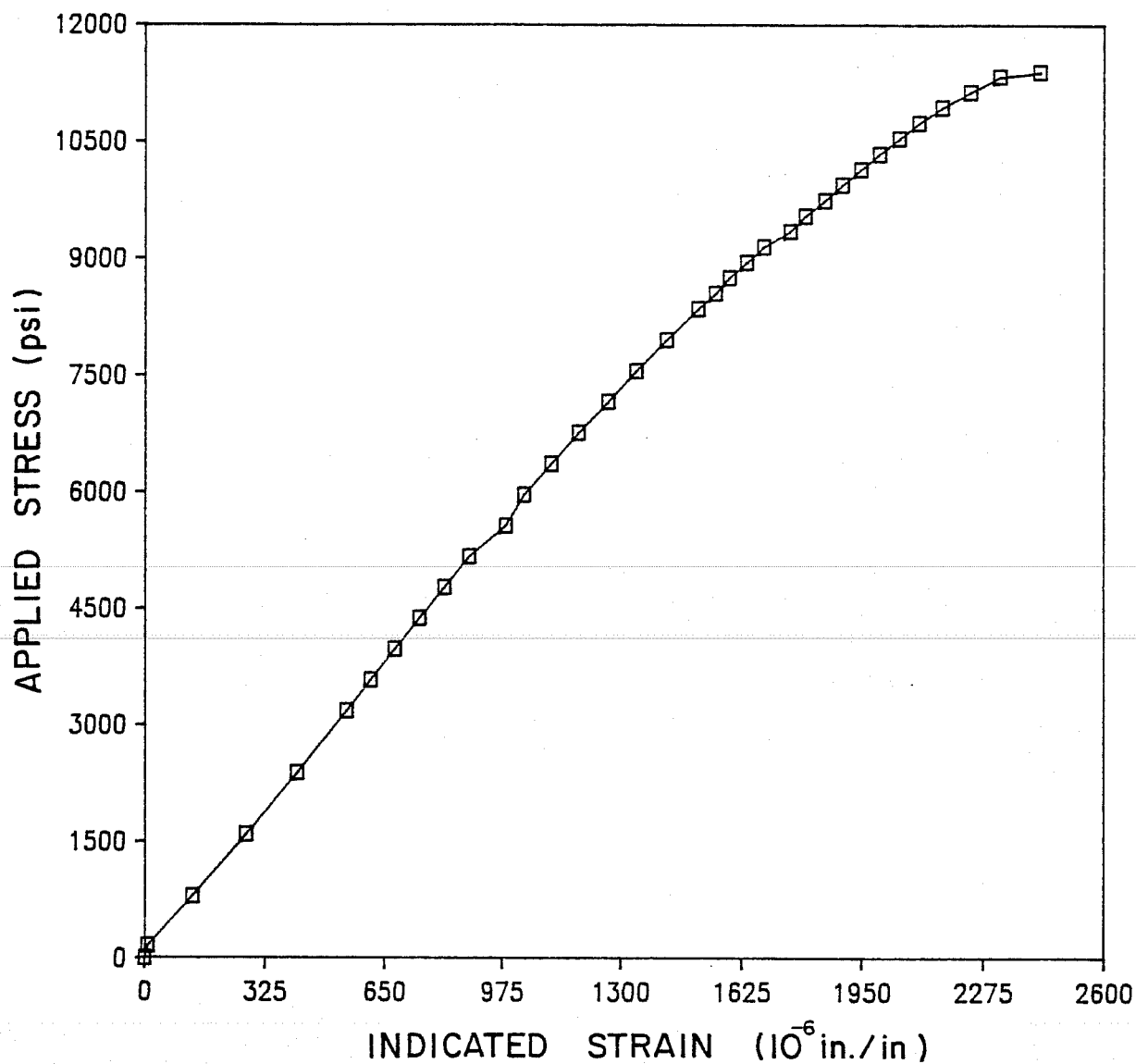
b) typical full ascending branch of stress-strain curve

Fig. 4.3 Typical Stress-Strain Curves from Concrete MOE Tests
(cont'd)
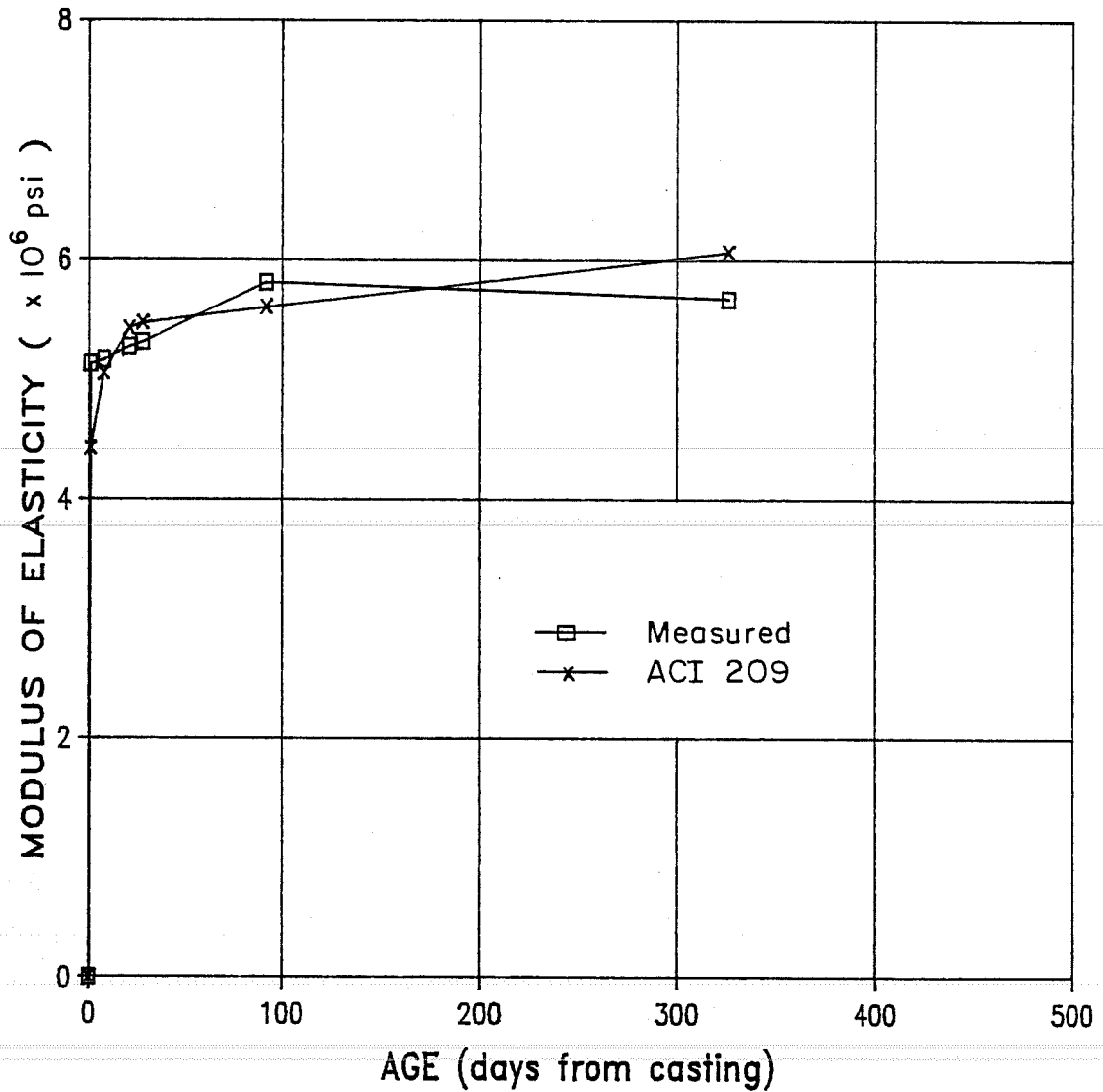
a) measured and predicted MOE curves for specimens L-I1&2

Fig. 4.4   MOE vs. Time Curves for Concrete from Field Specimens
Investigated
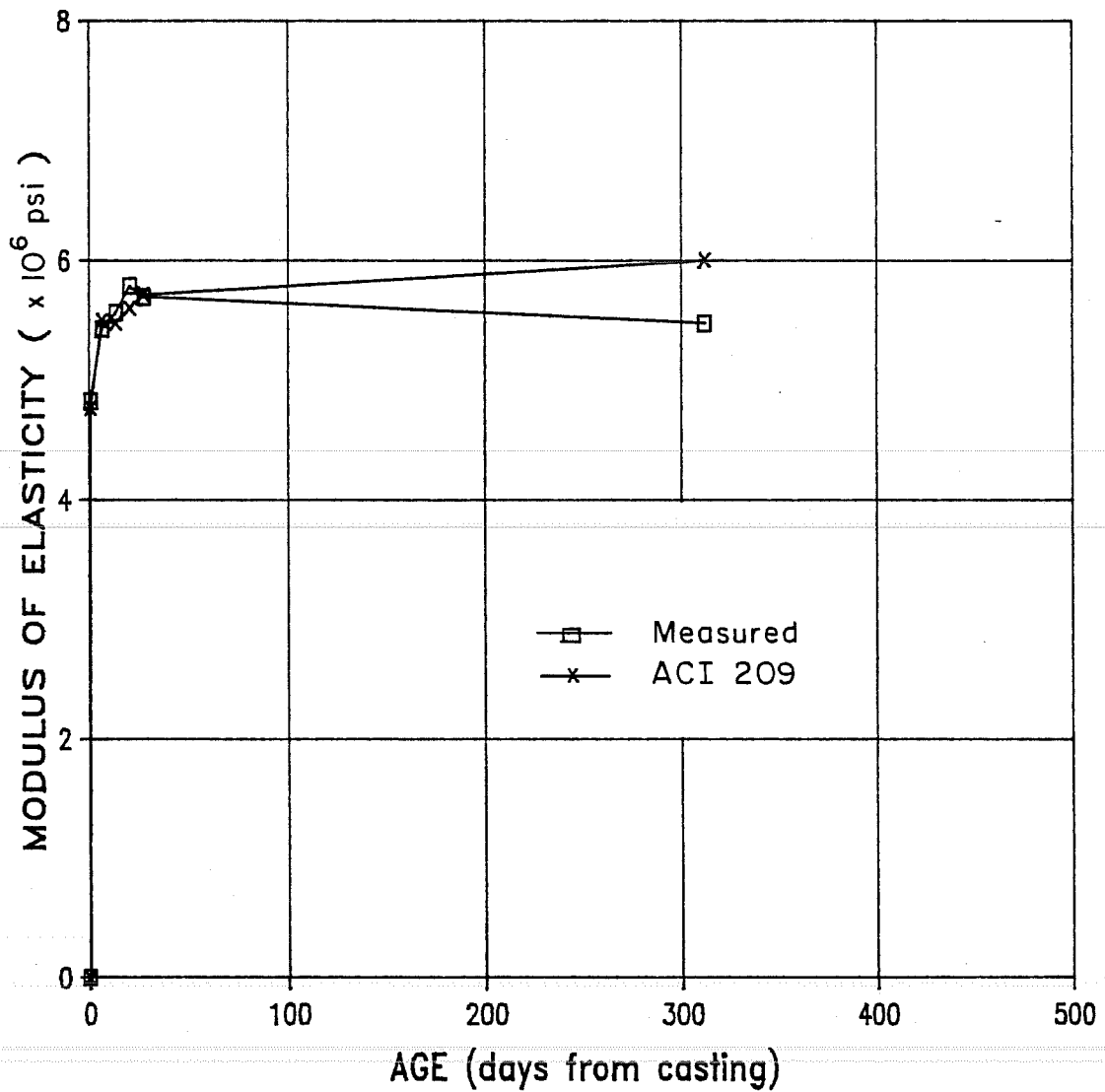
b) measured and predicted MOE curves for specimens L-01&2

Fig. 4.4 MOE vs. Time Curves for Concrete from Field Specimens
         Investigated (cont'd)
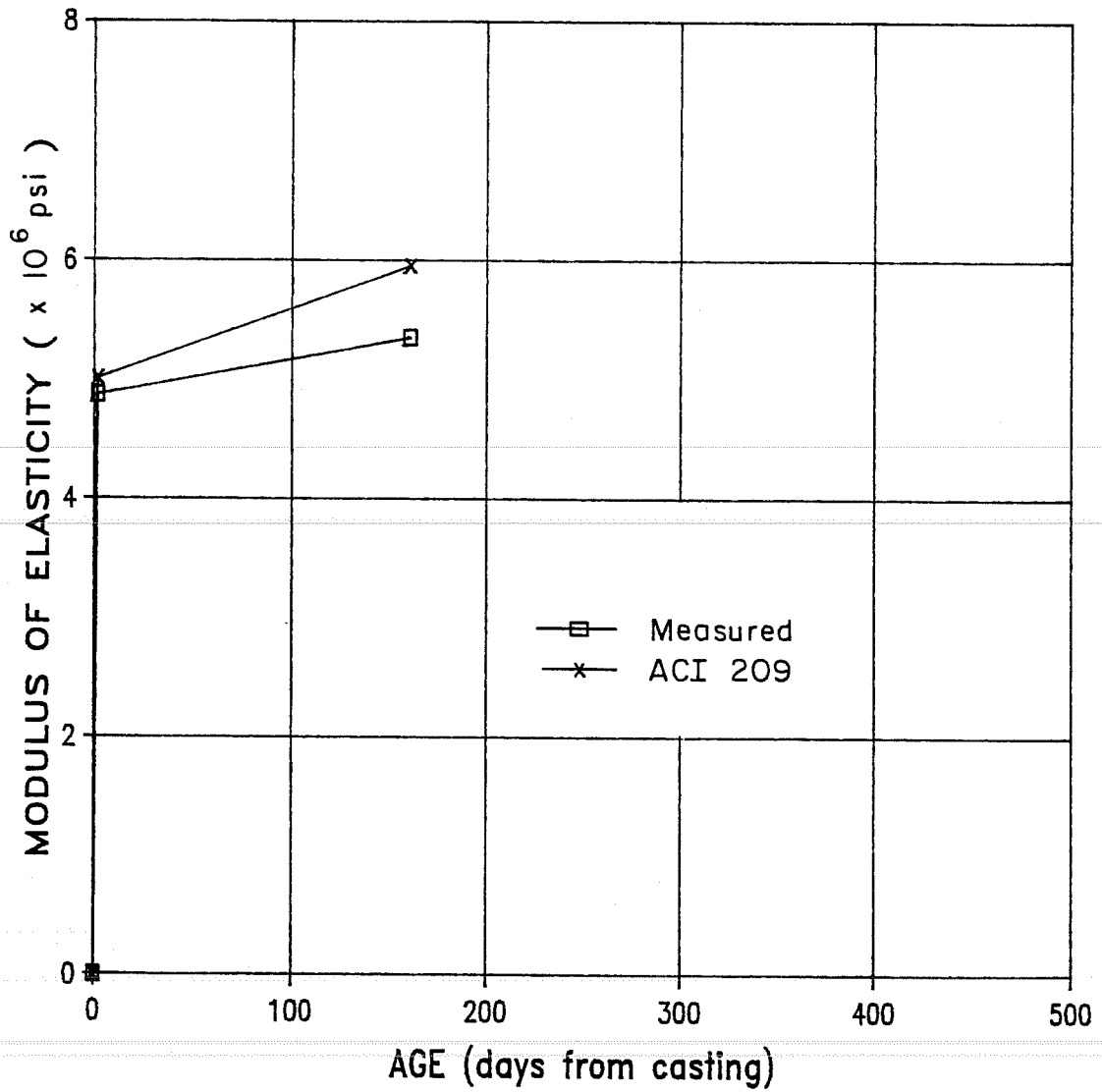
c) measured and predicted MOE curves for specimens H-01&2

Fig. 4.4 MOE vs. Time Curves for Concrete from Field Specimens
        Investigated (cont'd)
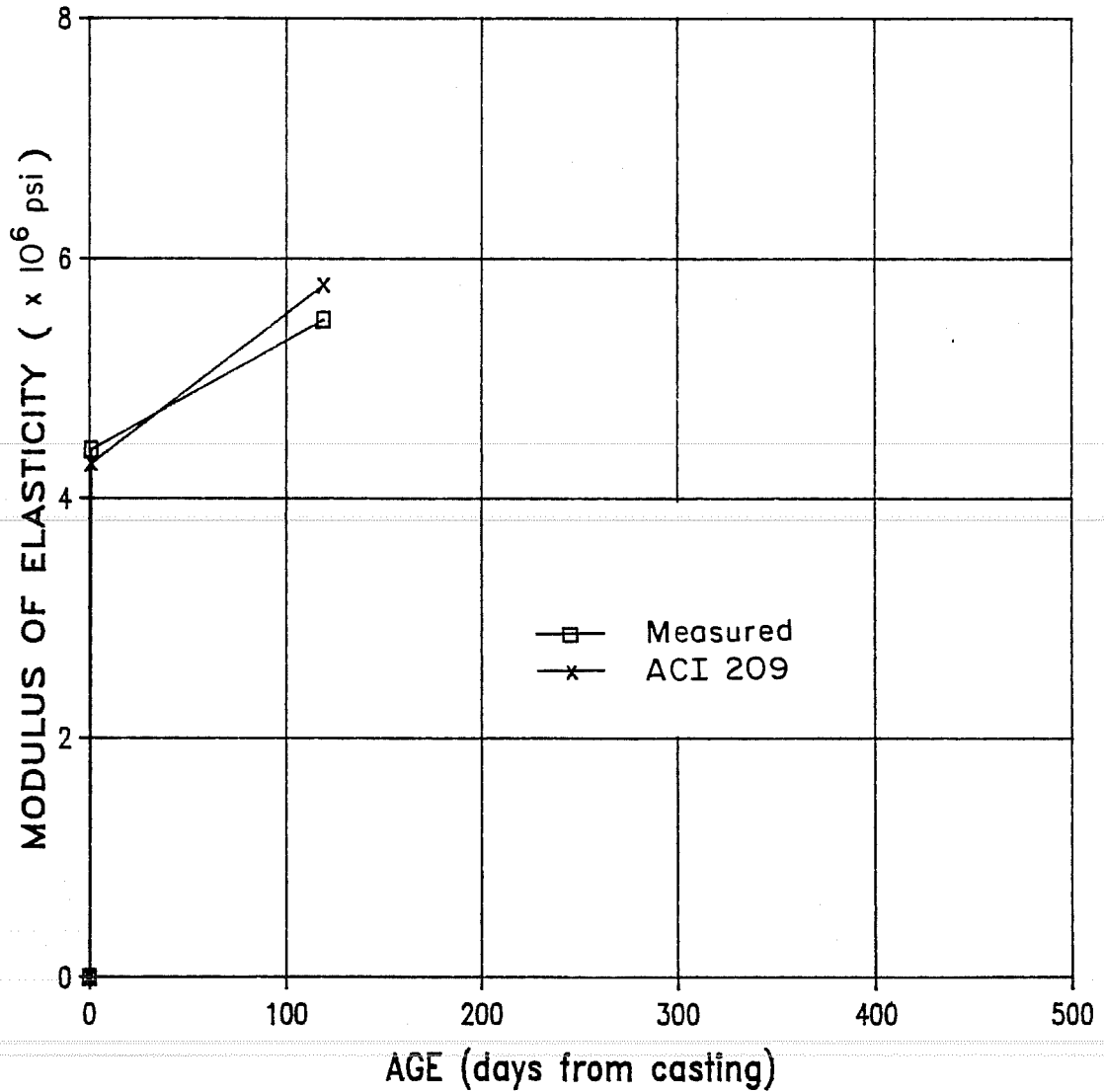
d)   measured and predicted MOE curves for specimens H-I1&2

Fig. 4.4   MOE vs. Time Curves for Concrete from Field Specimens
           Investigated (cont'd)

static modulus of elasticity for each specimen casting. The measured values are compared with the ACI 209 recommended functions. As was true with strengths, the early static modulus of elasticity predicted by the ACI 209 recommended function, $33w^{1.5}$ f'_c, is lower than the measured values but not as much as was the case with measured and predicted strengths and not for every casting (i.e., H-O series beam concrete had a lower measured initial modulus than was predicted). The compressive strength, f'_c, used to calculate the ACI 209 static modulus of elasticity is that measured rather than calculated.

If the ACI strength-gain function coupled with the ACI elastic modulus function were to be used in the analysis of girder camber, both the upward effect of eccentric prestress force and downward effect of the elastic loss of prestress would be overestimated.

4.2.4 Creep and Shrinkage Tests. Of the six creep and four shrinkage tests performed, only one of each was attempted under controlled environmental conditions. However, the relative humidity for this control test was allowed to vary from 62% to 83%. All test results must be interpreted, therefore, in light of the actual environmental conditions under which they were performed as mentioned previously. The remaining five creep tests and three shrinkage tests were performed outside the laboratory about 45 miles north of the plant but in conditions

quite similar in terms of general climate. However, tests CT-L-I and CT-L-O were both begun inside the laboratory and later transported to the outdoor testing area.

4.2.4.1 Creep Test Apparatus and Equipment. A typical apparatus used to load the creep specimens was shown in Fig. 2.12. The four steel bearing plates are 18 in. in diameter, 3.125 in. thick, and weigh about 225 lbs each. The three rods are 1.125 in. diameter by 6 ft long, A490, Grade B-7 all-threads. The three spring assemblies are each made up of two railroad car springs. The inner spring is 7.5 in. long and 4.25 in. in diameter. The outer spring is 8.25 in. long and 8 in. in diameter. The combined stiffnesses of the three spring assemblies for each creep test performed as determined at the time of loading are given in Table 4.3. The springs are spaced on 120 degree radii measured from the center of the plate and are as close together as possible. Next to each threaded rod is mounted a dial gage with least divisions of 0.001 in. The purpose of the dial gage is to:

1. determine the stiffness of the three-spring assemblies based on known changes of load during the initial loading of the specimens, and

2. monitor the change in load by measuring the average change in dial gage reading and multiplying this

average by the characteristic stiffness of the set of springs as determined in 1 above.

The characteristic spring stiffnesses for each creep test performed are given in Table 4.3 as previously noted. Initial loads were applied to the specimens using a 60 ton capacity hydraulic ram with an effective ram area (ERA) of 13.75 in ^{2}. Thus, the maximum allowable pressure at full load is 8727 psi. Upon initial loading of each set of creep specimens load was monitored by a strain indicator connected to a 100 kip capacity load cell placed between the hydraulic ram and the spherical head. The spherical head bore against the uppermost plate of the creep frame assembly. The load cell was calibrated on three different occasions using two different testing machines. The first two sets of creep cylinders were loaded in 5 kip increments based on the first calibration of the load cell while subsequent creep cylinders were loaded based on the second calibration. A third calibration was determined and an average curve used in the final evaluation of the creep tests load data. The difference of the indicated loads between the first and second calibrations and between the first calibration and the curve assumed in the data reduction is 7.53% and 4.44% respectively with the assumed curve falling between the other two. Thus, it is concluded that the loads assumed to be applied to all creep specimens based on load cell readings using an

TABLE 4.3 Characteristic Spring Stiffnesses
for Each Creep Test

Test	Spring Stiffnesses
CT-L-I	51.49 k/in.
CT-L-O	50.61 k/in.
CT-H-OTF	57.83 k/in.
CT-H-OBF	60.98 k/in.
CT-H-OAVE	60.67 k/in.
CT-H-ISTD	53.44 k/in.

TABLE 4.4 Creep Cylinders Information

Test	Date Cast	From Batches	Measured Slumps	Age at Loading
CT-L-I	06/25/84	1 & 2	7" & 4"	2 days
CT-L-O	07/09/84	1 & 2	2.25" & 5.5"	3 days
CT-H-OTF	10/02/84	1 & 2	8.875" & 8.5"	7 days
CT-H-OBF	10/02/84	1 & 2	8.875" & 8.5"	7 days
CT-H-OAVE	10/02/84	1 & 2	8.875" & 8.5"	10 days
CT-H-ISTD	11/12/84	1 & 2	7.25" & 9.25"	3 days

assumed average calibration curve are probably within ± 4% of the actual load magnitudes.

Concrete strains were measured on both the creep cylinders and the shrinkage, or "control", cylinders using the Demec system employed in the field.

4.2.4.2 Creep and Shrinkage Test Specimens. Table 4.4 contains relevant information concerning the creep specimens tested. Design information for each field casting has been previously given in Table 4.1.

For each creep and shrinkage specimen, the stainless steel gage points were located on three equally spaced lines oriented along the loading axis of the specimen and intersecting 120 degree radii at the top and bottom of the specimen. Circumferential lines were drawn approximately 2 in. from either end of the specimen. Using the Demec point setting bar gage points were attached with epoxy at each intersection of a longitudinal and circumferential line. This same procedure was used for setting points on the shrinkage, "control", cylinders.

Immediately after lines were drawn on the creep cylinders and before gage points were attached, each set of creep cylinders was joined together by:

1. clamping a cylinder mold casing around one of the cylinders,

2. pouring a 3/8-in. layer of hydrostone, a fast setting cement compound, into the cylinder mold on top of the upright cylinder,

3. sliding the second cylinder down inside the cylinder mold, pressing it against the hydrostone covered cylinder, and

4. clamping the cylinder mold casing tightly against the top cylinder.

After about 30 minutes the hydrostone was set and the cylinder mold casing could then be loosened and slid up the top cylinder far enough to provide forming for a 3/8-in. hydrostone cap. After leveling to ensure perfect vertical allignment the top cylinder was capped with hydrostone and the whole cylinder assembly flipped over to perform the same opperation on the opposite end. Much care was taken to ensure that the caps poured were as close to being perpendicular to the loading axis of the cylinders assembly as possible. These joining and capping procedures were employed to help minimize eccentric and non-uniform loading.

4.2.4.3 Loading and Monitoring Procedures. The procedures used in loading and monitoring the creep specimens can be divided into three major parts:

1. initial loading with previous and subsequent recording of Demec readings,

2. load monitoring with subsequent recording of Demec readings,

3. load adjustment with previous and subsequent recording of Demec readings.

The purpose of the initial loading portion of the procedures was to:

1. apply a load to the specimen of a magnitude close to the target load, and

2. establish the characteristic stiffness of the set of railroad springs so that the load could be monitored subsequently based on changes in dial gage readings.

The load monitoring portion of the procedures involved the recording of dial gage readings immediately before taking Demec readings so that the sustained load applied to the cylinders could be estimated. The load adjustment was desired whenever the sustained load was more than 2% lower than the target load. Unfortunately, for all but tests CT-L-I and CT-L-O, the adjustment was neglected resulting in sustained loads as much as 7% lower than the target load. Table 4.5 contains information concerning the initial loading and load maintenance for creep test performed.

The target loads (converted to applied stresses in Table 4.5) are the averages of the smallest and largest loads estimated to be applied to the creep cylinders at any time during

Table 4.5 Creep Test Information

Test	Initial Applied Stress	Target Applied Stress	Var. in Applied Stress	Initial Elastic Strain	Indicated Elastic Modulus	Status of Test
CT-L-I	2602 psi	2603 psi	1.92%	.000673	3,865,000	Ongoing
CT-L-O	2860 psi	2771 psi	4.22%	.000689	4,148,000	Terminated
CT-H-OTF	921 psi	860 psi	7.01%	.000212	4,352,000	Ongoing
CT-H-OBF	2374 psi	2299 psi	4.04%	.000504	4,714,000	Ongoing
CT-H-OAVE	1633 psi	1605 psi	3.02%	.002826	5,780,000	Ongoing
CT-H-ISTD	2211 psi	2091 psi	6.23%	.000462	4,784,000	Ongoing

the testing period. For tests CT-L-I and CT-L-O initial loading to a stress level of $0.4f'_c$ based on f'_c at the time of loading was attempted. Thus target loads for these two tests reflect the relative strengths of the specimens at the age of loading. For tests CT-H-OTF, CT-H-OBF and CT-H-OAVE initial loadings to stress levels of 876, 2270, and 1570 psi respectively were sought. This was done in an attempt to model the stresses at the top, bottom and an intermediate fiber of the girders at the time of release of prestress. These stress magnitudes were determined from an unpublished prestressed concrete design program called BRIDGE [49]. Unfortunately, because of time constraints, it was not possible to model the creep behavior of the girder concrete very well. The companion creep cylinders could not be loaded until 7 to 10 days of age while the girder concrete was loaded at an age of slightly less than one day. For the final creep test, CT-H-ISTD, an attempt was made to load the cylinders to $0.4f'_c$ based on f'_c at the time of loading. However, because of mechanical problems with the testing frame, this was not achieved. Thus, the target load for this test was something less than 40% of the cylinder strength at the age of loading.

4.2.5 <u>Creep</u> <u>and</u> <u>Shrinkage</u> <u>Tests</u> <u>Results.</u> The results of creep and shrinkage tests for each test performed are illustrated in Figs. 4.5a through 4.9b. It should be remembered
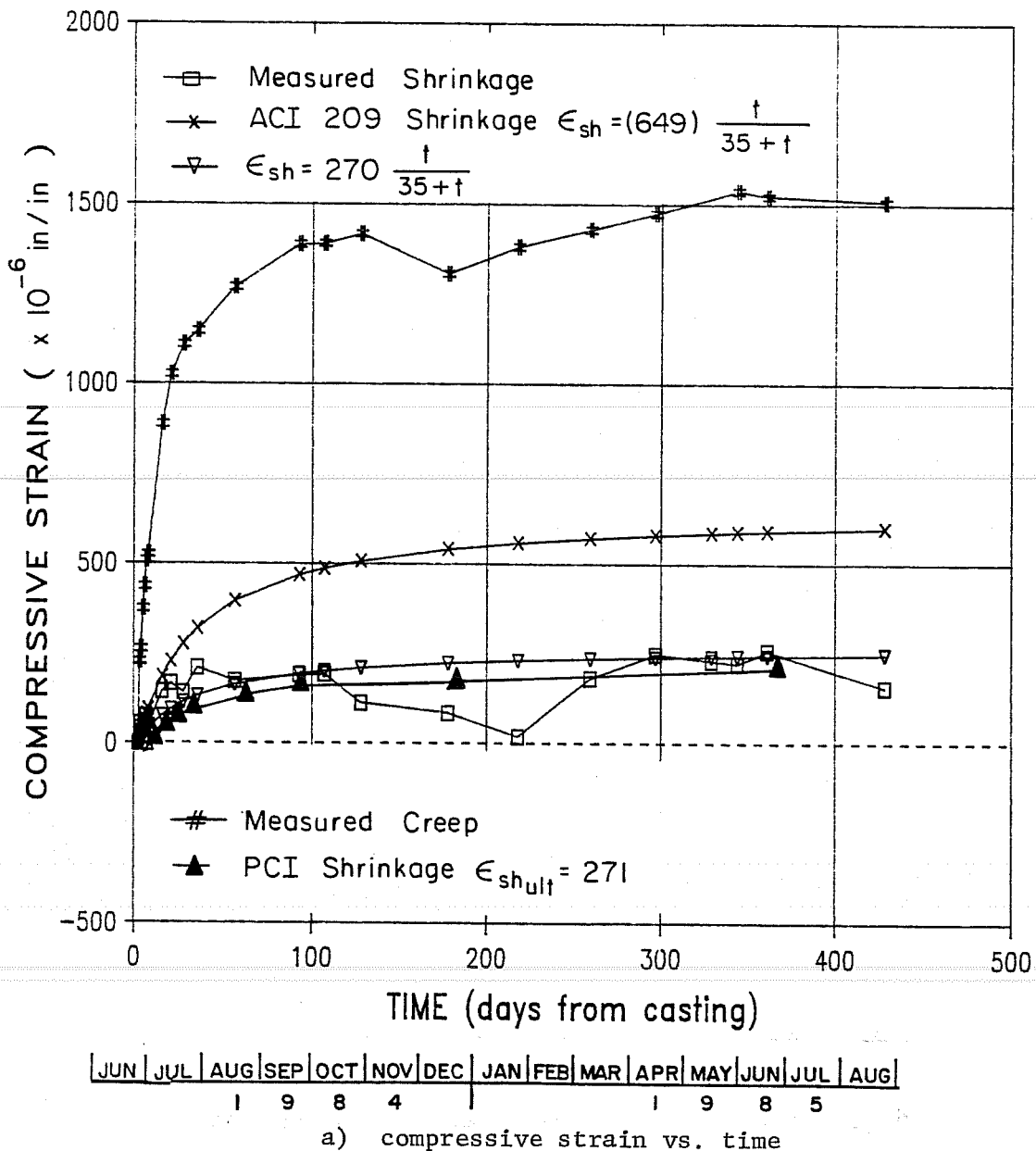
a) compressive strain vs. time

Fig. 4.5 Measured and Predicted Creep and Shrinkage of Companion
Concrete Cylinders for Test CT-L-I
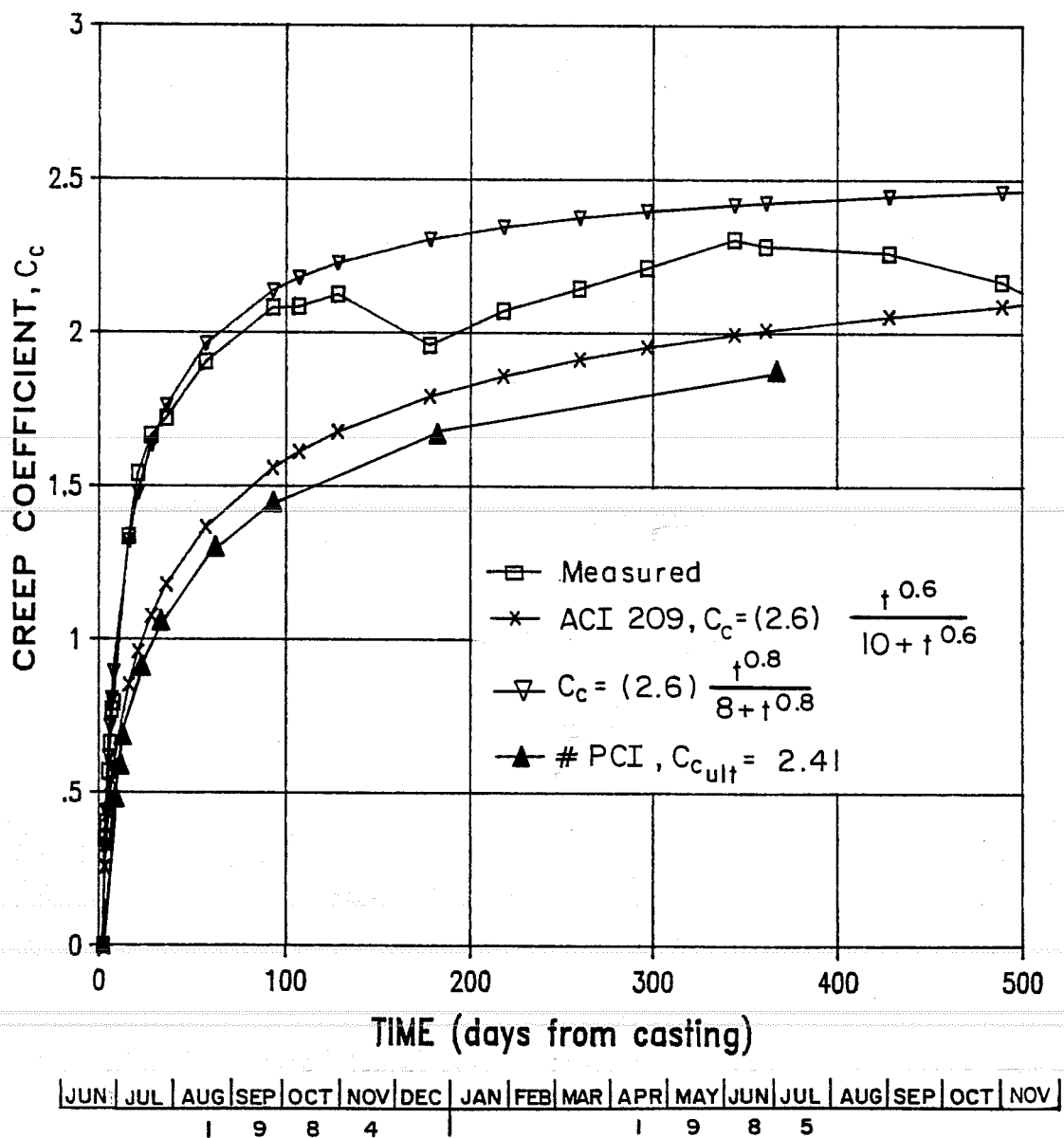
b)   creep coefficient curves

Fig. 4.5   Measured and Predicted Creep and Shrinkage of Companion
Concrete Cylinders for Test CT-L-I (cont'd)
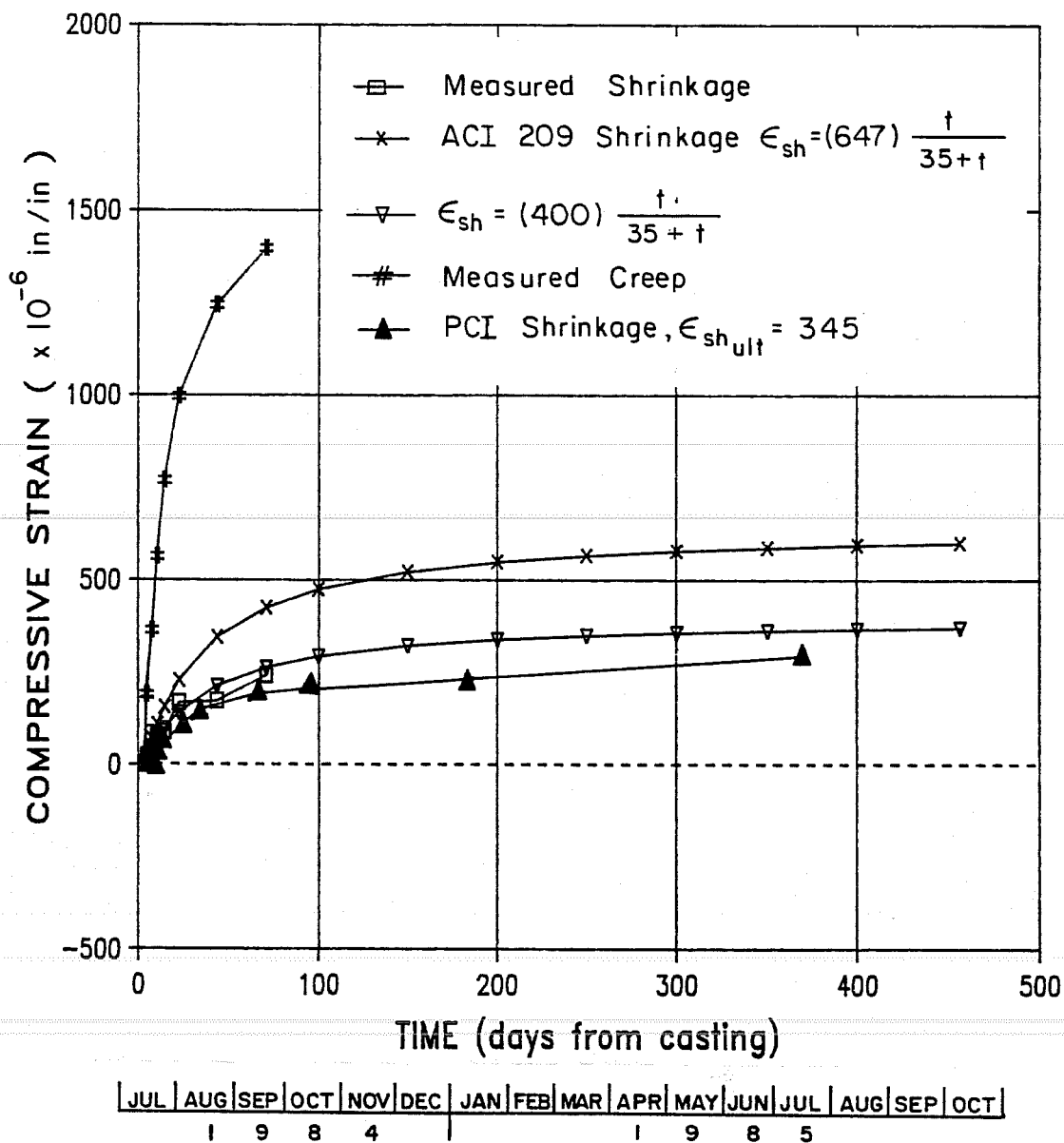
a) compressive strain vs. time

Fig. 4.6 Measured and Predicted Creep and Shrinkage of Companion Concrete Cylinders for Test CT-L-O
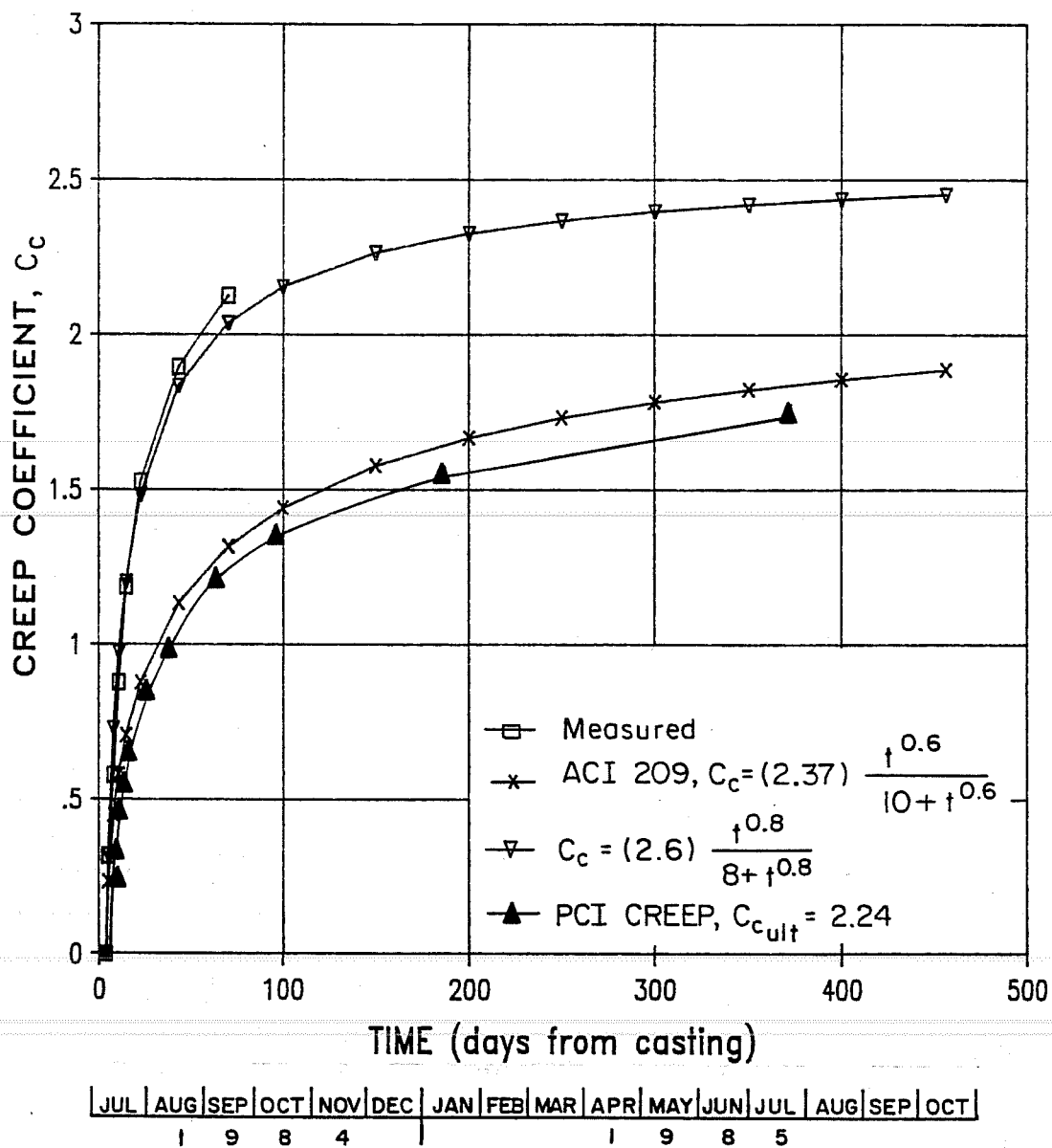
b) creep coefficient curves

Fig. 4.6 Measured and Predicted Creep and Shrinkage of Companion
Concrete Cylinder for Test CT-L-O (cont'd)
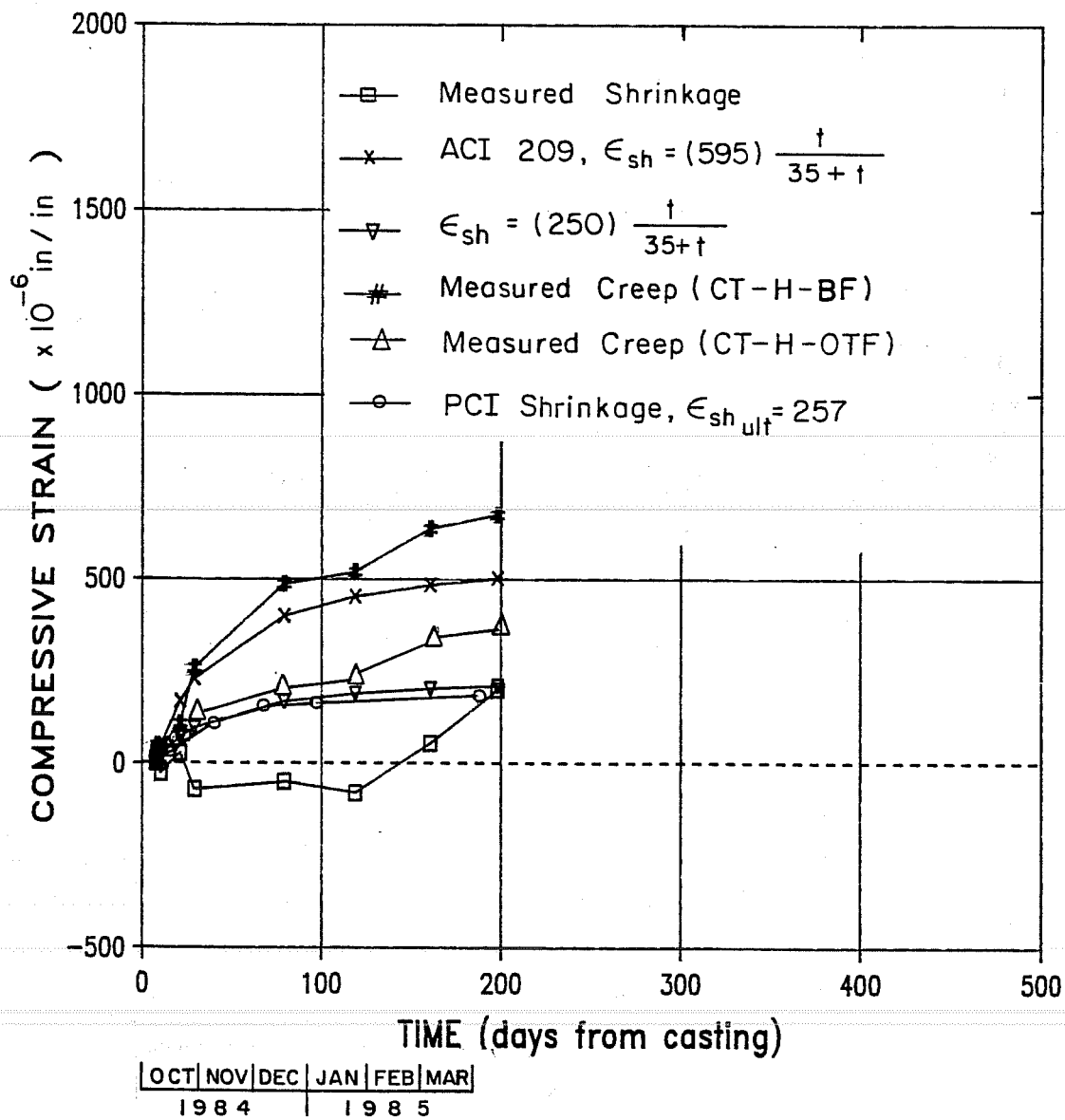
a) compressive strain vs. time

Fig. 4.7 Measured and Predicted Creep and Shrinkage of Companion
Concrete Cylinders for Tests CT-H-OTF and CT-H-OBF
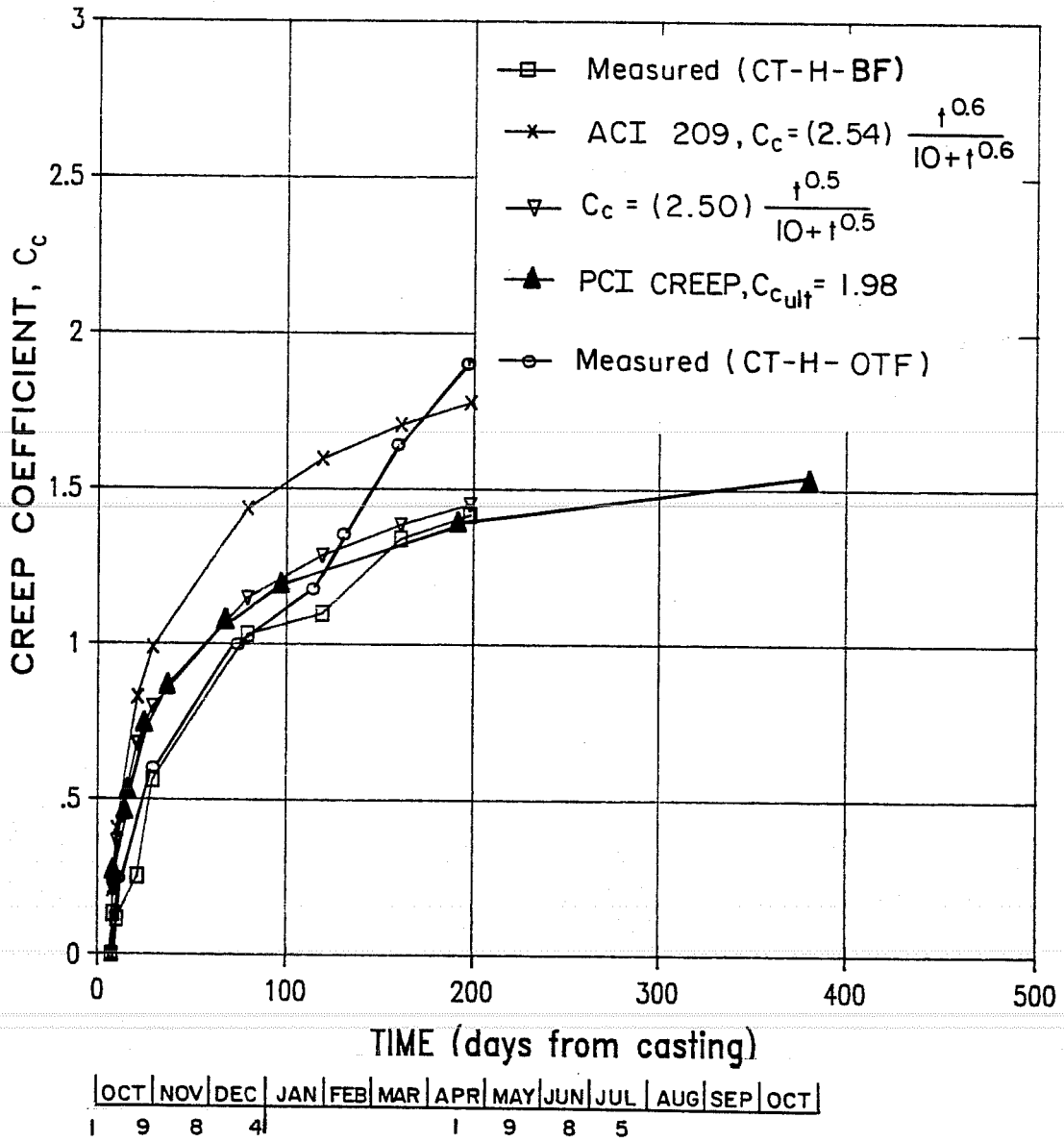
b) creep coefficient curves

Fig. 4.7 Measured and Predicted Creep and Shrinkage of Companion
Concrete Cylinders for Tests CT-H-OTF and CT-H-OBF (cont'd)
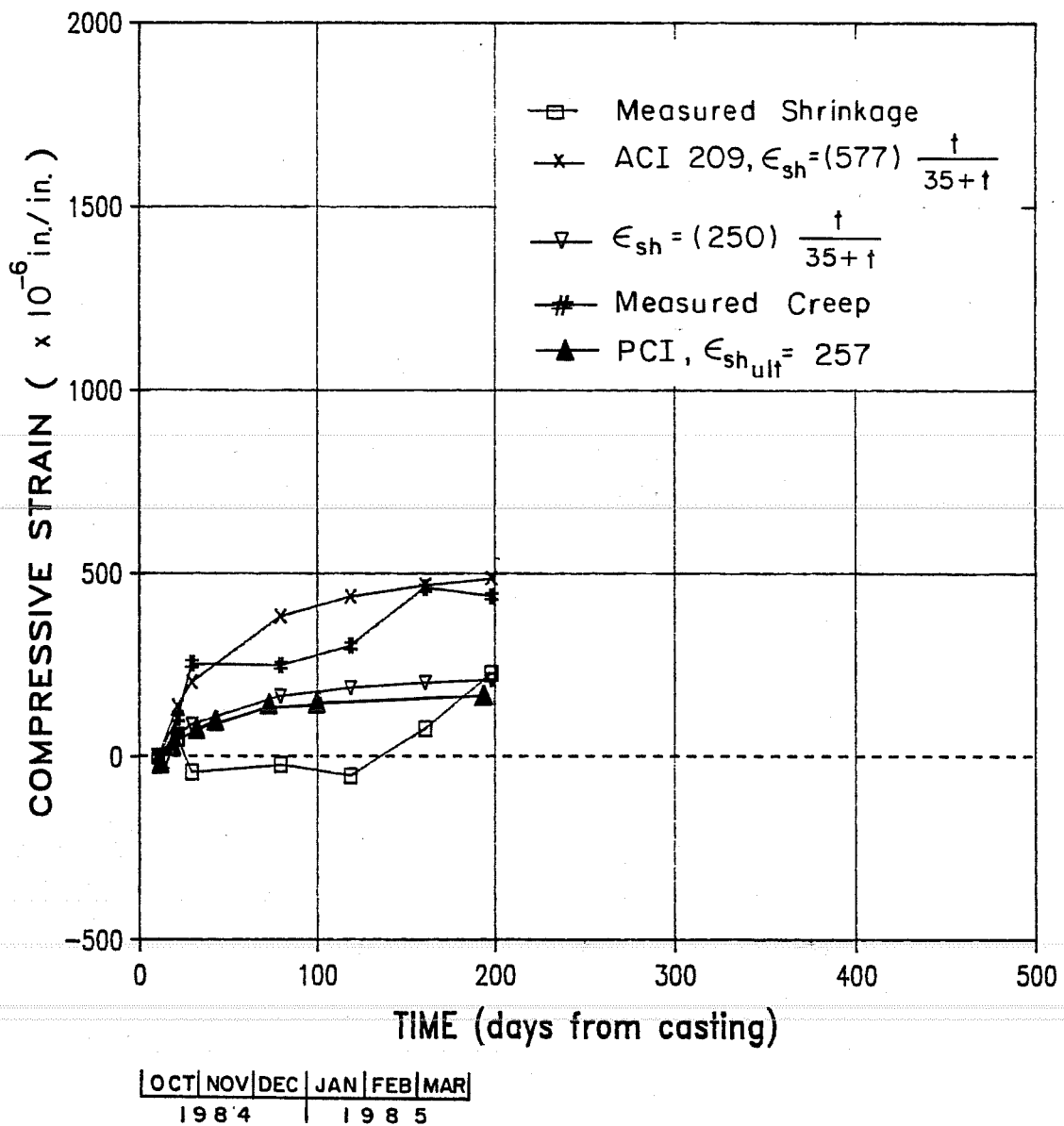
a)   compressive strain vs. time

Fig. 4.8   Measured and Predicted Creep and Shrinkage of Companion
Concrete Cylinders for Test CT-H-OAVE
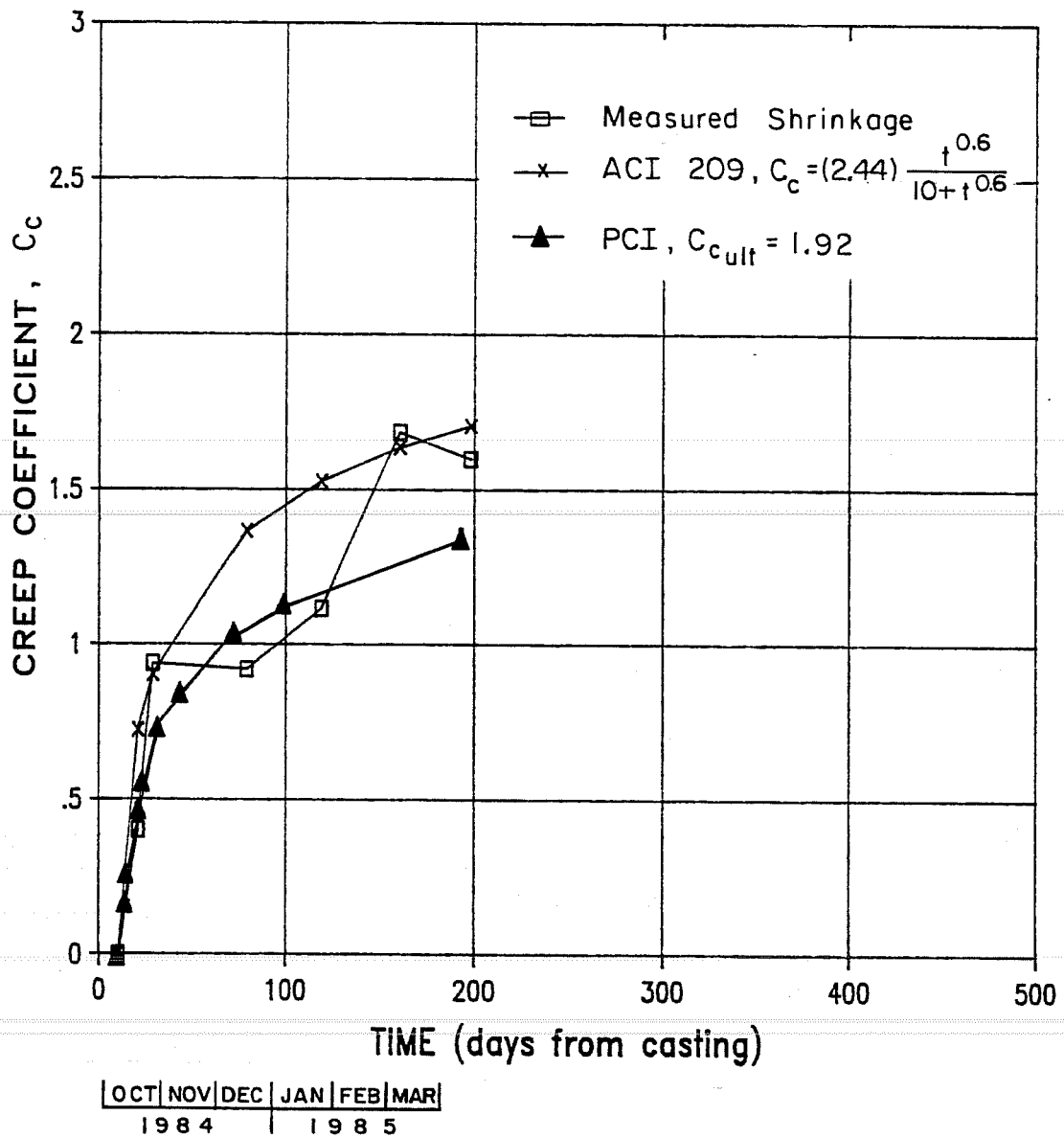
b) creep coefficient curves

Fig. 4.8   Measured and Predicted Creep and Shrinkage of Companion
Concrete Cylinders for Test CT-H-OAVE (cont'd)
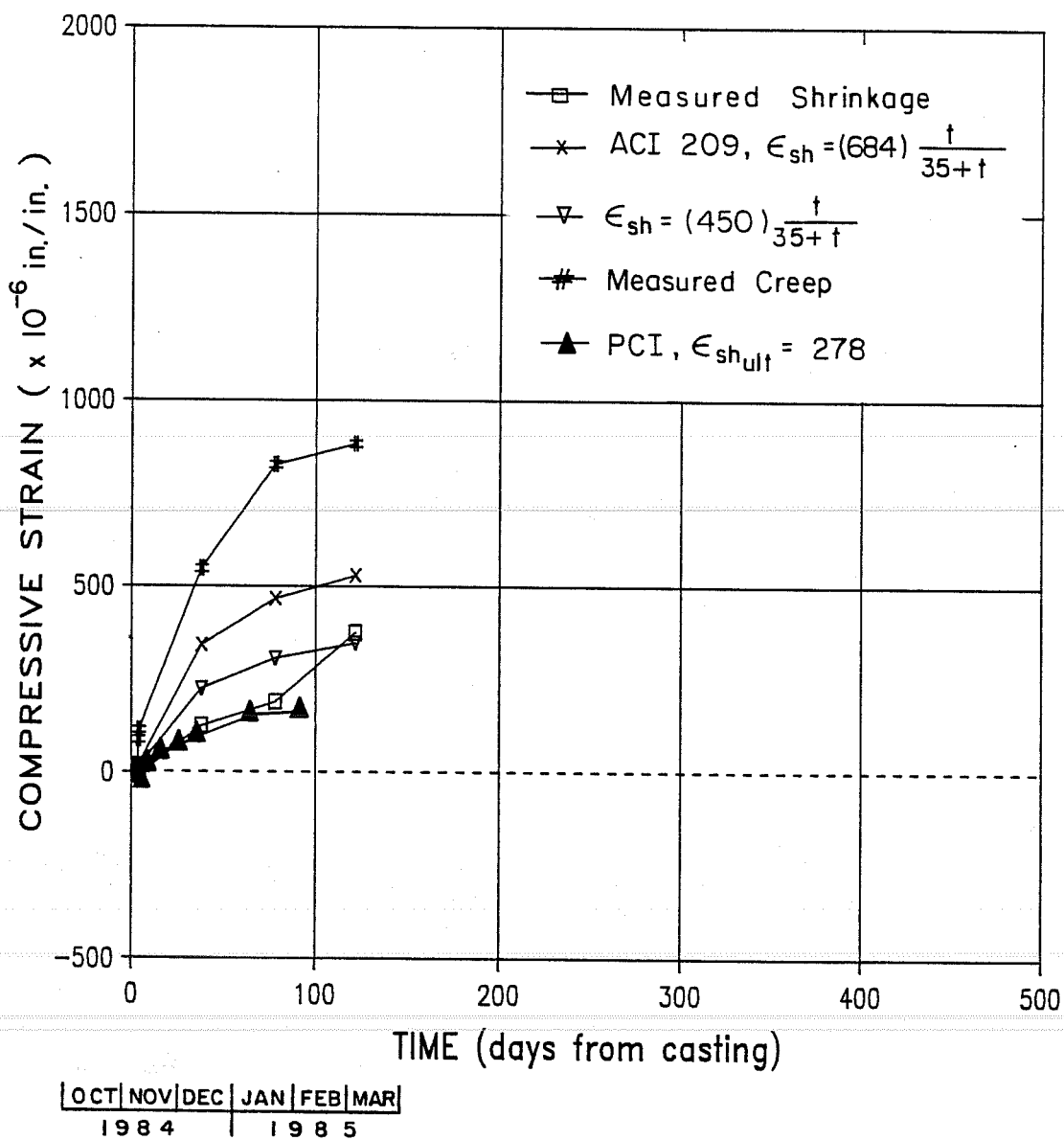
a) compressive strain vs. time

Fig. 4.9 Measured and Predicted Creep and Shrinkage of Companion Concrete Cylinders for Test CT-H-ISTD
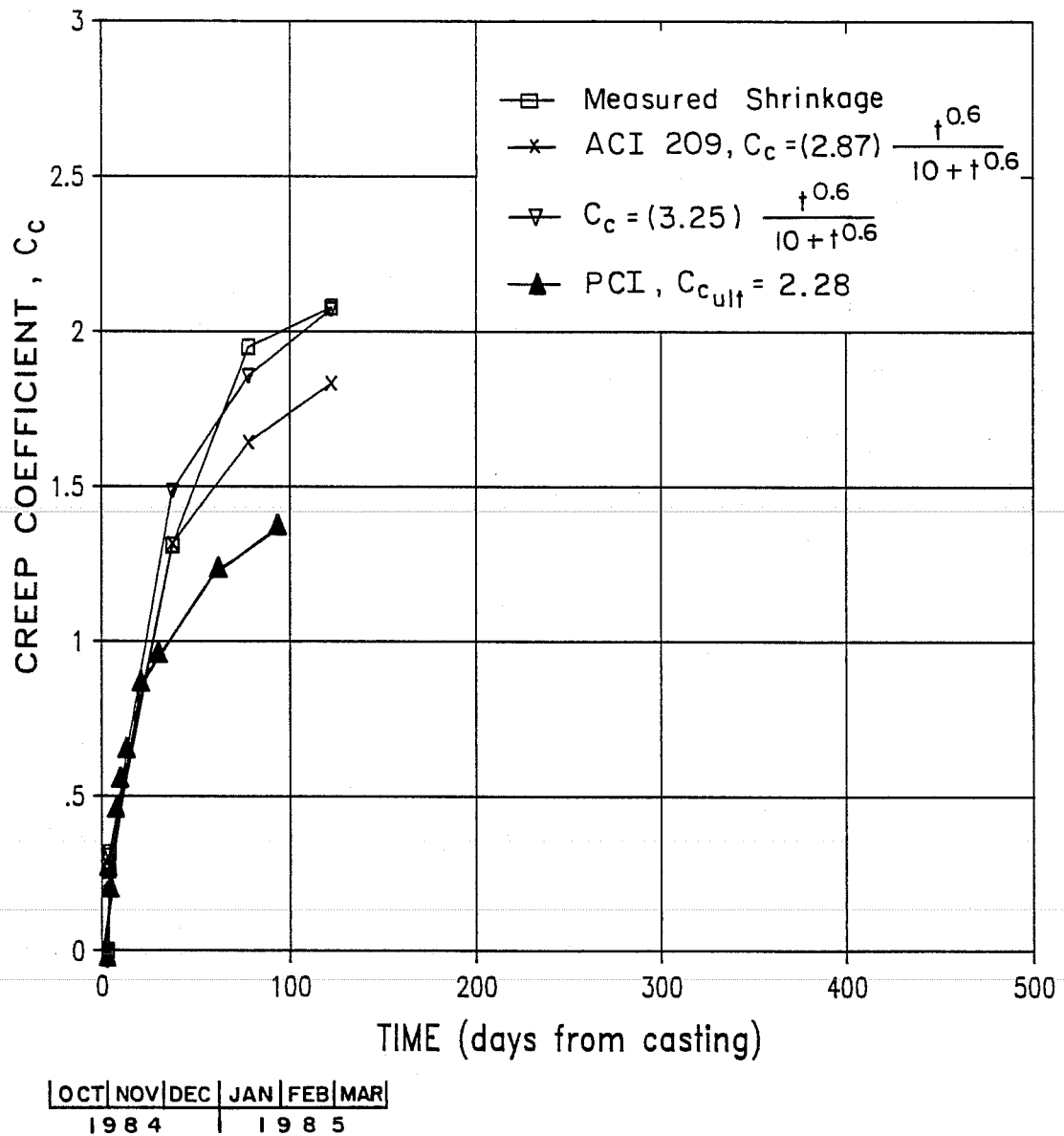
b) creep coefficient curves

Fig. 4.9   Measured and Predicted Creep and Shrinkage of Companion
Concrete Cylinders for Test CT-H-ISTD (cont'd)

that shrinkage cylinders were not placed in constant temperature and humidity environments.

In Fig. 4.5a, measured creep and shrinkage strains versus time are plotted against predicted shrinkage strains for Test CT-L-I. Both ACI 209 [2] and PCI Committee on Prestress Loss [36] recommended functions are used to predict shrinkage strains. Also, a fitted curve conforming to the shape and form of the ACI 209 recommended function is given. ACI 209 predicted shrinkage for most of the time was over twice that measured while the PCI Committee on Prestress Loss predicted shrinkage on the average was comparable to that measured for CT-L-I.

In Fig. 4.5b measured creep coefficient versus time is compared to predicted creep coefficient for Test CT-L-I. Both ACI 209 and PCI Committee on Prestress Loss recommended functions are used to predict creep coefficient curves. Also, a fitted curve corresponding to the form of the ACI 209 and the PCI Committee on Prestress Loss recommended functions yield creep coefficient versus time curves that underpredicted the measured creep coefficient for Test CT-L-I.

Figures 4.6a, 4.7a, 4.8a, and 4.9a are for CT-L-O, CT-H-OTF, and CT-H-OBF, CT-H-OAVE, and CT-H-ISTD respectively what Fig. 4.5a is for CT-L-I. The same conclusions regarding the relationships between measured and predicted creep and shrinkage apply to these last five tests as did to Test CT-L-I with the

exception that the measured creep coefficient curves for Test CT-H-OBF, CT-H-OTF, and CT-H-OAVE for the most part more closely fit the predicted curves. For test CT-H-OBF the ACI 209 predicted creep coefficient curve overpredicts the measured creep coefficient curve as it does for most of the time for the measured curve of Test CT-H-OTF.

4.3 Tests on Prestressing Steel

The prestressing steel engineering properties of interest, as noted in Sec. 2.1.2 were:

1.   time-relaxation relationships, and

2.   instantaneous elastic moduli.

In addition, tests needed to be performed to establish the indicated wire modulus based on the load-strain relationship of a SR-7 strain gage attached to an individual strand wire. This was necessary in order to properly interpret strand strain data gathered from the field specimen so that an evaluation of prestress loss due to strand shortening could be performed.

Tests were attempted in the laboratory to assess these prestressing steel properties but no reliable results were determined. As noted by Preston [40] the testing equipment and experience required to perform sufficiently accurate relaxation, strength and MOE tests on prestressing strand confines most such testing to the laboratories of prestressing steel suppliers.

Mill test reports and companion relaxation curves were obtained
from FWC and SWAI so that an assessment of strand properties
could be made. The proper strain strand properties (specifically
relaxation) could then be used as input into the analytical
model. This will be performed by Kelly [10].

PRESENTATION OF FIELD MEASUREMENTS

5.1   General

In this chapter the results of the field measurements
are presented and discussed. Measured cambers versus time for
each specimens are presented in Sec. 5.2. In Sec. 5.3 concrete
strains versus time are presented based on readings of the Demec
mechanical strain measuring system. Internal and ambient
temperature measurements and effects are discussed in Sec. 5.4.
Finally, strand strain data is discussed in Sec. 5.5.

5.2   Measured Time-Dependent Camber

Figures 5.1 through 5.8 and Table 5.1 detail the
measured time-dependent cambers for each beam investigated for
the period of time from casting of the beams until the beams were
placed on the bents at the bridge site. Note that immediate and
time-dependent cambers for each set of beams vary quite a lot
between sets. Contributing factors to these differences include:

1.   variations in concrete modulus of elasticity at the
time of prestress transfer,

2.   for initial cambers the time of taking readings for
each beam of a set causes differences in indicated
camber between beams,

Time Dependent Beam Camber
For Beam L-I1

Fig. 5.1 Measured Time-Camber of Specimen L-I1
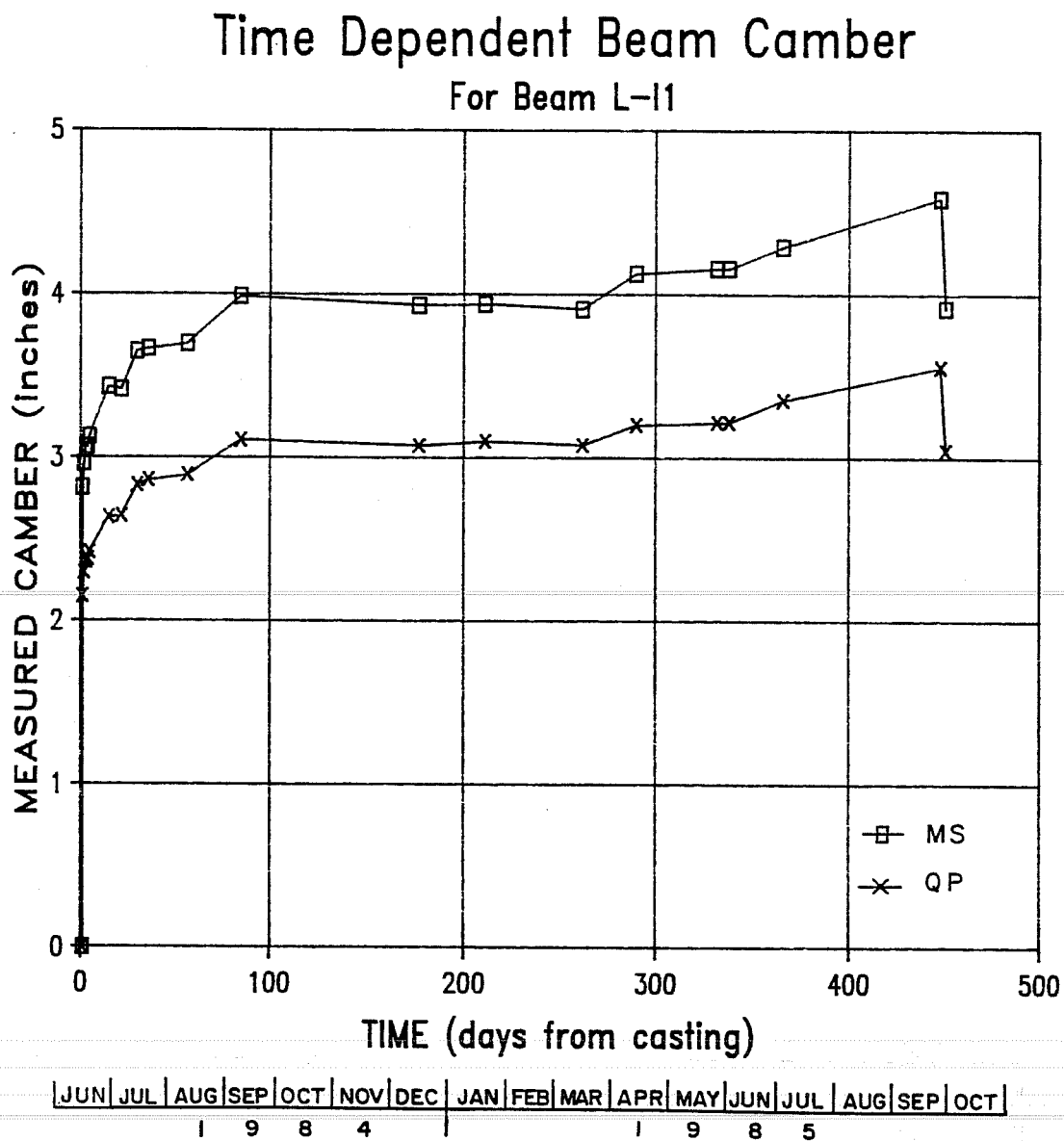
Time Dependent Beam Camber
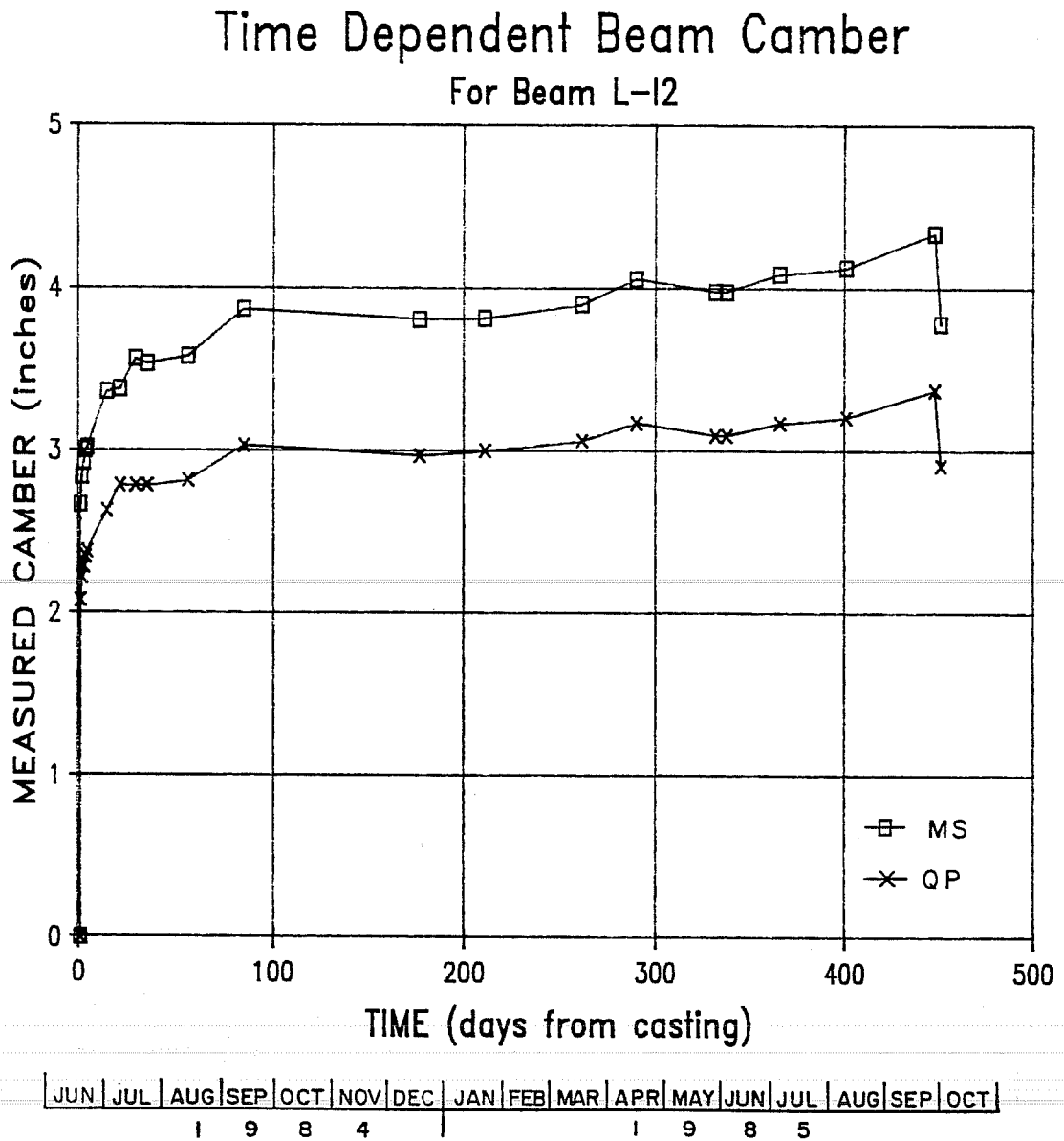
For Beam L-12

Fig. 5.2 Measured Time-Camber of Specimen L-I2

Time Dependent Beam Camber
For Beam L-01
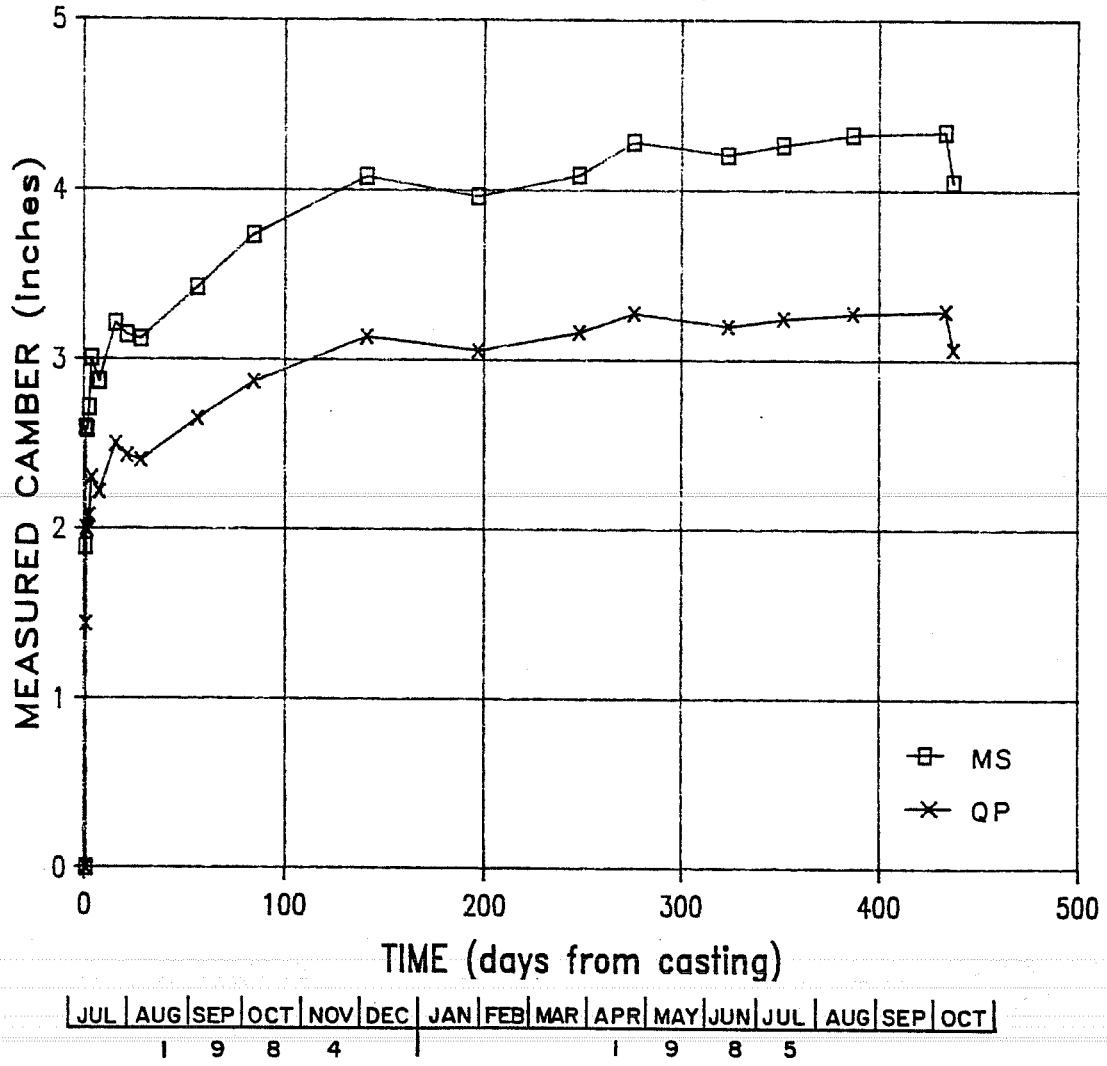
Fig. 5.3 Measured Time-Camber of Specimen L-01

Time Dependent Beam Camber
For Beam L-02
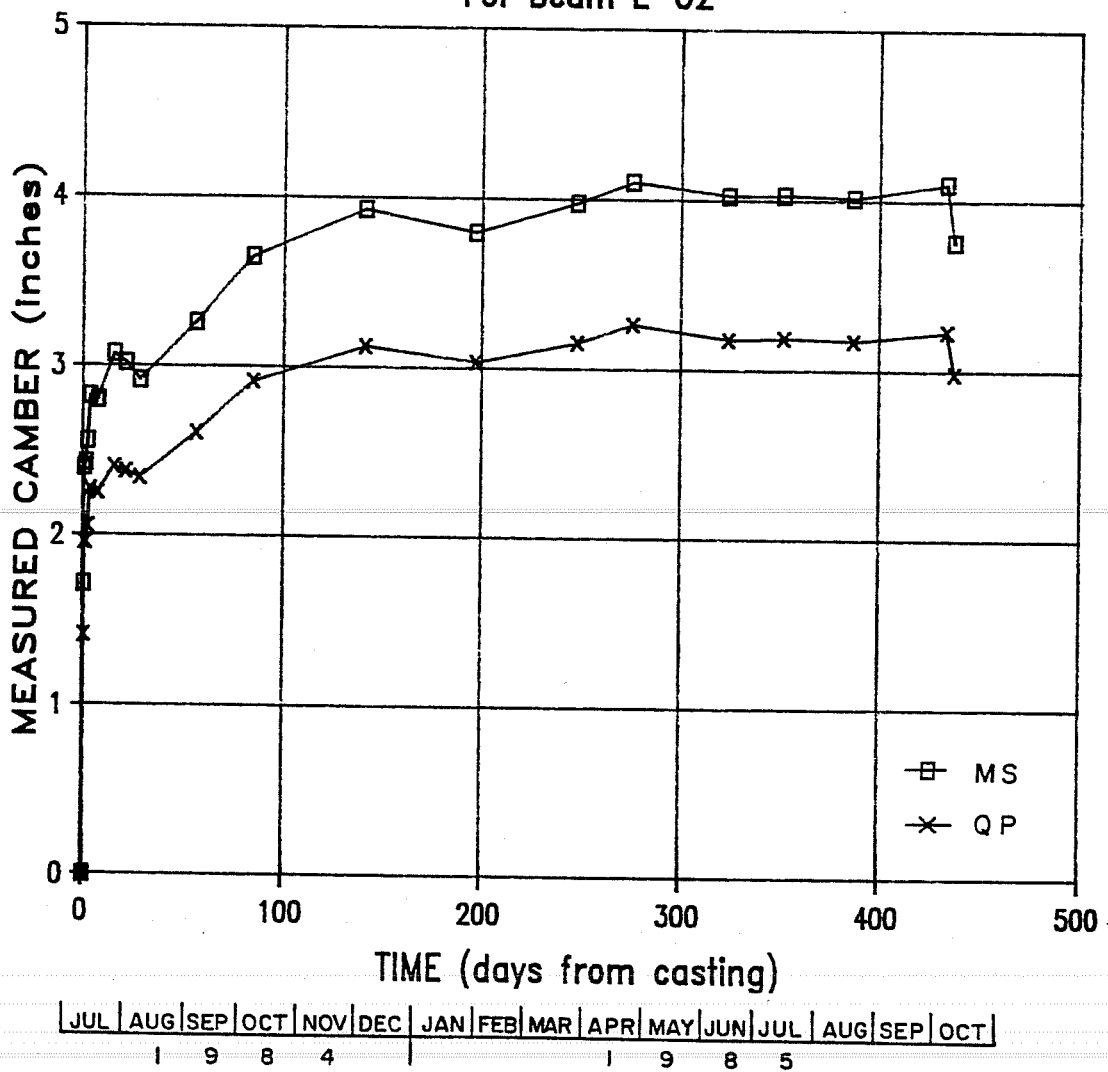
Fig. 5. 4   Measured Time-Camber of Specimen L-02

Time Dependent Beam Camber
For Beam H-01
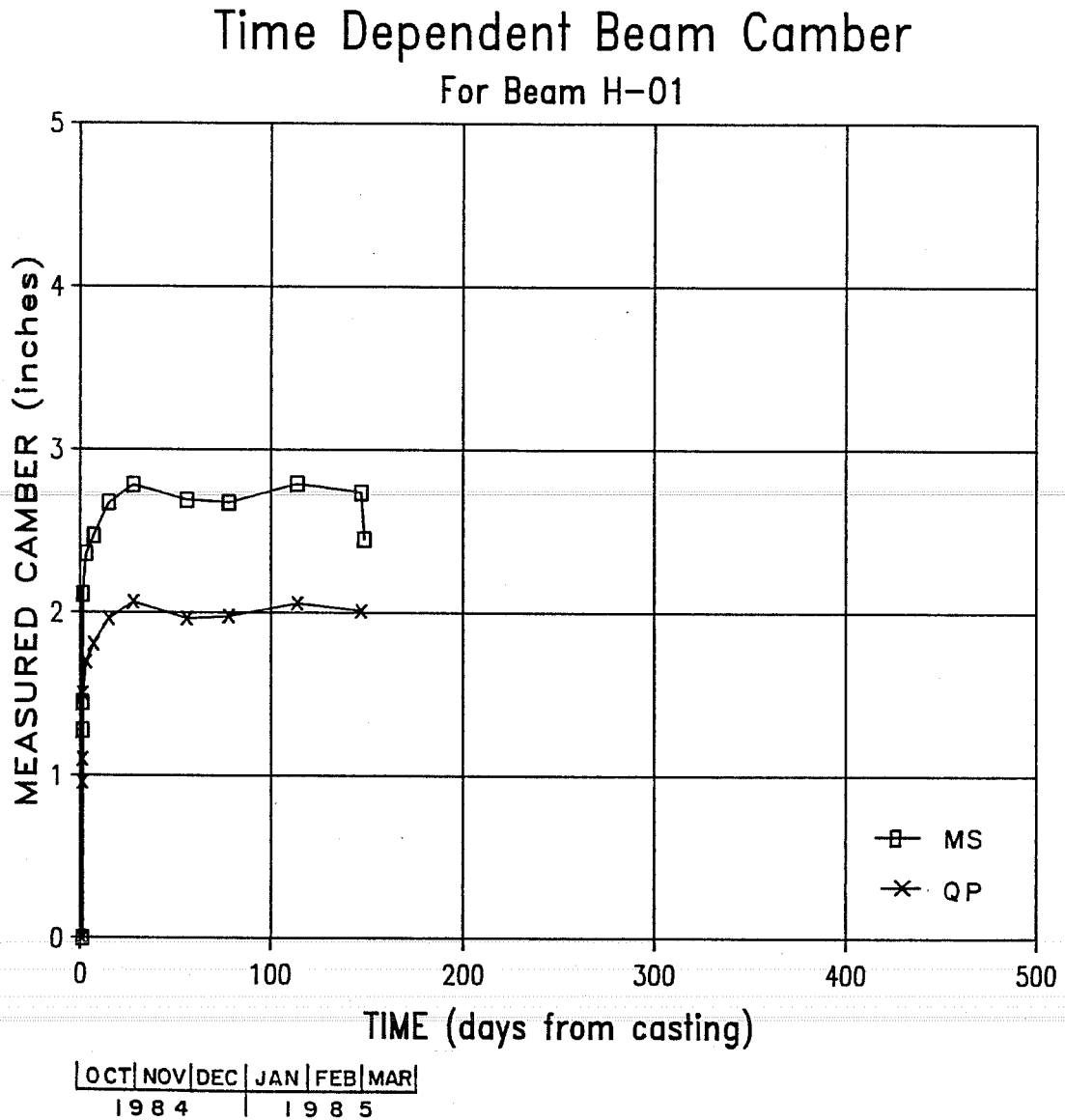
Fig. 5.5   Measured Time-Camber of Specimen H-01

Time Dependent Beam Camber

For Beam H-02
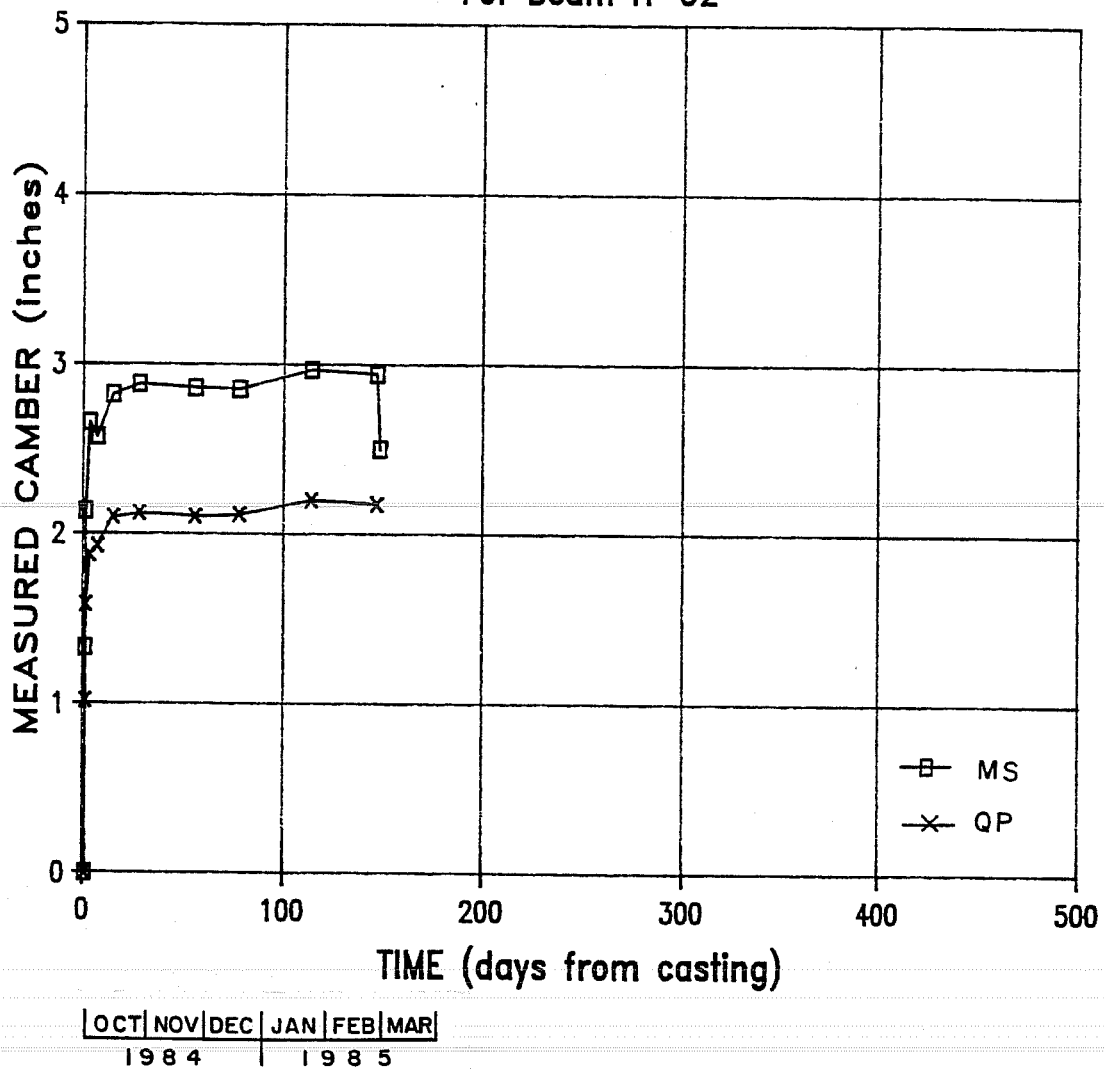
Fig. 5.6   Measured Time-Camber of Specimen H-02

Time Dependent Beam Camber
For Beam H–I1
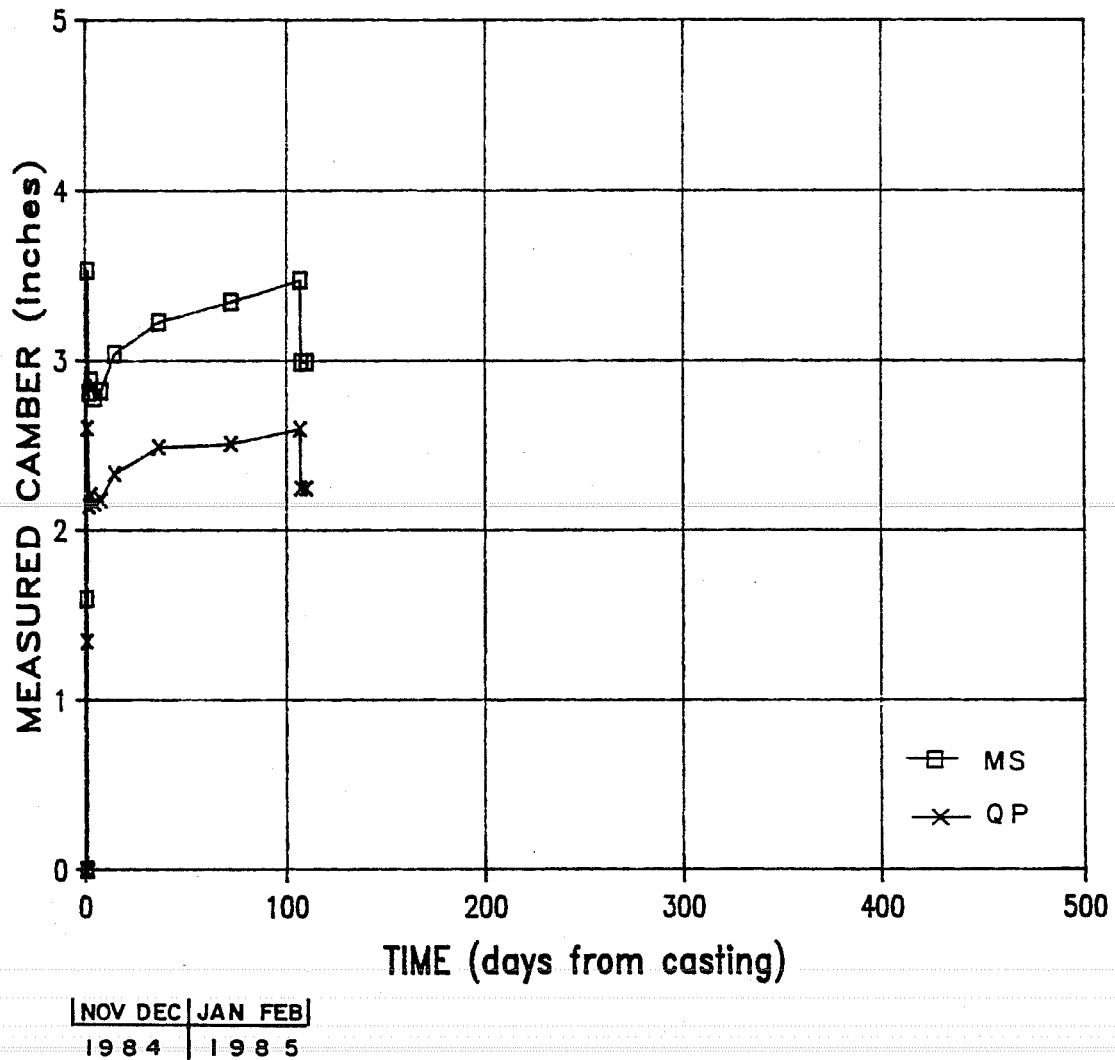
Fig. 5.7 Measured Time-Camber of Specimen H-I1

176

Time Dependent Beam Camber
For Beam H-12
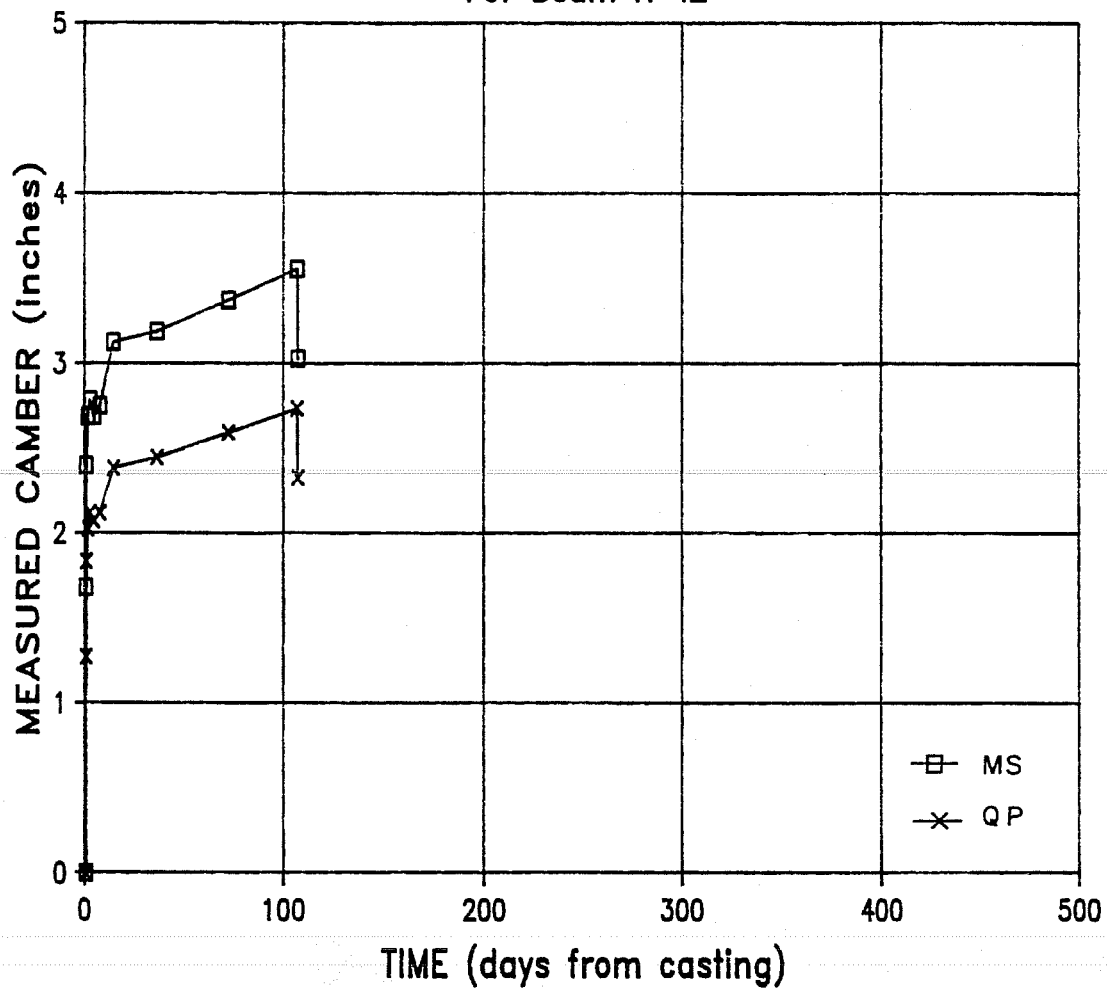
Fig. 5.8   Measured Time-Camber of Specimen H-I2

TABLE 5.1 Measured Beam Camber Summary

	L-I1	L-I2	L-01	L-02	H-01	H-02	H-I1	H-I2
Immediate Midspan Camber (in.) at Time of Prestress	N/A	N/A	1.89	1.71	1.27	1.33	1.59	1.68
Transfer Midspan Camber After Placed in Storage (in.)	2.81	2.66	2.59	2.40	2.11	2.13	2.66*	2.398
Midspan Camber From Setting Beam on Bents (in.)	4.59	4.34	4.34	4.10	2.73	2.94	3.47	3.55
Age of Girders When Placed on Bent (days from casting)	451	451	434	434	147	147	107	107
Midspan Camber at Time of Setting Beam on Bents (in.)	3.92	3.78	4.05	3.76	2.45	2.50	2.99	3.03

* reading taken one day after release

3. differences in design variables between low stress
    level and high stress level designs,

4. fabricating variations such as actual prestress force
    applied,

5. differences in support conditions between taking
    readings, with shorter span lengths frequently present
    when beams were being stored,

6. differences in age of beams at time of placement on the
    bents at the bridge site, and

7. differences in time dependent material properties.

The reason that beam H-I1 has such a large camber upon
its initial placement in storage is its temporary support
conditions. The temporary support (upon its initial placement in
storage) spacing for this particular beam was only 104 ft with
the north end support being 16 ft from the end of the girder.
The day following prestress transfer the beam was moved to a
different location in storage with more resonable spacing of the
supports and the measured camber decreased appropriately.

The average camber of L series beams at the time of
placement at the bridge site was 3.87 in. while that of H series
beams was 2.74 in. A major reason for this variation in beam
camber is certainly the age of the beams at the time of placing
them on bents at the bridge site. One could say the H series
specimens were stunted in camber growth because they were only an

average of 128 days old when shipped to the bridge site as compared to 444 days for L series beams.

Figures 5.1 through 5.8 indicate that most of the camber growth for each beam was completed within 100 to 150 days although the H-I series were still increasing in camber at a comparatively high rate when they were shipped to the bridge site at only 107 days old.

The curves have not been corrected for temperature gradients existing at the time of taking measurements. The effect of temperature gradients upon the measured camber can be illustrated by Fig. 5.9 which shows the deflected shape of a typical girder due to variations in temperature gradients and time. Figure 5.9 indicates that the effect of temperature gradients on the measured camber is small for individual beams placed in storage. Therefore, for this investigation no temperature corrections have been made for comparing measured cambers of different beams.

The shape of all camber-time curves are similar. The L-O series and H-I series were fabricated using SWAI low-relaxation strand as reported in Chapter 3 while L-I series and H-O series beams were fabricated using FWC low-relaxation strand. The relaxation properties of the strands produced by SWAI indicate a lower relaxation with time than those produced by FWC. A comparison of the time-cambers of the SWAI beams with those of

TEMPERATURE GRADIENTS
(Difference between Top and
Bottom Flange Temperatures)

AGE	MS	OP
140 days	8°F	4°F
196 days	1°F	1°F

140 days (Sunny)

196 days (Overcast)

SUPPORT
(85-294 days)

SUPPORT
(85-294 days)
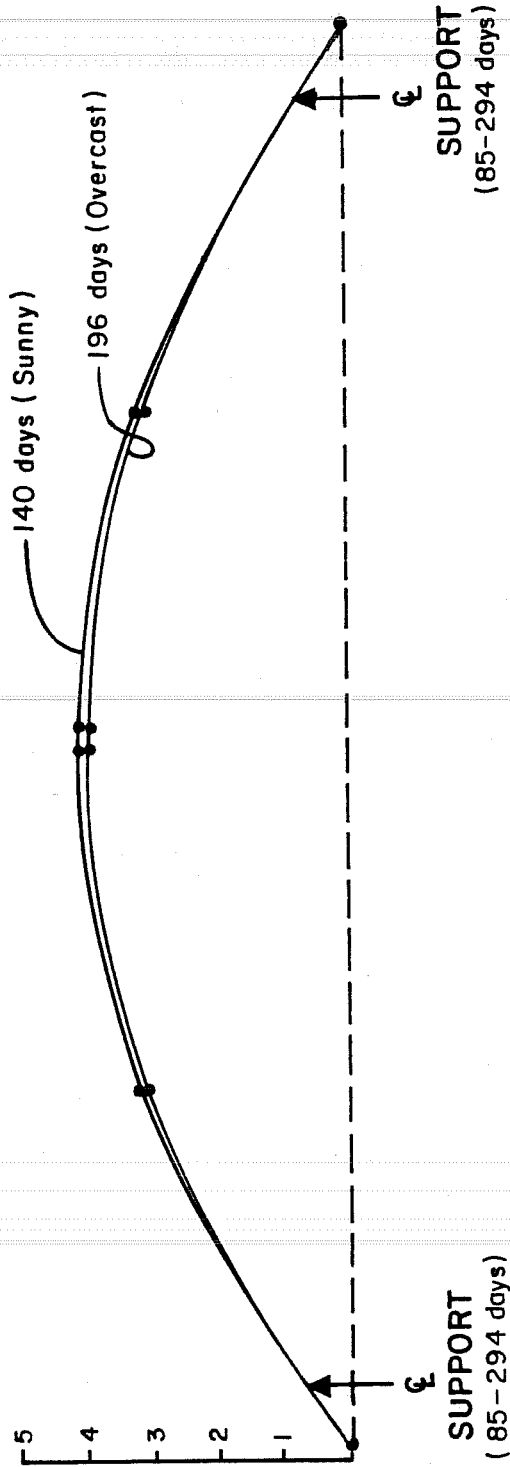
Fig. 5.9 Effect of Temperature Gradients on Measured Beam Camber

the FWC beams show that the SWAI beams camber growth did not
level off as quickly as did the FWC beams.

5.3 Measured Time-Dependent Surface Concrete Strains and Strain Distributions

Figures 5.10 through 5.15 show the time distribution of
surface concrete strains as measured using the Demec mechanical
strain monitoring system for each beam except those of the H-0
series. Because of problems in maintaining the Demec gage points
for the H-0 beams the strain data for these beams was erratic.
Also in apparent error is the midspan bottom fiber time-strains
for beam H-I1 as shown in Fig. 5.14c. Finally, as was noted in
Chapter 3, initial readings of strain gage lines for L-I series
beams were not completed prior to the beginning of prestress
transfer so the reported strains for these beams are smaller in
magnitude than the actual strains by the amount of unmeasured
strain.

Discontinuity in the time-strain curves are caused by:

1. random errors in taking Demec readings,

2. loss of reference to initial readings due to points falling off,

3. temperature differentials between taking readings,

4. changes in creep and shrinkage due to varying temperature and relative humidity, and

CONCRETE SURFACE STRAIN DATA FOR BM L-I1
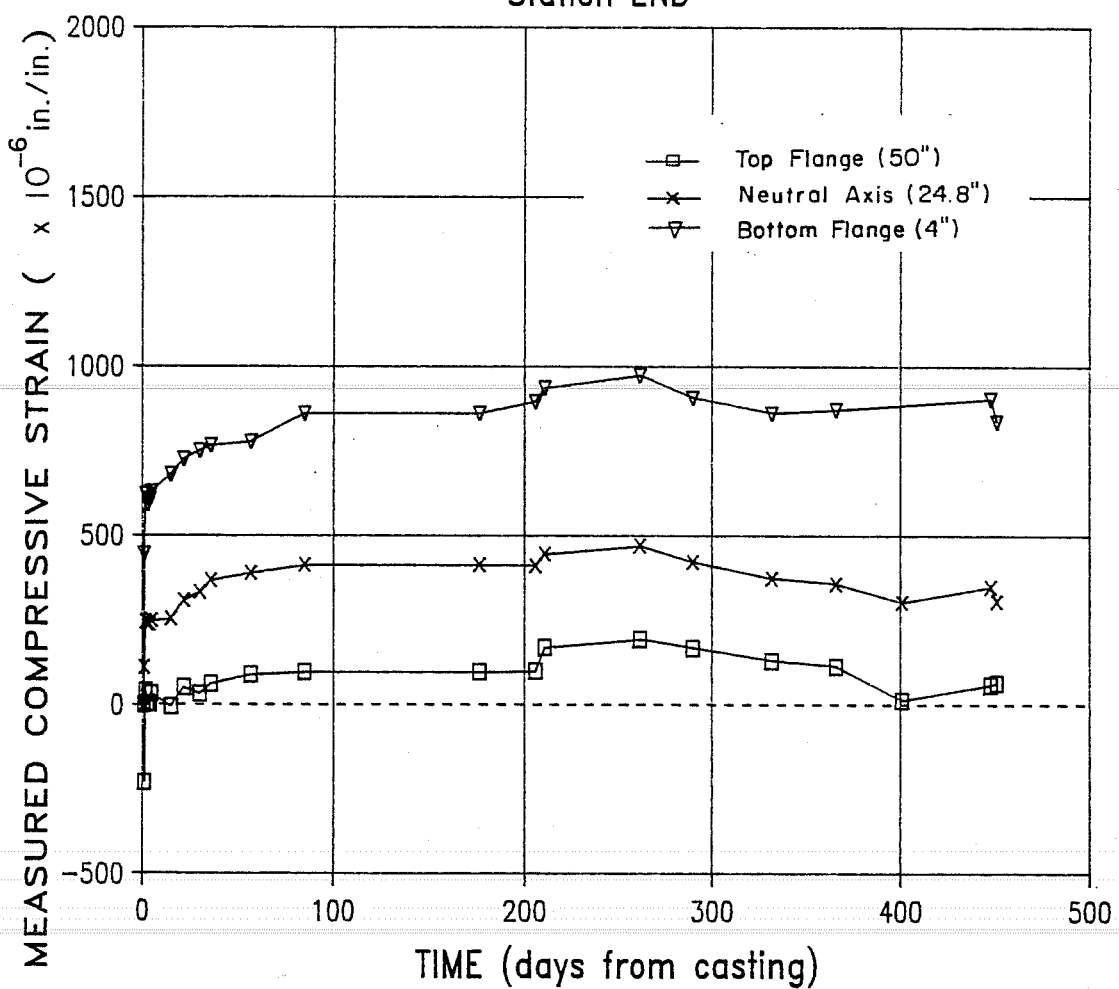
Station END

a) surface strains at station END

Fig. 5.10 Measured Concrete Surface Strains for Specimen L-I1
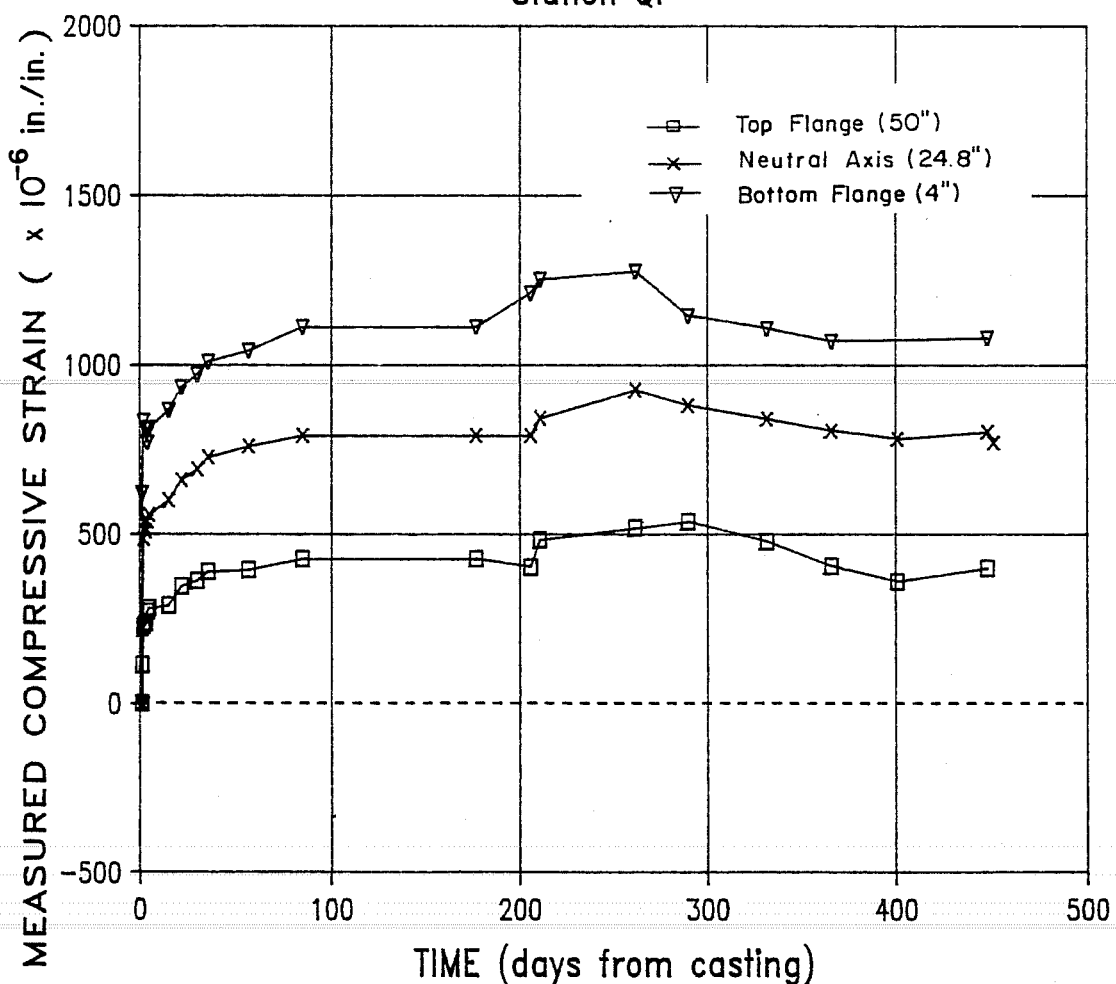
CONCRETE SURFACE STRAIN DATA FOR BM L–I1

Station QP

b) surface strains at station QP

Fig. 5.10   Measured Concrete Surface Strains for Specimen L-I1
            (cont'd)
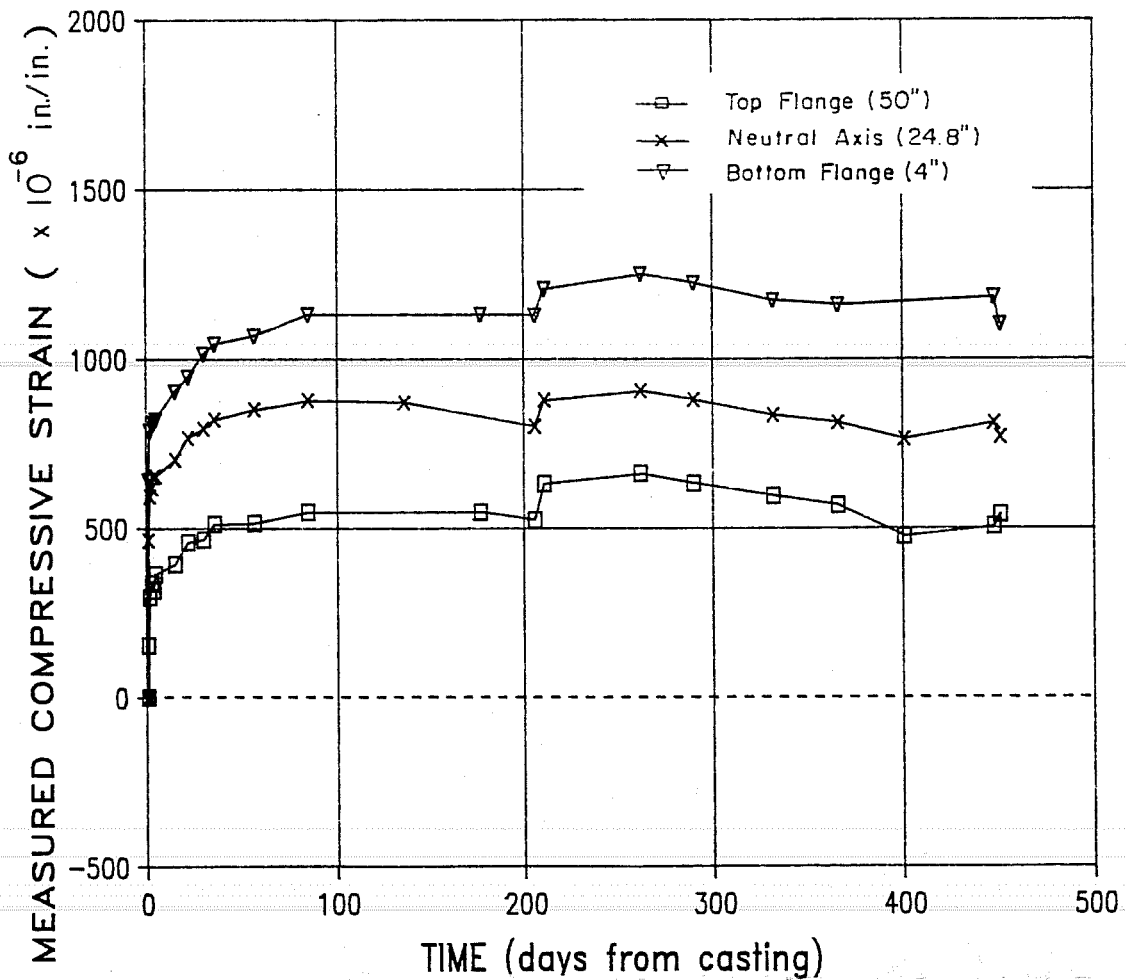
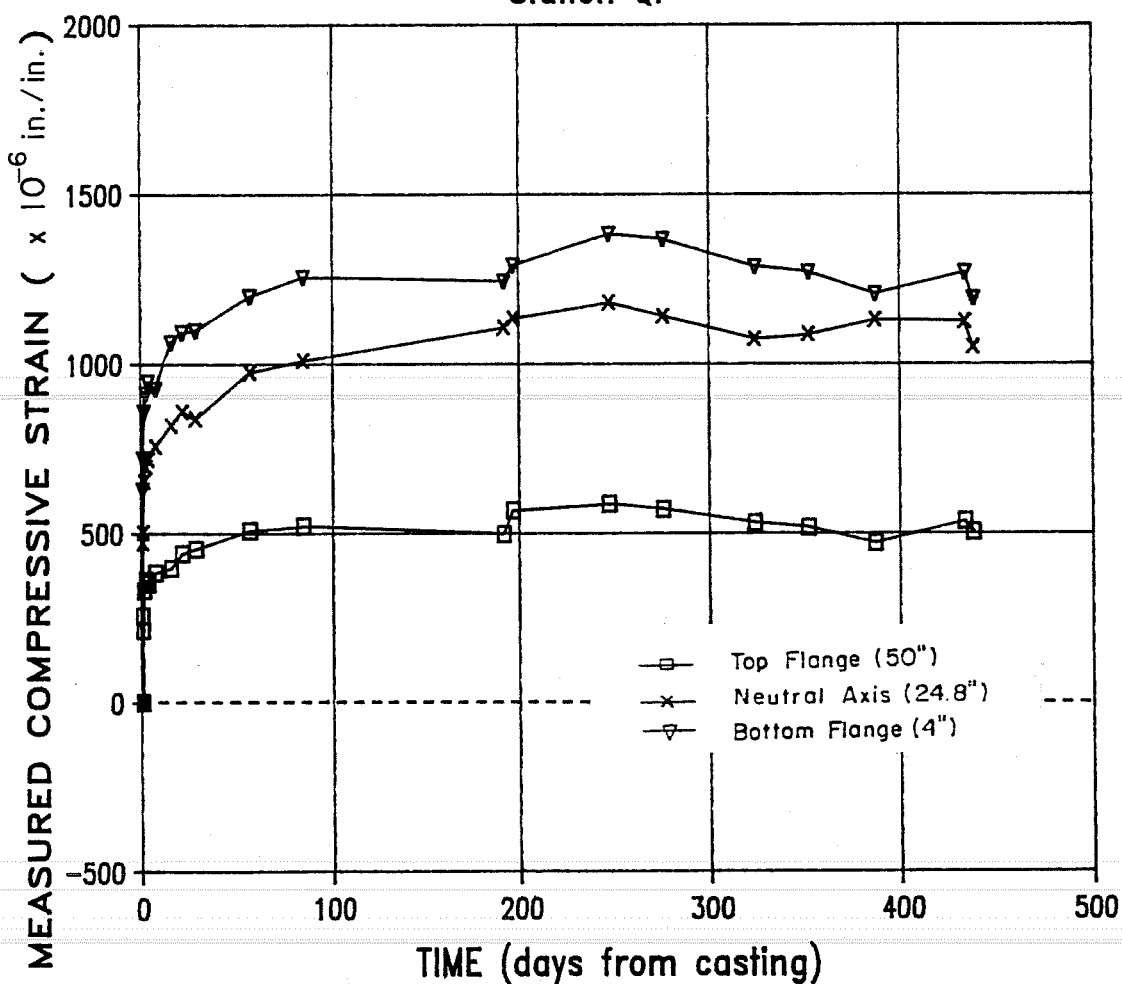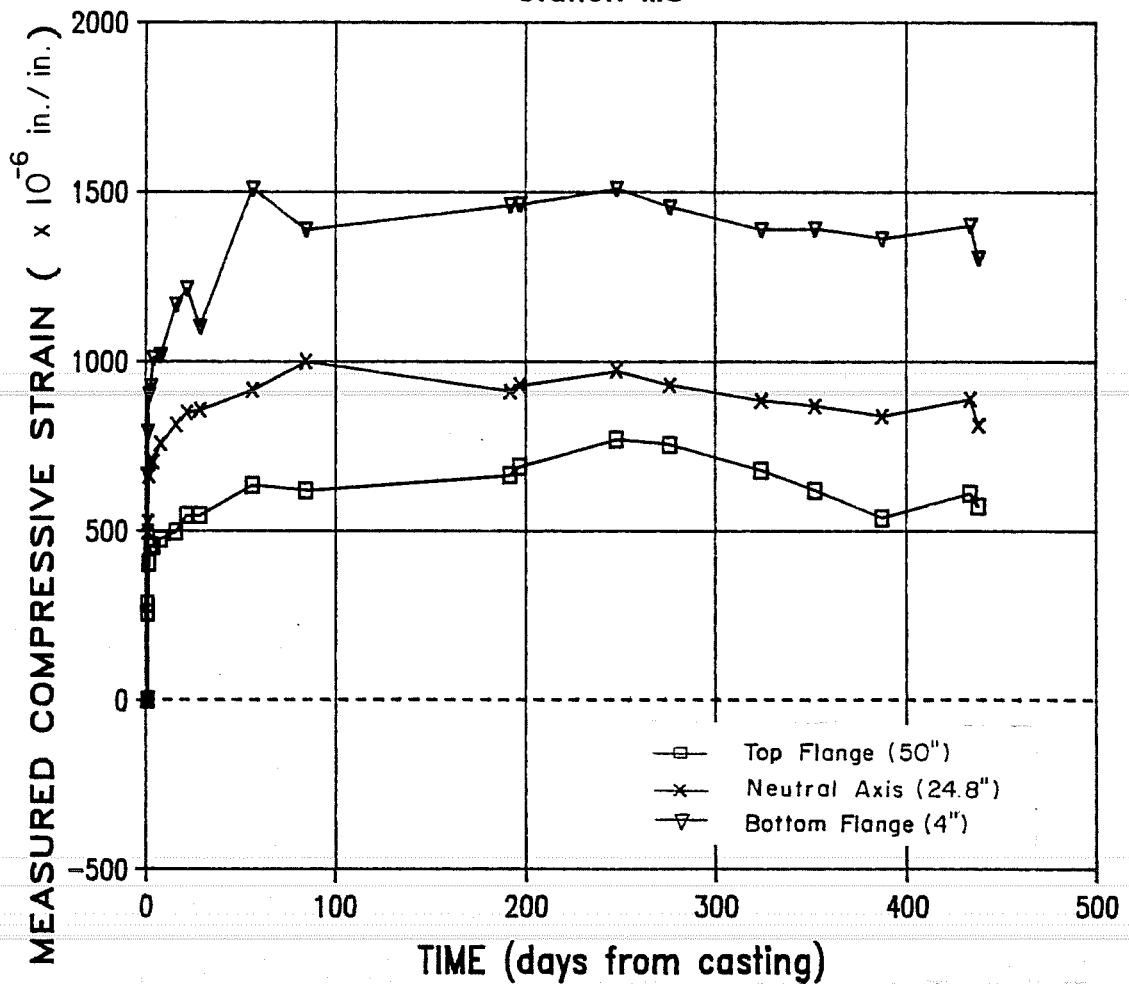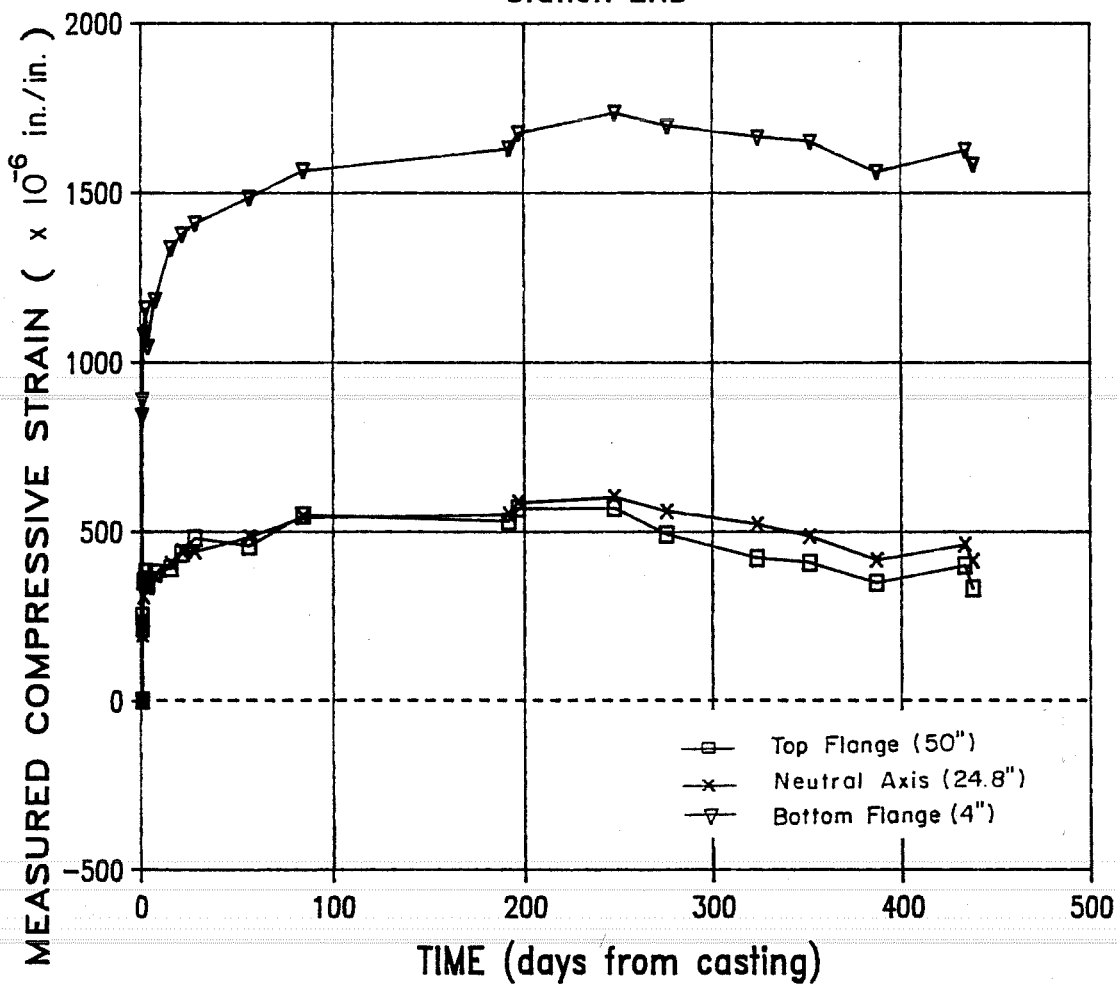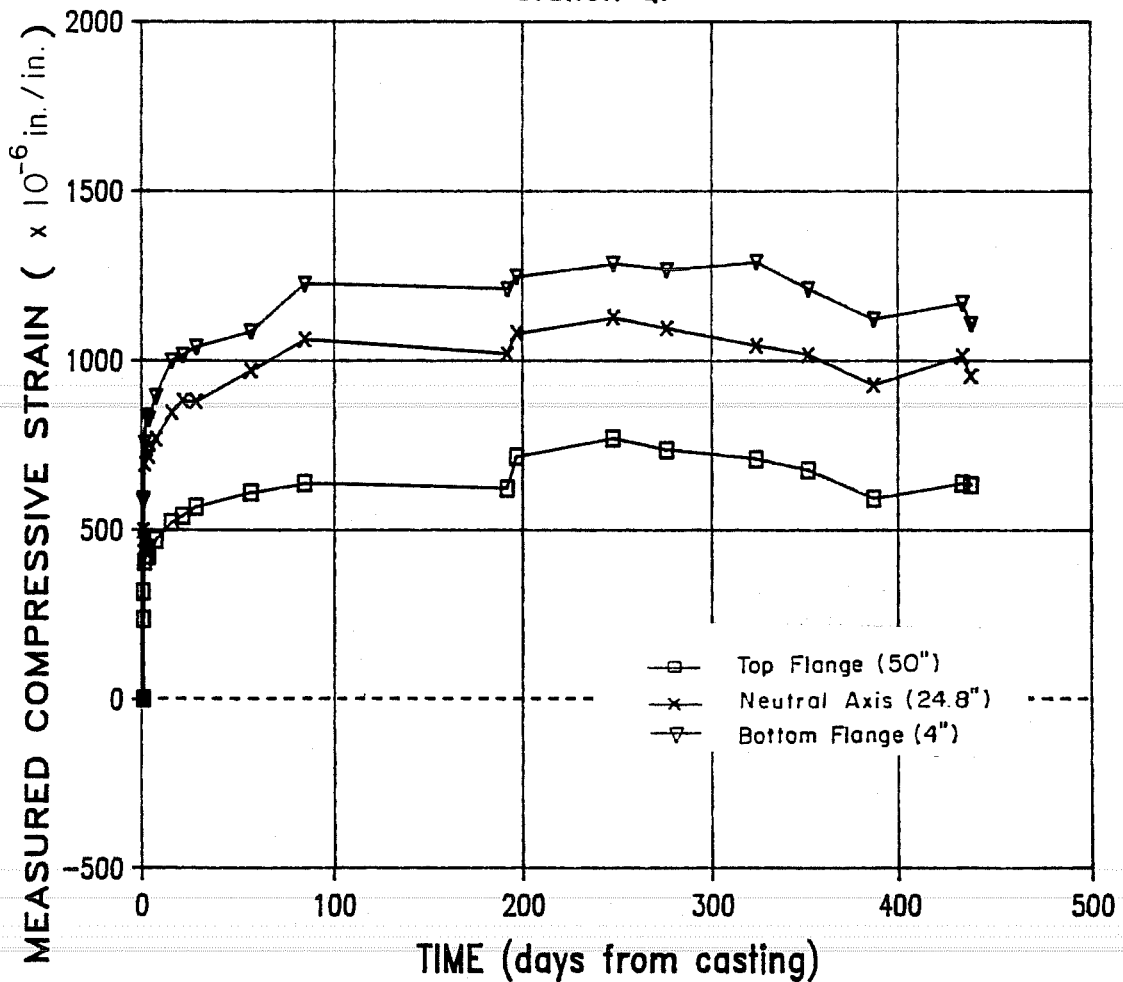# CONCRETE SURFACE STRAIN DATA FOR BM L-I1

Station MS

c)   surface strains at station MS

Fig. 5.10   Measured Concrete Surface Strains for Specimen L-I1
            (cont'd)

CONCRETE SURFACE STRAIN DATA FOR BM L-I2

Marked End

a) surface strains at station END

Fig. 5.11 Measured Concrete Surface Strains for Specimen L-I2
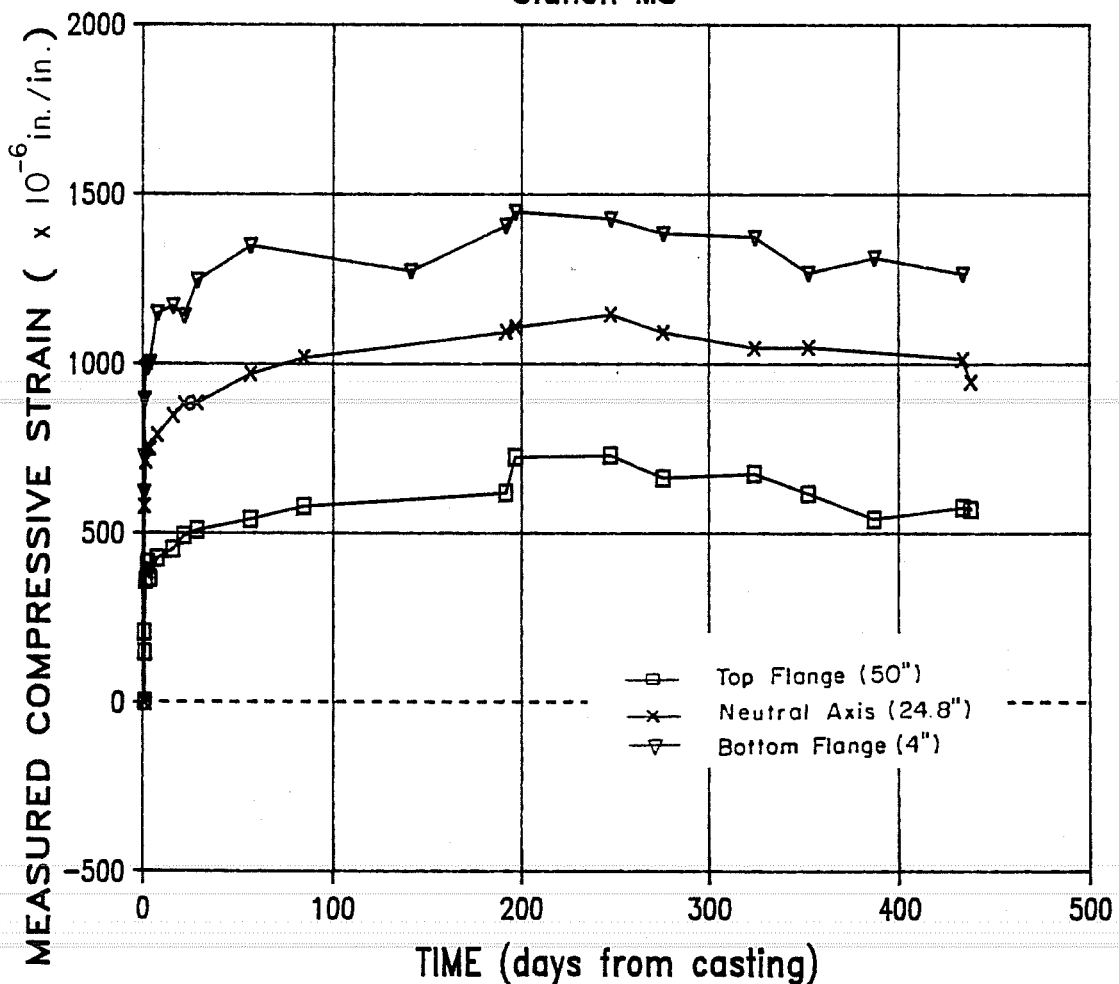
CONCRETE SURFACE STRAIN DATA FOR BM L-12

Quarter Point
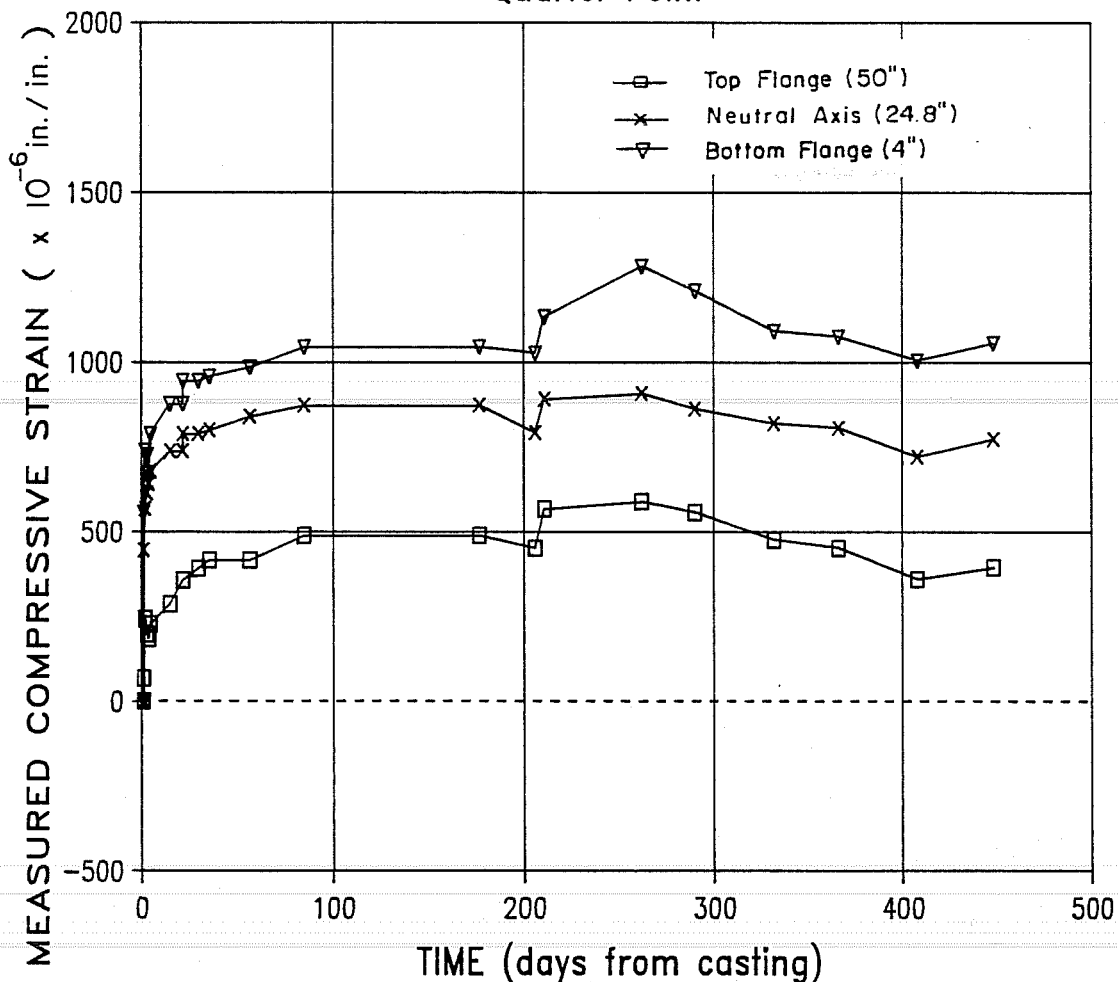
b)   surface strains at station QP

Fig. 5.11   Measured Concrete Surface Strains for Specimen L-I2
(cont'd)

CONCRETE SURFACE STRAIN DATA FOR BM L-12

Mid-span
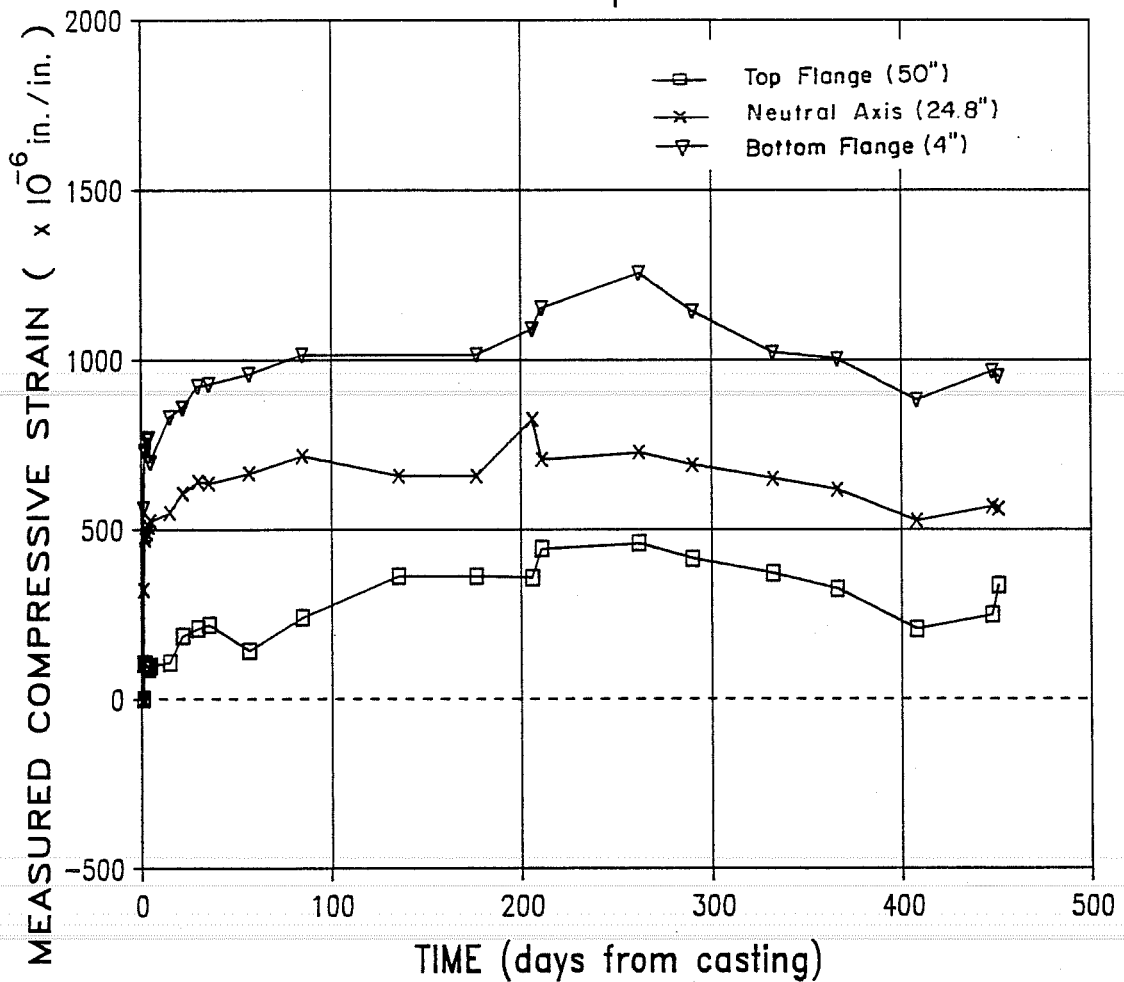
c) surface strains at station MS

Fig. 5.11 Measured Concrete Surface Strains for Specimen L-I2
(cont'd)

CONCRETE SURFACE STRAIN DATA FOR BM L-01

Station END

a) surface strains at station END

Fig. 5.12 Measured Concrete Surface Strains for Specimen L-01

189

b) surface strains at station QP

Fig. 5.12 Measured Concrete Surface Strains for Specimen L-01
(cont'd)

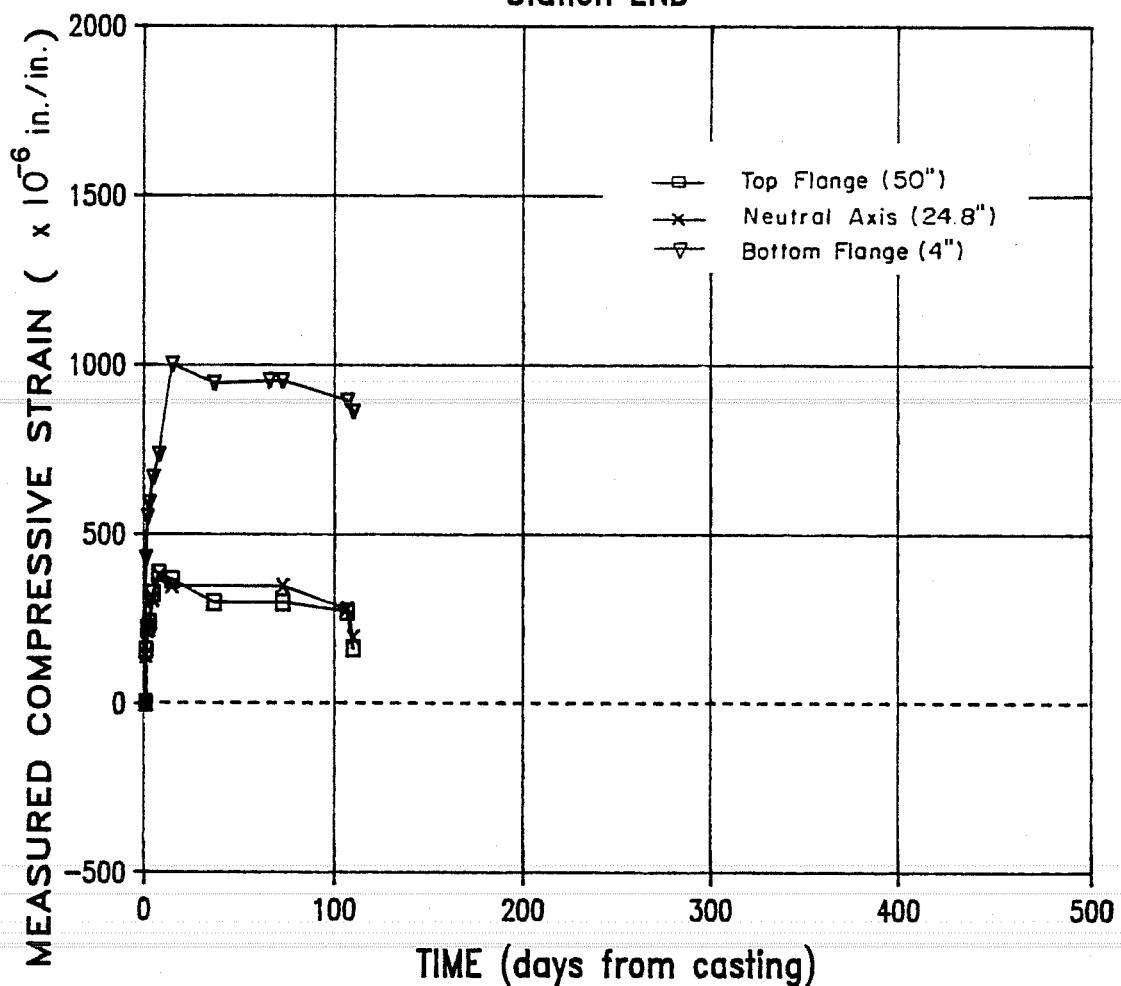# CONCRETE SURFACE STRAIN DATA FOR BM L-01

Station MS

c) surface strains at station MS

Fig. 5.12   Measured Concrete Surface Strains for Specimen L-01
            (cont'd)

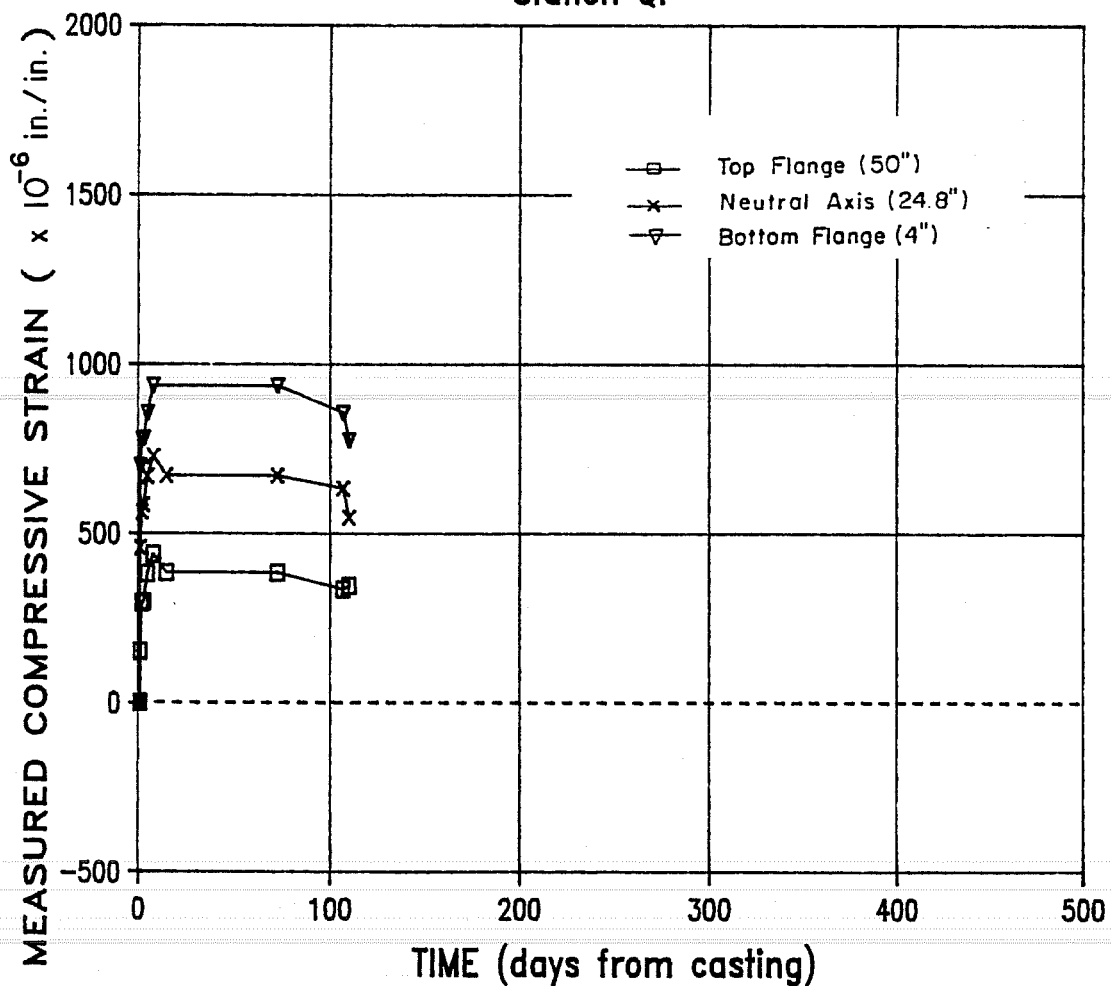# CONCRETE SURFACE STRAIN DATA FOR BM L-02

Station END

a) surface strains at station END

Fig. 5.13 Measured Concrete Surface Strains for Specimen L-02

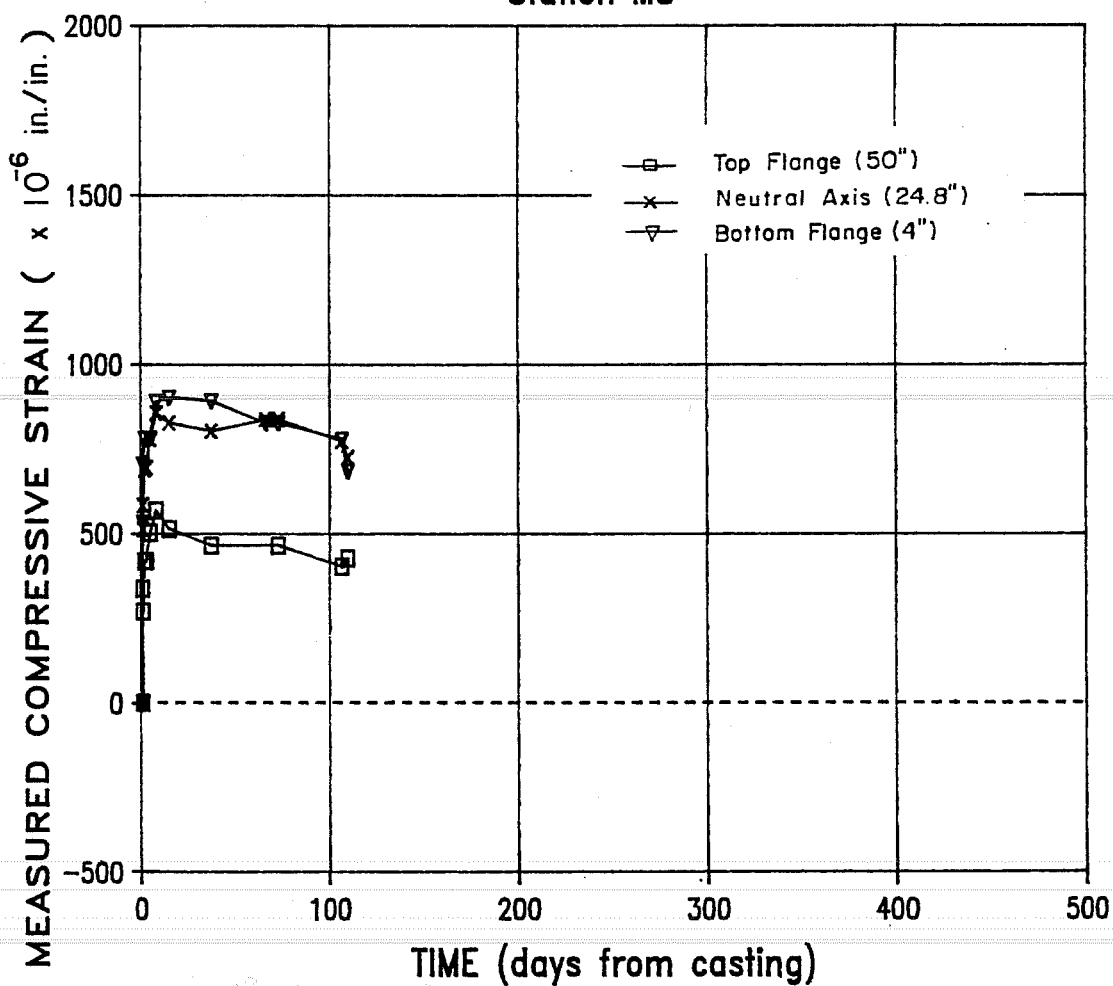# CONCRETE SURFACE STRAIN DATA FOR BM L-02

Station QP

b) surface strains at station QP

Fig. 5.13   Measured Concrete Surface Strains for Specimen L-02
            (cont'd)

c) surface strains at station MS

Fig. 5.13 Measured Concrete Surface Strains for Specimen L-02 (cont'd)

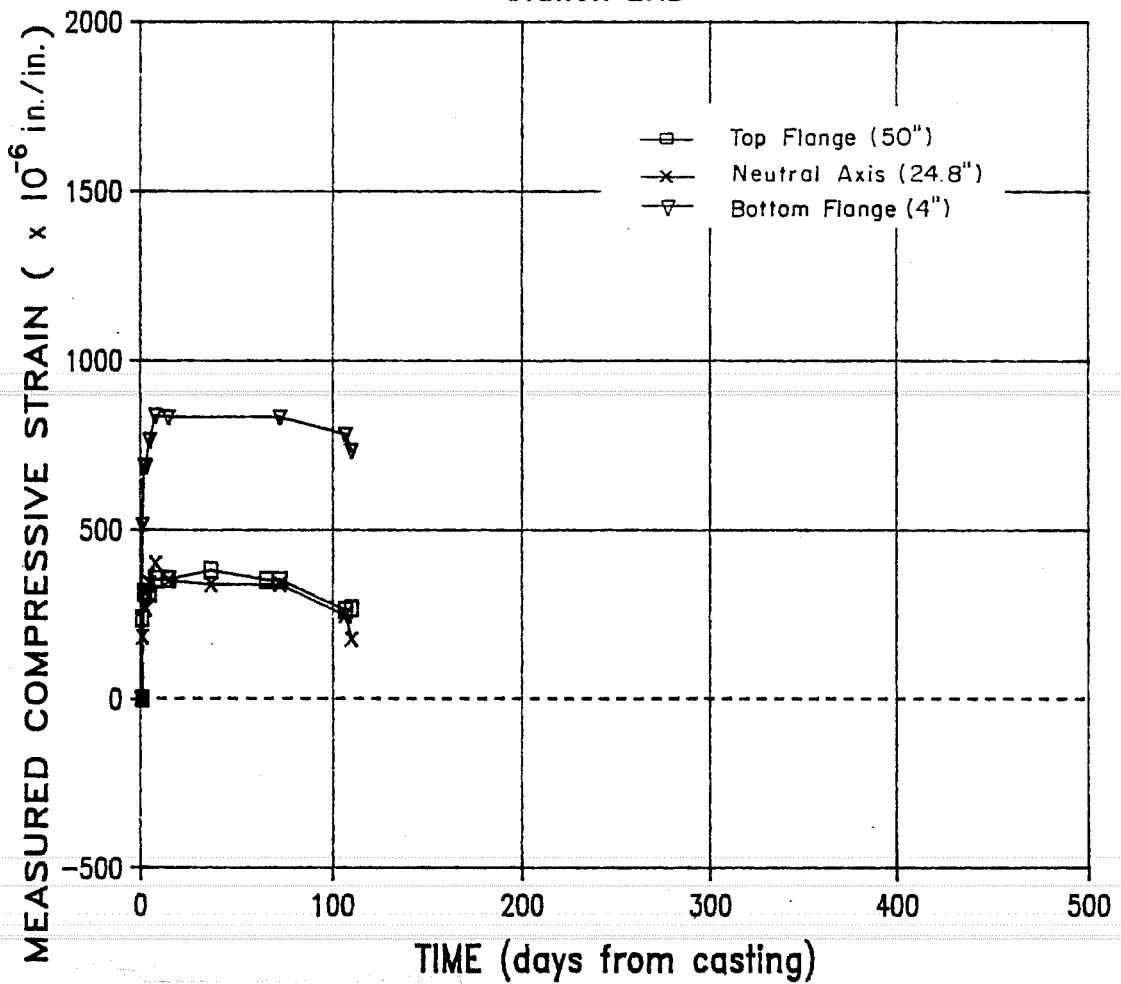# CONCRETE SURFACE STRAIN DATA FOR BM H-I1

Station END

Legend:
- Top Flange (50")
- Neutral Axis (24.8")
- Bottom Flange (4")

X-axis: TIME (days from casting)

Y-axis: MEASURED COMPRESSIVE STRAIN (x 10^{-6} in./in.)

| OCT | NOV | DEC | JAN | FEB | MAR |

1984   1985

a) surface strains at station END

Fig. 5.14 Measured Concrete Surface Strains for Specimen H-I1

CONCRETE SURFACE STRAIN DATA FOR BM H-I1

Station QP

b) surface strains at station QP

Fig. 5.14   Measured Concrete Surface Strains for Specimen H-I1
(cont'd)

CONCRETE SURFACE STRAIN DATA FOR BM H−I1

Station MS

c) surface strains at station MS

Fig. 5.14 Measured Concrete Surface Strains for Specimen H-I1
(cont'd)

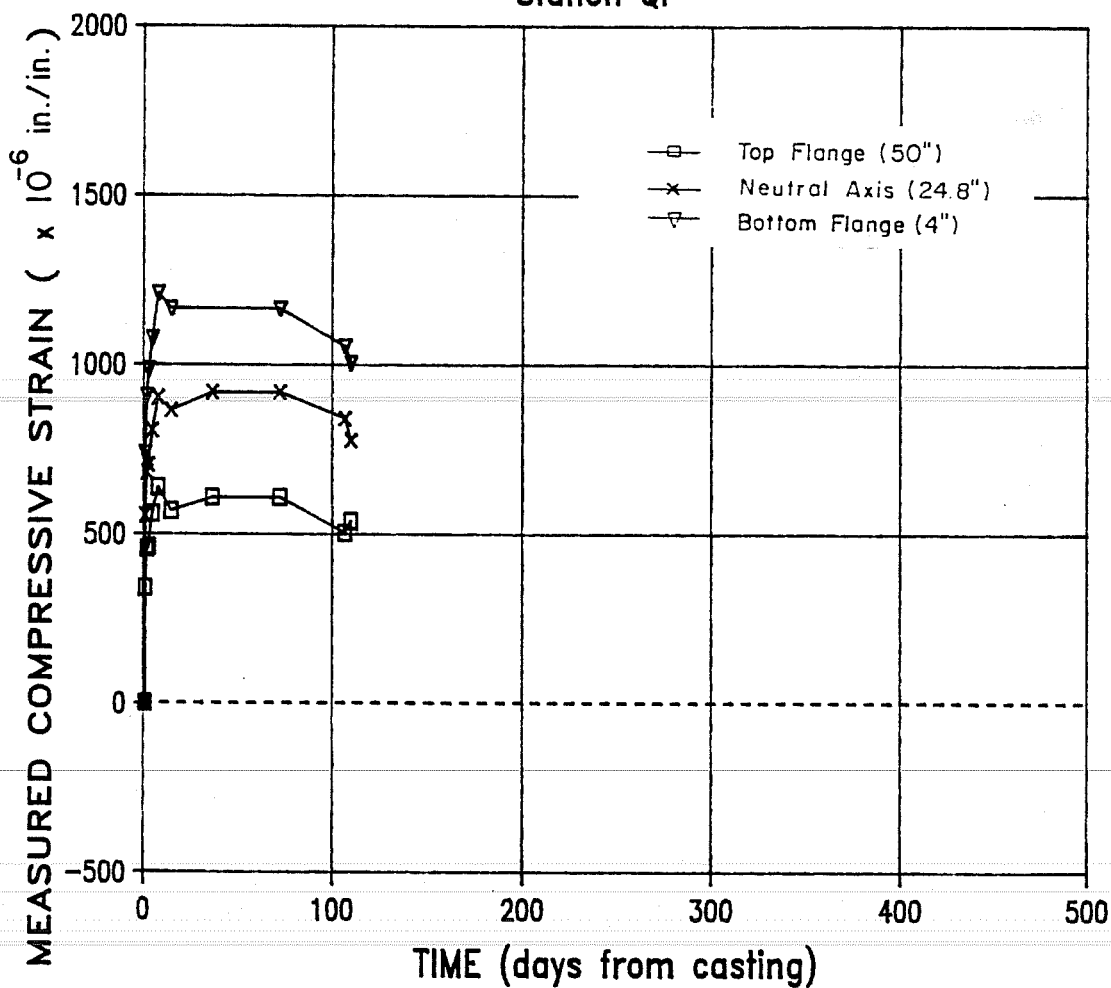# CONCRETE SURFACE STRAIN DATA FOR BM H-I2

Station END

a) surface strains at station END

Fig. 5.15 Measured Concrete Surface Strains for Specimen H-I2

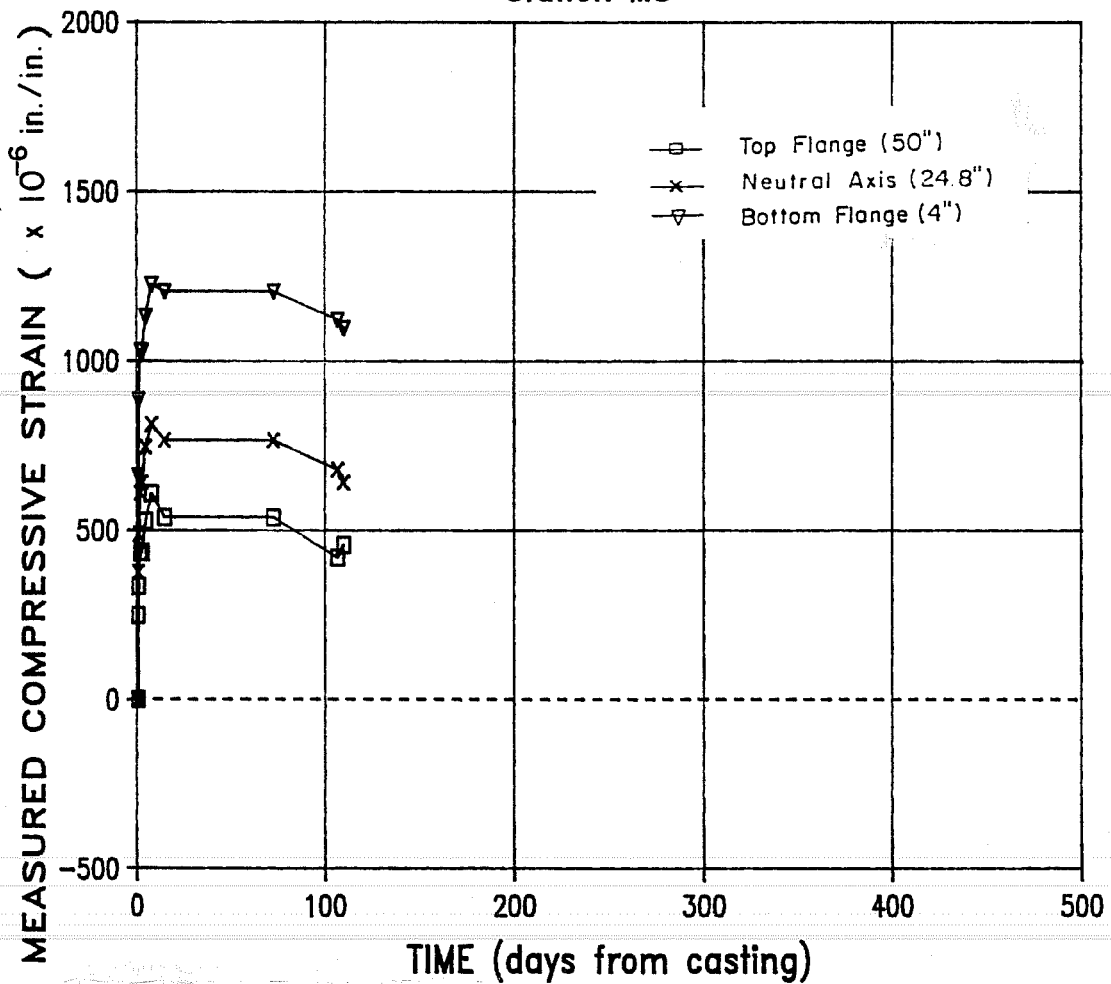# CONCRETE SURFACE STRAIN DATA FOR BM H-I2

Station QP

b) surface strains at station QP

Fig. 5.15   Measured Concrete Surface Strains for Specimen H-I2
(cont'd)

CONCRETE SURFACE STRAIN DATA FOR BM H−I2

Station MS


c) surface strains at station MS

Fig. 5.15 Measured Concrete Surface Strains for Specimen H-I2
(cont'd)

5.   variations in support conditions.

Discontinuity due to points falling off has the effect of making the strain-time curves flat from the time of taking the last reading while the points were still on until the time of replacing the points and taking new readings. Where these discontinuities occur a certain amount of actual strain is left unaccounted for.

Selected strain distributions across beam sections are shown in Fig. 5.16 through 5.19 and measured curvatures for each specimen at times of interest are presented in Table 3.2.. The distributions shown in each figure correspond to prestress transfer, initial storage, immediately prior to placement on bents and after placement on bents at bridge site respectively unless noted otherwise. No corrections to the strain distributions have been made for temperature effects.

Typical strain distributions at station END of L series beams (Fig. 5.16a and 5.17a) can be compared to those of H series beams (Fig. 5.17a and 5.19a). From these figures it is apparent that strain distributions near the end of the beams are highly non-linear. Initial strain distributions are comparable between L and H series beams near the ends except that compressive strains near the bottom fiber of L series are much larger than those of H series. This would indicate that the prestress force near the bottom of L series beams was greater
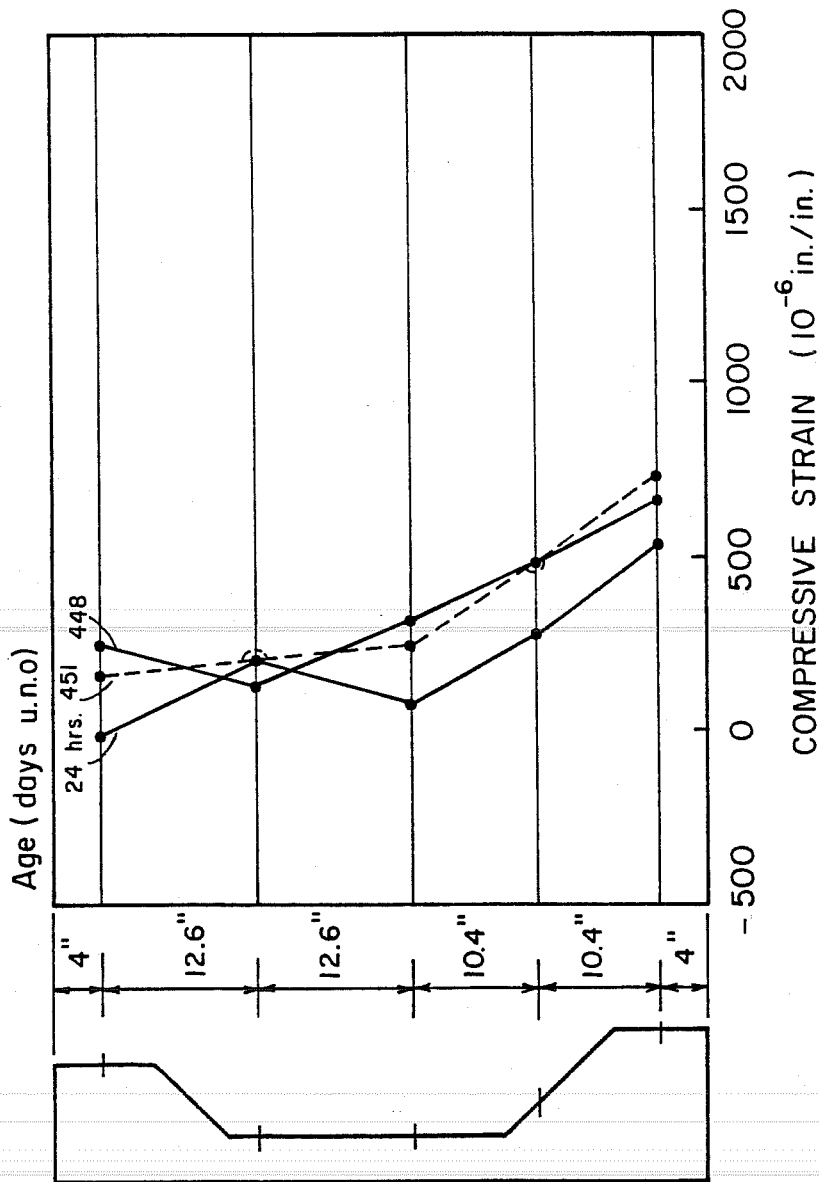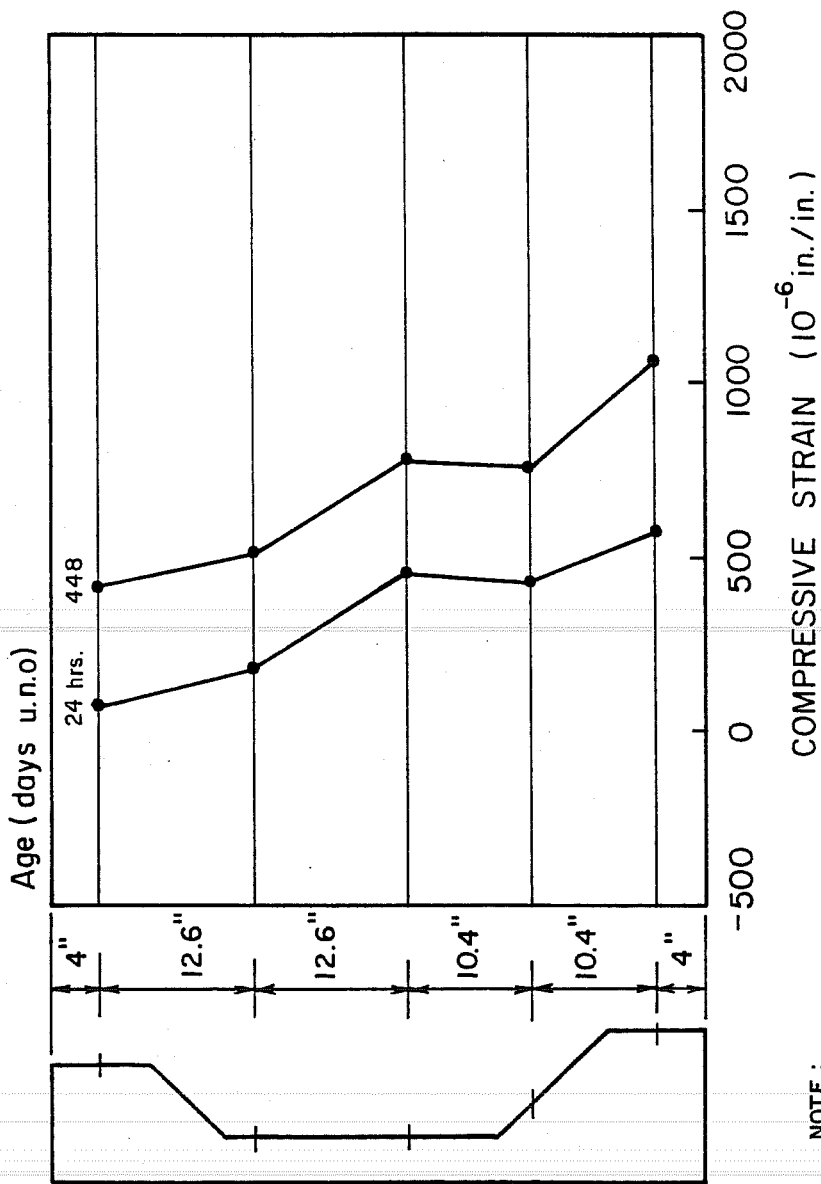
NOTE:
INITIAL STRAIN DISTRIBUTION UPON RELEASE IS NOT SHOWN.
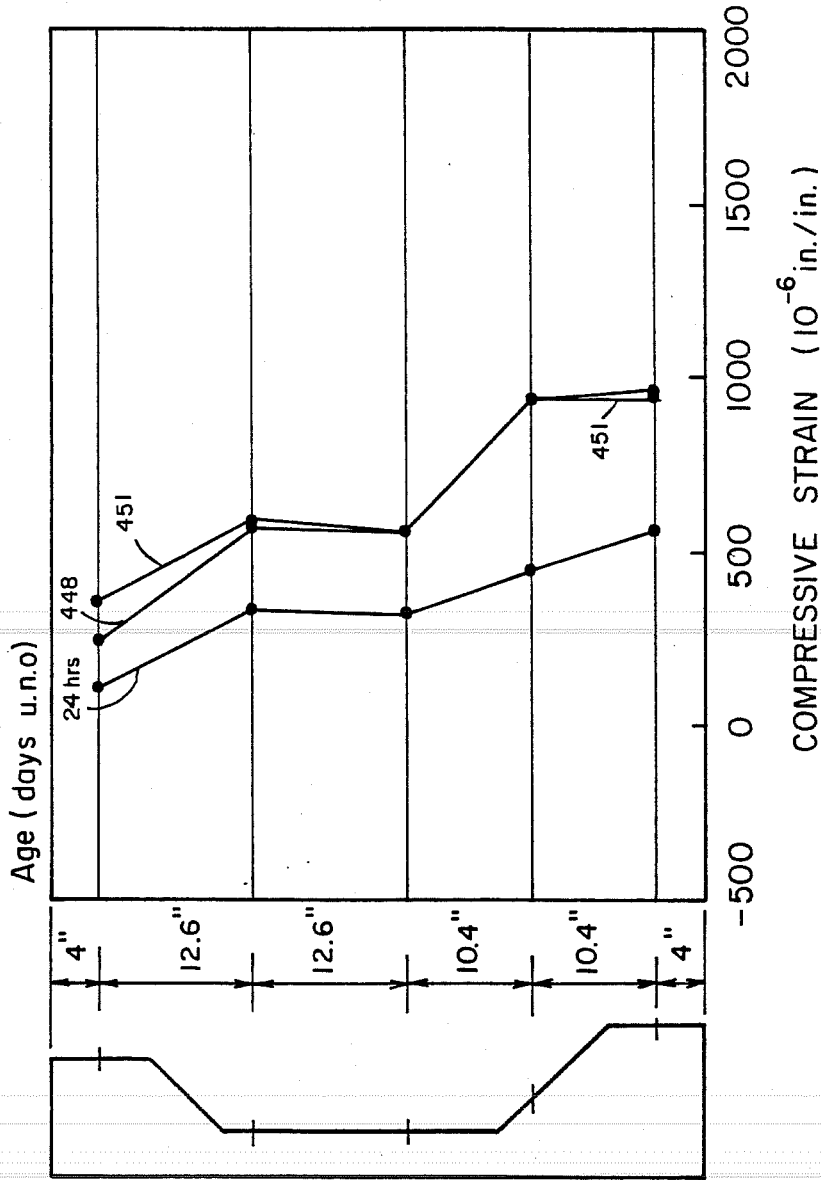a) strain distribution at station END

Fig. 5.16 Strain Distributions at Selected Ages for Specimen L-I2

NOTE :
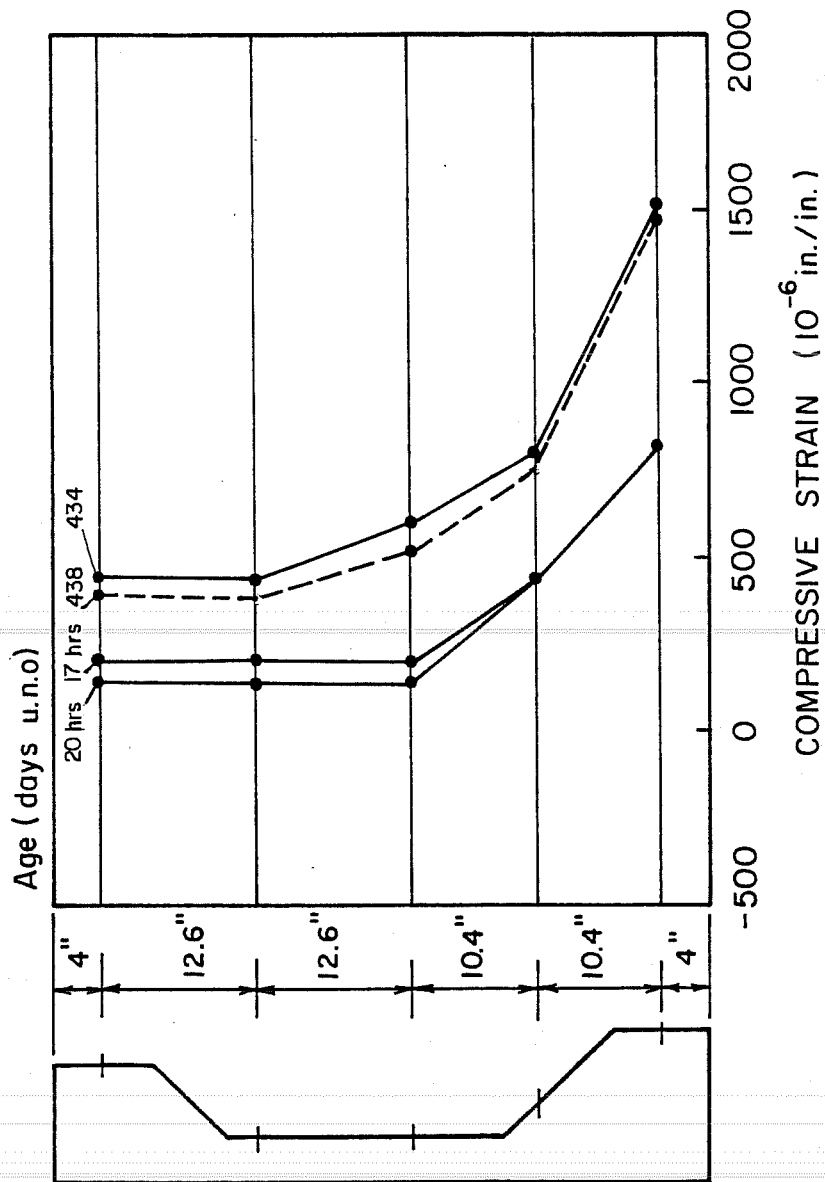
1. INITIAL STRAIN DISTRIBUTION UPON RELEASE IS NOT SHOWN.
2. STRAIN DISTRIBUTION AT TIME OF PLACING BEAM ON BENTS IS NOT SHOWN.

b) strain distribution at station QP

Fig. 5.16 Strain Distributions at Selected Ages for Specimen L-I2 (cont'd)

NOTE :
INITIAL STRAIN DISTRIBUTION UPON RELEASE IS NOT SHOWN.
c) strain distribution at station MS

Fig. 5.16 Strain Distributions at Selected Ages for Specimen L-I2 (cont'd)

Fig. 5.17 Strain Distribution at Selected Ages for Specimen L-01

b) strain distribution at station QP

Fig. 5.17 Strain Distributions at Selected Ages for Specimen L-01 (cont'd)

c) strain distribution at station MS

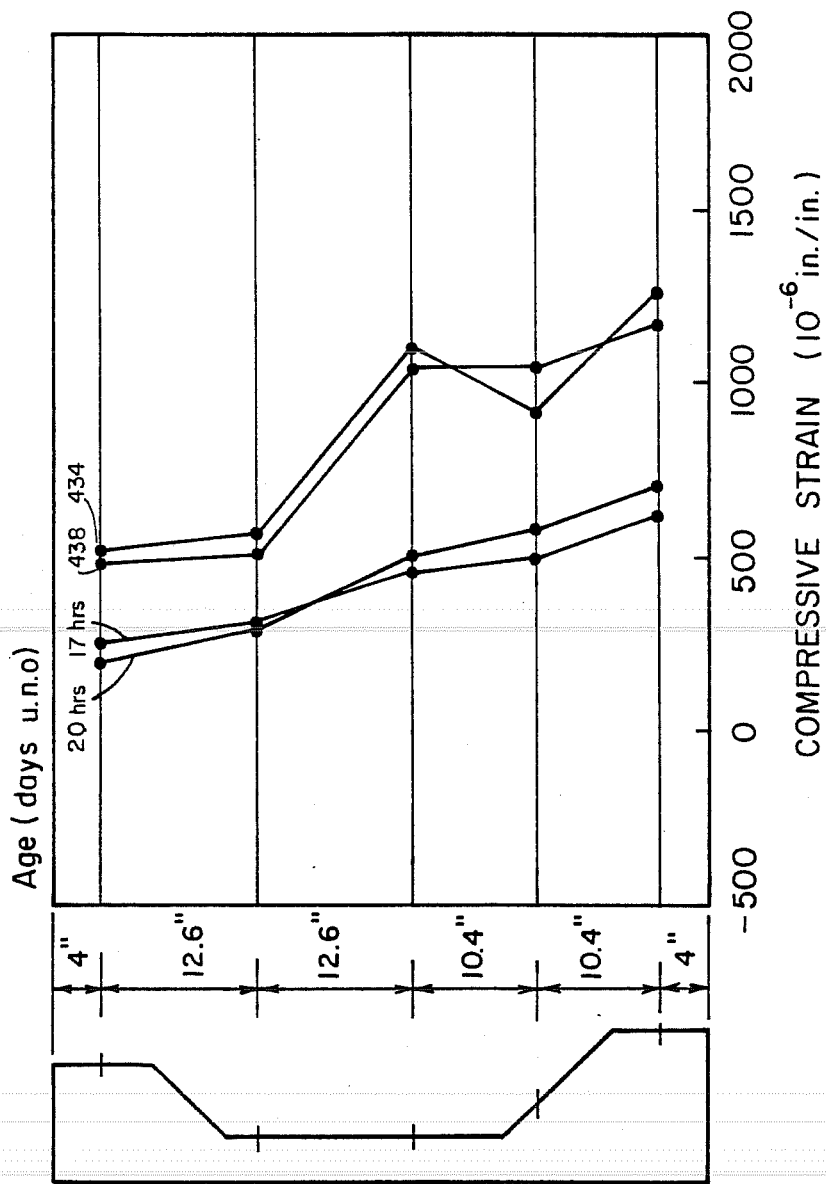Fig. 5.17 Strain Distribution at Selected Ages for Specimen L-01 (cont'd)

NOTE :
INITIAL STRAIN DISTRIBUTION UPON RELEASE IS NOT SHOWN.

a) strain distribution at station END

Fig. 5.18 Strain Distribution at Selected Ages for Specimen H-I1

NOTE:
INITIAL STRAIN DISTRIBUTION UPON RELEASE IS NOT SHOWN.

b) strain distribution at station QP

Fig. 5.18 Strain Distribution at Selected Ages for Specimen H-I1 (cont'd)

Strain Distributions at Selected Ages for Specimen H-I1

c) strain distribution at station MS

Fig. 5.18   Strain Distributions at Selected Ages for Specimen H-I1 (cont'd)

NOTE:
INITIAL STRAIN DISTRIBUTION UPON RELEASE IS NOT SHOWN.
a) strain distribution at station END

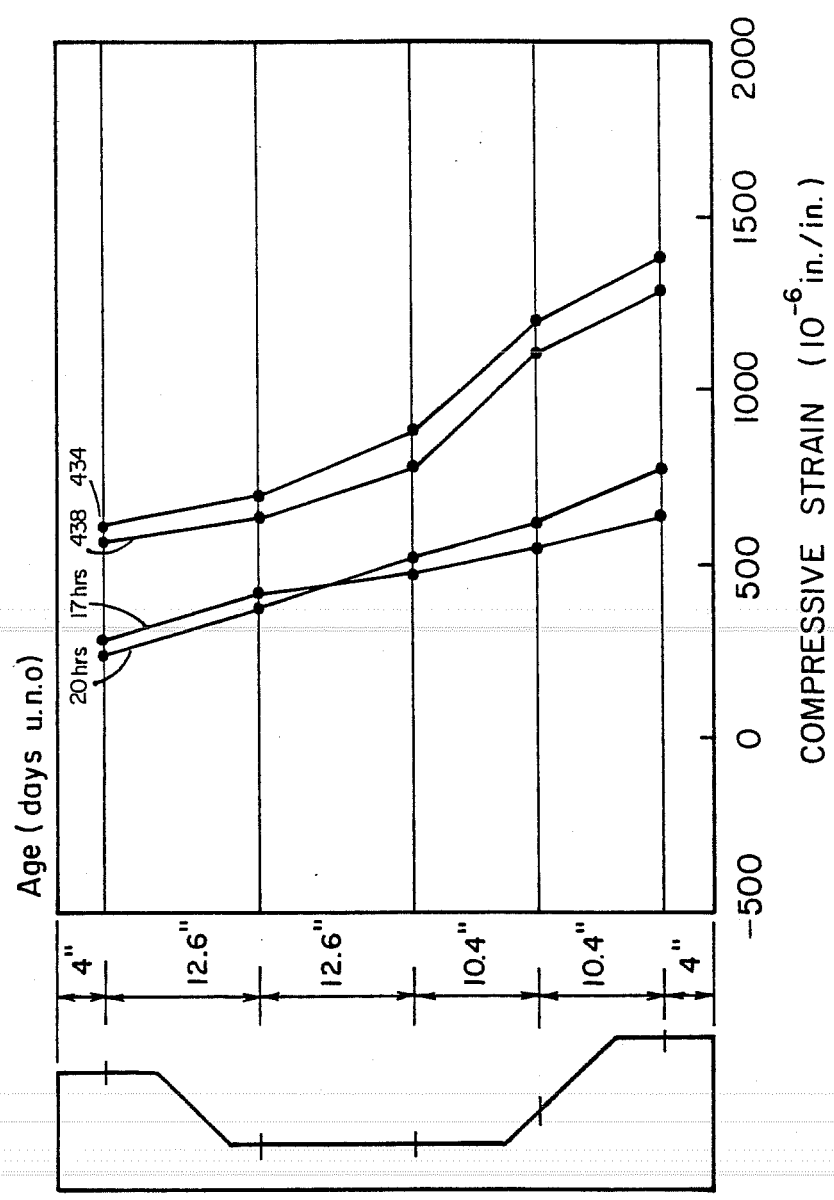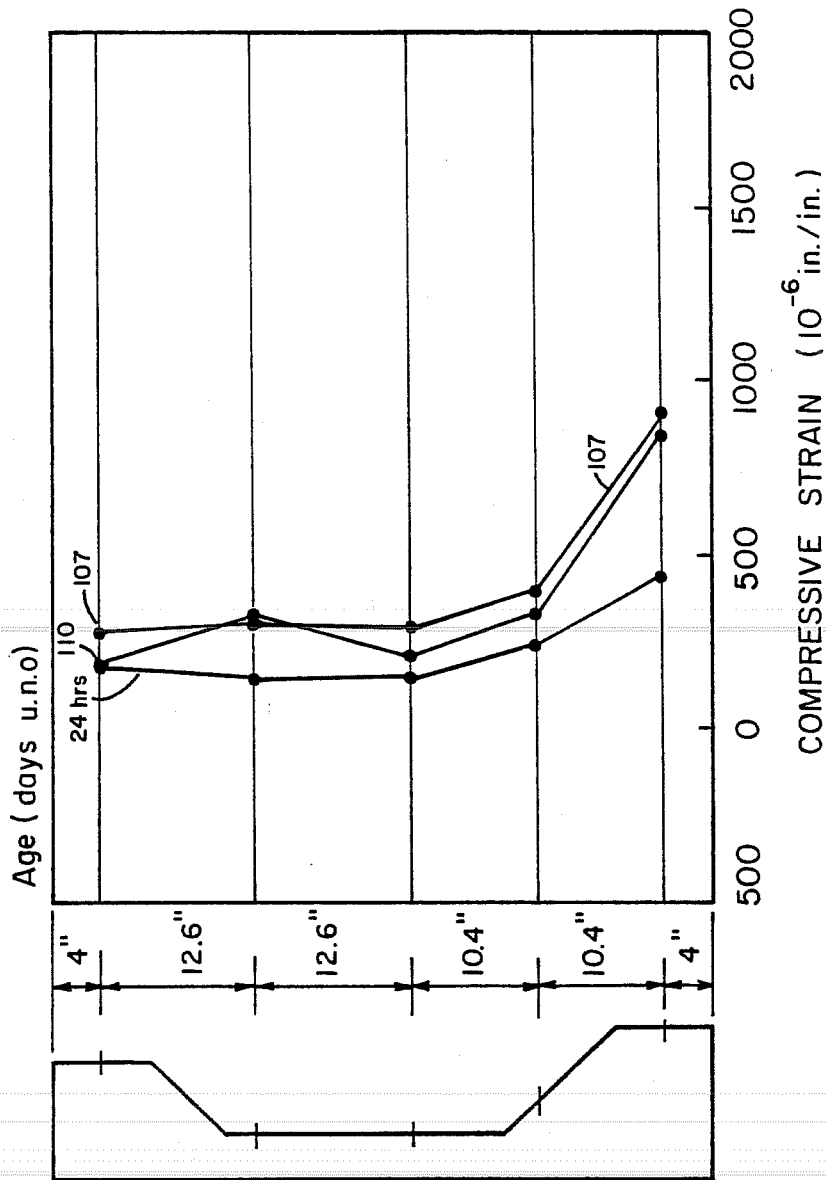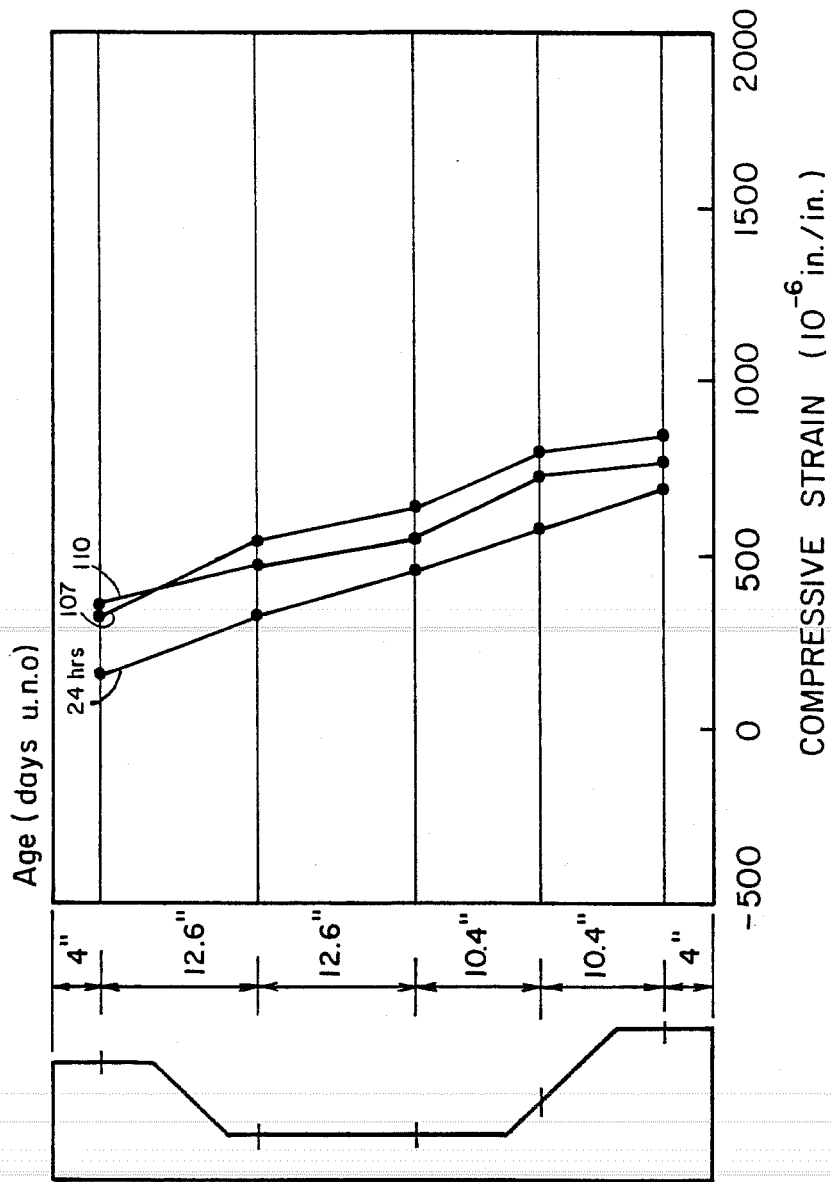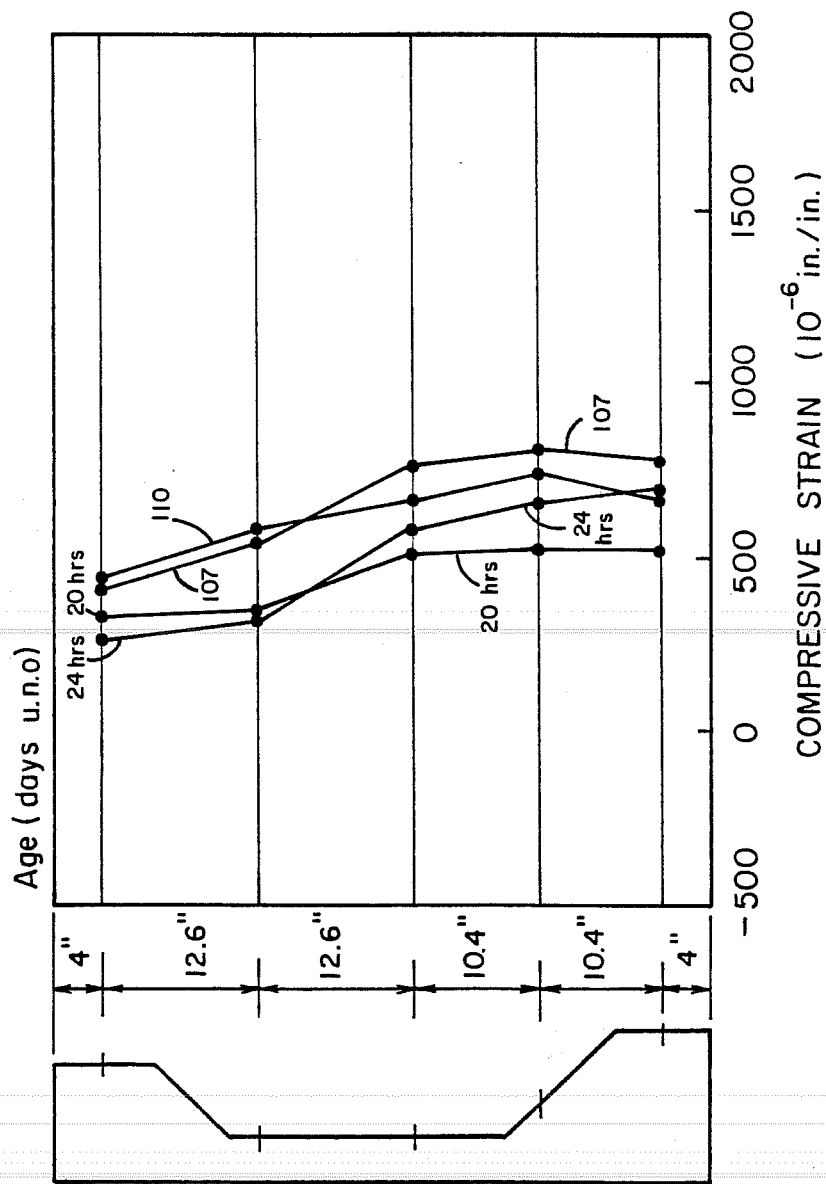Fig. 5.19 Strain Distributions at Selected Ages for Specimen H-I2
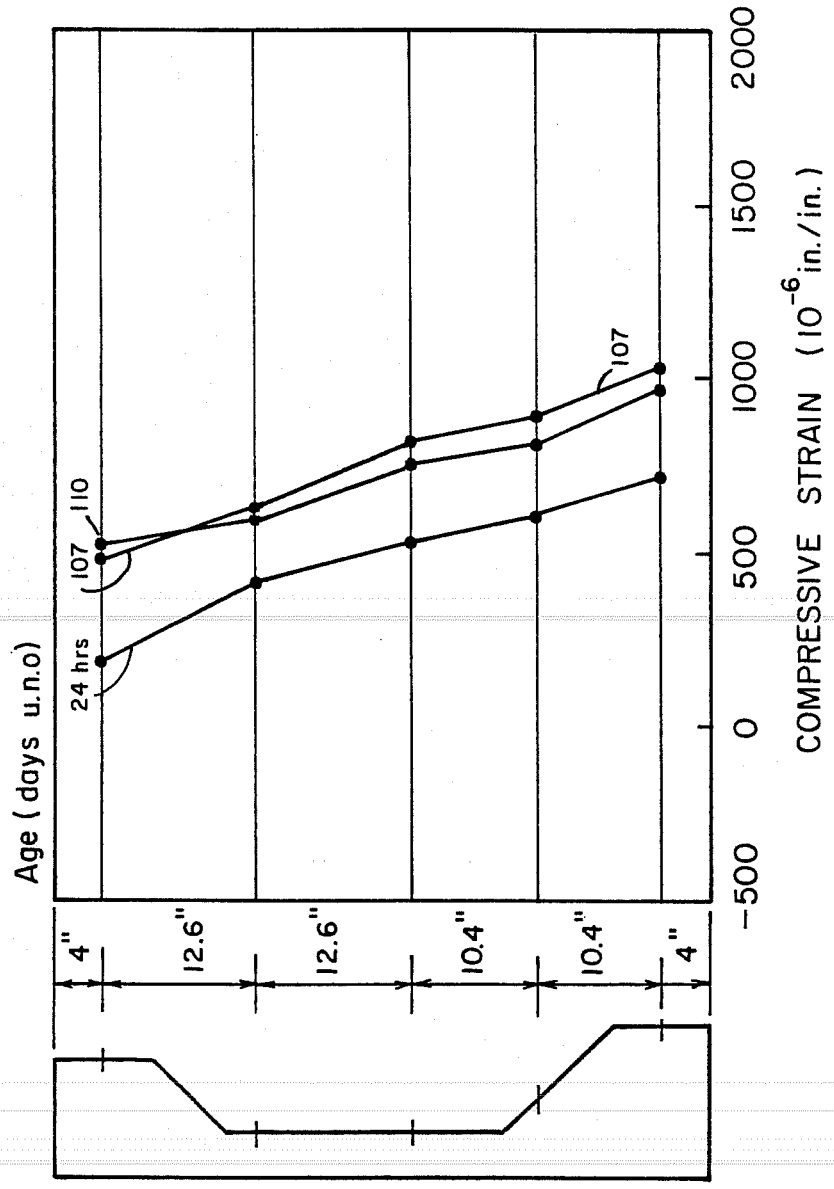
NOTE :
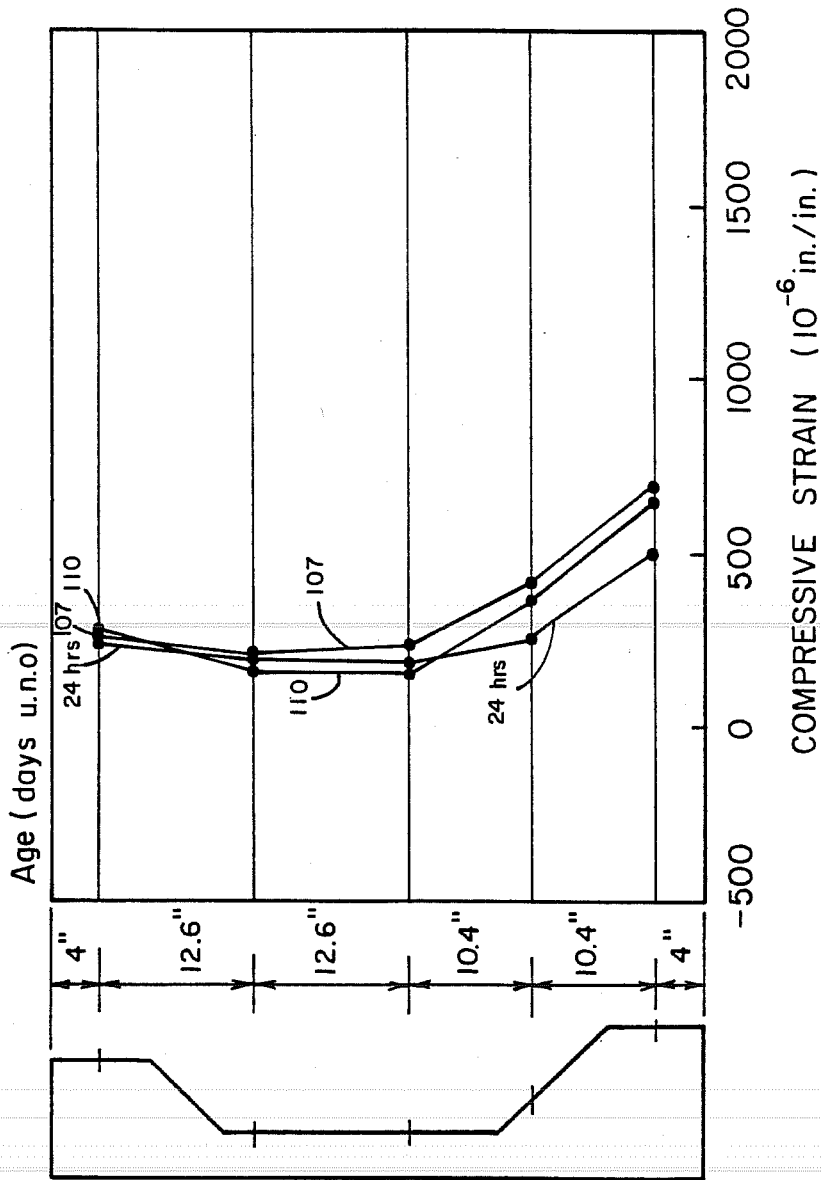INITIAL STRAIN DISTRIBUTION UPON RELEASE IS NOT SHOWN.

b) strain distribution at station QP

Fig. 5.19 Strain Distributions at Selected Ages for Specimen H-I2 (cont'd)
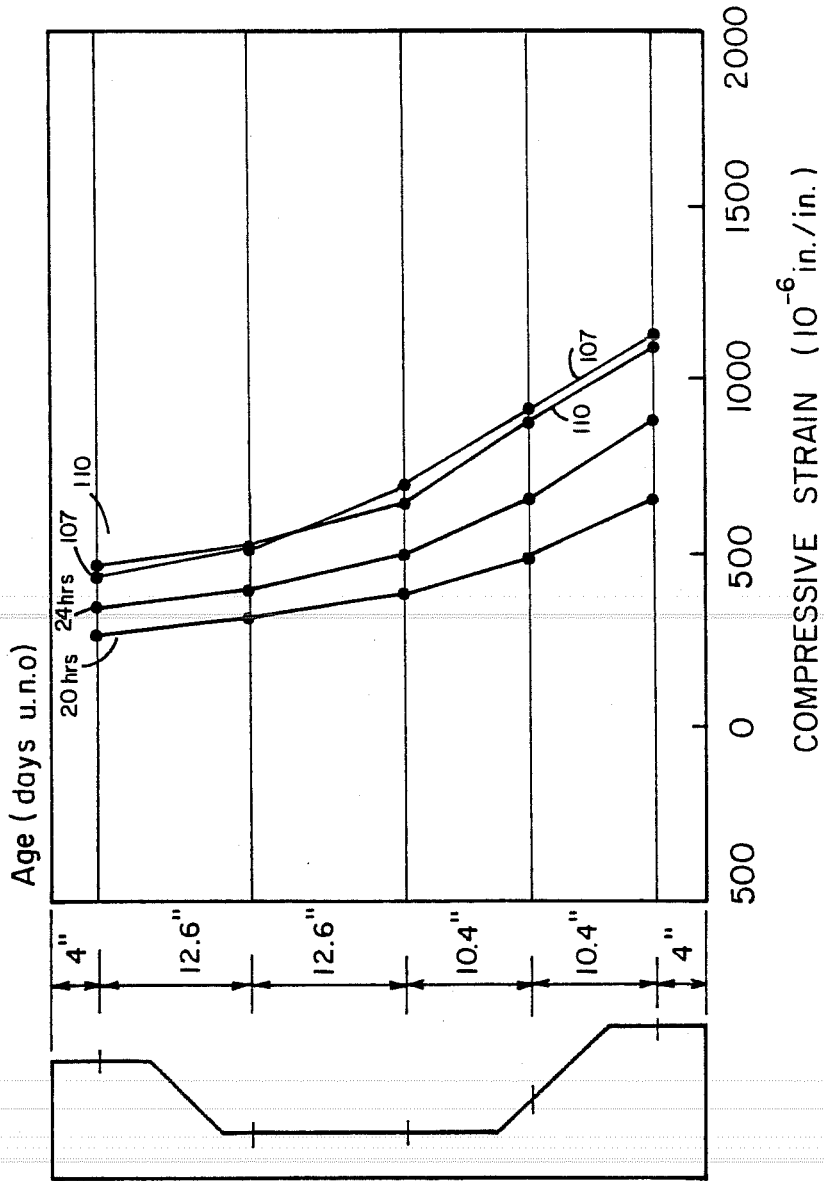
c) strain distribution at station MS

Fig. 5.19 Strain Distributions at Selected Ages for Specimen H-I2 (cont'd)

TABLE 5.2 Measured Beam Curvature Summary

	L-I1	L-I2	L-01	L-02	H-01	H-02	H-I1	H-I2
Immediate Mid-Span Curvature at Time of Prestress Transfer	N/A	N/A	-8.26	-8.98	N/A	N/A	-4.22	-8.98
Mid-Span Curvature After Beam Was Placed in Storage	-10.63*	-9.94	-11.63	-12.56	-10.22	-6.33	-9.46	-11.98
Mid-Span Curvature Prior to Setting Beam on Bents	-14.74	-15.63	-17.20	-16.02	-14.72	-12.52	-8.17	-15.28
Mid-Span Curvature Upon Setting Beam on Bent	-12.22	-13.37	-15.91	-15.09	N/A	N/A	-5.56	-13.94

*units are in 10^{-6} rad/in.

than that of H series beams. Subsequent strain distributions shown are resonable considering the amount of time passed and the change in support conditions upon placement on the bents at the bridge site.

Typical strain distributions at Station QP of L series beams (Fig. 5.16b and 5.17b) can be compared to those of H series beams (Fig. 5.18b and 5.19b). These figures show that at quarter points of the beams there is no significant difference between the strain distributions of L series beams and those of H series beams except that the magnitudes of the L series strains are larger than H series strains for long times. This indicates that the creep and shrinkage strains for the L series beams were larger than in the H series beams which is expected considering the differential ages of the beams at time of taking readings. Once again the changes in strain distribution with time and with changes in support conditions are resonable. Also, strain distributions are more nearly linear at Station QP than was the case at Station END.

The strain distributions at Station MS of L series beams (Fig. 5.16c and 5.17c) can be compared to those of H series (Fig. 5.18c and 5.19c). The same conclusions that were drawn from the quarter point strain distributions apply to these strain distributions. As before, plane section remain essentially plane at station MS for both L series and H series beams.

5.4   Internal and Ambient Temperature

Discontinuous plots of internal temperature versus time for beams L-I1 and H-01 as measured by copper-constantine thermocouples embedded in the concrete are given in Figs. 5.20 and 5.21.   These reported temperature-time distributions are similar to those recorded for beams L-01 and H-I1 respectively.

Discontinuous plots of ambient temperature versus time for beams L-I1 and H-01 as measured by a copper-constantine thermocouple exposed to the surrounding air are given in Figs. 5.22 and 5.23.   These reported temperature-time distributions are similar to those recorded for beams L-01 and H-I1 respectively.

5.5   Electronic Strain Gage Data

Unfortunately, the electrical resistance strain gages which were installed on the strands of one beam of each set cast did not exhibit long term stability.   The erratic nature of the strain readings recorded indicate that there may have been a problem with the switch boxes used or the gages themselves malfunctioned.   Care was taken in attaching the gages to the strands and each gage was checked for stability at each stage of its attachment so it is probable that the switch boxes did not function properly or the gages were damaged in some way during consolidation of the concrete.   Temperature was also a variable which might have affected gage performance.   Even short term
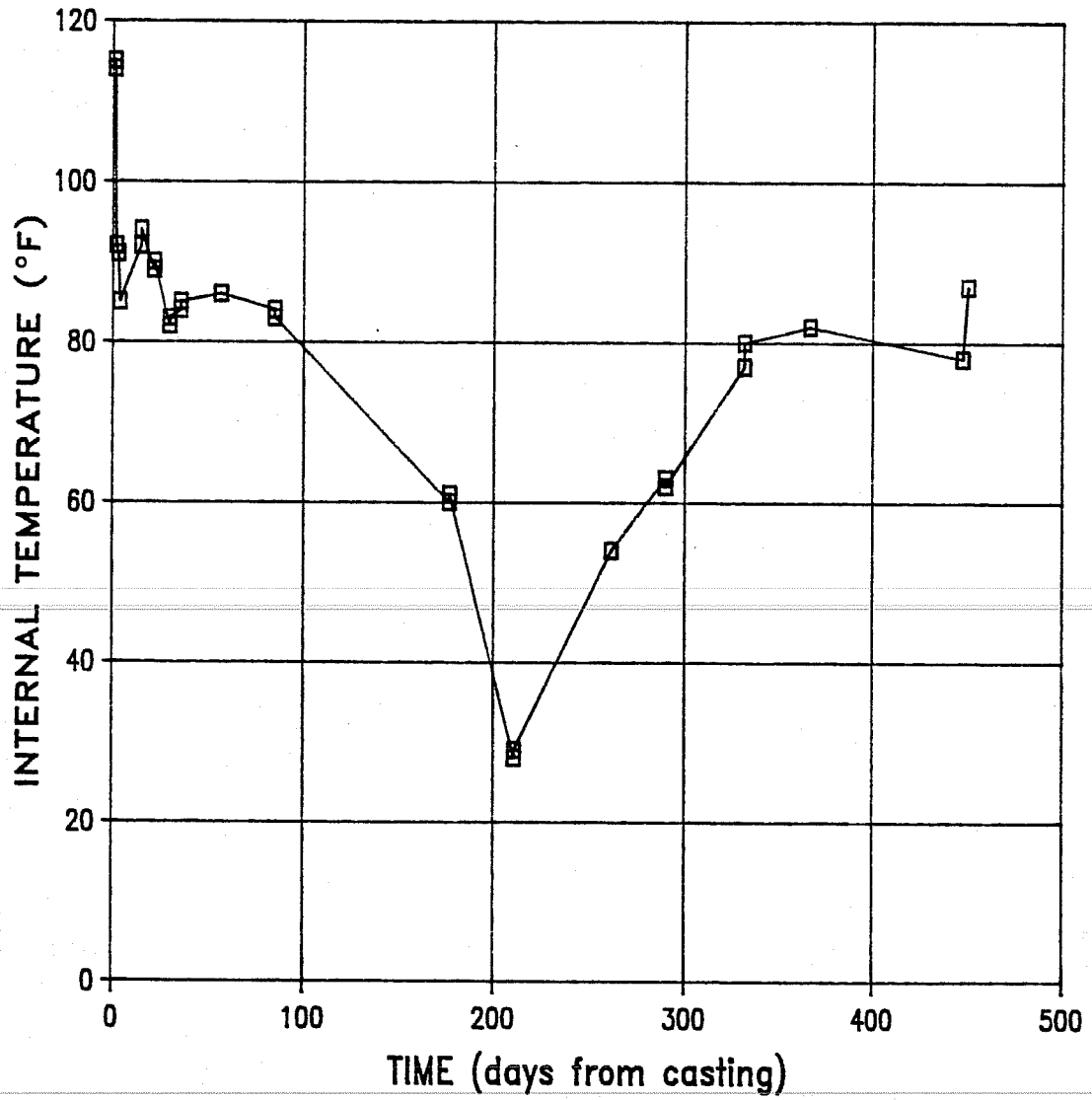
Fig. 5.20   Internal Temperature of Specimen L-I1 Measured During
            Each Instrumentation Monitoring Session
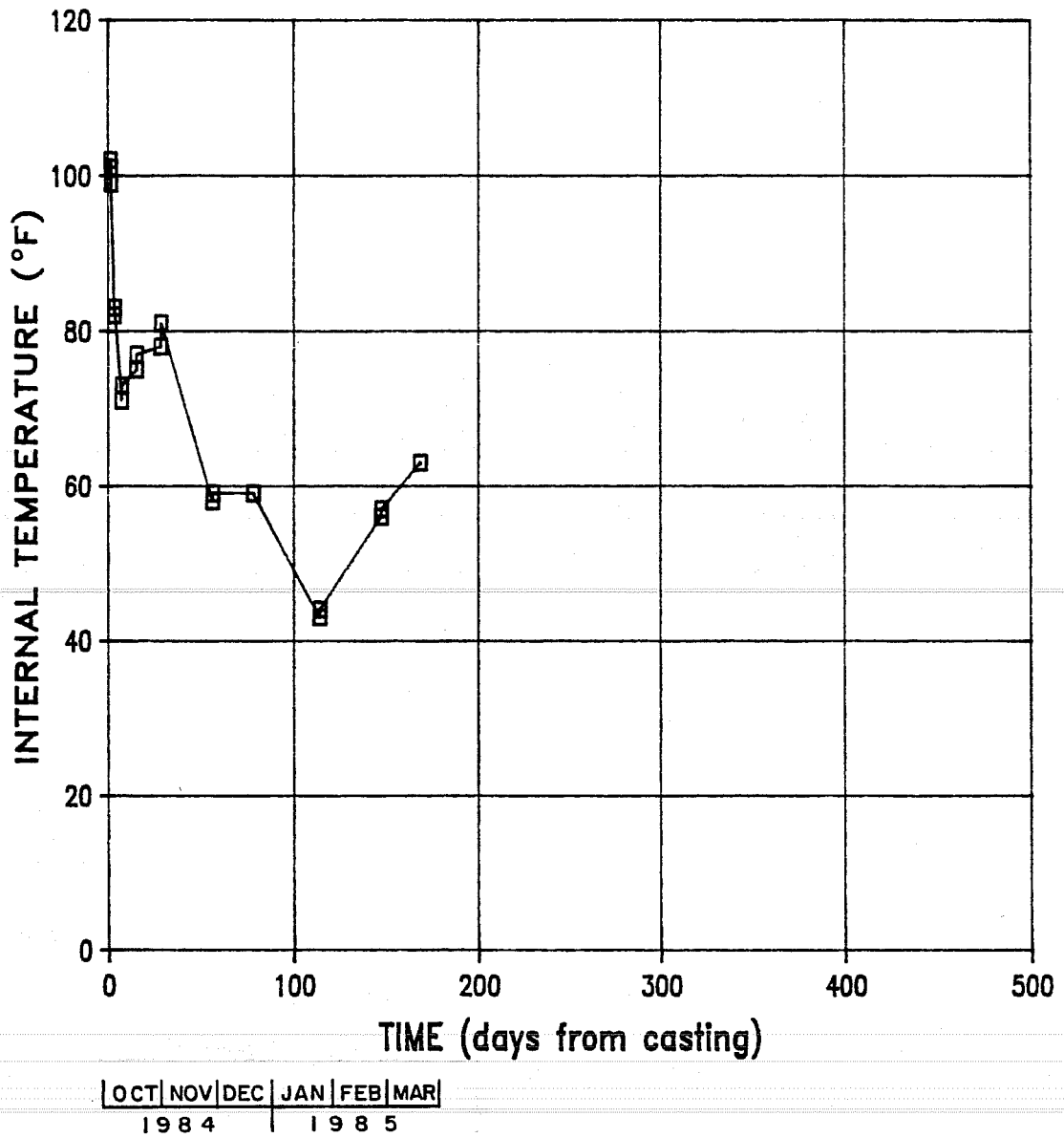
Fig. 5.21   Internal Temperature of Specimen H-01 Measured During
            Each Instrumentation Monitoring Session
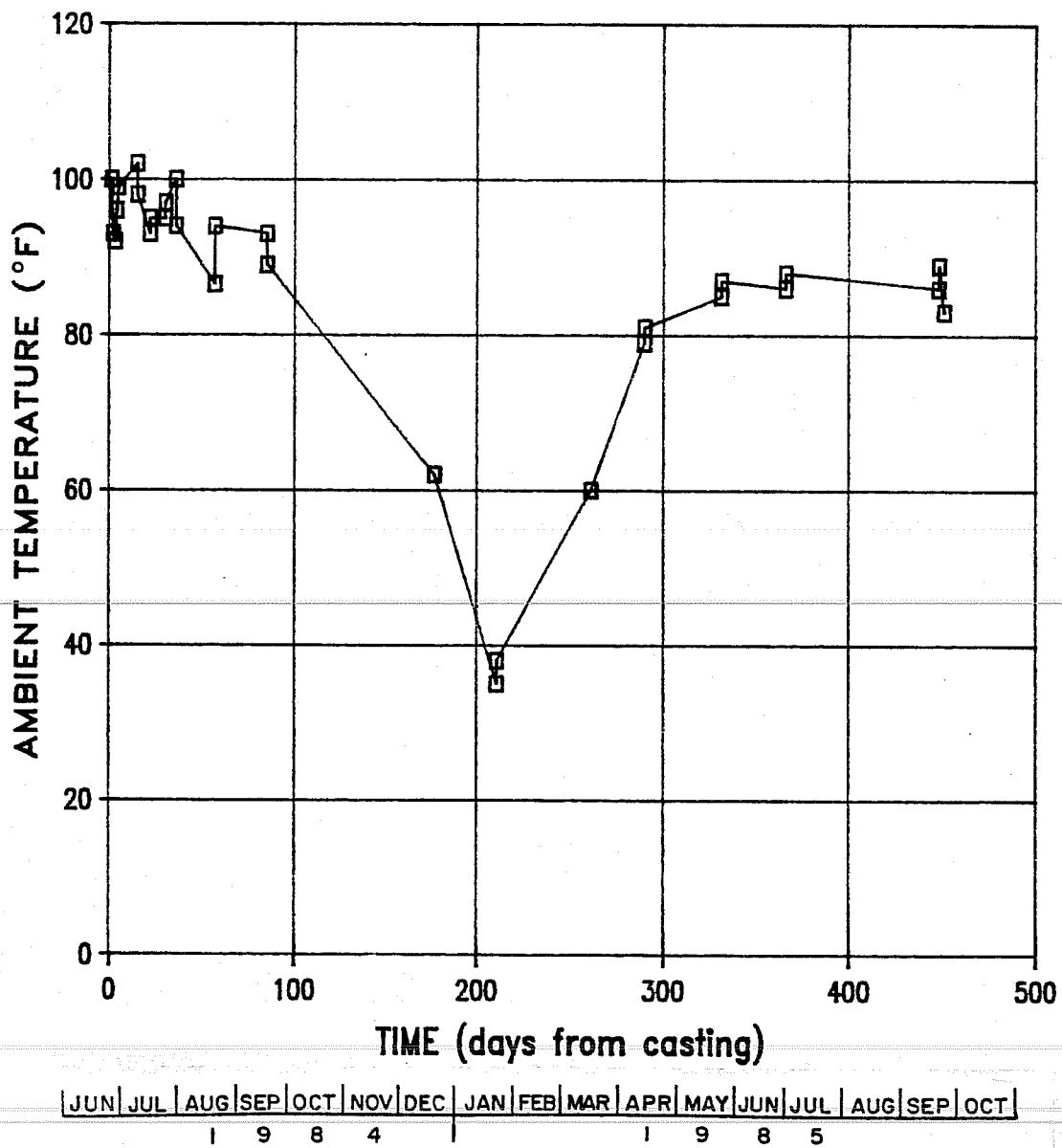
Fig. 5.22   Ambient Temperature for Specimen L-I1 Measured During
            Each Instrumentation Monitoring Session
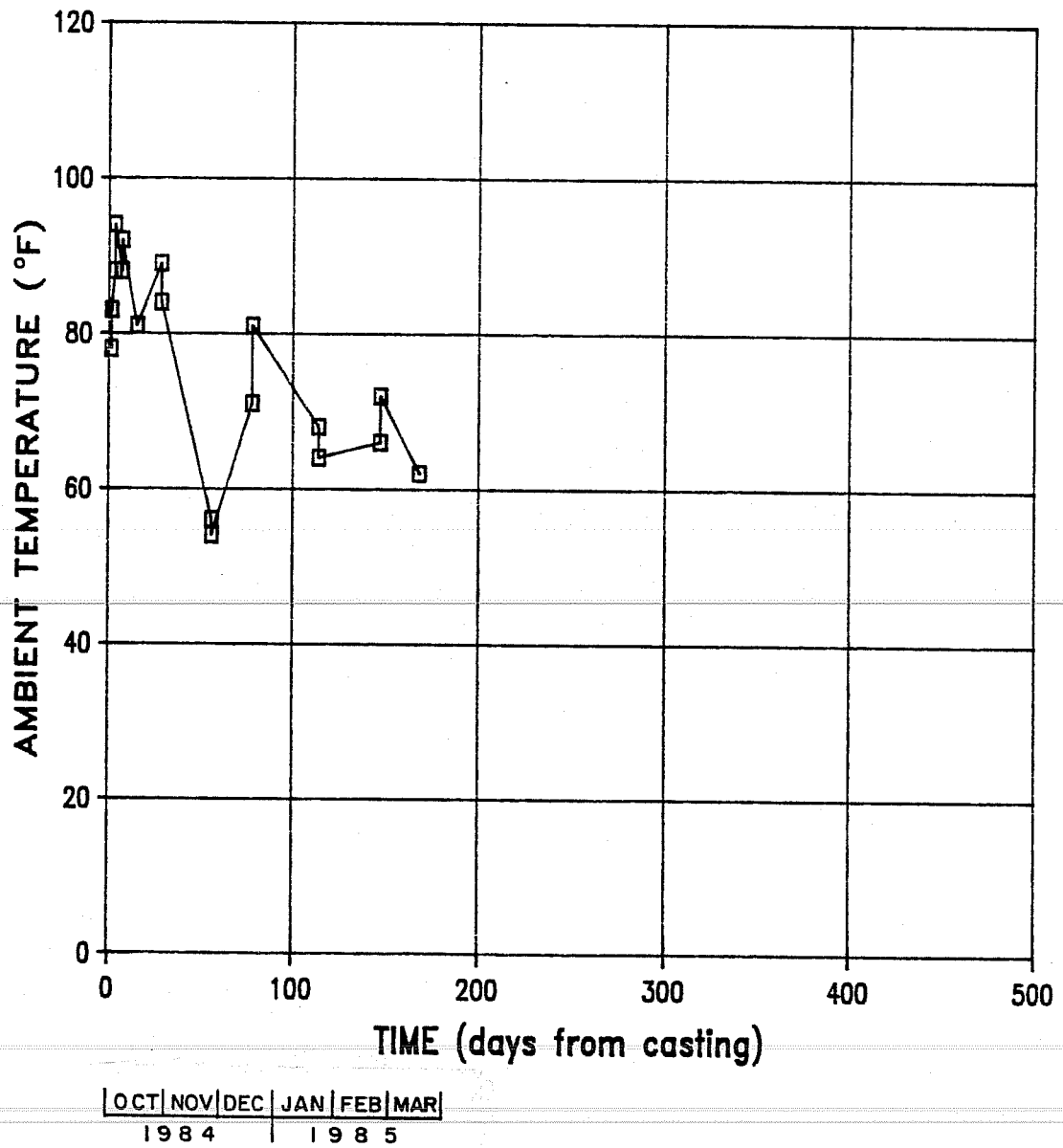
Fig. 5.23   Ambient Temperature for Specimen H-01 Measured During
Each Instrumentation Monitoring Session

strain gage behavior did not seem to be logical as most strain readings increased during prestress transfer indicating a tensile strain. This does not make sense as the strand strain should have decreased due to the initial elastic deformation and subsequent creep and shrinkage strains. Even when readings were taken immediately before and after prestress transfer a positive strain was indicated. In many cases the indicated strain eventually went negative. No consistent variation of indicated strain with temperature was found. In some cases the indicated strain increased with increasing temperature while in other cases the indicated strain goes in the opposite direction as the temperature.

C H A P T E R   6

CONCLUSIONS

6.1 General

The overall observation of the bridge girders which were instrumented and monitored in the casting yard is an ongoing one. Construction of the bridges has not been completed at the time of writing of this report. Thus, final information on material properties, construction operation dates, and final bridge dimensions are not yet available for input or comparisons with analytical programs. These steps will be completed by Kelly.

Conclusions in this chapter will focus on the adequacy and practicality of the various instrumentation systems and recommendations for their development and utilization.

6.2 Specific Conclusions

1. The field portable deflection measuring system using a tensioned wire calibrated by incremental weight-sag technique was an unqualified success. Repeatibility of readings was high and all deflection data is consistent and logical. The system was modified and used in a field investigation of a bridge in Happy, Texas, and was found to work well for load tests also.

221

2. The internal temperature measuring system using thermocouples worked well in practice and was easy to install.

3. Early age readings of the concrete surface strains using the Demec gage with standard gage points epoxied to inserts cast in the concrete were dependable. However, after several months the epoxy softened and many readings were lost. It was concluded that a tapered drilled hole in the metal insert instead of epoxied points would have been much more reliable.

4. The strand strain gage mounting and reference balancing system used did not give satisfactory performance in the field. Alternate procedures must be found.

5. A great deal of variability in typical girder deflections is due to the varied age of operations by the contractor on this specific project. Decisions such as which girders are to be cast or erected first greatly affect the age at placement on the piers. This was seen to greatly affect bridge camber.

6. Analytical studies should be run to determine the sensitivity of calculated deflections to the types of schedule and material variations noted in this study.

7. The properties of the materials of which a prestressed beam is constructed have a primary effect on beam

deformations. It is the writer's opinion that a lack of knowledge and understanding of the interaction of these material properties along with excessive tolerances in deck thickness and other dimensions effecting dead load have contributed to the problem of sagging beams in highway bridges in the state of Texas.

8. Extensive creep test programs can and should be conducted on mix designs used in prestressed concrete from several parts of the country from time to time to verify that theoretical models continue to yield realistic results. Also, modulus of elasticity test programs of high strength concrete from several regions should be performed under both controlled and ambient environmental conditions so that verification of theoretical models for the stiffening effect of aging concrete can be made.

REFERENCES

1. ACI Committee 209, "Effects of Concrete Constituents, Environment, and Stress on Creep and Shrinkage of Concrete," Designing for Effects of Creep Shrinkage Temperature in Concrete Structures, SP-27, American Concrete Institute, Detroit, 1971.

2. ACI Committee 209, "Prediction of Creep, Shrinkage, and Temperature Effects in Concrete Structures," Designing for Creep and Shrinkage in Concrete Structures, SP-76, American Concrete Institute, Detroit, 1982.

3. ASTM Committee A-1, Method A370-77, "Standard Methods and Definitions for Mechanical Testing of Steel Products," 1983 Annual Book of ASTM Standards, Vol. 01.04, American Society for Testing and Materials, 1983.

4. ASTM Committee A-1, Standard A416-80, "Standard Specification for Uncoated 7-Wire Strand for Prestressed Concrete," 1983 Annual Book of ASTM Standards, Vol. 01.05, American Society for Testing and Materials, 1983.

5. ASTM Committee C-9, Method C31-83, "Making and Curing Test Specimens in the Field," 1983 Annual Book of ASTM Standards, Vol. C 04.02, American Society for Testing and Materials, 1983.

6. ASTM Committee C-9, C39-83b, "Standard Test Method for Compressive Strength of Cylindrical Concrete Specimens," 1983 Annual Book of ASTM Standards, Vol. C 04.02, American Society for Testing and Materials, 1983.

7. ASTM Committee C-9, Method C469-81, "Static Modulus of Elasticity and Poisson's Ratio of Concrete in Compression," 1983 Annual Book of ASTM Standards, Vol. C 04.02, American Society for Testing and Materials, 1983.

8. ASTM Committee C-9, Method C512-76, "Standard Test Method for Creep of Concrete in Compression," 1983 Annual Book of ASTM Standards, Vol. C 04.02, American Society for Testing and Materials, 1983.

9. ASTM Committee E-28, Method E328-78, "Recommended Practice for Stress-Relaxation Tests for Materials and Structures," 1983 Annual Book of ASTM Standards, Vol. 03.01, American Society for Testing and Materials, 1983.

10. Kelly, D., "Deflection of Long-Span Prestressed Concrete Beams: Part 2," Master's Thesis, The University of Texas at Austin, August, 1986.

11. Armstrong, T. A., Leyendecker, E. V., and Breen, J. E., "Field Testing of Concrete Slab and Girder Bridges," Research Report Number 94-2, Research Project Number 3-5-86-94, Structural Model Study of Concrete Slab and Girder Spans, Center for Highway Research, The University of Texas at Austin, July 1969.

12. Atkins, W. G., "A Generalized Numerical Solution for Prestressed Concrete Beams," unpublished Master's Thesis, The University of Texas at Austin, August 1965.

13. Bazant, Z. P., "Thermodynamic Theory of Deformations of Concrete with Explanation of Drying Creep," reprinted from Structure, Solid Mechanics, and Engineering Design, The Proceedings of the Southhampton 1969 Civil Engineering Materials Conference.

14. Bazant, Z. P., and Panula, L., "New Model for Practical Prediction of Creep and Shrinkage," Designing for Creep and Shrinkage in Concrete Structures, SP-76, American Concrete Institute, Detroit, 1982.

15. Branson, D. E., "The Deformation of Noncomposite and Composite Prestressed Concrete Members," Deflections of Concrete Structures, Sp-43, American Concrete Institute, Detroit, 1974.

16. Buettner, D. R., and Hollrah, R. L., "Creep Recovery of Plain Concrete," ACI Journal, Proceedings, V. 65, No. 4, June 1968.

17. Chang, D. C., "Behavior of Multipanel Reinforced Concrete Frames Subjected to Vertical and Lateral Loads," published Ph.D. dissertation, The University of Texas at Austin, May 1977.

18. Corley, W. G., Sozen, M. A., and Siess, C. P., "Time-Dependent Deflections of Prestressed Concrete Beams," Bulletin No. 307, Highway Research Board, Washington D.C., 1961.

19. Fadl, A. I., and Gamble, W. L., "Time-Dependent Behavior of Noncomposite and Composite Post-Tensioned Concrete Girder Bridges," Structural Research Series No. 430, Engineering Experiment Station, University of Illinois, October 1976.

20. Gamble, W. L., "Field Investigation of a Continuous Composite Prestressed I-Beam Highway Bridge Located in Jefferson County, Illinois," Progress Report No. 5 of the Field Investigation of Prestressed Reinforced Concrete Highway Bridges, Project IHR-93, The Structural Research Laboratory, Department of Civil Engineering, Engineering Experiment Station, University of Illinois, Urbana, June 1970.

21. Ghali, A., and Favre, R., "Stresses and Deformations of Composite Members," private communication, 1985.

22. Grouni, H. N., "Prestressed Concrete--A Simplified Method for Loss Computation," ACI Journal, Proceedings, V. 70, No. 2, February 1973.

23. Hansen, T. C., and Mattock, A. H., "Influence of Size and Shape of Member on the Shrinkage and Creep of Concrete," ACI Journal, Proceedings, V. 63, No. 2, February 1966.

24. Hays, C. O., and Matlock, H., "A Nonlinear Analysis of Statically Loaded Plane Frames Using a Discrete Element Model," Research Report No. 56-23, Center of Highway Research, The University of Texas at Austin, May 1972.

25. Hernandez, H. D., and Gamble, W. L., "Time-Dependent Prestress Losses in Prestressed Concrete Construction," Structural Research Series No. 417, Engineering Experiment Station, University of Illinois, May 1975.

26. Houdeshell, D. M., Anderson, T. C., and Gamble, W. L., "Field Investigation of a Prestressed Concrete Highway Bridge Located in Douglas County, Illinois," Civil Enginerring Studies, Structural Research Series No. 375, Department of Civil Engineering, University of Illinois, Urbana, February 1972.

27. Huang, T., "Direct Method for Estimating Prestress Loss," *Transportation Research Record No. 547*, National Research Council, Congress on Steel Bridges, 1975.

28. Jones, H. L., and Furr, H. L., "Differential Camber in Prestressed Concrete Beams," *Research Report 193-1F*, Texas Transportation Institute, Texas A&M University, September 1977.

29. Koretsky, A. V., and Prichard, R. W., "Critical Assessment of the International Estimates for Relaxation Losses in Prestressing Strands," *Research Report No. CE25*, Department of Civil Engineering, University of Queensland, Australia, June 1981.

30. Kraai, P. P., "Concrete Drying Shrinkage: Facts or Fallacies," *Designing for Creep and Shrinkage in Concrete Structures*, SP-76, American Concrete Institute, Detroit, 1982.

31. Lo. Y., "Comparison of Analytical and Measured Performance of Pretensioned Prestressed Concrete Beams," unpublished Master's Report, The University of Texas at Austin, June 1975.

32. Lyse, I., "Shrinkage and Creep of Concrete," *ACI Journal, Proceedings*, V. 56, February 1960.

33. Mossiosian, V., and Gamble, W. L., "Time-Dependent Behavior of Noncomposite and Composite Prestressed Concrete Structures Under Field and Laboratory Conditions," *Structural Research Series No. 385*, Engineering Experiment Station, University of Illinois, May 1972.

34. Overman, T. R., Breen, J. E., and Frank, K. H., "Fatigue Behavior of Pretensioned Concrete Girders," *Research Report 300-2F*, Research Project Number 3-5-80-300, Center for Transportation Research, Bureau of Engineering Research, The University of Texas at Austin, November 1984.

35. Pauw, A., and Breen, J. E., "Field Testing and Analysis of Two Prestressed Concrete Girders," *The University of Missouri Bulletin*, Vol. 60, No. 52, Engineering Experiment Station Series, No. 46, University of Missouri, Department of Civil Engineering, Columbia, Missouri, November 1959.

36. PCI Committee on Prestress Losses, "Recommendation for Estimating Prestress Losses," *PCI Journal*, V. 20, No. 4, July-August 1975.

37. Peterman, M. B., and Carrasquillo, R. L., "Production of High Strength Concrete," *Research Report 315-F*, Center for Transportation Research, The University of Texas at Austin, October 1983.

38. Pierce, D. M., "A Numerical Method of Analyzing Prestressed Concrete Members Containing Unbonded Tendons," Ph.D. dissertation, The University of Texas at Austin, June 1968.

39. Poston, R. W., Bradberry, T. E., and Breen, J. E., "Load Tests of a Pretensioned Girder Bridge Near Happy, Texas," *Research Report 921-1F*, Research Project 3-40-85-921, Center for Transportation Research, Bureau of Engineering Research, The University of Texas at Austin, April 1985.

40. Preston, H. K., "Testing 7-Wire Strand for Prestressed Concrete--The State of the Art," *PCI Journal*, May-June 1985.

41. Rad, V. J., and Dilger, W. H., "Time-Dependent Deflections of Composite Prestressed Concrete Beams," *Deflections of Concrete Structures*, SP-43, American Concrete Institute, Detroit, 1974.

42. Reynolds, R. J., and Gamble, W. L., "Field Investigation of Prestressed Reinforced Concrete Highway Bridges: Instrumentation for Long-Term Field Investigations," *Progress Report No. 2 of the Field Investigation of Prestressed Reinforced Concrete Highway Bridges, Project IHR-93*, The Structural Research Laboratory, Department of Civil Engineering, Engineering Experiment Station, University of Illinois, Urbana, October 1967.

43. Shank, J. R., "The Mechanics of Plastic Flow of Concrete," ACI Journal, *Proceedings*, V. 32, November-December 1935.

44. Sinno and Furr, "Computer Program for Predicting Prestress Loss and Camber," *PCI Journal*, V. 17, No. 5, September-October 1972.

45. Slate, F. O., and Meyers, B. L., "Some Physical Processes Involved in Creep of Concrete," reprinted from Structure, Solid Mechanics, and Engineering Design, The Proceedings of the Southhampton 1969 Civil Engineering Materials Conference.

46. Suttikan, C., "A Generalized Solution for Time-Dependent Response and Strength of Noncomposite and Composite Prestressed Concrete Beams," Dissertation, The University of Texas at Austin, August 1979.

47. Tudros, M. K., Ghali, A., and Dilger, W. H., "Time-Dependent Prestress Loss and Deflection in Prestressed Concrete Members," PCI Journal, V. 20, No. 3, May-June 1975.

48. White, C. D., "Observations and Evaluation of the Composite Wing Girder Bridge at Bear Creek," unpublished Master's Thesis, The University of Texas at Austin, May 1984.

49. Castrodale, R. W., BRIDGE.BAS Version 1.0, "Basic Computer Program for Designing Pretensioned Prestressed Concrete Beams," September 1984.

V I T A

Timothy Ernest Bradberry was born in Birmingham, Alabama, on January 14, 1960, the son of Roland Ernest and Betty Rogers Bradberry. He graduated from Huffman High School, Birmingham, Alabama, in 1978, and entered Auburn University in Auburn, Alabama. In June, 1979, he began his Cooperative Education work being employed by Ingalls Iron Works Co., Birmingham, Alabama. In June, 1981, he was employed by Haradaway Constructors, Inc., Tampa, Florida, as a Cooperative Education student. He received the degree of Bachelor of Science in Civil Engineering in August, 1983. In September, 1983, he entered the Graduate School of the University of Texas at Austin. While working towards the degree of Master of Science in Civil Engineering, he was employed as a Research Assistant I at the Phil M. Ferguson Structural Engineering Laboratory.

Permanent address: 933 Eldorado Drive
                     Birmingham, AL 35235

This report was typed by Patricia Hinderson